Hort Innovation

Final Report

Improved tree and fruit nutrition for the Australian apple industry

Project leader:

Nigel Swarts

Delivery partner:

Tasmanian Institute of Agriculture

Project code:

AP14023

Project:

Improved tree and fruit nutrition for the Australian apple industry AP14023

Disclaimer:

Funding statement:

This project has been funded by Hort Innovation, using the apple and pear research and development levy and contributions from the Australian Government. Hort Innovation is the grower-owned, not-for-profit research and development corporation for Australian horticulture.

Publishing details:

ISBN 978-0-7341-4728-8

Published and distributed by: Hort Innovation

Level 7
141 Walker Street
North Sydney NSW 2060

Telephone: (02) 8295 2300

www.horticulture.com.au

Content

Summary

This four-year research program extended fertigation trials from PIPS 1, established ^{15}N whole tree recovery trials and a N, P and K fertigation trial, characterized soils from 40 different orchards from five apple growing regions and produced a decision support tool to assist grower and advisors strategically manage their nitrogen and irrigation resources. Key growers and advisors from across the Australian apple growing industry provided valuable insight into project activities ensuring appropriateness and relevance. Through strong collaboration with Plant and Food Research, New Zealand, and implementing field activities in commercial orchards, this project delivered cost effectively against the short and medium term outcomes anticipated at the start of the project and made an important contribution to the long term outcomes for the apple industry identified in the SIP.

We found that pre-harvest N (and other nutrients) were taken up by the tree much more efficiently than post-harvest N to the extent that we now question the validity of post-harvest N application. We made important recommendations to industry on a low input approach to N management that promotes greater N use efficiency without compromising fruit quality outcomes. We completed the first industry wide or multi-state assessment of soil health and soil-water characteristics of Australia's apple growing soils (www.applesoils.com), and learnt that (i) the structure or physical health (and therefore most likely the biological health) of apple growing soils varies widely between sites, even within the same soil order; and (ii) many sites were suffering from loss of soil carbon, surface compaction and sealing, loss of readily available soil water for sustaining growth and loss of tightly held water which provides resilience to moisture stress during drought. Using this information, we developed a nation-wide decision support tool to guide strategic on-farm irrigation and nutrient management – Strategic Irrigation and Nitrogen Assessment Tool for Apples (SINATA). The design of SINATA was strongly influenced by input from a reference group of leading growers and advisors. This tool incorporated research findings on (i) tree water use from PIPS I and PIPS II; (ii) multi-season nitrogen dynamics learned from the fertigation and ^{15}N trials; and (iii) soil physical, chemical and hydrological data from orchards across five main apple growing regions.

Awareness and findings of the project were extended via a wide range of platforms including national conferences and workshops, international conferences, articles in Australian Fruit Grower and Industry Juice and through the Future Orchards walks. Zoom presentations to the winter Northern and Southern Loop towards the end of the project generated a great deal of interest, discussion and intention to change practice, as well as industry push to address some key knowledge gaps in the management practices that promote the long term sustainability of Australian apple orchard soils. This has become an important component (AP19006) of the 3rd PIPS Research and Development Program.

Keywords

Apple, nitrogen, nutrition, fruit quality, nitrogen use efficiency, tree physiology, soils, phosphorus, potassium

Introduction

This project was developed as a collaborative effort between the Tasmanian Institute of Agriculture (TIA) and Plant and Food Research, New Zealand (PFR). We consulted an industry panel of growers and advisers who provided valuable input on the concepts for the project. The project was developed with key learnings from PIPS 1 in mind. From these discussions, key knowledge gaps that were identified that this project should address included:

- the sources, temporal patterns, and relative contributions to N supply of plant-available N in the orchard?
- peak N demand by the tree and how much is provided by internal tree N?
- development of a decision support tool for advisors and growers to assist with fertigation and irrigation management in all major apple-growing regions.

This project had two major sub-projects: (i) multi-season fertigation research trials that builds on findings from the fertigation project (AP12006) and (ii) the development of a decision support tool based on the SPASMO model that will guide advisor/grower optimisation of irrigation and fertigation application for four major growing regions in the country.

Sub project 1. Fertigation research. This sub project had four components:

- *Continuation of N and irrigation trials at Lucaston*. This trial established for AP12006 will continue for a total of five growing seasons creating one of the longest intensive nutrition trials ever completed in the POME fruit industry.
- *^{15}N recovery trial in mature apple trees*. There is limited understanding of the relative contribution of residual, end-of-growing-season N sources, to both N supply and N uptake and loss. This research was established to better understand nitrogen uptake efficiency in commercial apple orchards, peak demand for nitrogen and internal nitrogen dynamics. This research will provide an understanding of how fertiliser application approach, rates and timings can be managed to best satisfy the tree's N requirements, mitigate leaching and optimise productivity without a cost to fruit quality.
- *NPK fertigation trial*. As tree nutrition requires a balanced approach, research is required to better understand how the addition of N influences P and K uptake in commercially managed trees
- *Mineralisation trials*: Mineralisation as a source of N remains an understudied component of the overall nutrition budget for apple trees. This research will enable a better understanding of the rates of mineralization in a commercial apple orchard.

Sub project 2: Decision support tool (DST). This project had two components.

- *Soil characterisation*: Development of the DST required significant investment in soil parameterization including nationwide soil physical and chemical characteristics. In order for growers and advisers to have confidence in the tool, soils need to be locally characterised. At each site the model requires knowledge of the following soil properties for each soil layer, saturation, plant available water content, permanent wilting point, hydraulic conductivity, soil carbon and nitrogen distribution with depth including each of the soil carbon pools, as well as observation of root distribution.
- *Development of a user-friendly DST*. The DST underpinned by SPASMO, data from field N fertigation trials, multi-site regional soil characterisation, climate and tree physiological datasets will provide growers with a reliable assessment of their orchard's soil, water and nutrient status based on their irrigation and fertiliser inputs. Growers and advisors will be trained in the usage of the DST. This research will enable growers and advisers to explore different irrigation and fertilizer strategies and management practices for different soil types and climates in order to optimise yield achievement without cost to quality. This tool would also serve as a 'living' repository for R&D arising from PIPS1 and PIPS2, where model performance is incrementally improved as the findings from new research gets incorporated into the tools' calculations.

Methodology

The methods for each component of the two sub-projects are described below

Sub project 1: Fertigation trials

N and irrigation trial at Lucaston Park Orchards.

The fertigation trial at Lucaston was a continuation of the trial established for AP12006 with the final two seasons completed as part of this project (see final report AP12006 for more details for detailed methodology). The trial was initially established in 2012 with the first treatments applied in the post-harvest period of March 2013. The trial continued for five seasons concluding at harvest in March 2017. Two seasons of data was collected for this project and detailed fruit quality assessments were made and reported in Milestone 104. This trial investigated the influence of rate and timing of N application in the context of varying irrigation on 'Gala' fruit quality and productivity. This trial also facilitated research into nitrous oxide emissions (Appendix 1), water movement through the soil profile (Appendix 2), tree water use (Appendix 3) and N leaching (Appendix 4).

15N fertigation trials

Optimizing the utilization of applied nitrogen (N) in fruit trees requires that N supply is temporally well matched to tree demand. We investigated how the timing of N application affected uptake, allocation and remobilization within 14-year-old Gala/M26 apple trees (*Malus domestica Borkh*) over two seasons. In the 2017-18 season, ^{15}N-calcium nitrate was applied by weekly fertigation in four equal doses, commencing either four weeks after full bloom (pre-harvest) or one week post-harvest (post-harvest), or fortnightly, divided between pre- and post-harvest (50:50 split). Fertiliser uptake was monitored by fortnighly leaf sampling over the course of the season. Whole trees were destructively harvested at dormancy of the first season to quantify N uptake and allocation, and a second set of trees were excavated at fruit harvest of the second season to quantify the remobilization of N derived from fertilizer. Fruit quality and yeild from each tree was also assesed to determine the influence of N treatments. See Appendix 5 for the detailed experimental design and implementation of this trial.

NPK Fertigation trials.

Nutrient management via the application of fertilizer is a key factor determining the sustainable productivity of quality fruit. The challenges of negative environmental impacts from excessive fertilizer application, depletion of natural resources and increasing demand for sustainable production from retailers and consumers requires precise management of mineral nutrition in fruit production. The macronutrients N, P, and K particularly affect apple fruit quality and yield, yet few studies have investigated interactions in uptake between the key macronutrient minerals. and how/if these affect fruit quality and yield at harvest. This study aimed to examine interactions of N, P, and K fertilization at various rates on the tree and fruit uptake dynamics. The experiment was conducted from April 2018 to June 2019 over a growing season in a commercial 'Gala' orchard grown on M26 rootstock located in the Derwent Valley, southern Tasmania. This experiment was a 2 × 2 × 2 factorial completely randomized design of N, P and K fertilizer rate, replicated five times to give a total of 40 tree plots. Each plot consisted of three sampling trees and one buffering tree on both sides. Nitrogen fertilizer was delivered in the form of calcium nitrate either at the rate of 10 (N1) or 50 (N2) kg N ha^{-1}; phosphorus fertilizer was delivered in the form of calcium phosphate monobasic either at the rate of 10 (P1) or 40 (P2) kg P ha^{-1}; potassium fertilizer was delivered in the form of potassium sulphate either at the rate of 50 (K1) or 150 (K2) kg K ha^{-1}. Fertilizer treatments were divided equally over four successive weekly applications from 8th November 2018, 4 WAFB. Leaf laminar and petiole sampling was completed throughout the trial and fruit was harvested in March 2019 and subjected to full fruit quality analysis to determine the influence of fertiliser treatments. Full details of the trial design can be found in Appendix 6.

Mineralisation trial:

See Appendix 7 for summary of the mineralization research

Sub-project 2: Development of a DST

Soil Characterisation

Over the last decade the SPASMO (Soil Plant Atmosphere System Model) model has been developed by Plant and Food Research in New Zealand. In order to use and test this model for the Australian apple industry, soil data is needed. Unlike many crop-soil-climate models, SPASMO requires detailed soil physical characterisation of each soil layer including the soil water retention curve and saturated hydraulic conductivity. Overall, there is insufficient soil data and levels of mapping to identify the major soil types on which apples are grown, insufficient data for use with the SPASMO model, and no data that reports on the condition or 'health' of apple producing soils. Despite the economic importance of the Australian apple industry little is known about the types, characteristics and condition of Australia's apple growing soils. This study has sought to:

- identify the type and range of soils used for apple production
- determine the physical and chemical attributes of typical apple growing soils in four regions area
- provide soil data needed to support the development and adoption of tree crop simulation tools
- support growers to better understand and manage their soil resources,
- report on environmental condition or health of apple growing soils.

Detailed soil chemical, physical, structural and morphological assessments were completed on 40 orchard blocks from five growing regions across Australia. 31 of these were completed early on in the project with results reported in detail in Milestone 108. An additional nine sites were analysed from Western Australian orchard blocks as an additional milestone for the project. These soils samples were analysed in the same way as the earlier samples for consistency. Refer to www.applesoils.com for more information.

Development of SINATA

The primary model that is being developed from this project is called SINATA (Strategic Irrigation and Nitrogen Assessment Tool for Apples). This is a decision support tool that will guide advisors and growers on optimization of irrigation and fertigation application for the major apple-growing growing regions of Australia. The focus of SINATA is on water and nutrient (nitrogen) management, and to understand how irrigation and fertilizer application (types, rates, timings) can be managed to satisfy the tree's water and nitrogen requirements, mitigating leaching and optimising productivity without cost to fruit quality. The backbone underpinning this tool is the SPASMO model developed by Steve Green (PFR, NZ) and the data used to parametrise the model for Australian apple orchards has come from the nitrogen fertigation trials, tree water use (sap flow) research and the soil characterisation work. The background science to the model can be found in Milestone reports 103, 105, and 109. A final summary of the model is available in Appendix 8.

Outputs

This table was put together at the start of the project and summarises all the outputs from this project.

Level of the Program Logic	Measures	Progress at this Milestone
Outputs	No. of industry communication products (fact sheets, articles)	APAL Newsletter research summary (Dec 2016)- Tas Country article (Dec 2017) Article published in AFG (Jan 18), Factsheet prepared for the Fruit Growers Tasmania conference (May 2018), Postcard developed by PhD student Bi Tan (May 2018) APAL video published on Youtube (21/11/2018) Article published in AFG (June 2019) Fact sheet for FGT conference (June 2019) Australian Fruit Grower magazine article (Aug 2019) Industry Juice (Aug 2019)
	No. of industry training events (field days, workshops, interviews)	Presentation given at APAL speed updating event (Jun 2017) Presentation given by Steve Green at the International Sap flow conference (May 2017) Presentation given at ISHS Mineral Nutrition of Fruit Trees (Oct 2017) Presentation given at Fruit Growers Tasmania conference (May 2018) 1st interview with APAL for video completed in April 2018 Presentation given at Speed Updating associated with the Hort Connections conference (June 2018) 2nd interview with APAL and RMCG providing an overview of the project (June 2018) Research incorporated with PIPS 2 update for Future Orchards Loop (September 2018) Presentation given by Steve Green (Plant and Food Research, New Zealand) at International irrigation conference (April 2019) Presentation given at Fruit Growers Tasmania Winter Conference (May 2019) Presentation given at Hort Connections (June 2019) Presentation given at APAL Technical Forum at Hort Connections (June 2019) Presentation given at Fruit Growers Tasmania Apple Field Day (October 2019) Presentation given at APAL Industry Update (November 2019) PhD Student Bi Zhen Tan presented at American Society for Horticultural Science, Las Vegas, (July 2019) Presentations given for Future Orchards Northern and Southern loops (June 2020)
	Improved accuracy of SPASMO model for Australian key production regions (number of modules completed within model)	SPASMO/SINATA has been validated and verified for this final report

	Completion of DST	SINATA completed and submitted as part of this final report
	Completion of multi-season nitrogen budget	^{15}N trial completed for two growing seasons, 5 year nitrogen and irrigation fertigation trials and NPK fertigation trials have enabled a thorough understanding of N dynamics in apple orchards with data included in SINATA DST
	Completion of multi-site parameterisation	Completed for five regions with detailed report provided in Milestone 108 and developed into a webpage with support from RMCG www.applesoils.com
	Completion of climate and tree physiology dataset	Data collection from in field data logging and access to BOM data completed and used to parametrise the SINATA model. Additional data was obtained from OrchardNet Focus Orchards
Activities	No. of grower/advisor interviews to evaluate DST	N/A This wasn't able to be completed due to Covid-19
	No. of DST training events	SINATA was delivered by Nigel Swarts in the winter 2020 Northern and Southern Future Orchard Walk loop. We had originally planned to role SINATA out to three regions. Whilst this would have been preferable, the Future Orchard northern and southern loop enabled delivery to the eight regions and most likely had a greater reach.
	No. of fertigation and 15N trials completed	N and irrigation trials (Lucaston) and 15N trials (Derwent Valley) completed
	No. of N, P and K uptake trials completed	NPK Trial complete
	No. of N laboratory analyses completed	All 15N lab analysis now complete
	No. of soil characterisations completed	31 sites from Tasmania, NSW, SA and Victoria orchards have now been completed and an additional 9 sites from WA have now been included in the data set

Outcomes

This project has made an important contribution to the short, medium and long term outcomes anticipated at the project's commencement. Figure 1 shows the outcomes from the original MER document prepared for Milestone 102.

Figure 1. MER Outcomes for AP14023

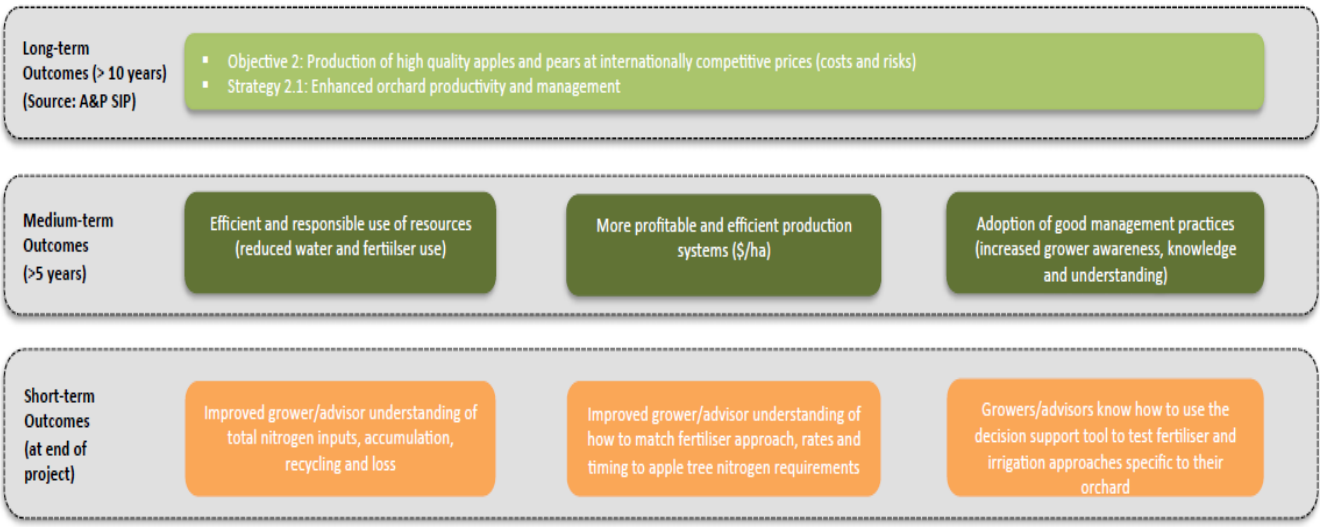

Key outcomes

Improved understanding of nitrogen and irrigation use efficiency

Through the five year fertigation trial at Lucaston Park Orchards and the 15N fertigation trial at Reid Fruits in the Derwent Valley we investigated how nitrogen inputs (pre and post-harvest) together with irrigation supply influence fruit quality outcomes and nitrogen recycling from season to season. We found that pre-harvest N (and other nutrients) were taken up by the tree much more efficiently than post-harvest N to the extent that we now question the validity of post-harvest N application. Whilst growers are rightfully concerned about the potential detrimental effect of pre-harvest N supply on fruit quality outcomes, our fertigation data suggests that with minimal N fertigation inputs (< 40kg N/ha), applied in small weekly doses, no negative impact to fruit quality outcomes will be observed. We have previously advocated for post-harvest N supply to avoid negative impacts on fruit quality, yet that was in the context of a much higher growers practice N rate. Since then, we have learnt that N recycled internally from season to season (from the ^{15}N whole tree excavations - Appendix 6), together with N uptake from mineralization processes, comprises a much larger portion of the seasonal N budget than we first thought. Through whole tree excavations and five years of yield monitoring and fruit nutrition assessments from fertigation trials, we have a much better understanding of N removal from crop harvest and N, P and K requirements for optimal fruit quality (*Long term outcome: Objective 2: Production of high quality apples and pears*). As such, we now advocate for a much lower rate of fertigated N applied pre-harvest to maximize uptake and therefore resource use efficiency. This will lead to substantial reductions in leaching (Appendix 4) and nitrous oxide emissions (Appendix 1) improving the long-term sustainability of commercial apple production (*Long-term outcome: Strategy 2.1 Enhanced orchard productivity and management*). Through the many channels of communication implemented as part of this project, growers and advisors will have an improved understanding of total nitrogen inputs, accumulation, cycling and loss in commercial apple orcharding (*Short term outcome*) as well as efficient and responsible use of resources (*Medium term outcome*).

Improvements in orchard management

For tree nutrition and water use management, research from each of the three fertigation trials and national soil

characterisation (www.applesoils.com) has led to best practice approaches for good orchard management. Fertigation research focused specifically on nitrogen have accurately determined tree nitrogen requirements (Appendix x) and periods of high N demand. Recommendations have been made to industry on how best to meet that demand without compromising fruit quality (see presentations to the Future Orchard Northern and Southern loop 2020). Given that nitrogen management cannot happen in isolation, we placed this research in the context of variable rate potassium and phosphorus fertigation to achieve a better understanding of a balanced approach to tree nutrition. Research findings showed there was significant flexibility in rates of nutrient supply before an influence on fruit quality outcomes was observed. The interaction of N, P and K application at a range of rates had limited effect on fruit quality, yet some influences in micro-nutrient uptake were observed suggesting that over time, regular monitoring of leaf and fruit nutrition is required to maintain balanced nutrient ratios (Appendix 6). Through regular communication across the variety of platforms adopted, growers and advisors will have an improved understanding of how to match fertiliser management (rates and timing) to meet tree demand and nitrogen requirements (*Short-term outcome*) and the adoption of good management practices (*Medium term outcome*) for tree nutrition.

Five years of sap flow monitoring in mature apple trees (yielding > 70t.ha) revealed how trees respond to the local microclimate. We now know exactly how much water apple trees consume throughout the season, under a wide variety of climatic conditions. Presenting this work to a grower forum in Tasmania, we were requested to place the sap flow equipment in young trees during the first years of development. Accordingly, sap flow equipment was installed in newly planted Jazz trees at Lucaston Park Orchards in southern Tasmania and data was collected for three seasons. This data helped parametrise the SPASMO model that underpins the DST SINATA which has been rolled out to industry. The information outputs from this tool will assist industry to develop sustainable irrigation schedules (*Short-term outcome*), for mature and newly planted orchards, that better match irrigation volumes with plant water demands.

Soil characterisation from 40 sites across five of Australia's most prominent growing regions revealed complex and challenging soil water interactions for growers in addition to some strong nutrient imbalances. A common theme that emerged from the analysis was the low organic carbon content seen throughout the wide variety of soil types represented and the challenge that is to tree water availability particularly in the lower rainfall regions. The Management recommendations for each soil type can be found at www.applesoils.com and presentations were made to growers at the Hort Connections conference (June 2019) and at the APAL Industry update (November 2019) to raise awareness of improved management practices (*Medium term outcome*).

Decision support tool: SINATA

Key to increased profitability and efficient production growing systems (*Medium term outcome*), is the use of decision support tools that are user friendly and assist growers and advisors with strategic management decisions. SINATA was developed to provide growers and advisors with an easy to use Microsoft Excel based tool that can help strategically manage irrigation and nitrogen resources (Appendix 8). The tool would provide a series of outputs suggesting monthly irrigation and nitrogen management strategies based on a set of inputs from the user. To achieve this outcome, the SPASMO model developed by Plant and Food Research New Zealand was parameterized with data collected from this project and the previous project (AP12006) ensuring relevance and reliability to Australian apple growing systems. Fruit and leaf nitrogen data was provided from ^{15}N fertigation trials, fruit quality outcomes and nitrogen management strategy was informed by the Lucaston fertigation trials, tree water use and nitrogen leaching was determined from sap flow and lysimeter data collected over five seasons, soil characterisation from each growing region and BOM climate data was used as an inputs for site selection and finally, crop phenology and yield data was sourced from OrchardNet. Together, this information serves as a repository of valuable research data for the apple industry into the future. The original short term outcome for this project was that growers know how to use the DST and that the outputs are specific to their orchard. Due to Covid-19 we experienced significant delays in the delivery of the DST from Plant and Food Research and we were unable to roll out SINATA face to face to growers and advisors. However, we were able to launch SINATA as part of the Winter series of Northern and Southern Future Orchard loops which enabled far greater reach and a larger audience. In addition, we were able to tailor the presentation to each region and detail how the soil characterisation work and climate data ensures the relevance of the DST to individual grower's sites (Short term Outcome).

Monitoring and evaluation

Effectiveness

We delivered project activities very effectively enabling strong outcomes for industry from the initial conception of the project to the presentation of project outcomes in the 2020 Winter Future Orchard Walk loops. Project activities built on research from AP12006 and findings from each of the sub-projects described above contributed to the success of the development of the SINATA tool. The project was a fully integrated and collaborative effort between TIA and Plant and Food Research New Zealand and benefited strongly from an initial grower workshop and regular discussions with the PIPS Biennial meeting panel.

The strength of project activities and the ability of the project to be delivered effectively comes from the implementation of field trials on commercial orchards. Each component of the fertigation trial sub-project was completed on farm with full involvement and collaboration with the grower and their staff. Initial trial design developed in consultation with the grower and the necessity to implement treatments in the context of standard management practice meant that trials could effectively deliver against the short, medium and long-term outcomes as described above.

One of the most effective components of the project was the characterisation of soils in each of the major growing regions. This required discussing field visits, site variation and soil type differences with individual growers from around the country. This was not only effective at engaging growers with the research, in particular those who don't necessarily read Australian fruit Grower, or attend Future Orchard walks, but also enabled important conversations about how orchard management can influence the long-term sustainability of their orchard. Easy access to detailed information about soils in apple growing regions around Australia enables effective decision making about irrigation requirements and orchard floor management.

Relevance

Nitrogen is often considered a black box in fruit tree crop nutrient management. This is often due to the inability to directly determine the short- and long-term benefits or issues around synthetic fertiliser application. Given that N is relatively cheap compared to the cost of labour and other inputs, there is a general approach to over supply almost a cheap insurance to producing a crop. Yet at the same time there is a legitimate concern that pre-harvest N supply will cause significant colour and maturity problems with fruit at harvest. This research has challenged some of the many myths around N fertigation and provides solutions to growers that are built on a legacy of sound science and long-term research trials. We aimed to increase grower awareness of apple tree nitrogen use and how best to achieve optimum fruit quality outcomes with efficient and well-timed supply. The relevance of the project to growers and advisors was evident from surveys for the mid-term review of the project. Key quotes included:

"This work is hugely relevant for my business. There has not been a lot of work done on this. We never *had much evidence on peak demand periods and where it goes in the tree. The last research of any quality was done in 1958 in peach trees. Most growers have a reasonable feel for it, but there is also a lot of wastage. There are also growers who don't put enough on". Orchardist*

"This research project is very relevant for my work and our business. Sometimes when I provide advice, I do wonder if I should be applying nitrogen. It has been a bit gut feel. It will be so nice to have some proper research behind it. Thresholds will be useful (without affecting fruit quality). I do pride myself on never recommending anything that won't do the job for a grower. This will give me a better evidence base to make these decisions". Orchardist

As such, this project will have important environmental outcomes. More efficient N use will certainly lead to reduced N leaching and reduce green-house gas emissions which is very important for the ever increasing environmentally conscious consumer.

Appropriateness

To ensure appropriateness of project activities, we engaged with industry and other researchers in the development of research trials and the shaping of the DST. We held an initial workshop at Grove Research station with growers and advisors who provided strong direction on the design of project trials and functionality of the DST. Those who attended the workshop continued to provide an informal sounding board throughout the life of the project to ensure that activities would deliver against project outcomes. Soon after the project started CI Swarts participated on the Future Orchards southern loop. Results from AP12006 were presented as well as initial concepts and an overview of this project, AP14023. Discussions with growers and in particular those who managed the Focus Orchards in each region provided significant input which gave confidence to the appropriateness of project design.

Industry engagement with the project at all stages is necessary to ensure that project findings and recommendations are communicated appropriately. Recognizing that this was a shortcoming of PIPS 1, we aimed to increase visibility and reach of the project among industry through regular communication across a variety of platforms. Integrating extension activities with Future Orchards was an important avenue for communicating research outcomes as was interviews for Youtube videos and presentations at speed updating events. Unexpectedly, during the Covid period, additional reach to growers and advisors across industry was made through Zoom presentations for the 2020 Winter series Future Orchard loops.

Efficiency

This project delivered project outcomes highly efficiently demonstrating value for money for levy payers. Most importantly, collaboration between TIA, Plant and Food Research NZ and commercial orchardists led to the establishment of a multidisciplinary team bringing all the necessary skills and experience to deliver project activities. Undertaking trials on commercial orchards both increased effectiveness and relevance of trial designs but importantly enabled cost-effective research to be completed with substantial in-kind support provided by the growers.

Project activities were delivered extremely cost effectively through the way in which personnel and infrastructure were resourced. TIA is a joint venture between the Tasmanian Government and the University with a mandate to support the sustainability of the Tasmanian Horticulture industries. With the close alignment of this mandate with the outcomes of this project, TIA contributed significant in kind staff time providing an extensive skill set to project activities. We leveraged a small portion of funds for this project (approx. $50k), to secure a 3.5 year PhD scholarship for Bi Zheng Tan who worked exclusively on this project delivering outcomes well above those originally anticipated.

TIA had recently invested in equipment for a dedicated Quarantine Soil Physics Laboratory providing capacity to undertake the soil characterisation work that would have otherwise been unable to complete. This infrastructure was provided in kind to the project substantially increasing the cost-effectiveness and capability of the activity. Evidence of this can be seen on the www.applesoils.com website which is now an important resource for industry.

Recommendations

The nitrogen (N) fertigation research undertaken on 'Galaxy Gala' at Lucaston (Tas) over AP12006 and AP14023 revealed the influence of pre- and post-harvest N management on the size and quality of fruit (at harvest and post-harvest) in a commercial apple orchard. Over five years of fertigation treatments, there were negligible differences in fruit quality, yield and tree growth outcomes between lower rate pre-harvest N supply and the higher rate post-harvest application. Yet, comparative N treatments showed that excess N supply pre-harvest can negatively influence fruit quality at harvest and during storage. This is due to substantially more efficient N uptake from pre-harvest N supply compared to post-harvest N supply learned from the ^{15}N uptake and remobilization trials. There is very limited demand for N post-harvest and with photosynthetic capacity of leaves reducing dramatically between March and May, there is limited draw of N into the tree canopy. This challenges the widely held belief that post-harvest N is required to build storage reserves for next season's growth and development. Whilst we certainly found evidence of fertiliser N placed in storage with post-harvest N supply, the efficacy of uptake was so low that the majority of N supplied remained in the soil and would likely be leached with the increased soil moisture from autumn and winter rainfall. In addition, our data clearly shows that not only does pre-harvest N supply, at a reduced rate, meet current season crop N demand, this management approach also ensures that adequate storage reserves are built for next season's requirements. Consequently, we recommend to growers and advisors that small, weekly applications of N commencing approximately four weeks after full bloom up to a maximum rate of 30 – 40 kg N/ha will more than adequately meet the demand of high yielding (> 70t/ha), high density commercially managed apple trees. This will dramatically increase the uptake efficiency of N in commercial apple orcharding reducing the risk of leaching during winter and the emissions of harmful nitrous oxide emissions under conditions amenable to denitrification.

There was limited interaction between the three irrigation rates and N treatments at the rates applied over the five-year experimental period. However, irrigation treatments demonstrated that greater irrigation significantly increased fruit size, but reduced firmness and total soluble solids at harvest. Whilst this information is not necessarily new for growers, it does help confirm the use of irrigation management prior to harvest to build or maintain fruit size to meet market requirements. Sap flow equipment installed at Lucaston and Shepparton (VIC) enabled a complete picture of the seasonal pattern of tree water use from mature (Lucaston) and young/developing apple trees (Lucaston and Shepparton) under varying irrigation treatments. Coupled with detailed weather information collected at each site, measurement of water fluxes enabled the development and calibration of the soil-water component of the Apple tree model SPASMO. Sap flow data revealed that high yielding trees will require upwards of 40L/day depending on local climatic conditions and this information was critical to the parameterization of the DST SINATA.

We highly recommend that growers and advisors make use of the www.applesoils.com website and the SINATA DST. Each apple major growing region across southern Australia (except the Stanthorpe/Applethorpe region) has been characterized with some important and consistent emerging themes among the suggested management approaches to long term sustainable healthy soils. There were clear knowledge gaps identified from this research that have become key components of AP19006, one of four projects that form PIPS 3.

SINATA as a decision support tool will help growers and advisors, who develop irrigation and nutrition management plans for growers, strategically determine their irrigation and N requirements for the season. With ground-truthed regional climate and soil data, coupled with yield and phenology data from OrchardNet, users can be confident of the applicability of the outputs provided by the tool. There are some clear data gaps such as soil moisture monitoring and site/orchard specific climate data which would add increased power to the tool. These gaps will be overcome with the next web-based version of the tool which will offer real time decision support in the context of site-specific climate and sensor datasets.

Refereed scientific publications

Swarts, N and Montagu, K* and Oliver, G and Southam-Rogers, L* and Hardie, M and Corkrey, R and Rogers, G* and Close, D, 2016. "Benchmarking nitrous oxide emissions in deciduous tree cropping systems", *Soil Research*, **54** (5) pp. 500-511. doi:10.1071/SR15326 ISSN 1838-675X (Appendix 1)

Hardie, M and Ridges, J and Swarts, N and Close, D, 2018. "Drip irrigation wetting patterns and nitrate distribution: comparison between electrical resistivity (ERI), dye tracer, and 2D soil-water", *Irrigation Science*, **36** (2) pp. 97-110. doi:10.1007/s00271-017-0567-3 ISSN 0342-7188 (Appendix 2)

Green, S* and Oliver, G and Swarts, N and Hardie, M and Clothier, B* and Close, D, (2018) "Measurement of sap flow in young apple trees using the average gradient heat-pulse method", *Acta Horticulturae 1222: Proceedings of the X International Workshop on Sap Flow*, 22-26 May 2017, Fullerton, USA, pp. 1-6. (Appendix 3)

Morris, M and Swarts, N and Dietz, C and Close, D, 2017. "Uptake efficiency and internal allocation of nitrogen in apple trees", *Acta Horticulturae 1217: VIII International Symposium on Mineral Nutrition of Fruit Crops*, 27-30 June 2017, Bozen-Bolzano, Italy, pp. 53-60. ISSN 0567-7572

Hardie, M., Green, S., Swarts N.D., Measuring and modelling nitrate fluxes in a mature commercial apple orchard (in Prep). Will be submitted to Plant and Soil in November 2020

Tan, B., Close, D.C., Swarts N.D., Interactions of nitrogen, phosphorus and potassium fertilization on 'Gala' apple tree nutrition (in prep). Will be submitted to Scientia Horticulturae in December 2020

Tan, B., Close, D.C., Quin, P., and Swarts N.D., Nitrogen Use and Allocation in Apple Trees: pre-harvest N supply optimizes uptake efficiency (in prep). Paper submitted to Tree Physiology on the 25th November 2020

Intellectual property, commercialisation and confidentiality

No project IP, project outputs, commercialisation or confidentiality issues to report

Acknowledgements

On behalf of the project team, we acknowledge the Apple and Pear Industry Research levy and Hort Innovation for the provision of funding for this project. We also acknowledge UTAS and TIA for the provision of in kind support for staff time and research infrastructure to undertake this work. We are grateful to TIA laboratory staff Justin Direen, Garth Oliver and Caroline Clay for their support and expertise. We express thanks to Phil Andrews, manager of the Horticulture Research Centre for his support in maintaining trees over the last three years. We acknowledge the large number of honours and masters students who made important contributions to project outcomes over the life of the project.

We are incredibly grateful to Andrew and Matthew Griggs from Lucaston Park Orchards, Tim Reid, Mark Salter, Andrew Hall, Nick Owens and Bradley Ashlin from Reid fruits for the provision of commercial orchards in which to conduct our research. We are grateful for their time and experience in discussing trial design and flexibility in making arrangements to accommodate us on farm and for their patience with the many staff and students that worked on farm. Reid Fruits provided 30 mature commercially managed trees for complete destructive harvest free of charge for our nitrogen research.

To the many growers who gave up their time and orchards allowing us to dig large trenches between tree rows for the soil characterisation work, we are very grateful. The quality and depth of this data set was made possible by their generosity and support.

We acknowledge Kristen Stirling from RMCG who provided MER support to this project and ongoing coordination of the PIPS program. We also gratefully acknowledge Ross Wilson and Craig Hornblow from AgFirst who provided extension support through the Future Orchards program.

Appendices

Appendix 1: Swarts et al 2016_N_2O emissions

Appendix 2: Hardie et al 2017_irrigation dye tracing

Appendix 3: Green et al 2017_Sap flow in apple trees

Appendix 4: Hardie et al 2020_ N fluxes (in prep)

Appendix 5: Tan et al 2020_ NPK (in prep)

Appendix 6: Tan et al 2020_15N (in prep)

Appendix 7: Soil Mineralisation

Appendix 8: SINATA summary

CSIRO PUBLISHING
Soil Research, 2016, **54**, 500–511
http://dx.doi.org/10.1071/SR15326

Benchmarking nitrous oxide emissions in deciduous tree cropping systems

Nigel Swarts[A,C], *Kelvin Montagu*[B], *Garth Oliver*[A], *Liam Southam-Rogers*[A], *Marcus Hardie*[A], *Ross Corkrey*[A], *Gordon Rogers*[B], *and Dugald Close*[A]

[A]Tasmanian Institute of Agriculture, University of Tasmania, Sandy Bay Campus, Tas. 7005, Australia.
[B]Applied Horticulture Research, Level 3 Biomedical Building, Australian Technology Park, 1 Central Avenue, Eveleigh, NSW 2015, Australia.
[C]Corresponding author. Email: nigel.swarts@utas.edu.au

Abstract. Nitrous oxide (N_2O) emissions contribute 6% of the global warming effect and are derived from the activity of soil-based microorganisms involved in nitrification and denitrification processes. There is a paucity of greenhouse gas emissions data for Australia's horticulture industry. In this study we investigated N_2O flux from two deciduous fruit tree crops, apples and cherries, in two predominant growing regions in eastern Australia, the Huon Valley in southern Tasmania (Lucaston – apples and Lower Longley – cherries), and high altitude northern New South Wales (Orange – apples and Young – cherries). Estimated from manual chamber measurements over a 12-month period, average daily emissions were very low ranging from 0.78 g N_2O-N ha^{-1} day^{-1} in the apple orchard at Lucaston to 1.86 g N_2O-N ha^{-1} day^{-1} in the cherry orchard in Lower Longley. Daily emissions were up to 50% higher in summer (maximum 5.27 g N_2O-N ha^{-1} day^{-1} at Lower Longley) than winter (maximum 2.47 g N_2O-N ha^{-1} day^{-1} at Young) across the four trial orchards. N_2O emissions were ~40% greater in the inter-row than the tree line for each orchard. Daily flux rates were used as a loss estimate for annual emissions, which ranged from 298 g N_2O-N ha^{-1} $year^{-1}$ at Lucaston to 736 g N_2O-N ha^{-1} $year^{-1}$ at Lower Longley. Emissions were poorly correlated with soil temperature, volumetric water content, water filled porosity, gravimetric water content and matric potential – with inconsistent patterns between sites, within the tree line and inter-row and between seasons. Stepwise linear regression models for the Lucaston site accounted for less than 10% of the variance in N_2O emissions, for which soil temperature was the strongest predictor. N_2O emissions in deciduous tree crops were among the lowest recorded for Australian agriculture, most likely due to low rates of N fertiliser, cool temperate growing conditions and highly efficient drip irrigation systems. We recommend that optimising nutrient use efficiency with improved drainage and a reduction in soil compaction in the inter-row will facilitate further mitigation of N_2O emissions.

Additional keywords: apples, cherries, fertiliser, global warming, greenhouse gas, nitrogen.

Received 4 November 2015, accepted 17 March 2016, published online 12 July 2016

Introduction

Nitrous oxide (N_2O) is a potent greenhouse gas (GHG) with 310 times the global warming potential of carbon dioxide (Ramaswamy *et al*. 2001). Despite comprising only 3.0×10^{-6} % of the earth's atmosphere, N_2O contributes ~6% of the warming effect caused by increased GHG emissions (Dalal *et al*. 2003). While the Australian Greenhouse Office (AGO 2001) estimates that agriculture is the second largest contributor of GHG emissions, agriculture contributes ~78% of all N_2O emissions. Furthermore, N_2O emissions from agricultural activities are expected to increase by 50% in the near future, due to greater fertiliser demand to meet the global food production needs (US EPA 2006).

An estimated two-thirds of global N_2O emissions are derived from the activity of soil-based microorganisms involved in nitrification and denitrification processes (Prather *et al*. 1995; Dalal *et al*. 2003). These processes and thus N_2O emissions are strongly influenced by both environmental factors, such as soil moisture, oxygen availability and soil and air temperature, as well as management practices, specifically fertiliser and irrigation use, but also inter-row weed management, soil compaction and organic matter flux due to pruning and thinning (Davidson 1992; Tiedje 1994).

Uncertainty as to the relative contribution of different agricultural sectors to N_2O emissions is in part due to scarcity of data, which is compounded by considerable variance between studies due to differences in soils, climate, and management practices (Barton *et al*. 2008; Denmead *et al*. 2010).

The horticulture sector of Australia's agriculture industries contributes approximately $8.7 billion to the national economy and is the third largest agricultural industry (Australian Bureau of Statistics 2012). The horticultural sector is diverse and

comprises many different commodities, each requiring its own unique production system including evergreen and deciduous fruit tree production, vegetable production, nuts, table grapes, turf and cut flowers. Consequently determining the N_2O emissions from horticulture is extremely complex. Despite the economic importance of the sector, emissions data for production horticulture are almost non-existent. Within the horticultural sector, apple and cherry production is estimated to occupy 10 600 ha (George 1999) or 37% of the total area for deciduous tree fruit crops. Apples and cherries are produced from higher altitude areas of southern Queensland and central New South Wales (NSW), to inland Victoria, Adelaide hills, Perth hills and south-western Western Australia and southern Tasmania.

Deciduous trees by their nature are highly effective utilisers of nitrogen (N) as they withdraw N from their leaves before leaf senescence into storage organs (roots, trunk and branches) during winter dormancy (Millard 1996). This stored N is remobilised for the current season's growth, which for some crops can contribute up to 50% of the total N requirement for the season (Millard and Neilsen 1989). Deciduous fruit tree crops are strong sinks for N, in which a large portion of N (30–60 kg ha^{-1}) is removed on an annual basis depending on crop load (Neilsen *et al*. 1997). As developing fruit have a strong demand for N over a short growth stage, growers tend to apply high rates of fertiliser to the soil over a short period pre-harvest to meet tree demands and/or post-harvest to facilitate storage of N by trees during winter dormancy. Similarly, deciduous fruit tree crops have a significant water requirement due to high crop water content (up to 85%) and transpiration losses during the summer months. N fertiliser application for mature apple trees broadly ranges from 30 to >200 kg N ha^{-1}, while irrigation requirements range from zero in rainfed areas to 1–5 ML ha^{-1} in cold climates and 5–9 ML ha^{-1} in Mediterranean climates (APAL 2013).

Given the paucity of GHG emissions data for the horticulture sector (Huang *et al*. 2012; Rowlings *et al*. 2013) there is an ongoing need to determine the spatial and temporal variations in N_2O fluxes from typical production systems within the sector. In response this study was established to determine annual N_2O emissions from two deciduous fruit tree crops, apples and cherries, in two predominant growing regions in eastern Australia: the Huon Valley, Tasmania and high altitude northern NSW. Furthermore, we sought to improve our understanding of the influence of environmental factors such as soil temperature, volumetric water content (VWC), water filled porosity (WFP), gravimetric water content (GWC) and matric potential (MP) on N_2O emissions in two deciduous fruit tree production systems. Results are discussed in the context of potential management strategies for mitigating N_2O emissions within the deciduous fruit tree crop industries.

Materials and methods

Trial sites

Tasmania

Two greenhouse gas monitoring sites were established in the Huon Valley, Tasmania, at Lucaston in an apple orchard, and Lower Longley in a cherry orchard. The Huon Valley has a cool temperate climate with an average daily maximum temperature of 21°C in summer and 12°C in winter. Over the study period, Lucaston and Lower Longley received a total of 801 and 806 mm of rainfall respectively (Table 1). Rainfall patterns were similar at both sites with fairly uniform monthly totals, reflected in the low standard errors over the study period, representing a typical Huon Valley rainfall scenario (Fig. 1). Soils used for orchards in the Huon Valley mostly consist of texture contrast Kurosols and Chromosols (Isbell 2002) derived from Quaternary alluvium.

The Lucaston site consisted of 12-year-old 'Royal Gala/Galaxy' trees on M26 rootstocks. Trees were grown in mounded rows running north-west–south-east trained as a central leader and spaced at ~1 m along rows and 4 m between rows. The orchard was irrigated during October–March with inline drippers (2.3 L h^{-1}) at 500-mm spacings along the tree line. Fertiliser was applied by a spreader along the mound shoulders as calcium nitrate at an annual rate of 40 kg N ha^{-1} split into a 15 kg N ha^{-1} pre-harvest (10 October 2013) and 25 kg N ha^{-1} post-harvest (3 April 2014). The Lower Longley site consisted of 12-year-old 'Simone' trees, grown on Colt rootstocks, pruned to a Spanish bush training system with tree spacing of 2 m and row spacing of 4.5 m. Row orientation was north-west–south-east with a considerable slope down from the northern end of the row. The orchard was drip-irrigated as described above and N was fertigated as six split fortnightly 25 kg N ha^{-1} of calcium nitrate and potassium nitrate along the tree line, commencing on 25 October 2013 at an annual rate of 150 kg N ha^{-1}.

Table 1. Site conditions of four orchards

	Site 1 Tas. Lucaston (apples)	Site 2 Tas. Lower Longley (cherries)	Site 3 NSW Orange (apples)	Site 4 NSW Young (cherries)
Location	42.993°S, 147.057°E	42.978°S, 147.141°E	33.296°S, 148.998°E	33.449°E, 148.209°S
Height above sea level (m)	53	330	863	439
Slope	3°	10°	2°	4°
Inter-row sward	Grass	Grass	Grass	Grass
Soil texture class	Sandy loam	Sandy loam	Loam	Sandy Loam
Soil type	Dermosol	Dermosol	Ferrosol	Ferrosol
Average crop yield per annum (t ha^{-1})	75	40	50	23
Annual rainfall (mm)	801	806	913	516
Monthly average (mm ± s.e.)	66.8 ± 9.6	67.5 ± 10.1	60.5 ± 9.3	39 ± 5.7
Ratio tree line : inter-row area per hectare	0.6	0.6	0.67	1.86

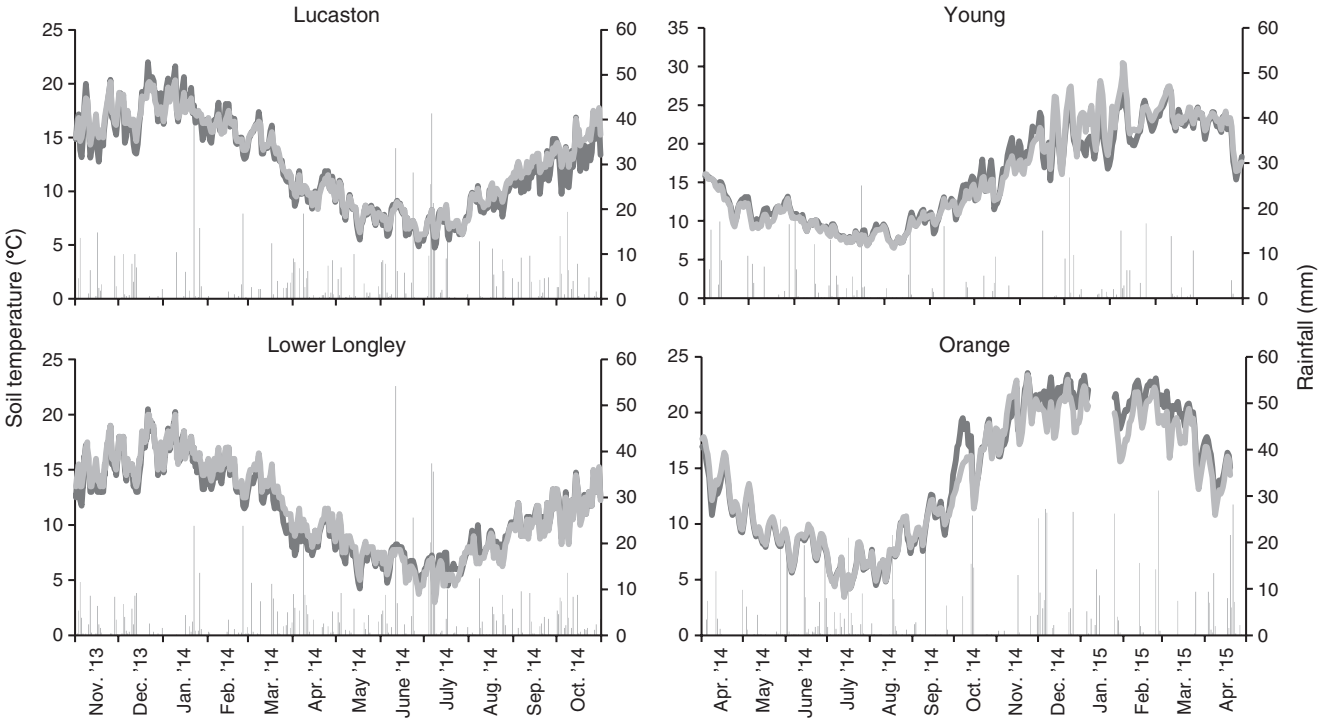

Fig. 1. Daily rainfall and average daily soil temperature from apple and cherry orchards in Tasmania and New South Wales.

NSW

Two greenhouse gas monitoring sites were established in NSW: an apple orchard at Orange and a cherry orchard at Young. The Orange site has a continental climate with a notable difference in mean maximum temperature between summer and winter (25.7°C and 10.6°C respectively). Rainfall in the region is generally uniform across the year, averaging 859 mm. The climate at the Young site is classified as cool temperate with uniform precipitation across the year, averaging 591 mm. The annual maximum mean temperature (1991–2015) is 30.1°C in summer and 13.2°C in winter. Over the study period, the orchards at Orange and Young received total rainfall of 913 and 516 mm respectively with uniform monthly totals reflected in low standard errors between the monthly averages (Table 1).

The Orange site consisted of 8-year-old 'Pink Lady' or 'Sundowner' apple cultivars on M106 rootstocks, planted in double rows (1.5 m), spaced at 2.1 m along rows and 6 m between rows. The orchard was irrigated with under tree drip irrigation from November to May (harvest). The N fertiliser was applied via three fertigation events (1 February 2014, 10 February 2015 and 28 February 2015). At each fertigation, 4.75 kg N ha^{-1} was applied as potassium nitrate and mono ammonium phosphate along the tree line, resulting in annual rate of 14.3 kg N ha^{-1}. The Young site consisted of 10-year-old 'Van' or 'Lapins' cherry cultivars on Mahaleb rootstocks planted in single rows, spaced at 4.65 m apart and 6 m between rows. The orchard was irrigated by under tree micro-sprinklers from October to December (harvest). A total of 58.5 kg N ha^{-1} of N fertiliser was applied during the 2014–15 sample period. This was applied by hand as 21.7 kg N ha^{-1} of ammonium nitrate to the tree row on the 8 August 2014, by fertigation as 9.2 kg N ha^{-1} of urea and calcium nitrate on the 15 October 2014 or as a post-harvest foliar spray at 27.6 kg N ha^{-1} on the 12 April 2015.

At all trial sites, herbicides were used to keep the tree line free of weeds. Pests and diseases were managed by the grower in accordance with commercial practices.

Soil N_2O emissions

N_2O emissions were measured using static non-flow through chambers, comprising a mounting collar and a detachable chamber. At the two Tasmanian field sites, chambers were ~9 L (240 mm diameter × 200 mm in height) with 0.046 m^2 surface area. Chambers were lined with Mylar to reflect UV and fitted with air-stones for passive pressure compensation to minimise the influence of heating from solar insulation. Collars were inserted 100 mm into the soil and remained in place throughout the trial. The collars each had three rows of 3.6-mm holes to allow for root penetration, and projected 50 mm above the soil surface. At Lucaston, eight static chambers were installed in October 2013, four in the tree line and four in the inter-row of the orchard. At Lower Longley, six chambers were installed, three in the tree line and three in the inter-row. At both sites, where chambers were installed in the tree line, 16-mm holes were drilled (then sealed) into the collar sidewall to allow the dripper irrigation line to pass through the collar. Each chamber top was fitted with an iButton (Maxim) temperature sensor that logged air temperature inside the chamber at 5-min intervals. For both sites, N_2O was sampled weekly during the peak growing season (November–April) and once monthly during the winter period (May–August). More frequent (every second day) sampling events coincided with fertiliser

application in November and March and a large rainfall event in July 2014. During collection events, the chamber top was secured to the collar with clips and a rubber O-ring to prevent air movement. The atmosphere in each chamber was sampled sequentially over a one-hour period at 0, 30 and 60 min intervals, starting at ~10 a.m. to represent the average daily temperature. Samples were extracted through a butyl rubber septa located centrally on the chamber top using a 25-mL glass gas-tight syringe (SGE, 25MDR-LL-GT,Melbourne Australia); the sample was then injected into a 12-mL Exetainer (Labco, High Wycombe, Buckinghamshire, UK) to ~2 atm.

At the two NSW field sites, the static non-flow through chambers were slightly smaller than those used in Tasmania (diameter 243 mm, height 205 mm and installed volume of 7.3 L) but otherwise the same. At each of the NSW sites, eight collars were installed in the tree line and eight randomly located in the inter-rows. Sampling was conducted every two weeks, and more frequently during the growing season (October–March). Chamber air samples were collected from the static chambers at 0, 30 and 45 min after lids were sealed using a 25-mL gas-tight syringe (SGE, 25MDR-LL-GT), and introduced into pre-evacuated 12-mL Exetainer (Labco) vials with grey silicon septa. Chamber temperature was measured during sampling using a TP3001 digital thermometer.

Gas analysis

Samples were analysed on an Agilent 7890A gas chromatograph fitted with a Gilson (GX 271) auto sampler. The system had two channels leading to μ-ECD and FID detectors. N_2O was analysed by μ-ECD. The sample was loaded onto a 1000-mL sample loop, and then injected onto a 1-m Porapak Q pre-column. Gases were then passed onto a 2-m Porapak Q column for further separation. The pre-column was back-flushed to remove moisture after the analytes had passed onto the analytical column. Relative standard deviation (based on seven replicate injections) for N_2O was <2%. For each batch of samples, a range of standards, controls and blanks were included for quality control purposes (van Zwieten *et al*. 2010).

Soil properties

At all sites, soil temperature was measured at 10 cm depth every hour using iButtons (DS1920, Maxim, San Jose, USA) temperature logger. In the Tasmanian sites, soil moisture probes (Decagon,10HS, Pullman, USA) were installed at 5–10 cm below the soil surface to record VWC ($cm^3\,cm^{-3}$) at hourly intervals in the inter-row and tree line under the irrigation dripper in two locations at Lucaston and one location at Lower Longley. In the NSW sites, VWC was measured in the tree line at 10, 20, 30 and 50 cm depth using a continuously logging capacitance soil moisture probe (EnviroSCAN, Sentek Sensor Technologies, Stepney, Australia).

In the Tasmanian field sites, soil was sampled along the tree line and inter-row of three experimental rows at three locations in November 2013 and July 2014. Soil samples were taken from 0–10 cm depth adjacent to the drippers in the tree line and next to the installed gas chambers in the inter-row. Samples were collected by 'pogo stick' in which four plugs were collected ~20 cm apart and mixed from which a representative subsample was obtained. Soil subsamples were air-dried, then gently disaggregated in a mortar and pestle and sieved to <2 mm. The NO_3^- content was determined by placing 8 g of dried soil in a 50-mL centrifuge tube which was extracted in 40 mL of 2 M potassium chloride over 18 h. The tubes were centrifuged at 12.6 *g* for 10 min and a 10-mL subsample was filtered through a 0.45-μm syringe filter. The NO_3^- analysis was performed on a Westco Smartchem 200 discrete analyser, following the US EPA Method 353.2 (US EPA 1993).

For all sites, total N (%) and total carbon (C, %) were also determined from a fine-ground sample (Retsch MM200 ball mill, Dusseldorf, Germany) of 20–30 mg using an oxidative combustion analyser (Perkin Elmer CHN-S 2400, Waltham, USA) (Table 2). Soil bulk density of the A1 horizon was determined at all sites using three 60 mm × 61 mm cores following Cresswell and Hamilton (2002). GWC was determined by drying the entire core at 105°C for 24 h. Total porosity (TP) and WFP were calculated from bulk density, assuming a particle density of 2.65 $g\,cm^{-3}$ and 98% saturation (Table 2). At the two Tasmanian sites, infiltration was measured in triplicate using a 20 mm diameter, single ring, constant head, infiltrometer in both the tree line and inter-row areas. The infiltration ring was inserted 3 cm and sealed on the outside with compacted soil slurry, water was maintained at head of 0.5–1.5 cm (variation due to surface elevation) for ~20–40 min to ensure establishment of steady-state conditions. Saturated hydraulic conductivity and sorptivity were estimated (Reynolds and Elrick 1990; Reynolds 2008) in which α (macroscopic capillary length equivalent to the wetting front suction) was estimated to be 0.12 (Table 1). At Lucaston, MP was calculated from the van Genuchten–Mualem equation (Mualem 1976; van Genuchten 1980). The soil water retention and conductivity parameters as input for the equation were determined using the extended HYPROP evaporative flux approach (Peters and Durner 2008). In the Tasmanian sites, a subsample of soil from each chamber location was sent to AgVita Analytical (Devonport, Tasmania) for labile C analysis using the permanganate method based on Weil *et al*. (2003). Potential N mineralisation was performed following the anaerobic incubation method of Curtin and Campbell (2008).

Data analysis

The flux rate, F_{N2O}, was calculated using Eqns 1 and 2 (Scheer *et al*. 2014). All N_2O flux rates were corrected for the actual air temperature during the measurement and recorded as μg N_2O-N $m^2\,h^{-1}$:

$$F_{N_2O} = \frac{b \times V_{CH} \times MW_{N_2O\text{-}N} \times 60 \times 10^6}{A_{CH} \times MV_{corr} \times 10^9} \quad (1)$$

where A_{CH} is basal area of the measuring chamber (m^2), *b* is increase in concentration (ppb min^{-1}), $MW_{N_2}O$-N is molecular weight of N_2O-N (28 $g\,mol^{-1}$), MV_{corr} is temperature-corrected molecular volume ($m^3\,mol^{-1}$) and V_{CH} is volume of the measuring chamber (m^3)

$$MV_{corr} = 0.02241 \times \left(\frac{273.15 + T}{273.15}\right) \quad (2)$$

where MV_{corr} is defined above, *T* is air temperature during the measurement (°C) and 0.02241 m^3 is the molar volume

Table 2. Soil physical characteristics from the four trial orchards
–, Denotes missing data

		Lucaston (apples)	Lower Longley (cherries)	Orange (apples)	Young (cherries)
Bulk density ($g\,cm^{-3}$)	Tree line	1.21	1.03	1.42	1.48
	Inter-row	1.32	1.18	1.53	1.49
Field infiltration rate ($cm\,h^{-1}$)	Tree line	13.77	11.66	–	–
	Inter-row	0.49	1.19	–	–
pH	Tree line	6.27	6.4	6.7	4.6
	Inter-row	6.37	6.5	6.6	5.8
Total N (%)	Tree line	0.26	0.23	0.14	0.11
	Inter-row	0.17	0.28	0.13	0.13
Nitrate ($mg\,kg^{-1}$)	Tree line	5.44	4.3	6.9	6.5
	Inter-row	2.53	3.1	5.7	5.7
Total organic C (%)	Tree line	4.31	3.31	1.6	1.3
	Inter-row	2.33	4.14	1.4	1.6
C : N ratio, soil	Tree line	16.6	14.4	11.3	12.1
	Inter-row	13.7	14.8	11	11.8
Labile C (ppm)	Tree line	400	345	–	–
	Inter-row	442	394	–	–
Mineralisation rate ($\mu g\,N\,g\,soil^{-1}\,day^{-1}$)	Tree line	0.76	–	–	–
	Inter-row	3.45	–	–	–

of an ideal gas at 1 atm and 273.15K (Aylward and Findlay 1974).

A linear regression (r) was computed using the Pearson's correlation coefficient to determine the quality of the slope relationship and flux rates were discarded if $r < 0.8$. Daily N_2O fluxes from each site were calculated by averaging hourly flux from each replicate and multiplying the data by 24. Cumulative seasonal fluxes for each site were calculated by integrating daily N_2O fluxes via linear interpolation over the study period.

Associations among N_2O emissions and soil environmental variables (soil temperature, VWC, WFP, GWC and MP) were assessed using Pearson's correlation in SPSS Version 22. Correlations were performed for each site, sampling location within site (tree line and inter-row) and for each season using the combined dataset from all sites. A multiple linear regression using a stepwise approach was used to develop a model to predict N_2O emissions from soil environmental variables using SPSS. This was undertaken in SPSS using the dataset from Lucaston, as this was the only site where data from all soil environmental variables were complete over the study period.

Auxiliary measurements

Emission factors were calculated uncorrected for background emission over the 12 months and expressed as the percentage of the total fertiliser N applied that was emitted as N_2O-N. The emissions intensity of each treatment was calculated as the ratio of N_2O emissions in relation to crop yield and relates to how much N_2O was emitted per tonne of fruit harvested. Direct N_2O emissions were converted to carbon dioxide equivalents (CO_2eq) within a 100-year horizon by multiplying by a radiative forcing potential equivalent to CO_2 of 310 (IPCC 2001). Yield-scaled emissions for this perennial system ($CO_2eq\,Mg^{-1}$) were calculated by dividing annual N_2O emissions ($CO_2eq\,ha^{-1}\,year^{-1}$) for the annual production cycle by total apple or cherry yield ($Mg\,ha^{-1}$). In each orchard, fruit yield was measured at harvest using Millennium Mechatronics pallet scales or by harvesting a random sample of whole trees and multiplying yield by orchard tree number.

Results

Site conditions

Average daily soil temperature ranged from 4°C in winter to 21°C in summer in the Tasmanian orchards and 5 to 26°C in the NSW orchards (Fig. 1). In Tasmania, daily soil temperature was consistently >13°C from early November to mid-April; whereas in NSW, daily soil temperature was >13°C between late September to mid-April (Fig. 1).

At Lucaston and Lower Longley, a substantially higher infiltration rate was observed in the tree line (13.77 and $11.66\,cm\,h^{-1}$ respectively) than the inter-row (0.49 and $1.19\,cm\,h^{-1}$ respectively) most likely due to mounding of the sandy loam topsoil at both sites for drainage purposes (Table 2). This was also reflected in an increased bulk density of the inter-row (1.32 and $1.18\,g\,cm^{-3}$ respectively) at both sites compared with the tree line (1.21 and $1.03\,g\,cm^{-3}$ respectively). Consequently, WFP was consistently higher along the inter-row than the tree line but never exceeded 80% or dropped below 40% over the study period (data not shown). Due to logger failure, only 60 days of soil moisture data was recorded at Lower Longley, where a similar trend was found for the period recorded. At Orange, bulk density of the inter-row was $1.53\,g\,cm^{-3}$ and was higher than the tree line ($1.42\,g\,cm^{-3}$);

however, at Young, bulk density of the inter-row (1.49 g cm^{-3}) was almost identical to the tree line (1.48 g cm^{-3}). Considerable variation in WFP was measured at the wetter Orange site, ranging from 15% in summer to 85% during winter. At Young, WFP ranged from 15% in summer to 65% in winter (data not shown).

Soil NO_3^- levels measured in November 2014 at Lucaston and Lower Longley were higher along the tree line (5.44 and 4.3 mg kg^{-1} respectively) than in the inter-row (2.53 and 4.14 mg kg^{-1} respectively). There was a similar trend for row and inter-row NO_3^{-1} levels at Orange (6.9 and 5.7 mg kg^{-1} respectively) and Young (6.5 and 5.7 mg kg^{-1} respectively) (Table 1). Total N (%), total organic C (%) and the C : N ratio were substantially higher in the Tasmanian than the NSW orchards. At Lucaston and Lower Longley respectively, labile C was substantially higher in the inter-row (442.3 and 394.3 ppm) than the tree line (400 and 344.7 ppm).

Temporal and spatial variability of N_2O emissions

Mean daily N_2O emissions over the 12-month period were very low, ranging from 0.78 g N_2O-N ha^{-1} day^{-1} in the apple orchard at Lucaston to 1.86 g N_2O-N ha^{-1} day^{-1} at the cherry orchard in Lower Longley. Mean daily N_2O emissions from the tree line were low (<1.31 g N_2O-N ha^{-1} day^{-1}) but similar across all orchards (Table 3). Mean daily emissions from the inter-row were consistently higher for each orchard but did not exceed 2.44 g N_2O-N ha^{-1} day^{-1}. The highest daily flux recorded (irrespective of sampling location) was 13.86 g N_2O-N ha^{-1} day^{-1} in the cherry orchard at Lower Longley, whereas the lowest daily flux of 0.09 g N_2O-N ha^{-1} day^{-1} was in the apple orchard at Lucaston. Mean daily emissions within seasons followed a similar trend of higher inter-row emissions than the tree line with few exceptions (Fig. 2). N_2O emissions were almost double in summer compared with other seasons for all orchards, with the exception of the cherry orchard at Young. Greatest variation in N_2O emissions within orchards was also observed in summer with daily inter-row fluxes twice that of the tree line at each site. N_2O emissions during winter (<0.9 g N_2O-N ha^{-1} day^{-1}) were consistently the lowest recorded for the Tasmanian orchards. In NSW, N_2O emissions were lowest (<0.91 g N_2O-N ha^{-1} day^{-1}) during autumn for Orange and summer for Young.

Cumulative emissions reached 890 g N_2O-N ha^{-1} $year^{-1}$ in the inter-row at Lower Longley but were as low as 230 g N_2O-N ha^{-1} $year^{-1}$ in the tree line at Lucaston (Table 3). The substantial spatial variation in daily N_2O fluxes within the tree line and inter-row static chamber replicates were reflected in the high standard errors. When added and corrected for the actual area within the orchard that the tree line and inter-row occupied, maximum cumulative emissions (736 g N_2O-N ha^{-1} $year^{-1}$) were recorded at Lower Longley with the least (298 g N_2O-N ha^{-1} $year^{-1}$) for Lucaston (Fig. 3).

Associations between daily N_2O fluxes and soil environmental variables for each orchard, sampling location and season are described in Table 4. Soil temperature showed a weak positive but significant correlation with N_2O emissions for all sites, with the exception of a negative correlation for Young ($r = -0.157$). Overall, N_2O emissions were negatively correlated with summer soil temperatures ($r = -0.211$). Indeed, at all sites, daily N_2O fluxes >5 g N_2O-N ha^{-1} day^{-1} were only observed for soil temperature >13°C. There were relatively weak, contrasting associations between soil temperature and N_2O emissions between the tree line and inter-row for all sites

Table 3. Mean for each season, minimum and maximum mean daily N_2O emissions (g N_2O-N ha^{-1} day^{-1}) and estimated cumulative yearly N_2O emissions (g N_2O-N ha^{-1} $year^{-1}$) from the manual chambers installed in apple and cherry orchards

Errors represent s.e.

		Lucaston (apples)	Lower Longley (cherries)	Orange (apples)	Young (cherries)
Mean		0.78 ± 0.30	1.86 ± 0.69	1.68 ± 0.24	1.55 ± 0.43
	Tree line	0.63 ± 0.09	1.31 ± 0.46	1.26 ± 0.21	1.23 ± 0.32
	Inter-row	0.93 ± 0.51	2.44 ± 0.93	2.10 ± 0.26	1.88 ± 0.54
Minimum	Tree line	0.14	0.41	0.52	0.2
	Inter-row	0.09	0.15	0.32	0.25
Maximum	Tree line	3.8	5.19	3.53	6.02
	Inter-row	5.53	13.86	5.72	5.33
Winter	Tree line	0.23 ± 0.04	0.76 ± 0.23	1.3 ± 0.19	1.45 ± 0.25
	Inter-row	0.17 ± 0.07	0.86 ± 0.32	1.22 ± 0.12	2.47 ± 0.4
Spring	Tree line	1.11 ± 0.04	1.08 ± 0.31	1.3 ± 0.13	1.29 ± 0.16
	Inter-row	1.08 ± 0.57	1.04 ± 0.26	2.91 ± 0.13	0.91 ± 0.13
Summer	Tree line	0.74 ± 0.13	2 ± 0.6	1.63 ± 0.35	0.56 ± 0.06
	Inter-row	2.02 ± 1.27	5.27 ± 2.12	3.43 ± 0.53	1.23 ± 0.23
Autumn	Tree line	0.44 ± 0.16	1.41 ± 0.71	0.79 ± 0.16	1.6 ± 0.83
	Inter-row	0.44 ± 0.14	2.59 ± 1.03	0.84 ± 0.27	2.91 ± 1.4
Cumulative	Tree line	230 ± 34	479 ± 169	468 ± 38	438 ± 22
	Inter-row	339 ± 187	891 ± 340	656 ± 102	619 ± 56

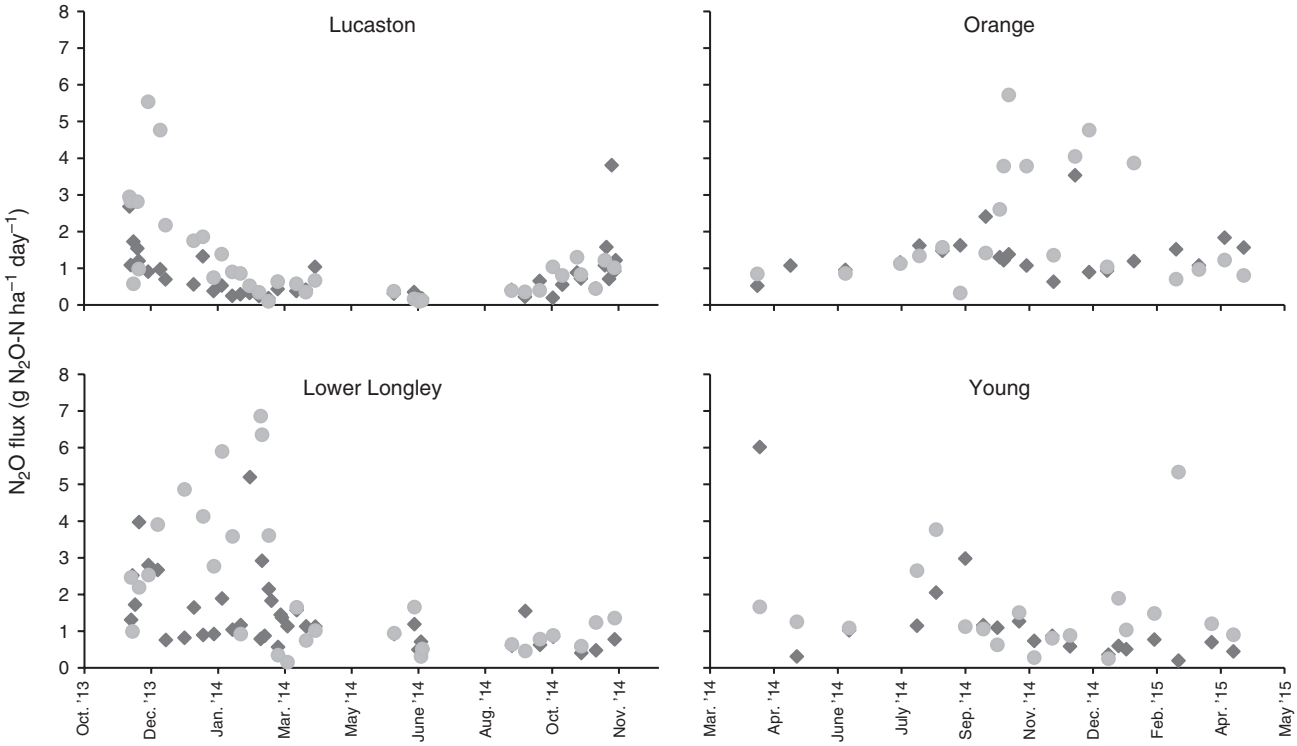

Fig. 2. Average daily N_2O (g N_2O ha^{-1} day^{-1}) emissions from apple and cherry orchards in Tasmania and New South Wales.

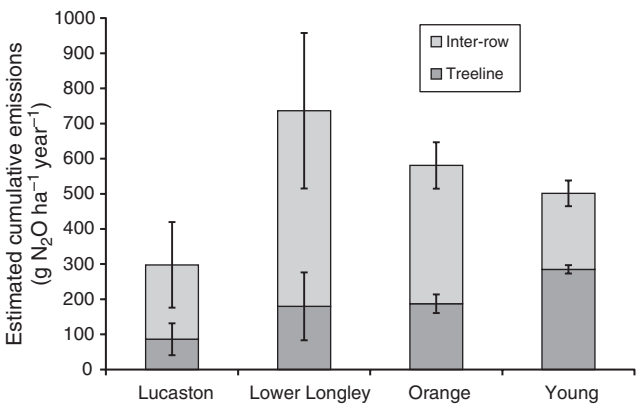

Fig. 3. Cumulative N_2O (g N_2O ha^{-1} $year^{-1}$) emissions from apple and cherry orchards in Tasmania and New South Wales.

with the exception of Lower Longley. N_2O emissions decreased as VWC and WFP increased at all sites, except Young in the tree line with an opposite effect ($r = 0.372$). The strongest association between N_2O emissions and WFP was during winter ($r = –0.506$), which matched the trends found within sites. N_2O emissions were consistently associated with decreasing GWC at all sites and within the tree line and inter-row. The strongest association was again in winter ($r = –0.743$), largely driven by data for Young. A very weak positive yet significant association between N_2O emissions and MP was found in the Lucaston tree line ($r = 0.159$).

The model produced from the stepwise regression analysis (Table 5), accounted for only 9% of the variability in the measured data driven by soil temperature (partial $r^2 = 0.072$) and WFP (partial $r^2 = 0.021$). Splitting the data into sampling location within the orchard improved the predictive capacity of the regression model to 24.5% for the tree line but reduced it to 3.7% for the inter-row, driven largely by soil temperature.

Discussion

Temporal and spatial variability of N_2O emissions

Average daily N_2O emissions averaged across the four orchards representing a temperate deciduous tree cropping system was 1.47 g N_2O-N ha^{-1} day^{-1}. Considerable variability in N_2O emissions was found between sites, within orchards and treatment replicates and between seasons, reflected in the high standard errors of the means (Table 3). The magnitude of the maximum daily values more closely followed N_2O emissions from Australian rainforests (Rowlings *et al*. 2012) than perennial tree crops receiving N fertiliser and irrigation (Pang *et al*. 2009; Rowlings *et al*. 2013; Xia *et al*. 2014; Ge *et al*. 2015). Pang *et al*. (2009) reported an average of 9.35 g N_2O-N ha^{-1} day^{-1} and Ge *et al*. (2015) reported an average of a much higher 36 g N_2O-N ha^{-1} day^{-1} for apple orchards in China – both were orders of magnitude above the average reported here. In another study of horticulture crops from sub-tropical soils, Huang *et al*. (2012) reported average daily N_2O emissions of 4.6, 5.9 and 3.3 g N_2O-N ha^{-1} day^{-1} for mango, custard apple and pineapple respectively.

Table 4. Associations between daily soil environmental conditions: soil temperature, volumetric water content (VWC), water filled porosity (WFP), gravimetric water content (GWC) and matric potential (MP), with N_2O emission rates measured using manual chambers from apple and cherry orchard soils over a 12-month period

Significance ($P < 0.05$ and $P < 0.01$) estimates are indicated by * and ** respectively; –, denotes missing data

	Soil temperature	VWC	WFP	GWC	MP
Site					
Lucaston	0.103*	–0.169**	–0.159**	–0.169**	0.03
Tree line	0.260**	–0.250**	–0.210**	–0.207**	–0.159*
Inter-row	0.11	–0.11	–0.11	–0.13	–0.02
Lower Longley	0.294**	–0.378*	–0.385*	–00.32	–
Tree line	0.229*	–0.39	0.20	–0.39	–
Inter-row	0.354**	–0.36	–0.42	–0.36	–
Orange	0.162*	–0.08	–0.01	–0.05	–
Tree line	–0.05	–0.07	–0.01	–0.27	–
Inter-row	0.249*	0.01	–	–0.26	–
Young	–0.157*	0.354**	0.362**	–0.55	–
Tree line	–0.348**	0.372**	0.362**	–0.83	–
Inter-row	–0.03	–0.83	–	–0.84	–
Season					
Autumn	0.03	–0.02	0.09	–0.02	0.15
Winter	–0.17	–0.506**	0.05	–0.743**	0.20
Spring	0.09	–0.02	0.07	–0.173*	0.14
Summer	–0.211**	0.07	0.06	0.01	–0.10

Table 5. Multiple regression analysis using a stepwise approach of the soil environmental variables on N_2O ($g\ N_2O\ ha^{-1}\ day^{-1}$) emissions from four deciduous fruit tree crop orchards

WFP, water-filled porosity; VWC, volumetric water content

	Parameter estimate	Standard error	*F*-value	*P*-value	Partial r^2	r^2
Lucaston ($n = 334$)						
Intercept	–0.408	0.169	17.042	0.016		0.093
Soil temperature	0.022	0.005		0.000	0.072	
WFP	–0.548	0.233		0.019	0.021	
Tree line ($n = 190$)						
Intercept	0.587	0.266	20.173	0.029		0.245
VWC	–1.862	0.910		0.042	0.102	
Soil temperature	0.020	0.005		0.000	0.091	
WFP	–1.048	0.495		0.035	0.052	
Inter-row ($n = 144$)						
Intercept	–0.714	0.173	5.419	0.000		0.037
Soil temperature	0.021	0.009		0.021	0.037	

The maximum daily flux from any of the four sites was 13.9 g N_2O-N ha^{-1} day^{-1}, which occurred in the inter-row where no N fertiliser or irrigation was applied. For all sites the maximum daily flux of the tree line, where N fertiliser and irrigation was applied, was in the range of 3.8–6.0 g N_2O-N ha^{-1} day^{-1} (Table 3).The absence of large N_2O emission pulses in this study is not considered to be an artefact of the sampling systems. While it is possible that static chamber sampling can miss pulse events, the frequency of sampling and reactive sampling around specific events (such as increased sampling in the spring and summer months following fertiliser application) in this study should have captured pulse events if they occurred. Furthermore, under the same sampling conditions, N_2O pulses exceeding 20 g N_2O-N ha^{-1} day^{-1} were observed in a companion study (N. Swarts unpubl. data) related to high fertiliser applications carried out by our research team. Therefore, we consider that the reported values for N_2O emissions from the four orchards of this study accurately reflected the processes occurring in this land-use.

The estimated annual soil N_2O emissions from four commercial perennial tree crop orchards in temperate south-east Australia varied within 0.30–0.74 kg N_2O-N ha^{-1} $year^{-1}$ (Fig. 3). These values represent very low annual N_2O emissions compared with other cropping systems (Scheer *et al*. 2012, 2013; Shi *et al*. 2013; De Antoni Migliorati *et al*. 2014). In contrast, N_2O emissions from apple orchards were reported as 3.22–44.30 kg N_2O-N ha^{-1} $year^{-1}$ in China (Pang *et al*. 2009; Xia *et al*. 2014). Furthermore, the results from this study are at the low end reported for grapes (0.56–3.92 kg N_2O-N ha^{-1} $year^{-1}$; Garland *et al*. 2014), and similar to those reported for almonds (0.53–0.80 kg N_2O-N ha^{-1} $year^{-1}$; Schellenberg *et al*. 2012).

Given the limitations of integrated scaling from manual chamber sampling (Smith and Dobbie 2001) as recognised above, this study suggests that Australian tree orchard systems are making relatively minor contributions to overall GHG emissions of the country; however, testing over multiple seasons and in a variety of orchard systems is required to further validate this finding. We propose that the low emissions found in this study were due to judicious management of irrigation and N fertiliser application through tree line drippers with regimes well suited to the local soils and tree uptake requirements.

The four commercial orchards, on which this study focussed, used frequent low-intensity irrigation via under tree drip or micro-sprinkler systems with fertiliser applied as multiple split applications. In this study, the VWC of the soil rarely exceeded field capacity as determined by the van Genuchten retention function at $\Psi = -10$ kPa, suggesting that the upper soil layers in the tree line would have remained aerobic for all but very short periods. Thus the irrigation management used across the four sites, which was based on objective soil water measures, would have minimised anaerobic soil conditions. This reduces the likelihood of denitrification being a major pathway for N_2O emissions (Russow *et al*. 2000; Rashti *et al*. 2015). Instead, it is likely that nitrification is the main pathway for N_2O emissions as oxygen availability is generally not limiting for the soil microorganisms when WFP is below 60–70% (Bollmann and Conrad 1998). This has additional significance in this study as 50–100% of the applied N was as NO_3^- (Table 1) and was not susceptible to loss via the nitrification pathway.

Across the four sites in this study, the rate of N fertiliser application was not a strong determinant of annual N_2O emissions. For example, the NSW apple orchard received only 10% of the N fertiliser (15 kg N ha^{-1}) applied to the Tasmania cherry orchard (150 kg N ha^{-1}) but the N_2O emissions (552 g N_2O-N ha^{-1} $year^{-1}$) were 75% of those from the Tasmania cherry orchard (736 g N_2O-N ha^{-1} $year^{-1}$). The use

of multiple split N-fertiliser applications would have more closely matched the N requirement of the trees during the growing season (Tagliavini *et al*. 1996). The lack of correlation between the rate of N fertiliser application and the magnitude of subsequent N_2O emissions in perennial crops was highlighted by Rowlings *et al*. (2013). The rate of N fertiliser clearly increases the risk of N_2O emissions, but the actual emissions are more closely associated with soil environmental conditions than the quantity of fertiliser.

N_2O emissions are biologically driven (Dalal *et al*. 2003) and it was expected that relatively low soil temperatures (<14°C for half the year) experienced at all four sites (i.e. temperate climate) and consistently distributed rainfall between seasons were likely to have played an important role in reducing N_2O production. Soil temperature, well known to be a major determinant of emissions timing and intensity and consequently, was significantly (although weakly) associated with N_2O emissions over the study period. Increased emissions were observed as expected, when soil temperatures were higher in three sites, with the exception of Young. At these three sites, the cherry crop at Lower Longley and the apple crops at Orange and Lucaston were not harvested until mid-February and late March respectively. This required considerable irrigation inputs that maintained relatively moist conditions in the orchard. In contrast, the cherry orchard at Young was harvested in late November and irrigation ceased completely at this time to conserve the limited water resource in the region. Although soil temperatures were the highest in Young in summer, soil moisture (VWC) was lowest, substantially limiting capacity for N_2O production.

Spatial variation in N_2O emissions is attributed to soil aeration as governed by gas diffusion (van der Weerden *et al*. 2012). This parameter is difficult to measure and so WFP is used as a proxy in field studies investigating N_2O emissions (Pang *et al*. 2009; Rowlings *et al*. 2012); however, gas diffusion in soils depends on the relative volumetric fractions of water and air. Furthermore, volumes of air and water in soil at given values of WFP will be influenced by the bulk density of the soil (Castellano *et al*. 2010). As such, Farquharson and Baldock (2008) proposed that VWC is more appropriate for estimating the spatial and temporal variability of N_2O emissions for different soils, and further supported by van der Weerden *et al*. (2012). In our study, relationships between VWC and WFP and N_2O emissions were consistently weak but almost identical for each site, sampling location and season with the exception of winter, when VWC was more strongly correlated. This was not surprising, as the TP and bulk density used to calculate WFPS from VWC were similar between the tree line and inter-row for each site. VWC and WFP for the Lower Longley, Lucaston and the inter-row at Young showed an atypical significant negative (weak) influence on N_2O emissions. Elevated emissions are linked to WFP > 60% (Chantigny *et al*. 1998; Helgason *et al*. 2005) and VWC > 0.55 $cm^3\ cm^{-3}$ (van der Weerden *et al*. 2012), conditions rarely seen in the orchards during the study period. For these sites, during winter when WFP and VWC were highest, soil temperatures were extremely low and accounted for the negative correlation observed and the moderately negative correlation between VWC and N_2O emissions in winter ($r = -0.506$). In stark contrast to this was the moderate positive correlation of VWC ($r = 0.372$) and WFP ($r = 0.362$) with N_2O emissions in the tree line at Young, most likely due to the early application of fertiliser and generally warmer soil temperatures of the site during the winter–spring periods.

Low N_2O emission rates were observed between late autumn through to early spring irrespective of the WFP and VWC (Table 4.). We attribute these emissions to the low soil temperatures which were in the range (on average) of 13 – 18°C over the four sites during the study period. Across the four sites, N_2O emissions classified as moderate (10–100 g N_2O-N ha^{-1} day^{-1}) from European cool temperate soils (Conen *et al*. 2000) or 16–160 g N_2O-N ha^{-1} day^{-1} from Australian tropical soils (Wang and Dalal 2010) were only observed for soil temperatures >14°C. However, as observed with other studies, single parameter correlations of soil environmental variables, while significant, only explained a small amount of the variation in N_2O emissions due to the preconditions required before N_2O emissions were observed (e.g. Ding *et al*. 2007; Schellenberg *et al*. 2012). Indeed, in this study, no consistent pattern emerged in the relationship between daily N_2O flux and soil temperature and soil water measurements either in the tree line or inter-row, between seasons or sites. This may be due in part to the overall very low emissions captured during the course of the study period, the high spatial and temporal variability within the dataset and that there were multiple interacting factors in this complex biogeochemical process. The stepwise regression analysis captured <10% of the total variability of the Lucaston dataset. Splitting the analysis between the tree line and inter-row improved the predictive capacity up to 24% for the tree line but reduced it to <4% for the inter-row. Soil temperature was a significant key predictor in all three models; however, partial coefficients were still very weak with $r^2 < 0.072$. The VWC was the best predictor in the tree line regression model, most likely due to the influence of irrigation via dripper lines over the apple growing season.

Tree line v. inter-row emissions

The 40% greater average N_2O emissions from the grassed inter-row at all sites, compared with the tree line were unexpected (Fig. 2, Table 2). In all orchards in this study, N fertiliser and irrigation were applied only to the tree line. As a result, the higher substrate availability and soil moisture would have been expected to be more conducive to N_2O emissions from the tree line. This should have been most pronounced in the cherry orchard where the equivalent of 150 kg N ha^{-1} was applied on the tree line along with irrigation, while no fertiliser or irrigation was applied to the inter-row. Despite this, average N_2O emission in the inter-row was almost double that of the tree line at this site (2.44 and 1.31 g N_2O-N ha^{-1} day^{-1} respectively).

Large N_2O emissions from the inter-row were observed in a vineyard with a legume cover crop but not when the inter-row was bare fallowed (Garland *et al*. 2014). Increased N_2O emissions are often observed due to the addition of C and N from plants, which stimulates nitrification and denitrification (Bouwman *et al*. 2002). Consequently, it is speculated that the grass sward in the orchard inter-rows would have increased the input of C into the soil and so stimulated greater microbial activity, particularly in the top 10 cm where the bulk of the grass

root mass exists. This is consistent with the inter-rows having higher labile C in the Tasmanian orchards and rates of N mineralisation at the Lucaston orchard (Table 2). At the Tasmanian sites, the orchards were heavily mounded (up to 40 cm) by scraping the sandy loam topsoil from the inter-row into the mound, to facilitate drainage and soil volume in the tree line, while leaving a very shallow, bleached, low-C A2 horizon above a deep clay subsoil within the inter-row. These soils had little macroporosity, which with compaction by tractor traffic means that they had little capacity to drain or store soil water, as demonstrated by the 10-fold reduction in infiltration compared with topsoils in the tree line. Consequently, during rainfall or irrigation soils in the inter-row rapidly approached field capacity compared with the more porous high C soils in the tree line.

Implications for management

Overall, the contribution of the apple and cherry orchards of the current study to global warming potential associated with N_2O emissions was very low on an area basis. When expressed on a yield basis, the emissions intensity was in the range of 1.6–3.2 and 4.6–6.4 kg CO_2eq Mg^{-1} for apples and cherries respectively. By comparison the N_2O derived emissions intensity of the major grain crops of wheat and maize were reported at 166 and 185 kg CO_2eq Mg^{-1} respectively (Linquist *et al*. 2012), or 80.8 CO_2eq Mg^{-1} for almond kernel (Schellenberg *et al*. 2012). The order of magnitude lower values estimated for apples and cherries were maintained even when the values were expressed on a dry matter basis, principally due to the low annual emissions from the orchard crops in this study. On a dry weight yield basis, the emissions intensity was in the range of 11.6–46.8 and 22.7–66.6 kg CO_2eq Mg^{-1} for apples and cherries respectively. The benefits of yield-scaling to produce emissions intensity is that it takes into account both the need for food production and environmental impacts, in this case contribution to global warming. Clearly, comparing fresh fruit to grains and other more dried products is complicated by the differing moisture contents. At present, there is no overarching system to allow different food products to be compared. However, the use of emissions intensity will be useful for comparing across differing production systems for the same food product. As an example, the Cool Farm Tool (Hillier *et al*. 2011) is used across the processing tomato industry globally to consider the global warming potentials of differing production systems. Extension of this approach more widely in the fresh food sector is still in its infancy but should be encouraged, as exclusive use of area-based impacts can lead to low-yielding management practices in the pursuit of reducing environmental impacts.

Based on the findings of this study, perennial cropping systems such deciduous fruit tree cropping have substantially lower N_2O emissions compared with other agricultural systems. It is highly likely that N_2O emissions would be lower in these systems generally given the length of time soil temperatures are <13°C, as these crops require winter chill to break dormancy in spring (Greer *et al*. 2006). However, given that fertiliser application in deciduous tree cropping systems is generally post-harvest during the warmer summer–autumn months when soil temperatures are at their highest, potential remains to mitigate emissions through increased fertiliser use efficiency. Although not tested here, optimising N fertiliser inputs to meet tree demand will facilitate a reduction in both emissions production and N leaching below the root zone, as more N is utilised by the trees. Further research to test emissions production under optimised fertiliser regimes will enable better determination of mitigation strategies based on fertiliser management.

Improved management of the inter-row areas, where consistently higher N_2O emissions were recorded, is possible – for example, bare fallow, but this will require consideration of the trade-off against potential increases in erosion and loss of soil C associated with bare fallow. Additionally, investigating the effect of growing cover crops, composting and side throwing of mower clippings and prunings to the tree line to increase soil C on N_2O emissions is necessary. Improved drainage in areas of the orchard prone to waterlogging is likely to mitigate N_2O emissions as well as using standard width machinery to minimise compacted areas of the inter-row.

Acknowledgements

The authors would like to thank the owners of the orchards for their considerable assistance during the monitoring. Andrew Griggs of Lucaston Park Orchards at Lucaston, Ross Affleck from Ridgy Didge Cherries at Lower Longley, Peter Darley from Day Dawn Orchard at Young and Geoff Hall from Geoff Hall Orchard in Orange. The project was funded under the Carbon Farming Futures program of the Federal Department of Agriculture, Fisheries and Forestry. Funding was also provided by Horticulture Innovation Australia Limited with co-investment from the Tasmanian Institute of Agriculture, Applied Horticulture Research and funds from the Australian Government. We acknowledge the two anonymous reviewers for their helpful comments on the earlier version of this manuscript.

References

Apple & Pear Australia Ltd (APAL) (2013) Guidelines for irrigation management for apple & pear growers. Available at http://apal.org.au/wp-content/uploads/2013/04/Apple_pear_guidelines_Irrigation_Management.pdf [verified 25 October 2015]

Australian Bureau of Statistics (2012) Agriculture production. Available at http://www.abs.gov.au/ausstats/abs@.nsf/Lookup/by%20Subject/1301.0~2012~Main%20Features~Agricultural%20production~260 [verified 29 October 2015].

Australian Greenhouse Office (AGO) (2001) 'National greenhouse gas inventory 1999 with methodology supplements.' (AGO: Australia)

Aylward GH, Findlay TJV (1974) 'SI chemical data.' 2nd edn. (John Wiley and Sons: New York, NY)

Barton L, Kiese R, Gatter D, Butterbach-Bahl K, Buck R, Hinz C, Murphy DV (2008) Nitrous oxide emissions from a cropped soil in a semi-arid climate. *Global Change Biology* **14**, 177–192.

Bollmann A, Conrad R (1998) Influence of O_2 availability on NO and N_2O release by nitrification and denitrification in soils. *Global Change Biology* **4**, 387–396. doi:10.1046/j.1365-2486.1998.00161.x

Bouwman AF, Boumans LJM, Batjes NH (2002) Emissions of N_2O and NO from fertilized fields: Summary of available measurement data. *Global Biogeochemical Cycles* **16**, 1058. doi:10.1029/2001GB001811

Castellano MJ, Schmidt JP, Kaye JP, Walker C, Graham CB, Lin H, Dell CJ (2010) Hydrological and biogeochemical controls on the timing and magnitude of nitrous oxide flux across an agricultural landscape. *Global Change Biology* **16**, 2711–2720. doi:10.1111/j.1365-2486.2009.02116.x

Chantigny MH, Prevost D, Angers DA, Simard RR, Chalifour FP (1998) Nitrous oxide production in soils cropped to corn with varying N

fertilization. *Canadian Journal of Soil Science* **78**, 589–596. doi:10.4141/S98-009

Conen F, Dobbie K, Smith K (2000) Predicting N_2O emissions from agricultural land through related soil parameters. *Global Change Biology* **6**, 417–426. doi:10.1046/j.1365-2486.2000.00319.x

Cresswell H, Hamilton G (2002) Bulk density and pore space relations. In 'Soil physical measurement and interpretation for land evaluation'. (Eds N McKenzie, K Coughlan, H Cresswell) pp. 35–58. (CSIRO Publishing: Melbourne)

Curtin D, Campbell C (2008) Mineralizable nitrogen. In 'Soil sampling and methods of analysis'. 2nd edn. (Eds MR Carter, EG Gregorich) pp. 599–606. (CRC Press: Boca Raton, FL)

Dalal RC, Wang W, Robertson GP, Parton WJ (2003) Nitrous oxide emission from Australian agricultural lands and mitigation options: a review. *Soil Research* **41**, 165–195. doi:10.1071/SR02064

Davidson EA (1992) Sources of nitric oxide and nitrous oxide following wetting of dry soil. *Soil Science Society of America Journal* **56**, 95–102. doi:10.2136/sssaj1992.03615995005600010015x

De Antoni Migliorati M, Bell MJ, Grace PR, Rowlings DW, Scheer C, Strazzabosco A (2014) Assessing agronomic and environmental implications of different N fertilisation strategies in subtropical grain cropping systems on Oxisols. *Nutrient Cycling in Agroecosystems* **100**, 369–382. doi:10.1007/s10705-014-9655-4

Denmead O, Macdonald B, Bryant G, Naylor T, Wilson S, Griffith DW, Wang W, Salter B, White I, Moody P (2010) Emissions of methane and nitrous oxide from Australian sugarcane soils. *Agricultural and Forest Meteorology* **150**, 748–756. doi:10.1016/j.agrformet.2009.06.018

Ding WX, Meng L, Cai ZC, Han FX (2007) Effects of long-term amendment of organic manure and nitrogen fertilizer on nitrous oxide emission in a sandy loam soil. *Journal of Environmental Sciences (China)* **19**, 185–193. doi:10.1016/S1001-0742(07)60030-8

Farquharson R, Baldock J (2008) Concepts in modelling N_2O emissions from land use. *Plant and Soil* **309**, 147–167. doi:10.1007/s11104-007-9485-0

Garland GM, Suddick E, Burger M, Horwath WR, Six J (2014) Direct N_2O emissions from a Mediterranean vineyard: event-related baseline measurements. *Agriculture, Ecosystems & Environment* **195**, 44–52. doi:10.1016/j.agee.2014.05.018

Ge S, Jiang Y, Wei S (2015) Gross nitrification rates and nitrous oxide emissions in an apple orchard soil in northeast China. *Pedosphere* **25**, 622–630. doi:10.1016/S1002-0160(15)30042-4

George AP (1999) Deciduous fruit production in Australia. Available at http://www.fao.org/docrep/004/ab985e/ab985e04.htm#bm04 [verified 25 October 2015]

Greer DH, Wünsche JN, Norling CL, Wiggins HN (2006) Root-zone temperatures affect phenology of bud break, flower cluster development, shoot extension growth and gas exchange of 'Braeburne'™ (*Malus domestica*) apple trees. *Tree Physiology* **26**, 105–111. doi:10.1093/treephys/26.1.105

Helgason B, Janzen H, Chantigny M, Drury C, Ellert B, Gregorich E, Lemke R, Pattey E, Rochette P, Wagner-Riddle C (2005) Toward improved coefficients for predicting direct N_2O emissions from soil in Canadian agroecosystems. *Nutrient Cycling in Agroecosystems* **72**, 87–99. doi:10.1007/s10705-004-7358-y

Hillier J, Walter C, Malin D, Garcia-Suarez T, Mila-i-Canals L, Smith P (2011) A farm-focused calculator for emissions from crop and livestock production. *Environmental Modelling & Software* **26**, 1070–1078. doi:10.1016/j.envsoft.2011.03.014

Huang X, Grace P, Weier K, Mengersen K (2012) Nitrous oxide emissions from subtropical horticultural soils: a time series analysis. *Soil Research* **50**, 596–606. doi:10.1071/SR11100

IPCC (2001) Climate change 2001: the scientific basis. In 'The climate change contribution of working group I to the third assessment report of the Intergovernmental Panel on Climate Change'. (Eds J Houghton, Y Ding, D Griggs, M Noguer, P Van der Linden, X Dai, K Maskell, C Johnson) p. 881. (Cambridge University Press: Cambridge)

Isbell RF (2002) 'The Australian soil classification.' (CSIRO Publishing: Melbourne)

Linquist B, van Groenigen KJ, Adviento-Borbe MA, Pittelkow C, van Kessel C (2012) An agronomic assessment of greenhouse gas emissions from major cereal crops. *Global Change Biology* **18**, 194–209. doi:10.1111/j.1365-2486.2011.02502.x

Millard P (1996) Ecophysiology of the internal cycling of nitrogen for tree growth. *Zeitschrift für Pflanzenernährung und Bodenkunde* **159**, 1–10.

Millard P, Neilsen GH (1989) The influence of nitrogen supply on the uptake and remobilization of stored N for the seasonal growth of apple trees. *Annals of Botany* **63**, 301–309.

Mualem Y (1976) A new model for predicting the hydraulic conductivity of unsaturated porous media. *Water Resources Research* **12**, 513–522. doi:10.1029/WR012i003p00513

Neilsen D, Millard P, Neilsen GH, Hogue EJ (1997) Sources of N for leaf growth in a high-density apple (*Malus domestica*) orchard irrigated with ammonium nitrate solution. *Tree Physiology* **17**, 733–739. doi:10.1093/treephys/17.11.733

Pang JZ, Wang XK, Mu YJ, Ouyang ZY, Liu WZ (2009) Nitrous oxide emissions from an apple orchard soil in the semiarid Loess Plateau of China. *Biology and Fertility of Soils* **46**, 37–44. doi:10.1007/s00374-009-0403-x

Peters A, Durner W (2008) Simplified evaporation method for determining soil hydraulic properties. *Journal of Hydrology* **356**(1–2), 147–162. doi:10.1016/j.jhydrol.2008.04.016

Prather M, Derwent R, Ehhalt D, Fraser P, Sanhueza E, Zhou X (1995) Other trace gases and tmospheric. In 'Climate change, 1994: radiative forcing of climate change and an evaluation of the IPCC IS92 emission scenarios'. (Eds J Houghton, LG Meira Filho, BJ Hoesung Lee, BA Callander, E Haites, N Harris, K Maskrell) p. 73. (University of Cambridge: Cambridge)

Ramaswamy V, Boucher O, Haigh J, Hauglustine D, Haywood J, Myhre G, Nakajima T, Shi G, Solomon S (2001) Radiative forcing of climate change. In 'Climate change 2001: the scientific basis: contribution of working group I to the third assessment report of the Intergovernmental Panel on Climate Change'. (Eds J Houghton, Y Ding, D Griggs, M Noguer, P Van der Linden, X Dai, K Maskell, C Johnson) pp. 349–416. (Cambridge University Press: Cambridge, UK)

Rashti MR, Wang WJ, Harper SM, Moody PW, Chen CR, Ghadiri H, Reeves SH (2015) Strategies to mitigate greenhouse gas emissions in intensively managed vegetable cropping systems in subtropical Australia. *Soil Research* **53**, 475–484. doi:10.1071/SR14355

Reynolds WD (2008) Saturated hydraulic properties: Ring infiltrometer. In 'Soil sampling and methods of analysis'. 2nd edn. (Eds MR Carter, EG Gregorich) Ch. 77, pp. 1043–1056. (Canadian Society of Soil Science, CRC Press: Boca Raton)

Reynolds WD, Elrick DE (1990) Ponded infiltration from a single ring: I. Analysis of steady flow. *Soil Science Society of America Journal* **54**, 1233–1241. doi:10.2136/sssaj1990.03615995005400050006x

Rowlings DW, Grace PR, Kiese R, Weier KL (2012) Environmental factors controlling temporal and spatial variability in the soil-atmosphere exchange of CO_2, CH_4 and N_2O from an Australian subtropical rainforest. *Global Change Biology* **18**, 726–738. doi:10.1111/j.1365-2486.2011.02563.x

Rowlings D, Grace P, Scheer C, Kiese R (2013) Influence of nitrogen fertiliser application and timing on greenhouse gas emissions from a lychee (*Litchi chinensis*) orchard in humid subtropical Australia. *Agriculture, Ecosystems & Environment* **179**, 168–178. doi:10.1016/j.agee.2013.08.013

Russow R, Sich I, Neue H-U (2000) The formation of the trace gases NO and N_2O in soils by the coupled processes of nitrification and

denitrification: results of kinetic ^{15}N tracer investigations. *Chemosphere. Global Change Science* **2**, 359–366. doi:10.1016/S1465-9972(00)00012-X

Scheer C, Grace PR, Rowlings DW, Payero J (2012) Nitrous oxide emissions from irrigated wheat in Australia: impact of irrigation management. *Plant and Soil* **359**, 351–362. doi:10.1007/s11104-012-1197-4

Scheer C, Grace PR, Rowlings DW, Payero J (2013) Soil N_2O and CO_2 emissions from cotton in Australia under varying irrigation management. *Nutrient Cycling in Agroecosystems* **95**, 43–56. doi:10.1007/s10705-012-9547-4

Scheer C, Rowlings DW, Firrel M, Deuter P, Morris S, Grace PR (2014) Impact of nitrification inhibitor (DMPP) on soil nitrous oxide emissions from an intensive broccoli production system in sub-tropical Australia. *Soil Biology & Biochemistry* **77**, 243–251. doi:10.1016/j.soilbio.2014.07.006

Schellenberg DL, Alsina MM, Muhammad S, Stockert CM, Wolff MW, Sanden BL, Brown PH, Smart DR (2012) Yield-scaled global warming potential from N_2O emissions and CH_4 oxidation for almond (*Prunus dulcis*) irrigated with nitrogen fertilizers on arid land. *Agriculture, Ecosystems & Environment* **155**, 7–15. doi:10.1016/j.agee.2012.03.008

Shi Y, Wu W, Meng F, Zhang Z, Zheng L, Wang D (2013) Integrated management practices significantly affect N_2O emissions and wheat–maize production at field scale in the North China Plain. *Nutrient Cycling in Agroecosystems* **95**, 203–218. doi:10.1007/s10705-013-9558-9

Smith KA, Dobbie KE (2001) The impact of sampling frequency and sampling times on chamber-based measurements of N_2O emissions from fertilized soils. *Global Change Biology* **7**, 933–945. doi:10.1046/j.1354-1013.2001.00450.x

Tagliavini M, Scudellazi D, Marangoni B, Toselli M (1996) Nitrogen fertilization management in orchards to reconcile productivity and environmental aspects. *Fertilizer Research* **43**, 93–102. doi:10.1007/BF00747687

Tiedje JM (1994) Denitrifiers. In 'Methods of soil analysis: Part 2. Microbiological and biochemical properties'. (Eds RW Weaver, A J. S. and PS Bottomley) pp. 245–267. (Soil Science Society of America: Madison, WI)

US EPA (1993) 'Method 353.2: determination of nitrate-nitrite nitrogen by automated colorimetry.' Revision 2. (US Environmental Protection Agency: Cincinnati, Ohio)

US EPA (2006) 'Global anthropogenic non-CO_2 greenhouse gas emissions: 1990–2020.' (United States Environmental Protection Agency, EPA 430-R-06–003: Washington DC)

van Genuchten MT (1980) A closed-form equation for predicting the hydraulic conductivity of unsaturated soils. *Soil Science Society of America Journal* **44**, 892–898. doi:10.2136/sssaj1980.03615995004400050002x

van der Weerden TJ, Kelliher FM, de Klein CAM (2012) Influence of pore size distribution and soil water content on nitrous oxide emissions. *Soil Research* **50**, 125–135.

van Zwieten L, Kimber S, Morris S, Downie A, Berger E, Rust J, Scheer C (2010) Influence of biochars on flux of N_2O and CO_2 from Ferrosol. *Australian Journal of Soil Research* **48**, 555–568. doi:10.1071/SR10004

Wang WJ, Dalal RC (2010) Assessment of the boundary line approach for predicting N_2O emission ranges from Australian agricultural soils. In '19th World Congress of Soil Science, Soil Solutions for a Changing World'. (N_2O Network: Brisbane, Australia)

Weil RR, Islam KR, Stine MA, Gruver JB, Samson-Liebig SE (2003) Estimating active carbon for soil quality assessment: a simplified method for laboratory and field use. *American Journal of Alternative Agriculture* **18**, 3–17. doi:10.1079/AJAA2003003

Xia Y, She D, Li Y, Yan X (2014) Impact of sampling time on chamber-based measurements of riverine nitrous oxide emissions using relative difference analysis. *Geoderma* **214–215**, 197–203. doi:10.1016/j.geoderma.2013.09.011

Irrigation Science
https://doi.org/10.1007/s00271-017-0567-3

ORIGINAL PAPER

Drip irrigation wetting patterns and nitrate distribution: comparison between electrical resistivity (ERI), dye tracer, and 2D soil–water modelling approaches

Marcus Hardie[1] · James Ridges[1] · Nigel Swarts[1] · Dugald Close[1]

Received: 19 February 2017 / Accepted: 17 December 2017

Abstract
Despite the widespread use of drip irrigation and fertigation, there is limited research on soil wetting patterns and nutrient distribution from drip emitters in agricultural soils. We compared the use of electrical resistivity imaging (ERI) with dye tracer patterns, measured soil nitrate distribution, and modelled changes in soil moisture and nitrate distribution, in a commercial apple orchard in southern Tasmania. Time-lapse two-dimensional ERI revealed wetting plumes beneath the emitters ranged from nil infiltration, to infiltration beyond 1.0 m depth. Lack of infiltration beneath some emitters was attributed to runoff caused by either water repellence or the surface leaf mulch, whilst infiltration to 1.0 m depth was attributed to preferential flow processes. The uncalibrated ERT was unable to discern the separate contributions from of solute concentration, moisture content and temperature to the change in electrical resistivity. The dye tracer study revealed the majority of the fertigated nitrate was retained in the A1 horizon, whilst the fertigated water infiltrated much deeper into the A2 and B2 horizons. The 2D modelling was not able to replicate the variations in infiltration demonstrated by the ERT, principally due to the lumped nature of the soil parameterisation, and inability of the model to simulate preferential flow. As such, use of modelling tools and texture-based guidelines for design and management of drip emitters is not recommended for the texture contrast soils.

Introduction

Drip fertigation involves the application of soluble nutrients through drip irrigation emitters. It is regarded as a precise and efficient method of supplying water and nutrients to crops, specifically perennial tree crops. Drip irrigation offers a large degree of control, enabling timely and precise placement of irrigation and nutrients to meet crop requirements, thereby minimising application to non-target areas and leaching of nutrients beneath the root zone (Gärdenäs et al. 2005; Thorburn et al. 2003). The shape of the wetted soil volume and nitrate distribution beneath emitters is influenced by factors such as; soil hydraulic properties, emitter discharge rates, emitter spacing, irrigation quantity and frequency, crop water uptake rates and root distribution (Gärdenäs et al. 2005; Naglič et al. 2014; Souza and Folegatti 2008; Subbaiah 2013).

Despite the wide spread use of drip irrigation and fertigation systems in many agricultural industries, there are relatively few studies which have measured soil water and nutrient distribution following fertigation in in situ agricultural soils (Klein and Spieler 1987). Instead, guidelines for the design and operation of drip irrigation systems (FAO 1997; Goldy 2012; Hung 1995) have been developed for generic soil texture classes (e.g., sand, loam, clay) which require modification by system designers and farmers to account for local conditions (Thorburn et al. 2003). These guidelines typically present soils as being uniform in which water and nutrients infiltrate in a three-dimensional flow pattern about the dripper (Klein et al. 1989). Consequently these guidelines typically ignore many of the complexities associated with infiltration into in situ soils, including; compaction, surface crusting, and preferential flows resulting from water repellence, macroporosity, and contrasting soil horizons (Bar-Yosef et al. 1988; Flury et al. 1994; Gerke et al. 2010; Jarvis 2007). The occurrence of preferential flow is especially important with drip irrigation systems, as localized ponding beneath emitters may facilitate infiltration

Communicated by N. Lazarovitch.

✉ Marcus Hardie
marcus.hardie@utas.edu.au

[1] Perennial Horticulture Centre, Tasmanian Institute of Agriculture, University of Tasmania, Private Bag 98, Hobart, TAS 7001, Australia

Published online: 05 January 2018

through surface connected macropores, shrinkage cracks and the development of finger flow (Clothier et al. 2008; Cote et al. 2003; Roth 2008).

Strategic and tactical management of drip irrigation and fertigation systems requires the ability to rapidly and non-destructively determine emitter wetting patterns (Devasirvatham 2009; Thorburn et al. 2003). Manual determination of emitter wetting patterns following infiltration such as augering or excavation are time consuming and result in damage to tree roots. Over the last two decades development of 2D soil water models and availability of geophysical proximal sensors has enabled non-destructive or minimally destructive means of predicting or inferring drip emitter wetting patterns and solute distribution (Samouëlian et al. 2005; Satriani et al. 2015; Subbaiah 2013).

A number of minimally invasive geophysical tools have been used to 'map' or spatially infer irrigation wetting patterns and solute distribution from drip emitters. Approaches include; electromagnetic induction (EM 38) (Coppola et al. 2016; Hossain et al. 2010; Misra and Padhi 2014), cosmic ray sensors (Han et al. 2016; Zhu et al. 2014), ground penetrating radar (Algeo et al. 2016; Satriani et al. 2015; Shamir et al. 2016), and electrical resistivity imaging (ERI) (Cassiani et al. 2015, 2016; Consoli et al. 2017; Michot et al. 2003; Moreno et al. 2015; Persson et al. 2015; Puy et al. 2016; Wehrer and Slater 2015). ERI or electrical resistivity tomography (ERT) produces 2D or cross section images of the soils resistance to the flow of electricity. Resistivity is influenced by soil texture, mineralogy, porosity, water content, solute concentration and temperature (Samouëlian et al. 2005). Time-lapse ERI before and after irrigation or fertigation events is therefore able to determine lumped spatial–temporal changes in soil moisture, solute concentration and soil temperature at a range of scales (Miller et al. 2008; Wehrer and Slater 2015).

Two-dimensional soil water modelling tools such as Hydrus-2D (Šimůnek et al. 2016) and WETUP (Cook et al. 2003; Kandelous and Šimůnek 2010) also have the ability to predict emitter wetting patterns and solute distribution under a wide range of soil types and management conditions. Kandelous and Šimůnek (2010) compared the ability of different modelling approaches for simulating surface and subsurface drip emitter patterns, they concluded that 'Hydrus-2D provides good predictions and should be selected over the other models' they evaluated. Hydrus-2D uses numerical methods to solve the Richards' equation for variably saturated water flow, the convection–dispersion equation for solute transport in the liquid phase and diffusion equations for solute transport in the vapor phase (Šimůnek et al. 2008, 2012, 2013; Šimůnek and van Genuchten 2007). Hydrus-2D has been successfully used to model fertigation and drip irrigation practices including; Cook et al. (2006a); El-Nesr et al. (2014); Li et al. (2015); Mguidiche et al. (2015); Naglič et al. (2014); Phogat et al. (2013); Phogat et al. (2014); Wang et al. (2014), however, its application in in situ soils is somewhat limited by difficulty parameterizing spatial–temporal variation in soil properties and limited ability to simulate preferential flow processes (Gerke et al. 2010; Šimůnek et al. 2003).

In Tasmania, approximately 26% of perennial horticulture (apples, cherries, vines) are located on texture contrast (TCS) or duplex soils (Cotching et al. 2009). These soils consist of a shallow sand to sandy loam topsoil over a clay subsoil. Infiltration into the TCS is often complex involving a number of preferential flow processes including; water repellence based finger flow, bypass flow through shrinkage cracks and macropores, and subsurface lateral flow above the A2 or B2 horizons (Chittleborough et al. 1994; Eastham et al. 2000; Hardie et al. 2013). Drip fertigation and irrigation into TCS is therefore expected to result in uneven, spatially heterogeneous, and largely unpredictable wetting patterns, as demonstrated by Hardie et al. (2012). This has important implications on irrigation and fertigation efficiency and effectiveness in commercial orchards, where the majority of nutrients are supplied by drip emitters.

This study was established in a commercial apple orchard growing on a texture contrast soils to:

1. Test the use of commercially available ERI tools for rapid non-destructive 'mapping' of fertigation infiltration patterns.
2. Compare fertigation infiltration patterns inferred by ERI to those predicted by Hydrus-2D, and to in situ measured values.
3. Determine the spatial distribution of irrigation and nitrate following fertigation.
4. Report the efficiency and effectiveness of a single drip fertigation and irrigation event.

Materials and methods

Field site characteristics

Location and climate

The trial was located in a commercial apple orchard within the Huon Valley, Tasmania, Australia (42°59′36.97″S, 147°59′29.04″E). The region has a temperate, maritime climate with an average rainfall of 745 mm, mean minimum and maximum temperature range of 5.8–17.1 °C, and mean daily sunshine hours of 5.5 h (BOM 2015). The orchard consisted of 10-year-old 'Galaxy' trees, grown on M26 rootstock, pruned to a central leader training system, with 2 m tree spacing, and 4.5 m row spacing, on a 0.3 m high

mounded tree row. The orchard had previously been irrigated by 2.3 L h^{-1} emitters spaced every 0.5 m along the tree line.

Soil properties

Prior to trial establishment, a handheld 4 m by 20 m electromagnetic induction survey (EM) was conducted using a Geonics EM38 in QP mode, and Garmin 12 XL GPS, to locate the trial in an area of relatively homogenous soils. Apparent conductivity maps were produced using SURFER version 8, employing default kriging settings and a low level of contour smoothing. The trial was located within an area in which the apparent conductivity varied from 5 to 9 mS cm^{-1}.

Soils were classified according to Isbell (2002) as Grey, Eutrophic, Humose–Bleached Kurosol (texture contrast), which consisted of a reworked A1 (0–0.30 m) sandy loam, over a rigid bleached silica cemented A2e horizon, and a mottled carbon rich (5.19%) light clay B21 horizon, over a mottled medium clay B22 horizon. Selected soil properties are presented in Table 1. Chemical analysis was conducted by CSBP laboratories, Western Australia according to Rayment and Higginson (1992).

Soil physical analysis

Soil core samples (5.0 cm × 5.2 cm and 6.0 cm × 9.0 cm) were collected in triplicate from each soil horizon for analysis of hydrological properties. Bulk density was determined at saturation using 5.0 cm × 5.2 cm cores according to McKenzie et al. (2002). Saturated hydraulic conductivity (K_{sat}) was determined on the 5.0 cm × 5.2 cm cores by Darcy's Law at a constant head of + 0.1 kPa. The soil water release curve was determined using the 6.0 × 9.0 cm cores by evaporative flux (Peters and Durner 2008; Wendroth et al. 1993) using HYPROP apparatus and tensioVIEW software (UMS 2013). The soil water retention curve was fitted using the bimodal (dual porosity) van Genuchten–Mualem equation (Durner 1994), which better represents macroporosity than the traditional van Genuchten–Mualem equation. Parameter values are presented in Table 1.

Fertigation and irrigation experiment

Fertigation and irrigation

The trial occurred over 4 days in February, 2013. Fertigation was conducted through Netafim 15–30 kPa pressure compensating emitters at 15 kPa with a solution of calcium nitrate (4.8 g L^{-1}) and dye tracer FCF Brilliant Blue (7.0 g L^{-1}). The dye tracer was added to the fertigation water to enable visualisation of infiltration pathways into the soil, and to guide soil sampling. Irrigation (0.2 dS/m) was conducted 20 h after fertigation through the existing farm 2.3 L h^{-1} irrigation emitters spaced at 0.5 m. High and low irrigation treatments were established in two adjacent 8.0 m long sections along a single tree row, each containing four trees. The low rate irrigation treatment was irrigated for 45 min, whilst the high irrigation rate treatment was irrigated for 90 min.

Electrical resistivity imaging

Two-dimensional electrical resistivity imaging (ERI) was conducted using a Wenner-alpha electrode array, which are highly sensitive to vertical variations in electrical

Table 1 Selected soil data

Soil horizon	Depth (cm)	Texture	Organic carbon (%)	$EC_{1:5}$ (dS/m)	pH ($CaCl_2$)	CEC (meq/100 g)	K_{sat} (mm/h)	Bulk density (g/cm^3)
Chemical and physical properties								
A1	0–30	Sandy loam	3.46	0.17	5.4	19.13	44	1.10
A2	30–50	Loamy sand	0.47	0.19	4.1	2.64	8.2	1.50
B21	50–70	Light clay	5.19	0.25	3.4	11.73	1.2	1.14
B22	70+	Medium clay	2.47	0.18	4.0	4.57	0.5	1.27
Soil horizon	Θr (cm/cm)	Θs (cm/cm)	α1 (1/cm)	η1	ω2	α2 (1/cm)	η^2	RMSE
Bimodal Durner van Genuchten–Mualem parameters								
A1	0.001	0.61	0.045	2.11	0.85	0.0071	1.16	0.0013
A2	0.11	0.34	0.020	1.57	0.29	0.0008	3.78	0.0011
B21	0.10	0.65	0.026	1.14	0.71	0.0010	1.70	0.0014
B22	0.10	0.55	0.031	1.70	0.80	0.0010	1.20	0.0016

CEC cation exchange capacity, *EC* electrical conductivity, *Ksat* saturated hydraulic conductivity. The RMSE refers to the fit between measures $\psi(\Theta)$ data pairs and the bimodal Durner van Genuchten–Mualem equation

resistivity (Furman et al. 2003). The 64 copper electrodes were inserted every 0.25 m, over a distance of 16 m, in the center of the orchard tree row that spanned the high and low irrigation treatment sections (Fig. 1). Electrodes were inserted to a depth of 0.10 m and left in place for the duration of the trial to ensure constant electrode position and contact resistance. Five ERI scans were conducted prior to excavation of the site. These occurred; (1) 2 h before fertigation, (2) 1 h after fertigation, (3) 20 h after fertigation, following which the irrigation was applied, (4) 46 h after fertigation which was also 26 h after the irrigation event, and (5) 66 h after fertigation, which was also 46 h after the irrigation event and immediately prior to excavation of the site. Data were acquired using an Allied Associated Geophysical Ltd Tigre resistivity meter at 12 levels in which measurements were repeated twice. Data acquisition typically took 110 min. The acquired apparent electrical resistivity data were inverted using the RES2DINV software version 3.59 (Loke 2010). Data were first assessed for erroneous measurements, and then inverted without temperature correction using standard least squares method and the half-cell resistivity option to improve resolution near the soil surface. Absolute error for individual inversions with up to seven iterations was between 1.3% and 1.5%.

Changes in electrical resistivity over time were determined by simultaneous time-lapse inversion in RES2DINV software version 3.59 (Loke 2010) using the 'minimise changes' and 'simultaneous inversion' options to ensure changes in model electrical resistivity were due to actual differences in electrical resistivity values, and not due to differences associated with inverting individual data sets, and to ensure that the inversion of later timesets were constrained by the first reference model. The time-constrain weight parameter was set to 1 to keep models for later time sets similar to the earlier time sets. Absolute error for time-lapse inversions were between 3.1% and 3.7%. Data are presented on a ratio basis to demonstrate relative change in moisture and or solute, and or temperature over time.

Dye tracer

Soil pits were excavated along the center of the tree row to a depth of 1.2 m in each of the two treatments 68–72 h after fertigation. Each pit revealed dye stained infiltration pathways beneath a single emitter in each of the two irrigation treatments (shown as the photographed area in Fig. 1). Both of the dye tracer stained infiltration pathways were photographed using a Cannon 200D SLR at 21 mm focal length. Images contained a large square metal scaled border to facilitate correction for radial and keystone distortion in Photoshop CS6. Dye stained pixels were separated from unstained pixels by adjusting hue and saturation channels, enabling the dye tracer to be extracted from the surrounding background image in Photoshop CS6 (Hardie et al. 2011). The dye stained images were converted to binary format in Image J software (Abramoff et al. 2004).

Nitrate and soil moisture measurements

Nitrate and soil moisture sampling was conducted for each of the two emitter dye tracer experiments (location shown in Fig. 1). A 2.00 × 1.00 m wire mesh with 0.10 × 0.10 m openings was placed over the dye stained excavation beneath the two emitter experiments to guide soil sampling. Approximately 20 g samples were obtained by removing soil to a depth of 0.01 m from every second grid square (i.e., at 0.2 × 0.2 m spacing). Samples were split for determination of gravimetric moisture content by drying for 24 h at 105 °C, and for storage at 3 °C for later determination of nitrate. Thawed samples were homogenised by grinding, to which potassium chloride solution (2 mol L^{-1}, 0.040 L) was added and agitated for 18 h, to induce nitrate extraction. Nitrate concentration was determined by Cd–Cu reduction according to the USEPA method 353.3 using a Smart Chem Westco Scientific Instrument cadmium reactor (O'Dell 1993). Separate analysis was performed with known nitrate samples with different levels of dye tracer to confirm that the dye tracer did not interfere with the colorimetric determination of nitrate.

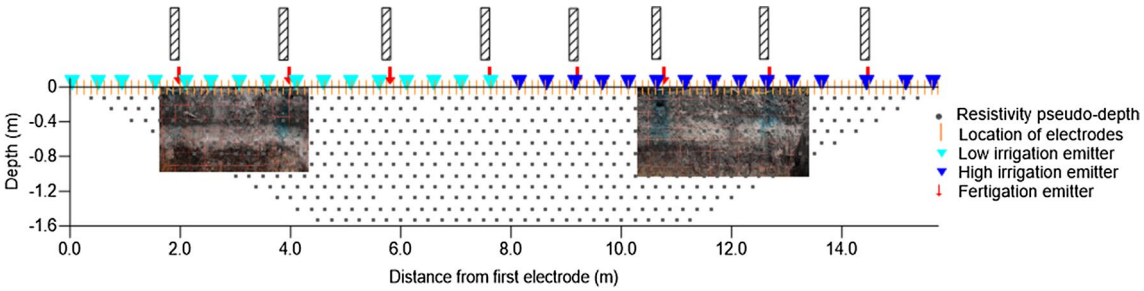

Fig. 1 Spatial representation of trial layout. Hashed bars indicate location of apple trees. Photos indicate depth and location of the two excavated dye tracers experiments, with low irrigation treatment on the left and the high irrigation treatment on the right

Nitrate and soil water modelling

Wetting patterns and solute distribution were modelled using Hydrus-2D with the bimodal (dual porosity) van Genuchten–Mualem equation (Durner 1994). The 16 m wide by 1.5 m deep experimental area was represented in a 2D vertical plane flow domain containing 5716 nodes and 10,962 elements with double the number of cells near the upper boundary. The flow domain had no-flow lateral boundaries, a free drainage lower boundary, and a no-flow upper boundary with emitters represented as time variable boundaries at 0.5 m spacings. For the two single emitter dye tracer experiments, infiltration from the emitters was simulated using the dynamic wetting option, in which the radius of the wetted area varied during infiltration, depending on the number of nodes required to maintain a negative pressure head at the soil surface (Gärdenäs et al. 2005; Naglič et al. 2014). As Hydrus-2D limits use of the dynamic wetting option to single emitters, infiltration for the 16 m long cross section experiment was simulated through a series of 0.25 m diameter circular time variable upper boundary nodes in which the number of nodes represented the width of saturated ponding beneath the emitters as indicated by the previous dynamic wetting simulations. Initial moisture contents were determined from hand auguring samples at six locations at four depths in an adjacent tree row prior to trial commencement. Representation of the spatial distribution of the four soil horizons was guided by apparent electrical resistivity and site photos. Nitrate transport was modelled using the Crank–Nicholson Scheme time weighting scheme, a longitudinal dispersivity of 5.0 cm, a transverse dispersivity of 0.5 cm and an adsorption isotherm coefficient of 0 as suggested by Gärdenäs et al. (2005). Nitrogen transformations and mineralization were not simulated due to the short duration of the experiment. As the site was covered with plastic between ERI readings, rainfall and evaporation were assumed to be zero.

Data visualization and statistical analysis

For the two excavated emitter experiments, the change in electrical resistivity 66 h after fertigation, the measured soil nitrate distribution, and the measured soil moisture were krigged and mapped as contour plots using default settings in SURFER 11 (Golden Software 2002). For the two excavated emitter experiments, statistical analysis was restricted to the soil nitrate and soil moisture sampling locations rather than krigged values. Values for the scaled TIFF layers (change in electrical resistivity, modelled soil moisture, and modelled soil nitrate) were determined by overlaying the TIFF layers with the location of the soil sampling grid, from which values for the change in electrical resistivity, modelled soil moisture, and modelled soil nitrate were recorded. As the dye images were binary, the relationship between the presence or absence of dye tracer versus soil moisture, nitrate concentration and the change in electrical resistivity were investigated using independent *T* test in SPSS V23. Whilst the relationship between the change in electrical resistivity, soil moisture, soil nitrate concentration, modelled soil moisture, and modelled soil nitrate were explored using bivariate two tailed Pearson correlation in SPSS V23. The influence of measured and modelled soil moisture, and nitrate concentration on the change in electrical resistivity at 66 h was evaluated using stepwise linear regression with an entry probability of 0.05 in SPSS v23.

Results

Electrical resistivity imaging

The time-lapse inversion of electrical resistivity demonstrated that the change in electrical resistivity associated with infiltration beneath the emitters was highly variable (Fig. 2). The time-lapse inversion of electrical resistivity immediately and 20 h following fertigation revealed that electrical resistivity decreased (blue) beneath 5 of the 8 emitters, whilst beneath 3 of the 8 emitters the electrical resistivity had both increased (red) and decreased (blue). Changes in electrical resistivity associated with increased soil moisture and increased solute concentration following fertigation were largely restricted to the upper A1 horizon (0–0.2 m depth). However, the emitter positioned 12.8 m from the first electrode indicated that the fertigation infiltrated to at least 1.0 m depth, presumably via some form of preferential flow (Fig. 2a, b). Increased electrical resistivity (red patches, Fig. 2) between 0 and 0.2 m depth in the hour after fertigation suggests there was a slight decrease in soil moisture or solute concentration between the two ERT acquisitions. This increase in electrical resistivity was attributed to either mobilization and dilution of existing soil solutes following irrigation, or internal drainage either between the two ERT acquisitions, or during the second ERT acquisition which took 110 min. Twenty hours after fertigation (Fig. 2b) the small areas of increased electrical resistivity (red) beneath the emitters was no longer apparent, whilst the size and shape of the infiltration plumes remained mostly unchanged (Fig. 2a, b). Interestingly, in both irrigation treatments, there was no evidence of wetting associated with 3–4 emitters in the low irrigation treatment, and 3 emitters in the high irrigation treatment. All emitters were observed to be flowing during the experiment.

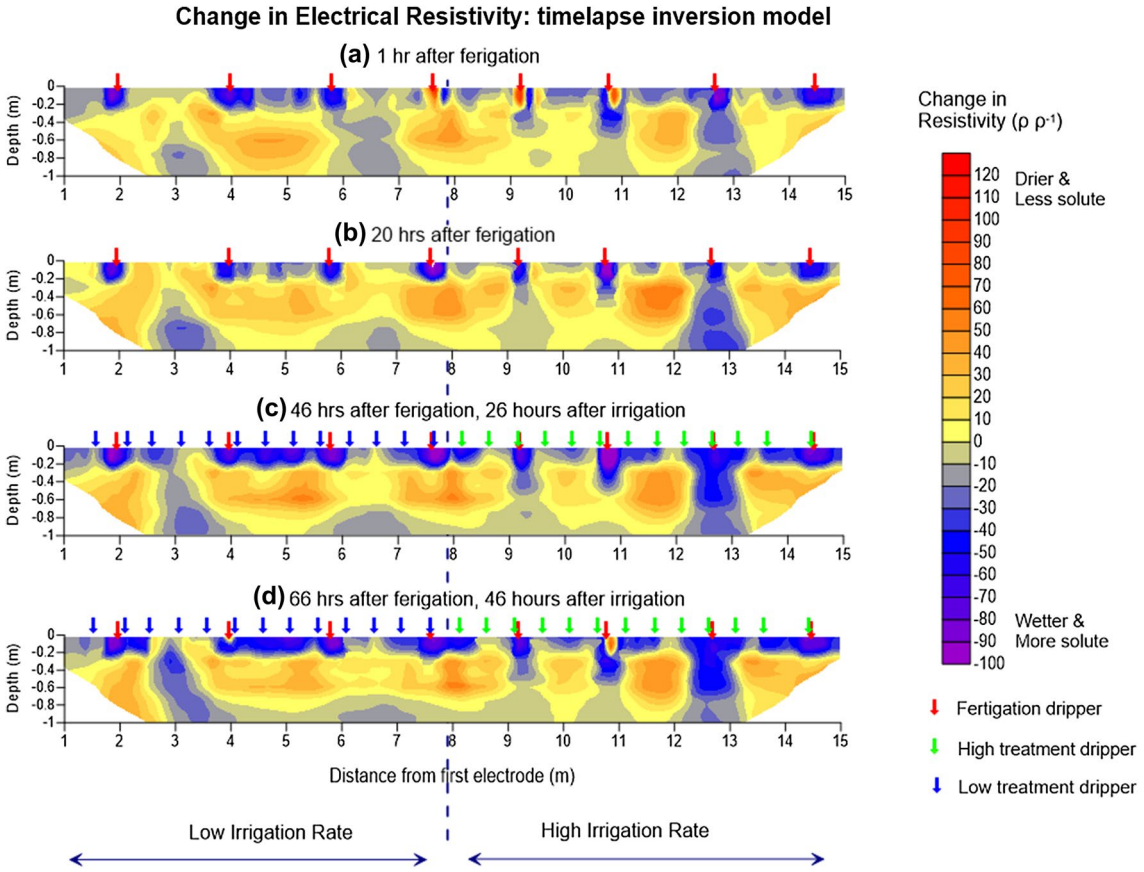

Fig. 2 Change in electrical resistivity: time-lapse inversion model demonstrating the change in electrical resistivity from the first reference model to **a** 1 h after fertigation, **b** 20 h after fertigation, **c** 46 h after fertigation and 26 h after irrigation, and **d** 66 h after fertigation and 46 h after irrigation. Dark blue arrows represent the location of the low irrigation treatment emitters, green arrows represent the location of the high irrigation treatment emitters, red arrows indicate the location of the fertigation emitters. Left side (1.0–8.0 m) low irrigation treatment. Right side (8.0–15 m) is the high irrigation treatment. (Color figure online)

Dye tracer and nitrate distribution

For the excavated high irrigation emitter, the dye tracer wetting pattern indicated that infiltration into the A1 horizon resulted from vertical infiltration with little lateral dispersion beyond the area of ponding beneath the emitter (Fig. 3a, b). Infiltration into the A2 horizon appeared to have resulted from a combination of both lateral movement of the dye tracer along the A1/A2 horizon boundary, and non-uniform sorptive flow into the A2 horizon resulting in the appearance of finger flow. The absence of dye staining in the B22 horizon indicates little if any of the water and or solute applied during the fertigation event infiltrated into the B22 horizon (Fig. 3a, b).

In contrast to the dye tracer distribution (Fig. 3b), the nitrate was almost entirely retained within the upper A1 horizon (0–0.25 m depth) (Fig. 3c) with the majority of the nitrate retained between 0 m and approximately 0.10 m depth, with a lower concentration of nitrate extending to 0.35 m depth. Other than the low concentration (0.02–0.04 mg g^{-1}) plume beneath 0.20 m depth, the measured soil nitrate distribution (Fig. 3c) appeared somewhat similar to that of the modelled nitrate concentration (Fig. 3g).

The change in electrical resistivity following fertigation and irrigation in the high irrigation treatment (Fig. 3e) was more uniform than either the dye tracer pattern (Fig. 3b) or the soil nitrate concentration (Fig. 3c). The change in electrical resistivity appeared as a fairly uniform band which extended to almost 0.40 m depth. As such, it appeared to be poorly related to the dye tracer distribution, soil moisture content and the nitrate distribution. The measured soil moisture distribution (Fig. 3d) appeared to be similar to the modelled soil water distribution (Fig. 3f) in which infiltration did not appear to have influenced soil moisture beyond the A1 horizon. Infiltration within the A1 horizon appeared to result from uniform flow in which the dye tracer appeared as a uniformly wetted vertical column directly beneath the ponded area beneath the emitter, as previously reported by Hardie et al. (2012).

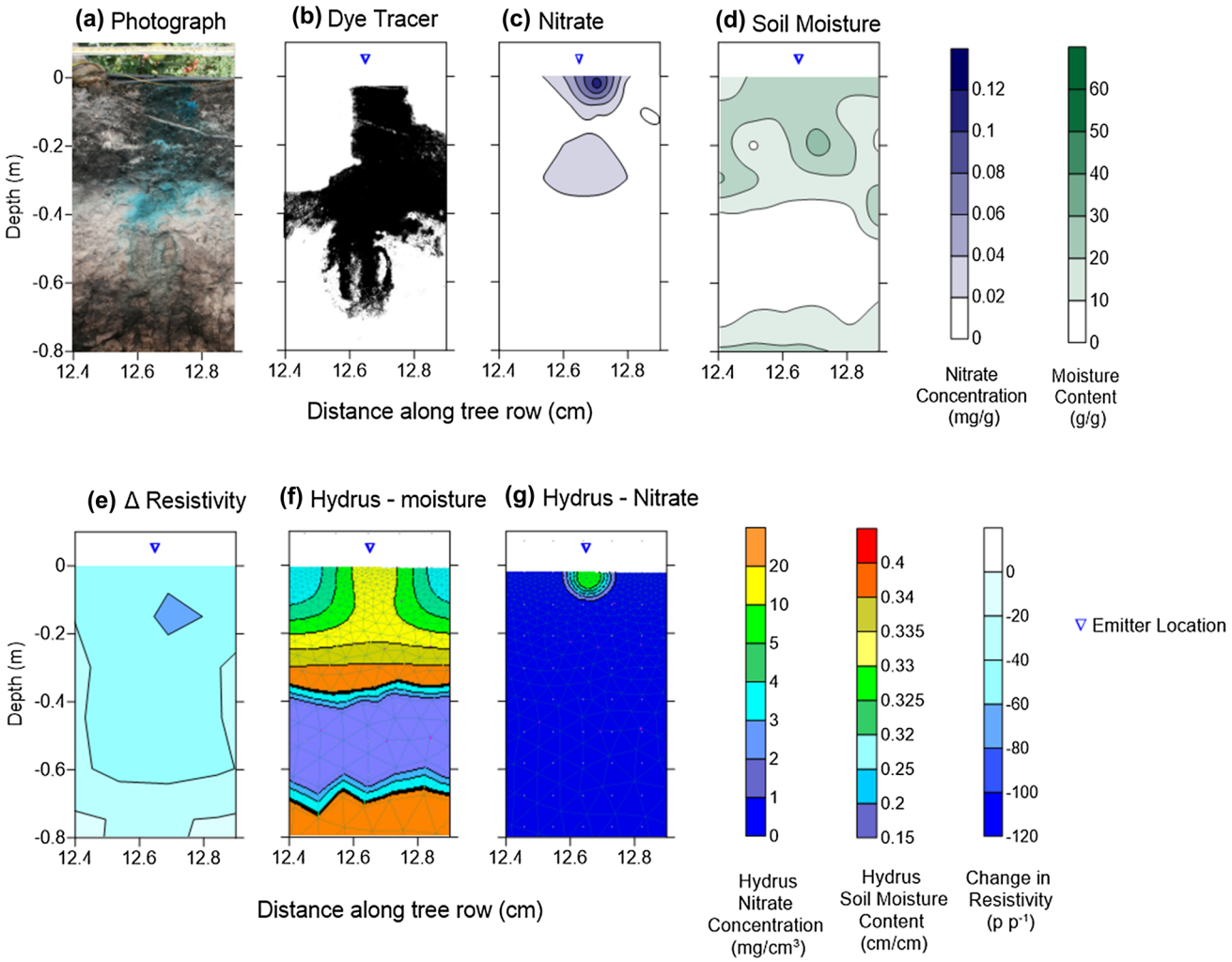

Fig. 3 Excavated emitter for the high irrigation treatment, **a** photograph of dye tracer stained soil profile, **b** extracted dye tracer pattern, **c** measured soil nitrate distribution, **d** measured soil moisture distribution, **e** ERI change in electrical resistivity 66 h after fertigation, **f** modelled (Hydrus-2D) soil moisture 66 h after fertigation, and **g** modelled (Hydrus-2D) soil nitrate 66 h after fertigation. Triangle marks location of emitter. (Color figure online)

In the low irrigation treatment, the dye tracer pattern (Fig. 4a, b) indicated that infiltration beneath the emitter resulted from preferential flow. The dye tracer pattern (Fig. 4b) showed that the fertigation ponded beneath the emitter and spread to the left along the soil surface where it infiltrated to only 0.03 m depth. Infiltration into the soil profile then occurred as a narrow finger which broadened with depth resulting in infiltration to 0.50 m depth (Fig. 4b).

The change in electrical resistivity (Fig. 4e) appeared to show increased electrical resistivity (decreased solute and moisture) immediately beneath the dripper to a depth of approximately 0.07 m, then a broad swale of decreased electrical resistivity (increased moisture and or solute) across the soil surface to a depth of approximately 0.20 m. The nitrate distribution pattern (Fig. 4c) was similar to that of the dye tracer (Fig. 4b) in that both demonstrate spreading along the soil surface and penetration into the near surface soil via a single narrow finger to the left of the emitter. Notably the nitrate did not penetrate as deep as the dye tracer. Unlike the high irrigation treatment, (Fig. 3c, g) in which the measured and modelled nitrate patterns appeared to be similar, in the low irrigation treatment the modelled nitrate concentration did not demonstrate spreading along the soil surface or the narrow deep infiltration through the A1 horizon (Fig. 4g).

Nitrate and soil water modelling

As expected, modelling indicated uniform and consistent infiltration of water and nitrate from each of the emitters (Fig. 5a). Twenty hours after fertigation, modelling predicted that fertigation had infiltrated to approximately 0.25 m depth, with minimal lateral dispersion away from the

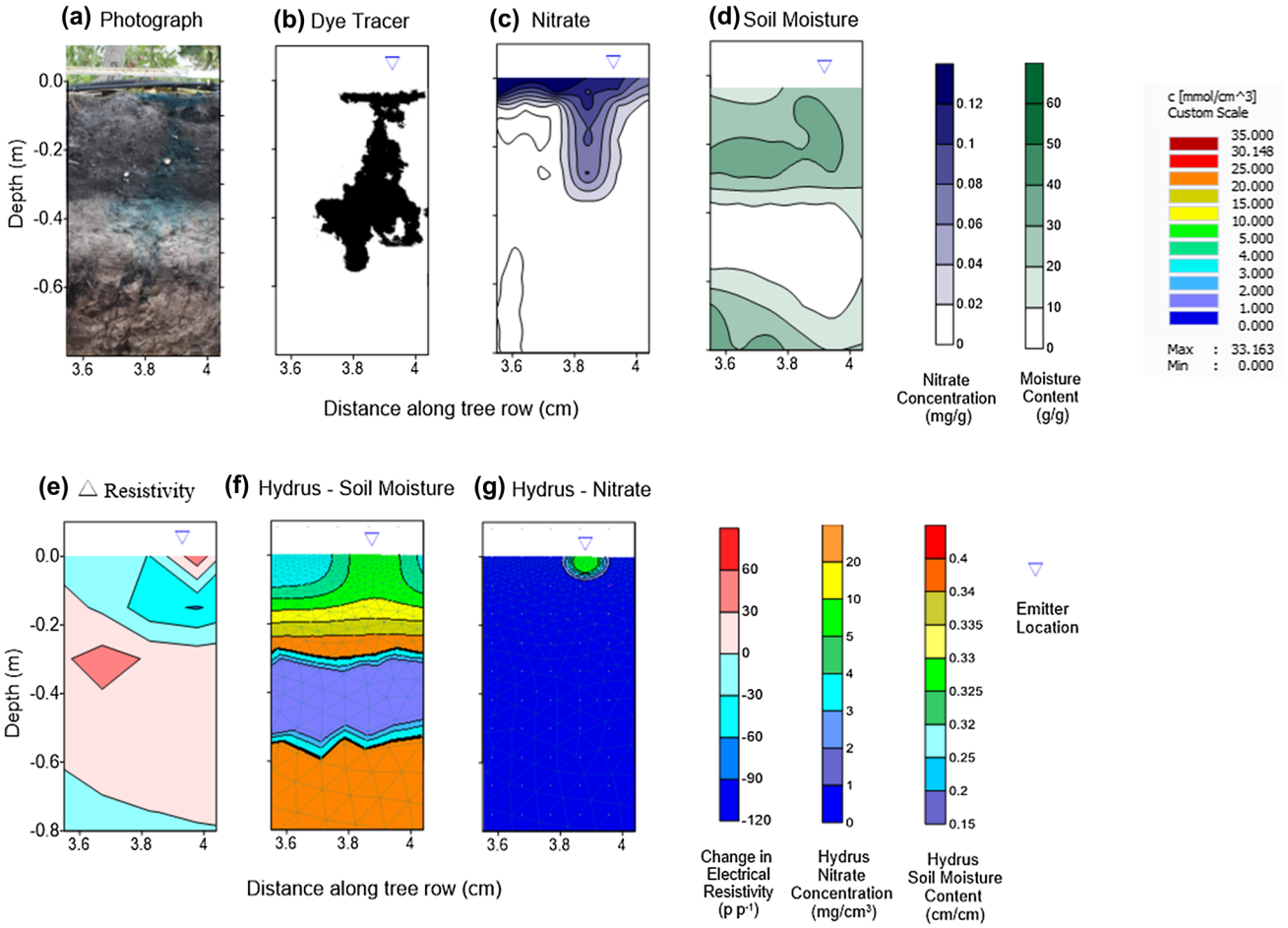

Fig. 4 Excavated emitter for the low irrigation treatment, **a** photograph of dye tracer stained soil profile, **b** extracted dye tracer pattern, **c** measured soil nitrate distribution, **d** measured soil moisture distribution, **e** ERI change in electrical resistivity 66 h after fertigation, **f** modelled (Hydrus-2D) soil moisture 66 h after fertigation, and **g** modelled (Hydrus-2D) soil nitrate 66 h after fertigation. Blue triangle marks location of emitter. (Color figure online)

emitters (Fig. 5a). However unlike the electrical resistivity (Fig. 2), the model did not indicate fertigation infiltrated into the B2 horizons via preferential flow (Fig. 5a). In keeping with the electrical resistivity, modelling indicated a slight reduction in the moisture content in the A2 and B22 horizons as a result of internal drainage. Yet, unlike the electrical resistivity, the modelling showed a slight accumulation of water at the A2/B21 soil boundary.

Sixty-six hours after fertigation, the model indicated the low irrigation treatment resulted in infiltration to approximately 0.35 m depth, and to 0.40 m depth for the high treatment (Fig. 5b). Modelling also demonstrated that emitter spacing was sufficient to adequately wet-up the remaining A1 horizon between emitters. This finding is in contrast to the ERI which demonstrated that little if any infiltration occurred beneath up to 6 of the emitters, and there was minimal wetting of the soil between the emitter plumes (Fig. 2c, d). Furthermore, the electrical resistivity 66 h after fertigation indicated preferential flow into the lower B22 horizon at emitters located 2.7 and 12.8 m from the first electrode, and into the A2 horizon at emitters located 9.3 and 10.8 m from the first electrode (Fig. 5a). These deeper infiltrations were not demonstrated by the model. The model indicated that the fertigated nitrate infiltrated to a depth of approximately 0.15 m depth in the area immediately beneath the emitters (Figs. 4g, 5c, d, g). Unlike the modelled soil moisture, these 'pockets' of nitrate remained discrete and did not form a continuous band within the A1 horizon, even after the subsequent irrigation event, which seemed to have diluted the nitrate concentration, rather than displaced the nitrate further down the soil profile (Fig. 5d).

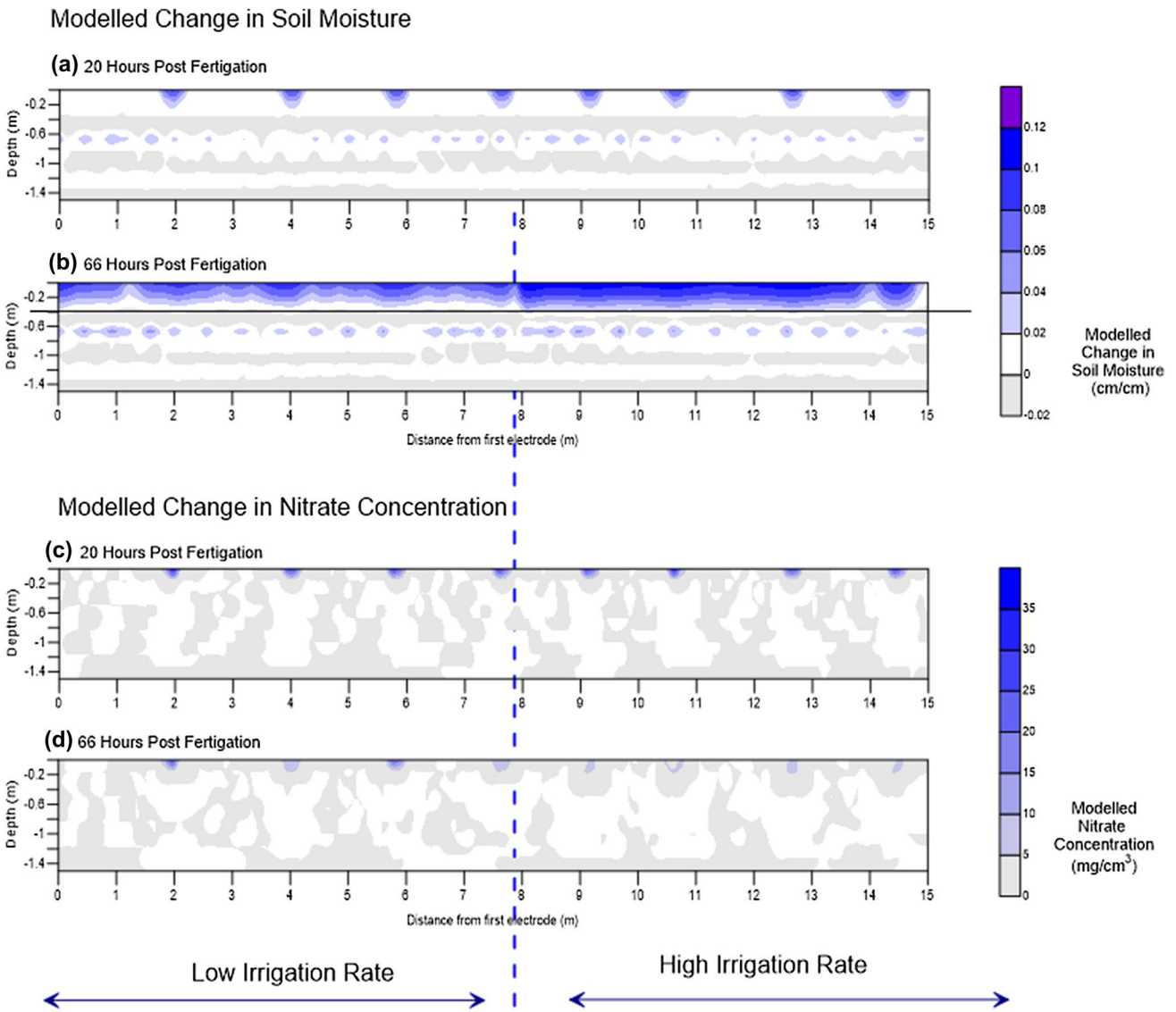

Fig. 5 Hydrus-2D modelled change in soil moisture, **a** 20 h after fertigation (before the irrigation), and **b** 66 h after fertigation. Hydrus-2D modelled nitrate concentration, **c** 20 h after fertigation (before the irrigation), and **d** 66 h after fertigation

Spatial associations between measured and modelled nitrate and soil moisture

In both irrigation treatments, the modelled soil moisture content was significantly lower ($p = 0.028$, 0.001) in the dye stained areas than in the unstained areas, the opposite of what was expected. In the high irrigation treatment, the dye stained areas had significantly ($p = 0.008$) lower change in electrical resistivity (wetter and more solute) than the unstained areas. In both the high and low treatments there was no significant difference in nitrate concentration, modelled nitrate concentration or moisture content between the dye stained and unstained areas (Table 2).

Change in electrical resistivity was significantly negatively correlated ($R^2 = 0.52$, $R^2 = 0.48$) with nitrate concentration in both the high and low irrigation treatments, and was significantly negatively correlated ($R^2 = 0.405$) with soil moisture, and the modelled soil moisture ($R^2 = 0.41$) in the low treatment (Table 2). The modelled soil moisture was significantly correlated with measured soil moisture in both the high and low irrigation treatments ($R^2 = 0.49$, $R^2 = 0.46$), and also with nitrate concentration ($R^2 = 0.283$) in the high treatment, and negatively correlated with electrical resistivity ($R^2 = 0.413$) in the low irrigation treatment (Table 2).

Multiple linear regression demonstrated that the change in electrical resistivity was most closely related to the

Table 2 Correlation between the change in electrical resistivity, measured and modelled soil moisture, and the measured and modelled nitrate distribution

	High irrigation treatment				Low irrigation treatment			
	Change in electrical resistivity	Measured nitrate concentration	Measured soil moisture	Modelled soil moisture	Change in electrical resistivity	Measured nitrate concentration	Measured soil moisture	Modelled soil moisture
Measured nitrate concentration	− 0.518**				− 0.480**			
Measured soil moisture	− 0.145	0.271*			− 0.405*	0.087		
Modelled soil moisture	0.199	0.283*	0.491**		− 0.413*	0.072	0.461**	
Modelled nitrate concentration	− 0.152	0.425**	0.244	0.107	− 0.005	0.346*	NA	− 0.016

NA not applicable, as the Hydrus solute distribution did not intersect the sampling points

*Denotes $P<0.05$, **denotes $P<0.001$

measured nitrate concentration (Beta = − 0.629, $P<0.0001$: Beta = − 0.537, $P=0.002$), followed by the modelled soil moisture (Beta = 0.392, $P=0.001$: Beta = − 0.331, $P=0.038$) in which the overall model fit was $R^2=0.41, 0.52$ for the high and low irrigation treatments respectively. No other variables were significant predictors.

Discussion

Comparison between ERI and Hydrus-2D

The ERI suggested that whilst most emitters resulted in infiltration to approximately 0.20 m depth, at two emitters infiltration penetrated to around 0.50 m depth, at a further two emitters infiltration penetrated to at least 1.0 m depth. In contrast up to 6 of the 26 emitters appeared to have had minimal if any infiltration. Checks confirmed all emitters were operating during the fertigation and irrigation events, such that we attributed the absence of infiltration beneath these 6 emitters to runoff to adjacent emitters, or runoff beyond the field of influence of the ERI due to either surface water repellence, compaction, or the presence of the surface leaf mulch. The variation in wetting patterns inferred from the ERI was somewhat greater than expected; however, drip irrigation systems are known to result in highly variable wetting patterns both horizontally and vertically (Cook et al. 2006b; Klein and Spieler 1987; Moreno et al. 2015).

The dye tracer experiments provided evidence to support findings from the ERI that infiltration beneath some of the emitters resulted from preferential flow processes. The dye tracer experiments indicated these processes to be finger flow in the A1 and A2 horizons, lateral flow along the A1/A2 soil horizon boundary, and bypass flow through shrinkage cracks and macropores in the B21 and B22 horizons. Similar preferential flow process have been reported in texture contrast soils by Hardie et al. (2011). Finger flow usually occurs in water repellent soils as a result of instability in the wetting front (Carrillo et al. 2000; Dekker and Ritsema 1996; Ritsema et al. 1998; Wang et al. 2000a, b), however, it may also form due to compression of entrapped soil air during infiltration (Wang et al. 1997, 1998b), or unsaturated infiltration at low application rates (Wang et al. 1998a; Yao and Hendrickx 1996). In both irrigation treatments the dye tracer appeared to have moved laterally along the A1/A2 soil horizon boundary as previously reported in other Tasmanian texture contrast soils (Hardie et al. 2011, 2013) rather than above the B2 horizons as is commonly cited in the literature (Eastham et al. 2000; Ticehurst et al. 2007).

By way of comparison to the ERI, the Hydrus-2D modelling indicated infiltration was relatively uniform and consistent between emitters within each of the two irrigation rate treatments. Furthermore the modelling indicated that for both treatments, the irrigation tended to wet-up the near surface soil between each of the emitters, which was not shown by the dye tracer or ERT studies. These results suggest that even with detailed site measurements, use of lumped parameter soil water models that do not consider non-equilibrium preferential flow process are unable to predict the depth and pattern of infiltration inferred from the ERI and dye tracer studies. Whilst Hydrus-2D and a number of other models have capacity to simulate preferential flow process, these models require additional parameters which are difficult to estimate without a priori knowledge of the type and extent of preferential flows. Furthermore while spatially explicit finite element models such as Hydrus-2D are able to be parameterized at very small scales, the amount of sampling and analysis required for such parameterization would be exhaustive, destructive, and not practical for assessment of irrigation performance in commercial orchards.

Comparison between approaches at the single emitter scale

The poorer than expected correlation between the change in electrical resistivity versus moisture content and or nitrate concentration at the single emitter scale were largely attributed to differences in measurement scale between the different approaches. For example, photogrammetry was able to discern the presence or absence of the dye tracer for individual 0.4 × 0.4 mm pixels, compared to the change in electrical resistivity which was determined from readings 250 × 250 mm apart, the nitrate concentration and soil moisture which were measured on a 200 mm × 200 mm grid, and the modelling which was conducted on cells spaced 20 mm to 50 mm apart. Koestel et al. (2009) also reported discrepancy between brilliant blue dye tracer concentration with 3D ERI, in which the ERI did not capture all the dye stained regions and underestimated sharp changes in solute concentration, which was in part attributed to the larger measurement scale of the ERI compared to the pixel size of the photographic images. Wehrer and Slater (2015) studied changes in soil moisture and solute transport in a large laboratory lysimeter using dye traces, 3D time-lapse electrical resistivity, tensiometers and capacitance soil moisture probes. They also reported that variations in water content over time were not exactly matched by the ERI, despite their ERI probes being spaced only 0.085 m apart, compared to 0.25 m in our study.

Infiltration of nitrate

Infiltration of nitrate into the A1 horizon was impeded relative to that of the dye tracer and therefore also the true wetting front. During infiltration movement of dye tracers is slower than that of the wetting front, due to absorption of the dye to soil particles, and thus the true wetting front is usually slightly ahead or deeper than indicated by dye staining patterns (Lipsius and Mooney 2006; Mon and Flury 2005). Anions such as nitrate are normally assumed to not become adsorbed by soil particles (Kowalenko and Yu 1996) and are therefore easily leached (Nováková and Nágel 2009), in which case the nitrate distribution should have been very similar to that of the wetting front and or slightly deeper than that of the dye tracer. Our findings that movement of nitrate during fertigation was impeded or moved more slowly than the infiltrating water is contradictory to expectations, but it is not unprecedented. As van der Laan et al. (2014) explains impeded movement of nitrate during infiltration may result from the presence of immobile water phases arising from the range in pore water velocities associated with the infiltrating water (Alletto et al. 2006; Clothier et al. 1995; Jarvis 2007) and or adsorption of nitrate to soil, most notably in tropical or acid soils (Kowalenko and Yu 1996).

Irrigation and fertigation efficiency

In recent years there has been growing concern about the potential for preferential flow to facilitate nitrate mobilisation to groundwater (Hu et al. 2015; Sheng et al. 2014; Smethurst et al. 2014; Williams et al. 2014). The ERI suggested that for all but two emitters, irrigation was largely restricted to the A1 and A2 horizons (approximately 0–0.40 m depth) which coincided with the highest observed root abundance at 0.30–0.35 m depth. Consequently, on a single event basis, irrigation and fertigation appeared to be highly effective and efficient. Furthermore even in the presence of preferential flows the fertigated nitrate appeared to be mostly retained in the A1 horizon. Consequently contamination risk or hazard posed by the presence of preferential flow processes transporting nitrate to shallow groundwater are somewhat less than what would otherwise be expected.

Conclusion

The ERI approach was a useful means of revealing spatial and temporal variations in infiltration patterns following drip fertigation and irrigation in a texture contrast soil. The ERI cross section demonstrated considerable variation in infiltration patterns and depth of infiltration between emitters, including infiltration to over 1.0 m depth, and no infiltration at all. These wetting patterns and those of the dye tracer differed markedly to those predicted by the model and 'texture based' emitter guidelines. Consequently results from this study suggest the use of 'texture based' emitter guidelines, and or lumped parameter soil water models are not supported for predicting emitter wetting patterns or designing irrigation systems in the texture contrast soils.

Uncalibrated use of ERI was unable to discern if changes in resistivity were due to changes in temperature, moisture or solute concentration. However simultaneous ERI, dye tracer and modelling studies revealed that changes in electrical resistivity were more strongly influenced by nitrate concentration than soil moisture content. Furthermore the dye tracer studies revealed that most of the fertigated nitrate was retained within the A1 horizon, whereas the infiltrating water penetrated through the A1 horizon, into the A2 and upper B2 horizons. Poor correlation between predicted nitrate and infiltration patterns versus and those revealed by the dye tracer and ERT studies were due to, differences in measurement scale between approaches, the limited ability of the model to simulate preferential flow process, and inability to parameterize the model at the individual emitter scale. To this end, results from this study indicate the potential to use small scale ERT surveys to improve model parameterization.

Acknowledgements The authors would like to thank the owners of the orchards for their considerable assistance during the monitoring of the orchards; Andrew Griggs of Lucaston Park Orchards at Lucaston. We would like to thank Dr Michael Roach for assistance with the ERI, Garth Oliver, Justin Direen and Abbas Almajmaie for assistance with field work. This project has been funded by Horticulture Australia Ltd under the 'Productivity, Irrigation, Pests and Soils' (PIPS) program, using the apple and pear industry levy, voluntary contributions from the New Zealand Institute for Plant and Food Research, and matched funds from the Australian Government.

References

Abramoff MD, Magelhaes PJ, Ram SJ (2004) Image processing with ImageJ. Biophotonics Int 11:36–42

Algeo J, Van Dam RL, Slater L (2016) Early-time GPR: a method to monitor spatial variations in soil water content during irrigation in clay soils. Vadose Zone J. https://doi.org/10.2136/vzj2016.03.0026

Alletto L, Coquet Y, Vachier P, Labat C (2006) Hydraulic conductivity, immobile water content, and exchange coefficient in three soil profiles. Soil Sci Soc Am J 70:1272–1280

Bar-Yosef B, Schwartz S, Markovich T, Lucas B, Assaf R (1988) Effect of root volume and nitrate solution concentration on growth, fruit yield, and temporal N and water uptake rates by apple trees. Plant Soil 107:49–56

BOM (2015) Climate statistics for Australian locations: Grove, Tasmania. Bureau of Meterology. http://www.bom.gov.au/climate/averages/tables/cw_094069.shtml. Accessed Jan 2015

Carrillo MLK, Letey J, Yates SR (2000) Unstable water flow in a layered soil: I. effects of a stable water-repellent layer. Soil Sci Soc Am J 64:450–455

Cassiani G, Boaga J, Vanella D, Perri MT, Consoli S (2015) Monitoring and modelling of soil–plant interactions: the joint use of ERT, sap flow and eddy covariance data to characterize the volume of an orange tree root zone. Hydrol Earth Syst Sci 19:2213–2225. https://doi.org/10.5194/hess-19-2213-2015

Cassiani G, Boaga J, Rossi M, Putti M, Fadda G, Majone B, Bellin A (2016) Soil–plant interaction monitoring: small scale example of an apple orchard in Trentino, North-eastern Italy. Sci Total Environ 543:851–861. https://doi.org/10.1016/j.scitotenv.2015.03.113

Chittleborough DJ, Smettem KRJ, Kirkby C (1994) Clay, phosphate and water movement through a texture contrast soil. Land and Water Resource Research and Development Corporation, for Project UAD1, LWRRC, Canberra

Clothier B, Heng L, Magesan G, Vogeler I (1995) The measured mobile-water content of an unsaturated soil as a function of hydraulic regime. Soil Res 33:397–414 doi. https://doi.org/10.1071/SR9950397

Clothier BE, Green SR, Deurer M (2008) Preferential flow and transport in soil: progress and prognosis. Eur J Soil Sci 59:2–13 https://doi.org/10.1111/j.1365-2389.2007.00991.x

Consoli S, Stagno F, Vanella D, Boaga J, Cassiani G, Roccuzzo G (2017) Partial root-zone drying irrigation in orange orchards: effects on water use and crop production characteristics. Eur J Agron 82:190–202. https://doi.org/10.1016/j.eja.2016.11.001

Cook FJ, Thorburn PJ, Fitch P, Bristow KL (2003) WetUp: a software tool to display approximate wetting patterns from drippers. Irrig Sci 22:129–134. https://doi.org/10.1007/s00271-003-0078-2

Cook FJ, Fitch P, Thorburn PJ, Charlesworth PB, Bristow KL (2006a) Modelling trickle irrigation: comparison of analytical and numerical models for estimation of wetting front position with time. Environ Model Softw 21:1353–1359. https://doi.org/10.1016/j.envsoft.2005.04.018

Cook FJ, Jayawardane NS, Rassam DW, Christen EW, Hornbuckle JW, Stirzaker RJ, Bristow KL, Biswas TK (2006b) The state of measuring, diagnosing, ameliorating and managing solute effects in irrigated systems. Technical Report No. 04/06, CRC for Irrigation Futures

Coppola A et al (2016) Calibration of an electromagnetic induction sensor with time-domain reflectometry data to monitor rootzone electrical conductivity under saline water irrigation. Eur J Soil Sci 67:737–748. https://doi.org/10.1111/ejss.12390

Cotching WE, Lynch S, Kidd DB (2009) Dominant soil orders in Tasmania: distribution and selected properties. Soil Res 47:537–548. https://doi.org/10.1071/SR08239

Cote CM, Bristow KL, Charlesworth PB, Cook FJ, Thorburn PJ (2003) Analysis of soil wetting and solute transport in subsurface trickle irrigation. Irrig Sci 22:143–156

Dekker LW, Ritsema CJ (1996) Uneven moisture patterns in water repellent soils. Geoderma 70:87–99

Devasirvatham V (2009) A review of subsurface drip irrigation in vegetable production, vol CRC. Irrigation futures irrigation matters series no. 03/09. CRC for Irrigation Futures

Durner W (1994) Hydraulic conductivity estimation for soils with heterogeneous pore structure. Water Resour Res 30:211–223

Eastham J, Gregory PJ, Williamson DR (2000) A spatial analysis of lateral and vertical fluxes of water associated with a perched watertable in a duplex soil. Austr J Soil Res 38:879–890

El-Nesr MN, Alazba AA, Šimůnek J (2014) HYDRUS simulations of the effects of dual-drip subsurface irrigation and a physical barrier on water movement and solute transport in soils. Irrig Sci 32:111–125. https://doi.org/10.1007/s00271-013-0417-x

FAO (1997) Small-scale irrigation for arid zones. Principles and options. Food and Agriculture Organisation of the United Nations (FAO), Rome

Flury M, Fluhler H, Jury WA, Leuenberger J (1994) Susceptibility of soils to preferential flow of water: a field study. Water Resour Res 30:1945–1954

Furman A, Ferré TPA, Warrick AW (2003) A sensitivity analysis of electrical resistivity tomography array types using analytical element modeling. Vadose Zone J 2:416–423

Gärdenäs AI, Hopmans JW, Hanson BR, Šimůnek J (2005) Two-dimensional modeling of nitrate leaching for various fertigation scenarios under micro-irrigation. Agric Water Manag 74:219–242. https://doi.org/10.1016/j.agwat.2004.11.011

Gerke HH, Germann P, Nieber J (2010) Preferential and unstable flow: from the pore to the catchment scale. Vadose Zone J 9:207–212. https://doi.org/10.2136/vzj2010.0059

Golden Software (2002) Surfer user guide: contouring and 3D surface mapping for scientists and engineers. Colorado

Goldy R (2012) Soil type influences irrigation strategy. Michigan State University extension. http://msue.anr.msu.edu/news/soil_type_influences_irrigation_strategy

Han X et al (2016) Simultaneous soil moisture and properties estimation for a drip irrigated field by assimilating cosmic-ray neutron intensity. J Hydrol 539:611–624. https://doi.org/10.1016/j.jhydrol.2016.05.050

Hardie MA, Cotching WE, Doyle RB, Holz G, Lisson S, Mattern K (2011) Effect of antecedent soil moisture on preferential flow in a texture-contrast soil. J Hydrol 398:191–201. https://doi.org/10.1016/j.jhydrol.2010.12.008

Hardie MA, Mitchelson H, Doyle R (2012) Efficiency and efficacy of drip irrigation in a Tasmanian Vineyard Irrigation performance was determined by dye tracer staining, soil hydraulic assessment and modelling. In: Paper presented at the proceedings of the 5th joint soil science Australia and New Zealand society of soil science conference, Hobart, 2–7 Dec 2012

Hardie M, Doyle R, Cotching W, Holz G, Lisson S (2013) Hydropedology and preferential flow in the Tasmanian texture-contrast soils. Vadose Zone J. https://doi.org/10.2136/vzj2013.03.0051

Hossain MB, Lamb DW, Lockwood PV, Frazier P (2010) EM38 for volumetric soil water content estimation in the root-zone of deep vertosol soils. Comput Electron Agric 74:100–109. https://doi.org/10.1016/j.compag.2010.07.003

Hu H, Mao X, Barry DA, Liu C, Li P (2015) Modeling reactive transport of reclaimed water through large soil columns with different low-permeability layers. Hydrogeol J 23:351–364. https://doi.org/10.1007/s10040-014-1187-0

Hung J (1995) Determination of emitter spacing and irrigation run time including plant root depth. In: Lamm FR (ed) Microirrigation for a changing world: conserving resources/preserving the environment. Proceedings of the fifth international microirrigation congress, Orlando, 2–6 Apr 1995. ASAE, St. Joseph, pp 292–296

Isbell RF (2002) The Australian soil classification, vol 4. Australian soil and land survey series. CSIRO Publishing, Melbourne

Jarvis NJ (2007) A review of non-equilibrium water flow and solute transport in soil macropores: principles, controlling factors and consequences for water quality. Eur J Soil Sci 58:523–546

Kandelous MM, Šimůnek J (2010) Comparison of numerical, analytical, and empirical models to estimate wetting patterns for surface and subsurface drip irrigation. Irrig Sci 28:435–444. https://doi.org/10.1007/s00271-009-0205-9

Klein I, Spieler G (1987) Fertigation of apples with nitrate or ammonium nitrogen under drip irrigation. II. Nutrient distribution in the soil 1. Commun Soil Sci Plant Anal 18:323–339

Klein I, Levin I, Bar-Yosef B, Assaf R, Berkovitz A (1989) Drip nitrogen fertigation of 'Starking delicious' apple trees. Plant Soil 119:305–314. https://doi.org/10.1007/bf02370423

Koestel J, Kasteel R, Kemna A, Esser O, Javaux M, Binley A, Vereecken H (2009) Imaging brilliant blue stained soil by means of electrical resistivity tomography. Vadose Zone J 8:963–975. https://doi.org/10.2136/vzj2008.0180

Kowalenko CG, Yu S (1996) Assessment of nitrate adsorption in soils by extraction, equilibration and column-leaching methods. Can J Soil Sci 76:49–57

Li X, Shi H, Šimůnek J, Gong X, Peng Z (2015) Modeling soil water dynamics in a drip-irrigated intercropping field under plastic mulch. Irrig Sci 33:289–302. https://doi.org/10.1007/s00271-015-0466-4

Lipsius K, Mooney SJ (2006) Using image analysis of tracer staining to examine the infiltration patterns in a water repellent contaminated sandy soil. Geoderma 136:865–875

Loke M (2010) RES2DINV ver 3.59 User Manual. Geotomo Software, Gelugor, Malaysia

McKenzie NJ, Coughlan KL, Cresswell HP (2002) Soil physical measurement and interpretation for land evaluation. CSIRO Publishing, Melbourne

Mguidiche A, Provenzano G, Douh B, Khila S, Rallo G, Boujelben A (2015) Assessing hydrus-2D to simulate soil water content (SWC) and salt accumulation under an SDI system: application to a potato crop in a semi-arid area of Central Tunisia. Irrig Drain 64:263–274. https://doi.org/10.1002/ird.1884

Michot D, Benderitter Y, Dorigny A, Nicoullaud B, King D, Tabbagh A (2003) Spatial and temporal monitoring of soil water content with an irrigated corn crop cover using surface electrical resistivity tomography. Water Resour Res 39:SBH141–SBH1420

Miller CR, Routh PS, Brosten TR, McNamara JP (2008) Application of time-lapse ERT imaging to watershed characterization. Geophysics 73:G7–G17. https://doi.org/10.1190/1.2073888

Misra RK, Padhi J (2014) Assessing field-scale soil water distribution with electromagnetic induction method. J Hydrol 516:200–209. https://doi.org/10.1016/j.jhydrol.2014.02.049

Mon J, Flury M (2005) Dyes as hydrological tracers. In: Lehr JH, Keeley J, Lehr J (eds) Encyclopedia of water. Wiley, New York

Moreno Z, Arnon-Zur A, Furman A (2015) Hydro-geophysical monitoring of orchard root zone dynamics in semi-arid region. Irrig Sci 33:303–318. https://doi.org/10.1007/s00271-015-0467-3

Naglič B, Kechavarzi C, Coulon F, Pintar M (2014) Numerical investigation of the influence of texture, surface drip emitter discharge rate and initial soil moisture condition on wetting pattern size. Irrig Sci 32:421–436. https://doi.org/10.1007/s00271-014-0439-z

Nováková K, Nágel D (2009) The influence of irrigation on nitrates movement in soil and risk of subsoil contamination. Soil Water Res 4:S131–S136

O'Dell J (1993) Method 353.2, Revision 2.0: Determination of nitrate-nitrite nitrogen by automated colorimetry. Environmental Monitoring Systems Laboratory, U.S. Environmental Protection Agency, Cincinnati, Ohio

Persson M, Dahlin T, Günther T (2015) Observing solute transport in the capillary fringe using image analysis and electrical resistivity tomography in laboratory experiments. Vadose Zone J. https://doi.org/10.2136/vzj2014.07.0085

Peters A, Durner W (2008) Simplified evaporation method for determining soil hydraulic properties. J Hydrol 356:147–162

Phogat V, Skewes MA, Cox JW, Alam J, Grigson G, Šimůnek J (2013) Evaluation of water movement and nitrate dynamics in a lysimeter planted with an orange tree. Agric Water Manag 127:74–84. https://doi.org/10.1016/j.agwat.2013.05.017

Phogat V, Skewes MA, Cox JW, Sanderson G, Alam J, Šimůnek J (2014) Seasonal simulation of water, salinity and nitrate dynamics under drip irrigated mandarin (*Citrus reticulata*) and assessing management options for drainage and nitrate leaching. J Hydrol 513:504–516. https://doi.org/10.1016/j.jhydrol.2014.04.008

Puy A, García Avilés JM, Balbo AL, Keller M, Riedesel S, Blum D, Bubenzer O (2016) Drip irrigation uptake in traditional irrigated fields: the edaphological impact. J Environ Manag. https://doi.org/10.1016/j.jenvman.2016.07.017

Rayment GE, Higginson FR (1992) Australian laboratory handbook of soil and water chemical methods. Australian soil and land survey handbook. Inkata Press, Melbourne

Ritsema CJ, Dekker LW, Nieber JL, Steenhuis TS (1998) Modeling and field evidence of finger formation and finger recurrence in a water repellent sandy soil. Water Resour Res 34:555–567

Roth K (2008) Scaling of water flow through porous media and soils. Eur J Soil Sci 59:125–130. https://doi.org/10.1111/j.1365-2389.2007.00986.x

Samouëlian A, Cousin I, Tabbagh A, Bruand A, Richard G (2005) Electrical resistivity survey in soil science: a review. Soil Tillage Res 83:173–193

Satriani A, Loperte A, Soldovieri F (2015) Integrated geophysical techniques for sustainable management of water resource. A case study of local dry bean versus commercial common bean cultivars. Agric Water Manag 162:57–66. https://doi.org/10.1016/j.agwat.2015.08.010

Shamir O, Goldshleger N, Basson U, Reshef M (2016) Mapping spatial moisture content of unsaturated agricultural soils with ground-penetrating radar. International archives of the photogrammetry, remote sensing and spatial information sciences—ISPRS archives, pp 1279–1285. https://doi.org/10.5194/isprsarchives-XLI-B8-1279-2016

Sheng F, Liu H, Wang K, Zhang R, Tang Z (2014) Investigation into preferential flow in natural unsaturated soils with field multiple-tracer infiltration experiments and the active region model. J Hydrol 508:137–146. https://doi.org/10.1016/j.jhydrol.2013.10.048

Šimůnek J, van Genuchten MT (2007) Chap. 22: contaminant transport in the unsaturated zone: theory and modelling. In: Delleur JW (ed)

The handbook of groundwater engineering, 2nd edn. CRC Press, Boca Raton, pp 22.21–22.38

Šimůnek J, Jarvis NJ, van Genuchten MT, Gardenas A (2003) Review and comparison of models for describing non-equilibrium and preferential flow and transport in the vadose zone. J Hydrol 272:14–35

Šimůnek J, van Genuchten MT, Sejna M (2008) Development and applications of the HYDRUS and STANMOD software packages and related codes. Vadose Zone J 7:587–600

Šimůnek J, Van Genuchten MT, Šejna M (2012) Hydrus: model use, calibration, and validation. Trans ASABE 55:1261–1274

Šimůnek J, Jacques D, Langergraber G, Bradford SA, Šejna M, Van Genuchten MT (2013) Numerical modeling of contaminant transport using HYDRUS and its specialized modules. J Indian Inst Sci 93:265–284

Šimůnek J, van Genuchten MT, Šejna M (2016) Recent developments and applications of the HYDRUS computer software packages. Vadose Zone J. https://doi.org/10.2136/vzj2016.04.0033

Smethurst PJ, Petrone KC, Langergraber G, Baillie CC, Worledge D, Nash D (2014) Nitrate dynamics in a rural headwater catchment: measurements modelling. Hydrol Process 28:1820–1834. https://doi.org/10.1002/hyp.9709

Souza CF, Folegatti MV (2008) Characterization spatial and temporal patterns of water and solute distribution. American Society of Agricultural and Biological Engineers. Annual international meeting 2008, ASABE 2008,. pp 2327–2339

Subbaiah R (2013) A review of models for predicting soil water dynamics during trickle irrigation. Irrig Sci 31:225–258. https://doi.org/10.1007/s00271-011-0309-x

Thorburn PJ, Cook FJ, Bristow KL (2003) Soil-dependent wetting from trickle emitters: implications for system design and management. Irrig Sci 22:121–127. https://doi.org/10.1007/s00271-003-0077-3

Ticehurst JL, Cresswell HP, McKenzie NJ, Glover MR (2007) Interpreting soil and topographic properties to conceptualise hillslope hydrology. Geoderma 137:279–292

UMS (2013) HYPROP user manual. UMS GmbH München, Art. no. HYPROP

van der Laan M, Annandale JG, Bristow KL, Stirzaker RJ, Du Preez CC, Thorburn PJ (2014) Modelling nitrogen leaching: are we getting the right answer for the right reason? Agric Water Manag 133:74–80. https://doi.org/10.1016/j.agwat.2013.10.017

Wang Z, Feyen J, Nielsen DR, Van Genuchten MT (1997) Two-phase flow infiltration equations accounting for air entrapment effects. Water Resour Res 33:2759–2767

Wang Z, Feyen J, Ritsema CJ (1998a) Susceptibility and predictability of conditions for preferential flow. Water Resour Res 34:2169–2182

Wang Z, Feyen J, van Genuchten MT, Nielsen DR (1998b) Air entrapment effects on infiltration rate and flow instability. Water Resour Res 34:213–222

Wang Z, Wu L, Wu QJ (2000a) Water-entry value as an alternative indicator of soil water-repellency and wettability. J Hydrol 231–232:76–83

Wang Z, Wu QJ, Wu L, Ritsema CJ, Dekker LW, Feyen J (2000b) Effects of soil water repellency on infiltration rate and flow instability. J Hydrol 231–232:265–276

Wang Z, Li J, Li Y (2014) Simulation of nitrate leaching under varying drip system uniformities and precipitation patterns during the growing season of maize in the North China Plain. Agric Water Manag 142:19–28. https://doi.org/10.1016/j.agwat.2014.04.013

Wehrer M, Slater LD (2015) Characterization of water content dynamics and tracer breakthrough by 3-D electrical resistivity tomography (ERT) under transient unsaturated conditions. Water Resour Res 51:97–124. https://doi.org/10.1002/2014WR016131

Wendroth O, Ehlers W, Hopmans JW, Kage H, Halbertsma J, Wosten JHM (1993) Reevaluation of the evaporation method for determining hydraulic functions in unsaturated soils. Soil Sci Soc Am J 57:1436–1443

Williams MR, Buda AR, Elliott HA, Hamlett J, Boyer EW, Schmidt JP (2014) Groundwater flow path dynamics and nitrogen transport potential in the riparian zone of an agricultural headwater catchment. J Hydrol 511:870–879. https://doi.org/10.1016/j.jhydrol.2014.02.033

Yao TM, Hendrickx JMH (1996) Stability of wetting fronts in dry homogeneous soils under low infiltration rates. Soil Sci Soc Am J 60:20–28

Zhu Z, Tan L, Gao S, Jiao Q (2014) Observation on soil moisture of irrigation cropland by cosmic-ray probe. IEEE Geosci Remote Sens Lett 12:472–476. https://doi.org/10.1109/LGRS.2014.2346784

Measurement of sap flow in young apple trees using the average gradient heat-pulse method

S.R. Green[1,a], G. Oliver[2], N. Swarts[2], M. Hardie[2], B.E. Clothier[1] and D. Close[2]

[1]Plant and Food Research Institute, Palmerston North, Manawatu, New Zealand; [2]Tasmanian Institute of Agriculture, University of Tasmania, Hobart, Tasmania, Australia.

Abstract

The average gradient heat-pulse method (CHMP-AG) has been used to monitor sap flow in very young (1-year-old) apple trees, from budburst through until leaf fall. Data are presented to illustrate how CHPM-AG can resolve the full range of sap flux densities in these small trees. The methodology has been implemented by making a very simple software change to existing CHPM instrumentation.

Keywords: irrigation, transpiration, crop ET, modelling

INTRODUCTION

There is a lot of interest from the sap-flow scientific community in being able to measure low and reverse flows in the stems and roots of woody plants. Low flows are of particular interest at night for they can provide evidence of a recharge of the plant's water status (Oliveira et al., 2005) and may also provide an early indicator of plant water stress (Fuentes et al., 2009). Reverse flows, particularly in roots, are also of interest to quantify the redistribution of water from wetter to drier parts of the root-zone (Burgess et al., 2001; Ferreira et al, 2018).

We have used the compensation heat-pulse technique (CHPM; Marshall, 1958; Swanson and Whitfield, 1981) to study sap flow in the orchard trees for more than 30 years. During that time, we have developed instrumentation that is simple, probes that are robust, and measurements that are reliable and accurate (Green and Clothier, 1988; Green et al., 2003). The compensation method uses two temperature probes placed asymmetrically either side of a line heater that is radially inserted into the tree stem. Following the application of a brief heat-pulse (e.g., 100 J over 2-4 s), the time delay for an equal temperature rise at both sensors is used to calculate a heat-pulse velocity (V_H). A theoretically-derived calibration factor is then used to correct the heat-pulse measurements (V_C) for any probe-induced effects of wounding (Green et al., 2009). The technique is theoretically sound and practically simple. However, the CHPM has a recognised poor resolution at low flows (<3 cm h^{-1}) and there is no way to measure reverse flow using the standard CHPM analysis.

Testi and Villalobos (2009) reported a modification of the CHPM, called the "calibrated average gradient" (CAG) method. The CAG method consists of averaging the temperature difference signal (ΔTa) after the heat-pulse is applied, then deriving an empirical function $V_C = f(\Delta Ta)$ that is linear in the low-flow domain (10 cm $h^{-1} < V_C < 25$ cm h^{-1}) where V_C is still measurable with the traditional CHPM. The calibrated function depends only on the sensor characteristics and the thermal properties of the wood (Green and Romero, 2012). Moreover, it can be implemented with only a simple change to the analysis software and without changing any of the hardware.

This paper presents a selection of data from a field study of the water and nutrient balance of young apples trees. We describe how sap flow was measured using the CHPM-AG method. We also show how the trunk sap flow is related to the prevailing microclimate. The overall goal of our measurements is to obtain parameters (i.e., a crop factor) to model the soil water balance of the apple orchard.

[a]E-mail: Steve.Green@plantandfood.co.nz

MATERIALS AND METHODS

Study area

Field experiments were carried out during the growing season of 2016/17 using 1-year-old (non-fruiting) trees at the Lucaston orchard near Hobart in Tasmania (42.96°S; 147.02°E). The trees are *Malus* × *domestica* 'Scilate' (Trade name Envy™) on root stock 102. They were planted in the winter of 2015 and had been in the ground for one year prior to instrumentation. The orchard block is planted at a spacing of 1.2 m, in north facing rows spaced at 3.2 m. This is a high-density planting of new trees on a dwarfing rootstock.

Irrigation was set at the grower-applied rate using pressure-compensated drippers, spaced at 50 cm along the tree line. A single rain gauge was placed under one of the drippers to monitor the irrigation volumes. A weather station was located in a neighbouring block, some 100 m away, to record the local microclimate (global shortwave radiation, air temperature, relative humidity, wind speed and rainfall) once every 30 min. Our measurements span the period from just after budburst until just prior to leaf fall, i.e., the complete growing season.

Transpiration

Six neighbouring apple trees were instrumented shortly after bud-burst (a mid-November installation date). Single sets of heat-pulse probes (model HP2TC, Tranzflo NZ Ltd, Palmerston North, New Zealand) were placed in the tree stems, which varied in diameters of between 30 and 40 mm, including bark of 2 mm thickness. The sensors were made from 19-g stainless hypo-tube with thermocouples at depths of 5 and 15 mm. The probes were installed at a height of approximately 0.75 m above the soil surface, and they were positioned using the standard spacing of 5 mm upstream and 10 mm downstream from the heater probe. The tree stem was then wrapped in aluminium foil for thermal insulation.

The transpiration rate (T, L day^{-1}) was measured using our standard compensation heat-pulse method (Green and Clothier, 1988) to resolve sap flux densities J_S > 5 cm h^{-1}). The average-gradient method (Testi and Villalobos, 2009) was used to resolve the flows J_S < 5 cm h^{-1}. In practice, the power output from the heaters was regulated to deliver the same amount of heat energy (50 J) each time the heaters were fired. This was achieved by measuring the supply voltage just prior to heating, and then adjusting the heating time to deliver the requisite amount of heat energy.

A Campbell data logger (model CR1000, Campbell Scientific, Logan, USA) was used to control the heater output and then measure the cross-over time (t_Z, s) following the application of a 2.0-s heat pulse. We also recorded the average temperature-difference signal, ΔT, over the time interval 0 to 90 s.

Sap flow was calculated from t_Z values using the approach outlined by Green et al. (2003, 2009). These calculations included a correction for the effect of wounding. A wound diameter of 2.0 mm was assumed for the 1.6 mm diameter drill holes used. This is the same wound factor that we have previously used for apples (Green and Clothier, 1988).

Trunk sap flow (T, L h^{-1}) was determined by multiplying the depth-wise pattern of SFD by the relative area of conducting sapwood using the simple annulus approach suggested by Hatton et al. (1990). Data were collected at 30-min interval throughout the entire growing season.

Weather station and ET_0 estimates

A weather station was located at the site to measure global solar radiation (LI200, Licor, USA), air temperature and relative humidity (HMP60, Vaisala, Sweden), wind speed at 3 m (Maximum, USA), and rainfall (Pronamic, Denmark) using a Campbell data logger (model CR1000). The weather data were used to estimate hourly and daily values of the reference evapotranspiration (ETo) using the standard crop-factor approach (FAO-56; Allen et al., 1998). The transpiration of the apple trees is related to ET_0 through the dimensionless crop factor, K_C:

$$ET_C = K_C . ET_O \quad (1)$$

where ET_C is the crop water use and K_C is found from the ratio of the measured daily sap flow to the corresponding daily evaporative demand.

RESULTS AND DISCUSSION

Firstly, we examine the ΔT signals that quantify the temperature gradient between the upstream (closer to the heater) and the downstream (further from the heater) sensors. Values of ΔT averaged over the first 90 s are strongly correlated with V_C measured by the CHPM (Figure 1). The relationship is a very stable across the five months of measurements. A three-day time-centred filter was used to calculate a new response function for each day. The CHPM-AG data show no significant short-term drifts over time. Furthermore, over the course of the growing season we observed a very high correlation coefficient (r^2>98%), which indicates a very stable relationship between V_C and f(ΔT).

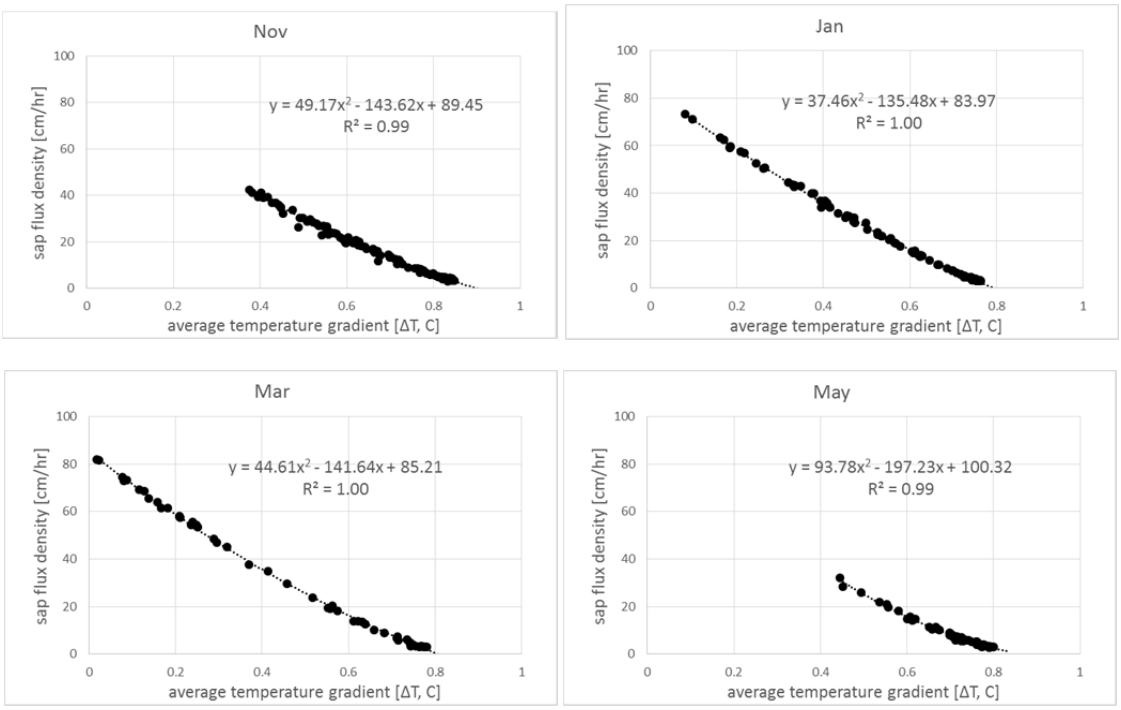

Figure 1. The functional relationship between sap flux density (V_C) measured by CHPM and the average temperature gradient (ΔT) recorded during the first 90 s following the application of a heat-pulse.

Figure 2 shows the diurnal pattern of sap flux density (i.e., tree water use divided by trunk cross-section) recorded during late February and early March in one of the trees. During these twelve days any nocturnal sap flows were typically close to zero. At first sight there seems to be almost no benefit in using the revised CHPM-AG method, rather than the standardized CHPM method, since the nocturnal flows on these days were typically very low. During the daytime, recorded sap flows were much higher than we had expected, given the low leaf area of these young trees. The peak sap flux densities were relatively high (>90 cm h^{-1}) and in a range that the alternative heat-ratio method (HRM) would not be able to resolve (Madurapperuma et al., 2009; Green and Romero, 2012).

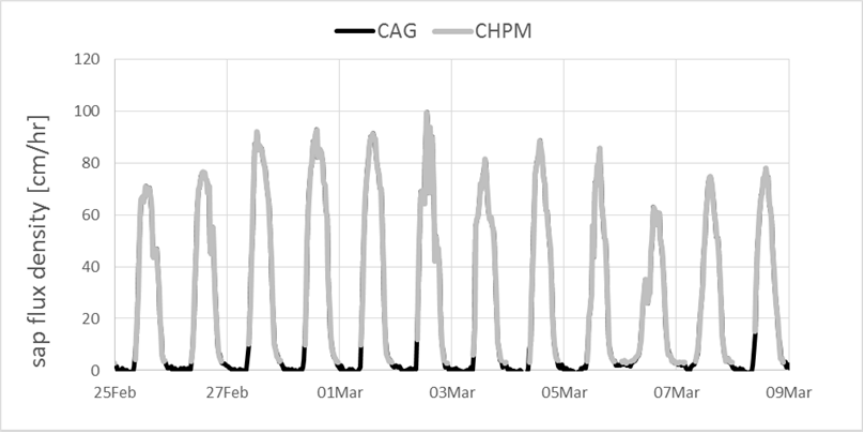

Figure 2. The diurnal pattern of sap flux density (J_S, cm h^{-1}) measured in a 1-year-old apple tree ('Envy') at the Lucaston orchard, Tasmania. The value of J_S was calculated from the ratio of measured sap flow (T, L h^{-1}) divided by the trunk cross-sectional area (A, cm^2). The black line shows the improved resolution at low flows that is achieved using the CPHM-AG method in these young apple trees.

We now look at the tree's sap flow in response to the local microclimate. Essentially there are two main driving forces for transpiration: the radiant energy from the sun (R_S, W m^{-2}) and the vapour-pressure deficit of the air (VPD, kPa). On most days there was a very good correspondence between sap flow and the global shortwave radiation (Figure 3). In general, the sunny days (e.g., December 13) had much higher rates of transpiration compared to cloudy days (e.g., December 10). There was also a very good correspondence between transpiration and VPD (Figure 4). On nights with warm air temperatures and higher wind speeds (e.g., December 9-10) we observed elevated VPDs and significant levels of nocturnal sap flow whereas on the cooler nights with lower wind speeds (e.g., December 16-19) the rates of nocturnal sap flow were negligible.

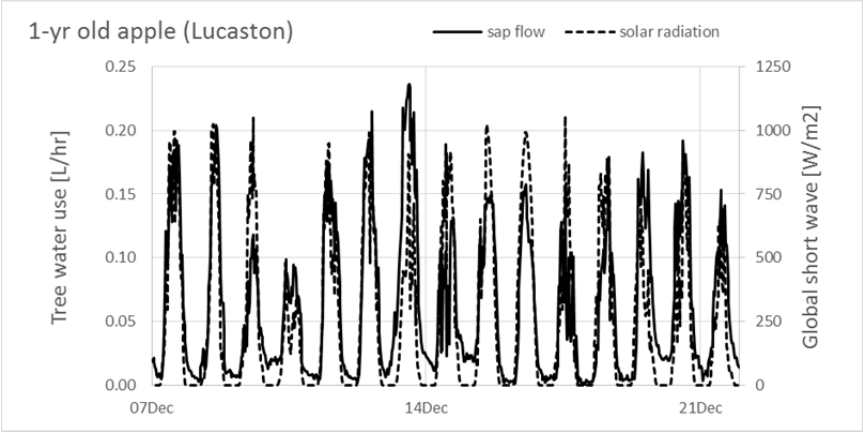

Figure 3. The solid line shows the diurnal pattern of the average tree water use (T, L h^{-1}) in six 1-year-old apple trees ('Envy') at the Lucaston orchard, Tasmania. The corresponding diurnal pattern of global shortwave radiation (R_G, kPa) is shown by the dashed line.

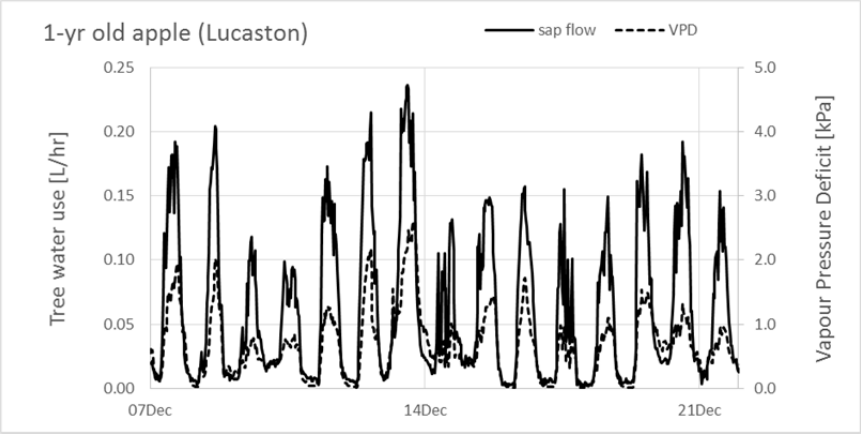

Figure 4. The solid line shows the diurnal pattern of the average tree water use (T, L h^{-1}) in six 1-year-old apple trees ('Envy') at the Lucaston orchard, Tasmania. The dashed line shows the diurnal pattern of the vapour pressure deficit of the air (VPD, kPa) which remains elevated on warm and windy nights.

Half-hourly sap flow data have been integrated, on a daily basis, to provide a picture of the seasonal pattern of tree water use (Figure 5). The peak transpiration rate for these 1-year-old trees occurred in late January and was 2.5 L $tree^{-1}$ day^{-1}, on average. As expected, the daily rates of transpiration 'tailed-off' at the shoulders of the season, being half the peak rate at the start of December and once again by the end of March. Sap flow at the end of May was essentially zero as the evaporative demands had decreased and the leaves have begun to senesce and fall off. The results of Figure 5 confirm the appropriate crop-factor for these young trees (K_C=0.12 during mid-season). This knowledge is essential for calculating an equitable and sustainable irrigation strategy for the orchard.

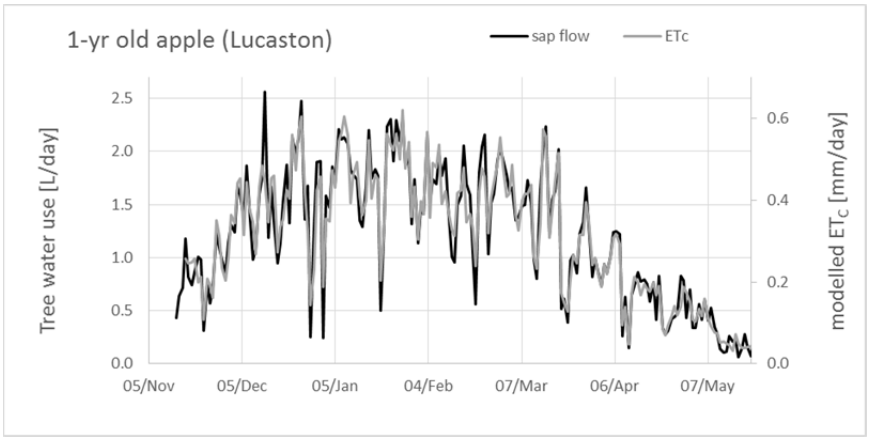

Figure 5. The black line represents the seasonal pattern of the average daily tree water use (T, L day^{-1}) in 1-year-old apple trees ('Envy') at the Lucaston orchard, Tasmania. The grey line represents daily tree transpiration, as calculated using the FAO-56 crop factor approach (Allen et al., 1998). The two y-axes can be rescaled using the effective tree density (= 3.84 m^2 $tree^{-1}$). Thus, the actual tree water use equals ETc multiplied by 3.84 m^2.

CONCLUSIONS

The academic goal here was to demonstrate the stability of the empirical function V_C = f(ΔT) that is used by the CHPM-AG method to resolve the low flows. The slope of the linear part of the 'calibration curve' (Figure 3) will depend on a number of factors, including 1)

probe spacing and geometry, 2) wood moisture content, 3) length of the time-averaging window, 4) heater output, and many other factors. Nonetheless, we observe a very stable calibration curve throughout the whole growing season of these young apple trees. The implicit 'self-calibrating' feature of CHPM-AG means we can now resolve our measurements across the full range of sap flux densities.

ACKNOWLEDGEMENTS

This research comes from a collaborative project between the Tasmanian Institute of Agriculture (TIA) and Plant & Food Research, New Zealand (PFR). The project is funded by Horticulture Innovation Australia Ltd (HIA) under Project Code AP14203.

Literature cited

Allen, R.G., Pereira, L.S., Raes, D., and Smith, M. (1998). Crop Evapotranspiration Guidelines for Computing Crop Water Requirements. FAO Irrigigation.and Drainage Paper *56* (Rome, Italy: FAO), pp.300

Burgess, S.S.O., Adams, M.A., Turner, N.C., White, D.A., and Ong, C.K. (2001). Tree roots: conduits for deep recharge of soil water. Oecologia *126* (*2*), 158–165 https://doi.org/10.1007/s004420000501. PubMed

Ferreira, M., Green, S.R., Conceição, N., and Fernández, J.E. (2018). Assessing hydraulic redistribution with the compensated average gradient heat-pulse method on rain-fed olive trees. Plant Soil *425* (*1-2*), 21–41 https://doi.org/10.1007/s11104-018-3585-x.

Fuentes, S., Collins, M., Rogers, G., Acevedo, C., and Conroy, J.P. (2009). Nocturnal heat-pulse sap flow as a sensitive system to assess drought effects on grapevines: an irrigation scheduling application? Acta Hortic. *846*, 167–176 https://doi.org/10.17660/ActaHortic.2009.846.17.

Green, S.R., and Clothier, B.E. (1988). Water use of kiwifruit and apple trees by the heat-pulse technique. J. Exp. Bot. *39* (*1*), 115–123 https://doi.org/10.1093/jxb/39.1.115.

Green, S.R., and Romero, R. (2012). Can we improve heat-pulse measurements to measure low and reverse flows? Acta Hortic. *951*, 19–29 https://doi.org/10.17660/ActaHortic.2012.951.1.

Green, S.R., Clothier, B.E., and Jardine, B.J. (2003). Theory and practical application of heat pulse to measure sap flow. Agron. J. *95* (*6*), 1371–1379 https://doi.org/10.2134/agronj2003.1371.

Green, S., Clothier, B., and Perie, E. (2009). A re-analysis of heat pulse theory across a wide range of sap flows. In VII International Workshop on Sap Flow. Acta Hortic. *846*, 95–104 https://doi.org/10.17660/ActaHortic. 2009.846.8.

Hatton, T.J., Catchpole, E.A., and Vertessy, R.A. (1990). Integration of sapflow velocity to estimate plant water use. Tree Physiol. *6* (*2*), 201–209 https://doi.org/10.1093/treephys/6.2.201. PubMed

Madurapperuma, W.S., Bleby, T.M., and Burgess, S.O. (2009). Evaluation of sap flow methods to determine water use by cultivated palms. Environ. Exp. Bot. *66* (*3*), 372–380 https://doi.org/10.1016/j.envexpbot.2009.04.002.

Marshall, D.C. (1958). Measurement of sap flow in conifers by heat transport. Plant Physiol. *33* (*6*), 385–396 https://doi.org/10.1104/pp.33.6.385. PubMed

Oliveira, R.S., Dawson, T.E., Burgess, S.S., and Nepstad, D.C. (2005). Hydraulic redistribution in three Amazonian trees. Oecologia *145* (*3*), 354–363 https://doi.org/10.1007/s00442-005-0108-2. PubMed

Swanson, R.H., and Whitfield, D.W.A. (1981). A numerical analysis of heat pulse velocity theory and practice. J. Exp. Bot. *32* (*1*), 221–239 https://doi.org/10.1093/jxb/32.1.221.

Testi, L., and Villalobos, F.J. (2009). New approach for measuring low sap velocities in trees. Agric. For. Meteorol. *149* (*3-4*), 730–734 https://doi.org/10.1016/j.agrformet.2008.10.015.

Appendix 4: Draft manuscript, Hardie et al_Nitrate and irrigation flux

Measuring and modelling nitrate fluxes in a mature commercial apple orchard.

Marcus Hardie[a], Steve Green[b], Garth Oliver[a], Nigel Swarts[a], Brent Clothier[b], Dugald Close[a], Roberta Gentile[b]

[a] Tasmanian Institute of Agricultural Research, University of Tasmania, PB 98, Hobart, Tasmania 7001.

[B] Plant and Food Research, PB 11600, Palmerston North 4442, New Zealand

[*]Corresponding author. Fax +61 3 6226 2642 E-mail: Marcus.Hardie@utas.edu.au

Abstract

Leakage of nitrogen from intensive agriculture to groundwater and waterways is a potential source of environmental harm. Nitrate leaching beneath a commercial 10-year-old 'Galaxy' apple orchard was investigated using a coupled measurement and modelling approach. Sapflow (tree water use), climate, soil moisture, deep drainage and nitrate leaching beneath the root zone were monitored for up to 30 months in order to parameterise and calibrate the Soil Plant Atmosphere System Model (SPASMO). Deep drainage and nitrate leaching were highly variable and did not appear to be influenced by irrigation rate. Over the 30 month monitoring period, drainage beneath the rootzone averaged 93/mm/yr, whilst nitrate leaching averaged 33.2 kg/Ha/yr, equivalent to 55 % of the applied fertilizer. Nitrate concentration in the leachate exceeded the World Health Organisation threshold for drinking water of 50 mg/L in 44 out of 279 samples. Long term modelling indicated the average amount of drainage and nitrate leaching were 136 mm/yr and 11.4 kg/ha/yr, respectively. Scenario analysis indicated that few options existed to reduce nitrate leaching at the site.

Introduction

Nitrogen (N) is the most used fertilizer in orchards, and is often over-applied as an 'insurance policy' to achieve maximum productivity (Dong et al., 2004; Fernández-Escobar et al., 2004). Excess application of N fertilizer and irrigation increases production costs, can reduce fruit quality (Albornoz, 2016), and poses a risk to the environment (Swarts et al., 2016a), and potentially human health through groundwater contamination (Di and Cameron, 2002; Ongley, 1996). It is well recognised by orchardist that increasing the rate of nitrogen application can increase vegetative growth, bud development and yield, but at a cost to fruit quality, as excess nitrogen decreases fruit colour and firmness through delayed maturation (Neilsen et al., 2004; Oberly and Boynton, 1966; Stefanelli et al., 2010). Nitrogen application and management in deciduous fruit trees is complex, as the trees accumulate and store carbohydrates and nutrients at the end of the growing season for remobilisation in the following spring (Loescher et al., 1990).

Most Australian perennial tree crops are irrigated by drip or microspray irrigation to which soluble nutrients are often applied in a combined practice called fertigation. Drip fertigation is regarded as a precise and efficient method of supplying water and nutrients due to the large degree of control over application timing, placement and amount (Klein et al., 1989; Van der Kooij et al., 2013). In theory, this high degree of control should enable growers to accurately meet tree water and nitrogen requirements, thereby minimising losses via leaching beneath the root zone (Gärdenäs et al., 2005; Thorburn et al., 2003). Much of the difficulty in managing fertigation in commercial apple orchards results from the complexity of nitrogen transformations, rapid mobilisation of nitrogen through the soil, and the internal dynamics of tree storage and remobilisation of nitrogen (Lehmann and Schroth, 2003; Neilsen and Neilsen, 2002) combined with the relatively shallow, low density nature of apple tree roots (Sokalska et al., 2009). Most perennial tree crops apply fertiliser based on standard recommendations irrespective of irrigation requirement, crop load, tree size, quality specifications, or the soil's capacity to retain and supply nutrients.

Many soil-water-crop models have been developed to simulate soil water and nutrient movement in agricultural soils including; RZWQM (Ma et al., 1998; Saseendran et al., 2004), APSIM (Keating et al., 2003), CropSyst (Stöckle et al., 2003), SWAP (Crescimanno and Garofalo, 2005; van Dam et al., 1997), CERES (Jones and Kiniry, 1986), HYDRUS (Phogat et al., 2013; Šimůnek and van Genuchten, 2008). However, few have the complexity of processes needed to simulate nitrogen mobilisation, storage and transformation processes that occur in apple production systems. Furthermore, in most cases the data required to parameterise and calibrate the large number of input parameters required to account for these processes is usually lacking. Consequently, this study has adopted a coupled measurement – modelling approach to capture and monitor the major nitrogen sources, transformations pathways, and fate of nitrogen in a mature commercial apple orchard. The purpose of this study was to;

- Quantify rates of nitrate leaching in a typical, mature commercial apple orchard.
- Evaluate the ability of SPASMO to estimate real world irrigation and nitrogen mobilisation, storage, transformation processes, and fate, especially nitrogen leaching.
- Explore how fertiliser and irrigation management can be optimised to minimise nitrate leaching.

Methods

Field site

The trial was located in a commercial apple orchard in the Huon Valley, Tasmania, Australia (42°59'36.97"S, 147°59'29.04"E), reported in Swarts et al. (2016a) and Hardie et al. (2018). The region has a temperate, maritime climate with an average rainfall of 745 mm, distributed evenly throughout the year, mean minimum and maximum temperature range of 5.8 – 17.1 °C, and mean daily sunshine hours of 5.5 hours (BOM, 2015). The orchard consisted of 10-year-old 'Galaxy' trees, grown on M26 rootstock pruned to a central leader training system, with 1 m tree spacing, and 4 m row spacing (2100 trees/ha), on a 0.3 m high mounded tree row. The orchard was drip irrigated by a single lateral 13 mm in-line drip emitters (Netafim) located in the centre of the row, which delivered 2.3 L/h at 0.5 m spacing.

Soils

Soils were classified according to Isbell (2002) as Grey, Eutrophic, Humose – Bleached Kurosol (duplex or texture contrast). The soil profile consisted of a reworked A11p (0-0.12 m) sandy loam, over a A12 (0.12 - 0.30 m) sandy loam, over a rigid bleached silica cemented A2e horizon (0.30 - 0.52 m), which overlayed a mottled carbon rich light clay B21 horizon (0.52 – 0.70 m), over a mottled medium clay B22 horizon (0.70 - 0.90 + m).

Soil physical properties (Table 1) were determined from a single location adjacent the trial area. Soil cores (5.0 cm x 5.2 cm and 6.0 x 9.0 cm) were collected in triplicate from each of the four soil horizons. Bulk density was determined at saturation for the 5.0 cm x 5.2 cm cores according to McKenzie et al. (2002). The soil water release curve was determined on the 6.0 x 9.0 cm cores using the evaporative flux method according to the procedure described by Wendroth et al. (1993) and Peters and Durner (2008) using the HYPROP approach with tensioVIEW software (UMS, 2013). The soil water retention curve was fitted using the van Genuchten-Mualem equation (Mualem, 1976; van Genuchten, 1980). Saturated hydraulic conductivity (K_{sat}) of the A11 horizon was measured in triplicate using a 20 mm diameter, single ring, constant head, infiltrometer in both the treeline and inter-row areas following (Reynolds, 2008; Reynolds and Elrick, 1990) in which alpha was estimated to be 0.12 cm^{-1}. Saturated hydraulic conductivity (K_{sat}) of the A2e, B21 and B22 horizons was determined on 5.0 cm x 5.2 cm cores by Darcy's Law at a constant head of +0.1 kPa. Soil chemical analysis was conducted by CSBP laboratories, Western Australia according to Rayment and Higginson (1992) (Table 2).

Table 1: Soil physical properties at Lucaston experimental field site.

		Van Genuchten Parameters					
Horizon	Depth [cm]	α [1/cm]	η [-]	m [-]	θr [L/L]	θs [L/L]	K_{sat} [cm/d]
A11	5-12	0.066	1.190	0.159	0.027	0.599	1422
A12	25-30	0.018	1.234	0.189	0.000	0.560	191
A2	30-50	0.015	1.220	0.180	0.000	0.344	511
BHS	50-70	0.040	1.102	0.092	0.300	0.604	27
B22	70 +	0.252	1.148	0.129	0.300	0.716	1149

Table 2: Selected soil chemical properties at Lucaston experimental field site.

Horizon	Depth (cm)	Texture	Organic Carbon (%)	$EC_{1:5}$ (dS/m)	pH ($CaCl_2$)	CEC (meq/100g)	NH_4 (meq/100g)	NO_3 (meq/100g)
A1p	0-30	Sandy Loam	3.46	0.17	6.1	19.13	3.5	12.5
A2	30-50	Loamy Sand	0.47	0.19	6.1	2.64	5	6
BHS	50-70	Light Clay	5.19	0.25	5.5	11.73	2	3
B22	70 +	Medium Clay	0.71	0.18	4.0	4.57		

CEC is the cation exchange capacity, EC is electrical conductivity in a 1:5 dilution,

Trial Design

The research presented in this manuscript is a subset of a larger randomised irrigation by fertigation block design described in Swarts et al. (2016b). The randomised block experiment consisted of four tree rows as replicates, three irrigation rate treatments (high 4 L/hr, medium 2.3 L/hr, and low 1.6 L/hr) and five nitrogen fertigation treatments and a zero rate control, in which only the split 30 kg/N/ha Pre harvest and 30 kg/N/ha Post Harvest nitrogen treatment were monitored for nitrogen leaching, soil moisture and sap flow, in a single replicate plot for each of the three irrigation treatments. Each of the 60 replicates consisted of four trees, two of which were guard trees, with the two middle trees used for monitoring and sampling. Results reported in this manuscript were limited to the 50% nitrogen Pre and 50% nitrogen post fertigation treatment.

Fertilizer and Irrigation Management

Nitrogen was applied at 60 kg-N/ha/yr which was equivalent to 29 kg-N per tree. This rate was determined in discussion with industry as being the upper range of industry practice in order to represent current over use of N fertilizer. Nitrogen was applied through the drip irrigation system as fertiliser grade $Ca(NO_3)_2$ mixed with water in a 220 L drum header tank and delivered via a fire-fighting pump at constant 70 kPa (Fig. 3). Fertiliser application followed standard fertigation practise in which a 10 min water only wetting up period was followed by a 40 min application of the nitrogen treatments followed by a 10 min water only rinse. At each application interval, treatments (including the control 0 N) were applied once/week for four weeks in approximately 50 L water. Timing of fertigation events was at the grower's discretion based on current agronomic best practice. Pre-harvest fertigation treatments commenced in November 2012, 2013 and 2014 coinciding with the first irrigation application for the season and timed to match maximum demand by the tree during leaf canopy development. Post-harvest treatments were applied in March/April 2013, 2014 and 2015.

Table 3: Irrigation and Nitrogen treatments per growing season

Growing Season	Nitrogen (Kg-N/tree/yr)	Irrigation Treatment (mm) High	Medium	Low	Rainfall (mm) 1 July -30 June
2012-13	29.04	*	*	*	635
2013-14	29.04	445	267	178	909
2014-15	29.04	189	113	76	851

* Missing data due to logger failure.

Tree water use

Tree water use (mm/ha/day) was determined using the standard crop-factor approach (FAO 56) (Allen et al., 1998) as;

$$ET_C = K_C ET_0$$

In which ET_C is the combined crop evaporation and transpiration, K_C is the crop factor which is related to the amount of light intercepted by the leaf canopy as a function of the leaf-area index, LAI (m^2 of leaf per m^2 of ground area) (Green et al., 2003b), and ET_0 is reference evapotranspiration, calculated daily by the Penman-Monteith equation from global radiation, air temperature, relative humidity and wind speed obtained from the Grove Bureau of meteorology station located 2 km from the field site.

The K_c mid was determined directly from measurements of trunk sap flow. Sap flow probes (HP4TC-S, Tranzflo NZ Ltd, Palmerston North, New Zealand) were installed in three trees in separate replicates of the high irrigation treatment. The probes comprised two 1.8 mm diameter temperature probes and a 1.8 mm diameter heater probe, each containing 4 thermocouples housed in a stainless steel hypodermic tube insulated with a Teflon sheath. Measurements were taken using the compensation heat-pulse method (Green et al., 2003a; Green and Clothier, 1988), controlled by a CR1000 datalogger (Campbell Scientific, Logan, USA) with a standard probe spacing of 5 mm upstream and 10 mm downstream from the heater probe. Sap flow readings were conducted every 30 minutes and summed up to give a value of the daily water use. Leaf area measured in April 2014 from the monitored trees averaged 8.33 m^2, 7.73 m^2 and 6.83 m^2 in the high, medium and low irrigation treatments respectively.

Soil moisture

Soil moisture content was measured using TDR (time-domain reflectometry) in a single replicate of the 50% nitrogen Pre and 50% nitrogen Post fertigation treatment for each of the high, medium, and low irrigation treatments. Thirteen probes were placed directly under the drip line and 9 were placed in the inter-row. Nine probes were placed at 0-30 cm, 7 at 0-60 cm and 6 at 0-90 cm depth. Data was collected via a CR1000 logger installed with a Campbell Scientific TDR100, 3x SDMX multiplexer. Unfortunately, many of the TDR sensors were irreparably damaged in September 2013 due to root punning operations.

2.3 Drainage collection and leachate analysis

Twelve drainage flux meters (DFM Tranzflo NZ Ltd, Palmerston North, New Zealand) or passive-wick lysimeters (Green et al., 2012a) were installed to monitor quality and quantity of drainage water beneath the rootzone at 60 cm depth. Passive-wick flux meters operate by maintaining tension on the base of the soil via a fiberglass wick which creates a self-priming hanging-water column (Gee et al., 2009; Gee et al., 2004) (Figure 1). Nine 200 mm diameter x 2000 mm PVC DFM's were installed in the tree row beneath or adjacent a fertigation emitter. Three DFM's were installed in a single replicate for each of the high, medium and low irrigation rate treatments. An additional three DFM's were installed on the mound shoulder of the high irrigation treatment, approximately 0.3 m from the tree-line and midway between two trees. Installation of each DFM involved carefully hand auguring to a depth of 60 cm in which each soil layer was placed in individual buckets for repacking the DFM. A mechanised hole auger was used to extend the holes to 2.0 meters depth. Before installation, each DFM was packed with wetted diatomaceous earth, then a layer of pure silica sand followed by each soil layer in turn from deepest to shallowest to the top of the DFM. After installation, the remaining soil from the original hole was repacked around the DFM to the surface (Figure 1).

Drainage samples were manually collected from the flux meter reservoirs every month between 15th November 2010 and 3rd February 2014. Filtered aliquots of approximately 30 - 40 mL were extracted from each fluxmeter and stored at -20 °C. Nitrate content was determined by Cd-Cu reduction according to the US EPA Method 353.3 (O'Dell, 1993). Monthly nitrate flux (kg-N/Ha) was calculated by the volume of collected leachate (cm^3), divided by the surface area of the flux meter (cm^2), multiplied by the nitrate concentration (mg/L) of the leachate, divided by 10.

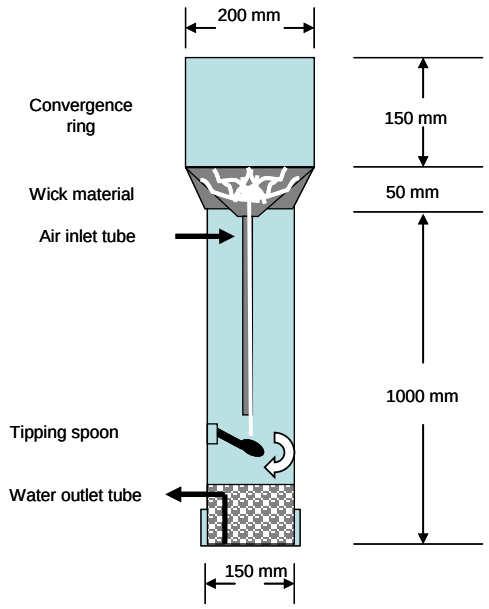

Figure 1: Passive wick lysimeter (drainage flux meters, DFM) used to monitor water and nutrient fluxes (Adapted from Gee et al. (2009)).

SPASMO Soil Plant Atmosphere System Model

SPASMO (Soil Plant Atmosphere System Model) is a generic 1D daily time step soil – plant – climate model developed to simulate water and solute transport through a one-dimensional soil profile (Cichota and Snow, 2009; Green et al., 2003c). SPASMO has been widely used in research for evaluating nitrogen leaching (Green et al., 2012a; Green et al., 2003c; Rosen et al., 2004), determining crop water use (Green et al., 2002; Green et al., 2012b; Green et al., 2007; Green et al., 2003d), and simulating pesticide transport in soils (Cichota and Snow, 2009; Close et al., 2003; Greven et al., 2007; Sarmah et al., 2005). Water and nutrient fluxes are calculated on a daily time step in which the potential for nutrient leaching is determined by mass balance (Green and Clothier, 2016b). The model accounts for fertilisation, plant uptake, volatilisation, exchange and transformation in the soil including recycling of nutrients and organic material to the soil biomass (Cichota and Snow, 2009; Green and Clothier, 2016a; Green et al., 2012a; Green et al., 2003d). The soil water balance is calculated by considering the inputs (rainfall and irrigation) and losses (plant uptake, evaporation, runoff and drainage) of water from the soil profile. Water movement through the soil profile is simulated using a capacity model similar to that of which allows the specification of a mobile and an immobile fraction to account for macropore flow. Crop water use is estimated daily using the standard crop-factor approach (FAO 56) (Allen et al., 1998). Surface runoff is modelled using the Soil

Conservation Service (SCS) curve number approach which is predicted from daily rainfall plus irrigation. Nutrient runoff is modelled using the Revised Universal Soil Loss Equation (RUSLE, Renard et al. 1991). The soil nitrogen balance accounts for nitrogen uptake by plants, exchange and transformation processes in the soil, loss of gaseous nitrogen to the atmosphere, fertiliser application, and the leaching of nitrogen below the root zone. SPASMO considers both organic nitrogen (i.e. in the soil biomass) and the mineral nitrogen (i.e. urea, ammonium and nitrate) detailed in Green et al. (2007) and (Rosen et al., 2004). Dissolved nitrate is considered to be mobile and to percolate freely through the profile, whilst movement of dissolved ammonium is retarded. The soil can receive inputs of organic carbon and organic nitrogen from decaying plant residues which are added to the litter layer of the topsoil (Green et al., 2003b).

Model parameterisation was based on a combination of measured values (e.g. soil water retention, bulk density, climate, sapflow, soil carbon content) from which appropriate values for the model inputs were derived. Values for other parameters (e.g. light use efficiency, dry-matter allocation fractions and rate constants for mineralisation) were derived from literature values or past research at other sites (Ref). Model output was compared to measured values and where necessary values were 'tuned' to improve model performance.

Scenario analysis

Model simulations were conducted over a range of values to explore the effects of site characteristics and management on nitrogen leaching, including; soil water holding capacity, tree size, rainfall, irrigation amount, and fertilizer rate (Table 4). Simulations were conducted at a nitrogen fertiliser rate of 60 kg/ha (except the nitrogen fertilizer scenarios), using four applications pre-harvest and two applications post-harvest. In order to simulate the effects of different soil types on the water balance and nutrient flux, the plant available water content (PAWC) between field capacity (-10 kPa) and the permanent wilting point (-1500 kPa) over the soil profile to 100 cm depth was varied 70 % to 130 % from the current PAWC of 184 mm. Likewise, the long term average rainfall (1980–2014) of 726 mm (Bureau of Meteorology, Grove) was varied 70% to 130% to explore the effects of variable rainfall. The base irrigation value (217.5 mm) was determined by triggering the model to irrigate to field capacity when half the readily available soil moisture (RAW) had been extracted from the root zone. Model simulations were conducted for irrigation trigger points between 30% and 150% of the base (50% RAW) value. Variation in tree size or age on the water and nitrogen balances was mimicked by manipulating the FAO56 crop factor (K_C).

Table 4: Base (existing) model values and the range of simulated values used in the scenario analysis.

Model parameter	Base value		Simulated values			
			Lower Range		Upper Range	
PAWC (mm)	Measured	184	70 %	128	130 %	240
Rainfall (mm)	Long Term Average	726	70 %	508	130 %	944
Irrigation trigger (mm)	50% RAW	218	30% RAW	66	150% RAW	327
N fertilizer (kg/ha)	Current practice	60	0 %	0	200 %	120
Tree size (Kc)	Measured	0.75	Young tree	0.15	Mature tree	0.90

RAW refers to readily available water content - approximately 50% of plant available water content

RESULTS

Tree water use, sap flow and Kc factors

Tree water use (sap flow) occurred between mid-September and early May, peaking at around 15 L/tree/day in late January (Figure 2). Average sap flow for the 2013-2014 season was 8.58 (L/tree/day), 6.39 (L/tree/day) and 6.47 (L/tree/day) for the high, medium and low irrigation treatments respectively. Differences in sapflow between treatments were attributed to differences in leaf area measured in April 2014 which averaged 8.33 m^2, 7.73 m^2 and 6.83 m^2 in the high, medium and low irrigation treatments respectively.

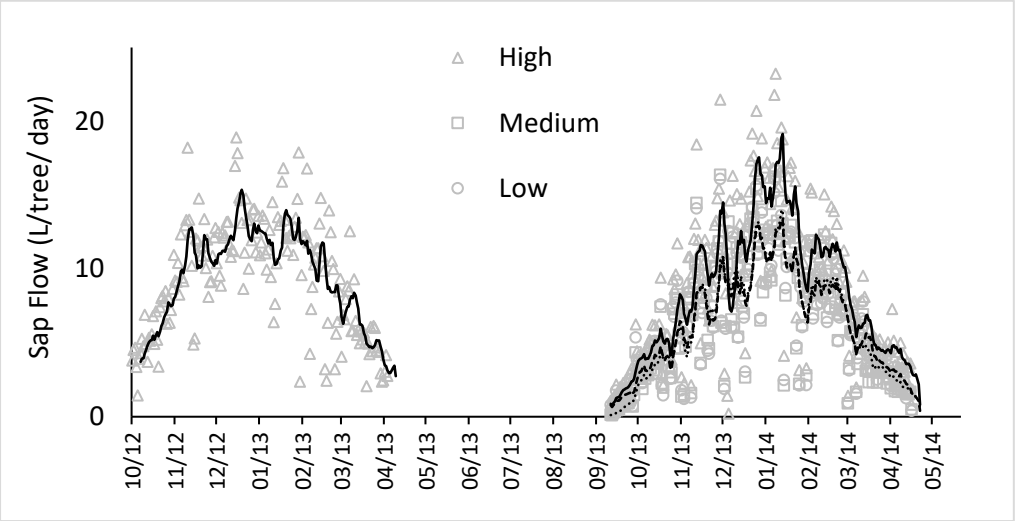

Figure 2: Sap flow (L/tree/ day) for the high, medium, and low irrigation treatments for the 2012/13 (high treatment only) and 2013/14 growing seasons. Lines represent a seven day moving average. Solid line is the high treatment, dotted line is the medium treatment, and the dashed line is the low treatment.

The crop factor (Kc) increased from budburst (late September) through to late December then plateaued between late December and harvest (mid-March) (Figure 3). The mid-season $K_{C\ mid}$ values relate to irrigation treatment and thus LAI, ranging from 0.71, to 0.53, and 0.52 for the high, medium and low irrigation treatments, respectively. Measured Kc values were substantially lower than the recommended $K_{c\ mid}$ factor for apples of 0.9 (Allen et al., 1998). Post-harvest K_C values are noted to decline after early April in the low and medium irrigation treatments, presumably due to leaf senescence. No decline in K_C was observed in the high irrigation treatment. Notably, the mid-season crop factors were similar ($K_{C,\ mid}$ = 0.71) between both years.

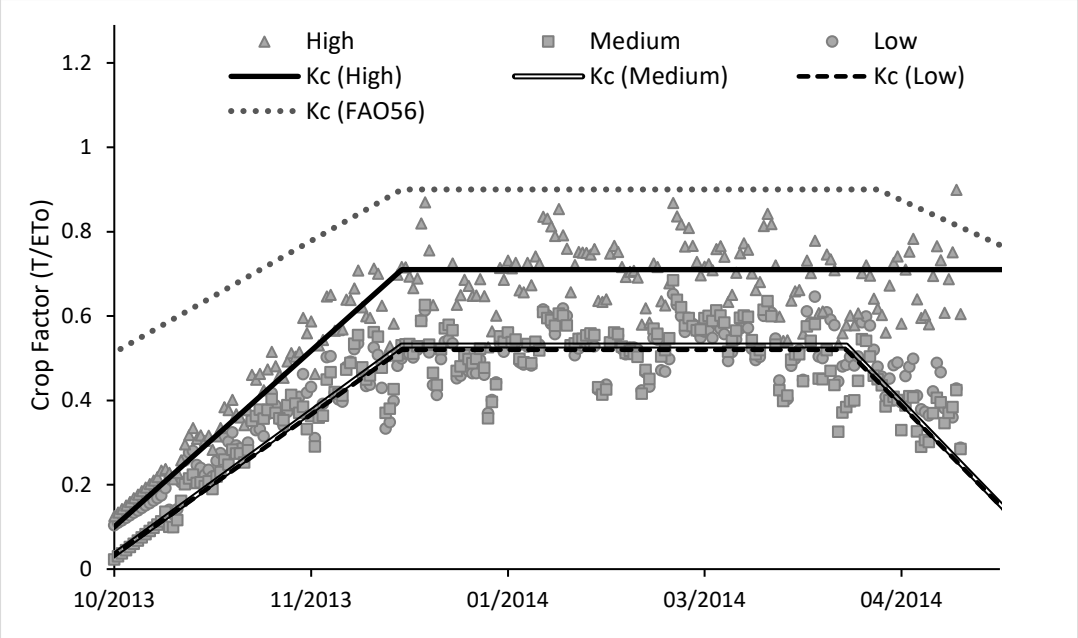

Figure 3: Measured crop factor (T/ETo) and fitted Kc curves for the high, medium and low irrigation treatments over the 2013/14 growing season. Dotted line indicates FAO56 recommended mid-season Kc for apples of 0.9.

Correlation between trunk sap flow and SPASMO estimates of daily tree water use were 0.38 in the 2012-2013 season and 0.48 in 2013 -2014 season. However, on a bi-monthly basis the measured and modelled tree water use appeared remarkably similar, as demonstrated by the 15 day moving average plots (Figure 4).

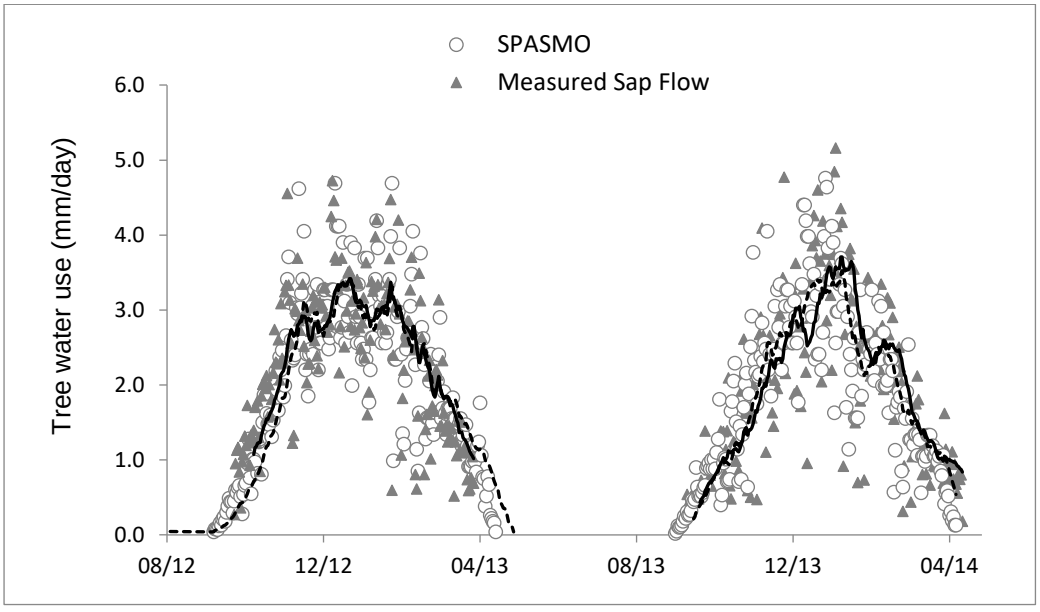

Figure 4. Seasonal comparison between measured tree water use (mm/day) by sap flow and SPASMO model, using a crop factor of Kc = 0.71. Lines represent 15 point moving average for SPASMO model (dashed), and measured values by trunk sap flow (solid).

Soil Moisture

Soil moisture between October 2012 and September 2013 was not greatly influenced by irrigation treatment (Figure 5). Within the tree rootzone (0-60 cm depth), the medium irrigation treatment had the highest average cumulative soil moisture content of 176 mm, followed by the low treatment at 167 mm, and lastly the high irrigation treatment at 163 mm. However, at 15 cm depth, the irrigation treatments appeared to influence soil moisture as the average soil moisture content over the 11 month monitoring period in the high irrigation treatment was 27.79, 25.85 and 23.48 %vol in the high, medium and low irrigation treatments respectfully.

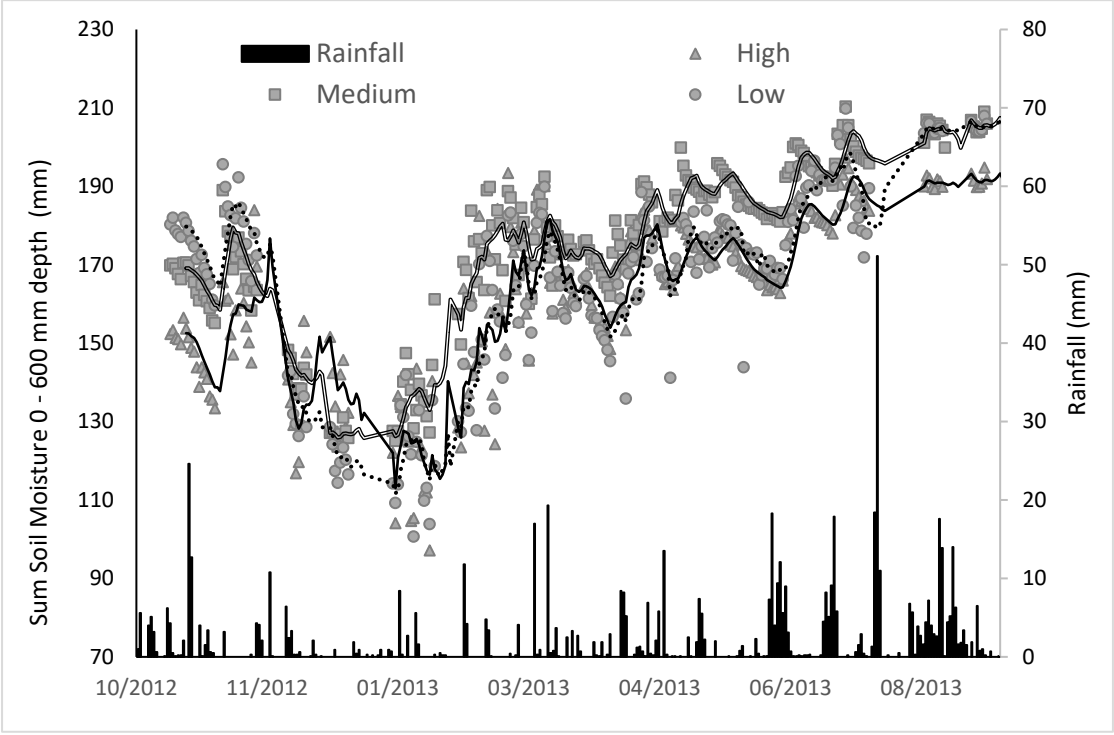

Figure 5: Sum of soil moisture (mm) between 0 and 600 mm depth (left axis), and rainfall (right axis). Gaps in data indicate periods of logger failure. Lines represent 7 day moving average. The solid line is the high treatment, the double line is the medium treatment, and the dotted is the low treatment.

Drainage

Drainage rates were extremely variable within and between the irrigation treatments, in which the cumulative drainage over the 30 month monitoring period ranged from 13 to 45 mm/yr (mean 34mm/yr) in the medium treatment, followed by 53 to 138 mm/yr (mean 94 mm/yr) in the high

treatment, 94 to 197 mm (mean 152 mm) in the low treatment, and 53 to 183 mm/yr (mean 212 mm/yr) in the shoulder area adjacent the high treatment. The average annual leaching from the three treatments (excluding shoulder area) was 93/mm/yr, or 122 mm/yr for the three treatments including the shoulder area. Large drainage events (> 50 mm) mostly occurred in winter, between July to October in 2013 and June and July in 2014, whilst a smaller drainage event (20 mm) occurred in February 2015, following 162 mm rainfall between January and February. Monthly drainage flux was moderately correlated with irrigation application (R^2 = 0.20), soil moisture (0-45 cm depth) R^2 = 0.43 - 0.55, and rainfall R^2 = 0.05 – 0.29 depending on irrigation treatment.

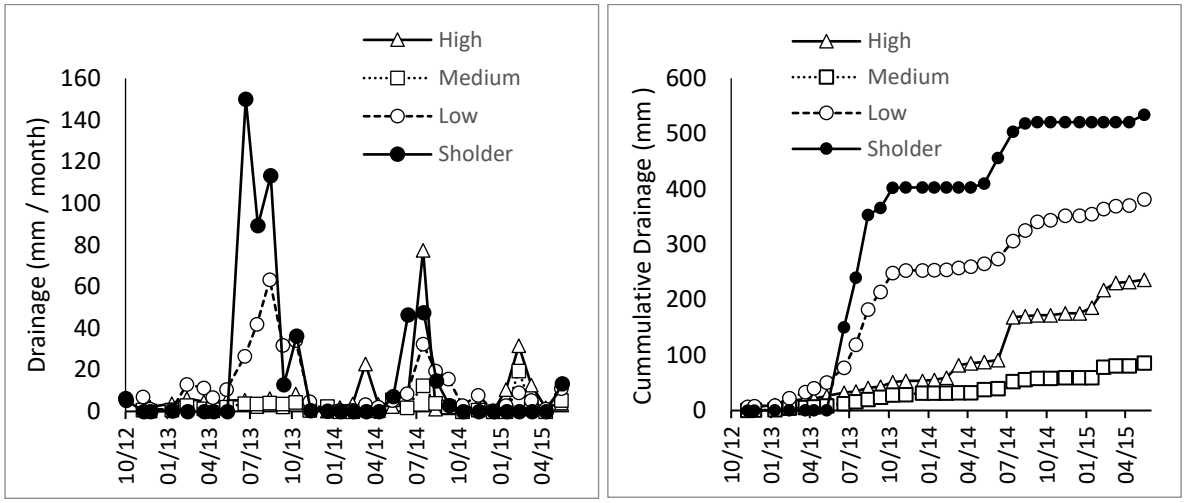

Figure 6: (a) Average monthly drainage flux, and (b) cumulative drainage below 60 cm depth in the high, medium and low irrigation treatments and adjacent shoulder area.

Nitrate Concentration in Leachate

Nitrate concentration of the recovered leachate from the lysimeters was highly variable, both between and within treatments, as well as over time (Figure 7). Nitrate concentration was not overly related to rainfall in which R squared values were 0.02, 0.17 and 0.24 for the High, Medium and Low treatments respectively. The highest nitrate concentrations occurred in the Low and Medium irrigation treatments. A large 'spike' in nitrate concentration occurred in the last measurement in May-June 2015. This 'spike' was observed shortly after the post-harvest nitrogen fertigation treatments were applied and following 101 mm monthly rainfall however similar spikes were not observed in previous years in which monthly rainfall in May 2013 was 41 mm, and 64 mm in 2014. Nitrate concentration in the shoulder area adjacent the tree row was noted to be lower than the other treatments.

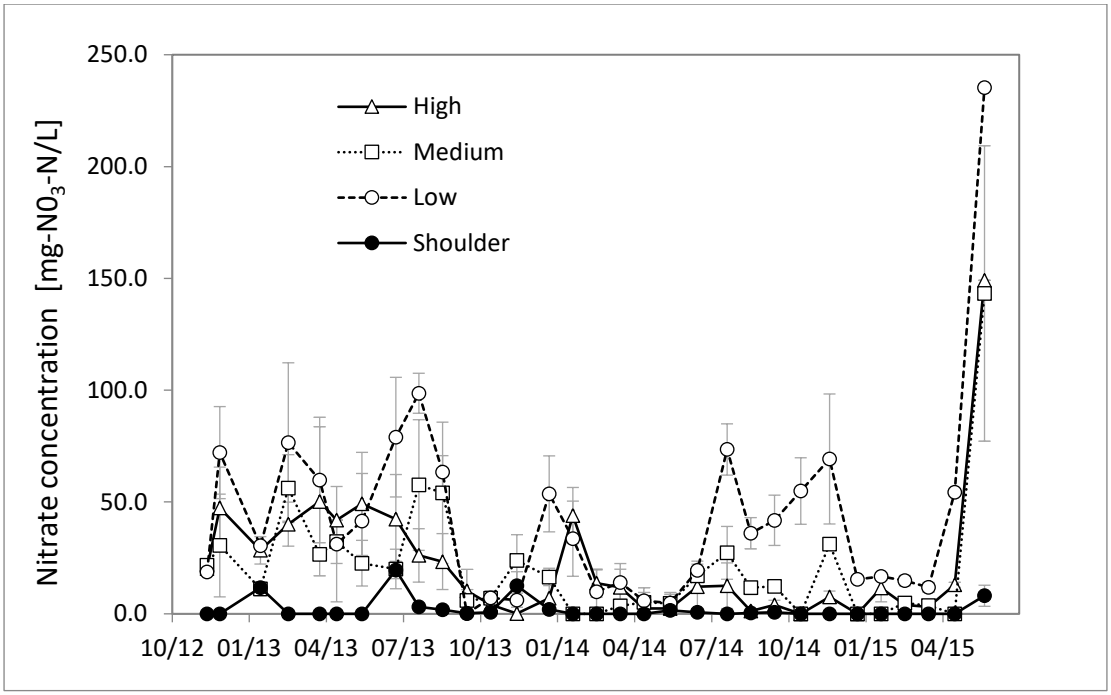

Figure 7: Effect of irrigation treatment on nitrate concentration over the 30-month monitoring period. Error bar indicates SE

Nitrate flux

Nitrate leaching was highly variable. For example, in May-June 2015 two adjacent fluxmeters in the same irrigation treatment recorded 0.0 and 77.2 kg-N/ha/month. The average nitrate flux from under the tree row (all irrigation treatments) was 33.2 kg/ha/yr. Nitrate leaching was not related to the irrigation treatments as leaching from the High and Medium irrigation treatments averaged 9.70 kg-N/ha/yr and 10.62 kg-N/ha/yr respectively, compared to 79.20 kg-N/ha/yr in the Low treatment. Nitrate flux was event based in which 50 % of all nitrate flux and 41 % of all drainage occurred over a 3 month period between June to August 2013, especially in low treatment and shoulder area (Figure 8). Notably, the nitrate flux appeared to be more closely related to the drainage flux than the concentration of nitrate in the drainage water. The measured water and nitrate balance for the 30 month monitoring period is presented in Table 5.

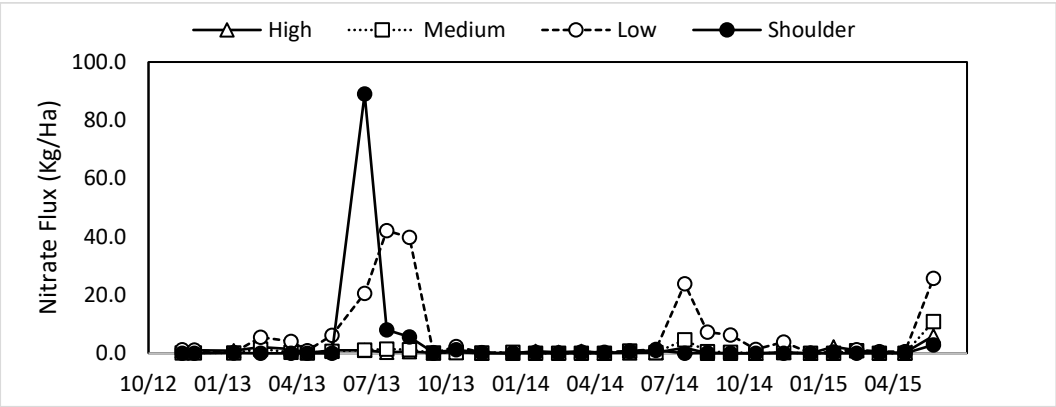

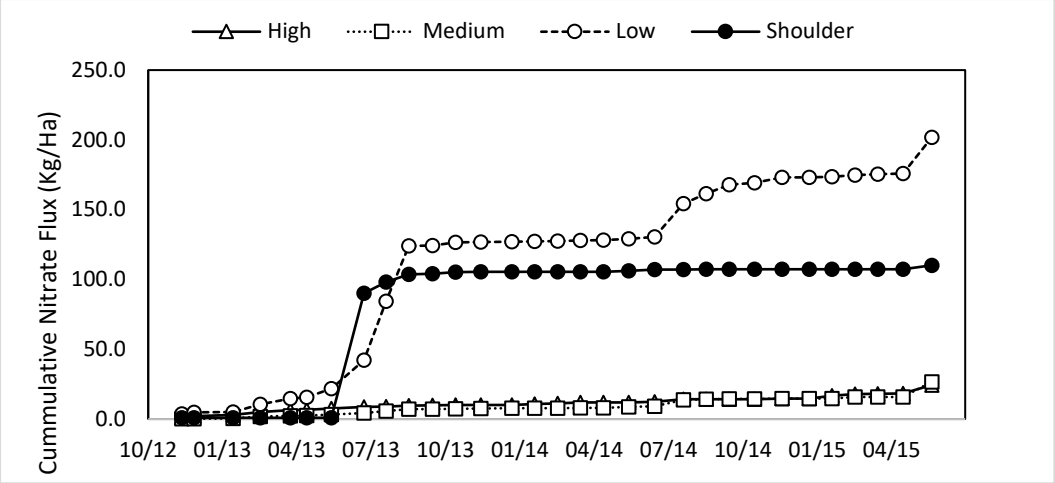

Figure 8: (a) Nitrate flux and (b) cumulative flux of nitrate by treatment over the 30-month monitoring period.

Table 5: Water and nitrogen budget by irrigation treatment for the 2012-2013, 2013-2014, and 2014-2015 seasons

	Late 2012-2013			2013-2014			2014-2015		
Irrigation treatment	Low	Medium	High	Low	Medium	High	Low	Medium	High
Rainfall (mm)	313	313	313	995	995	995	846	846	846
Transpiration (mm)			430			408			416
Drainage (mm)	26.5	16.2	32.3	196	27.3	59.2	108	46.3	145
Leached Nitrogen kg/ha	19.2	3.1	7.6	107.4	5.7	4.4	72.7	17.9	12.3
Yield kg /ha	23.5	33.9	31.4	42	42	42	35	35	35

Data is presented as July to June season. Monitoring commenced 20/10/2012, first leachate sampling occurred on 28th, November 2012. All data is measured or derived from measured values.

Long term average simulations

The long term average simulations using climate data from 1980 to 2015 demonstrated that the 2013-2014 and 2014-2015 growing seasons had substantially higher rainfall at 995 mm and 846 mm than the long term average of 726 mm. The measured amounts of drainage from beneath the tree row (exclude shoulder) were 25.0, 94.2, and 99.8 mm/yr for the 2012-2013, 2013-2014, and 2014-2015 seasons respectively, whereas the long term modelling indicated the average seasonal drainage was 136 mm/yr. Likewise the average measured nitrate leaching over the three growing seasons were 9.96, 39.16, and 34.3 kg/ha, respectively, whereas the long term modelling indicated the average nitrate leaching was 12.5 kg/ha/yr (Table 6).

SPASMO indicated that tree age or canopy size (modelled as Kc factor) had a substantial effect on all aspects of the water balance (excluding rainfall), in which the irrigation requirement ranged from 80

mm/yr/ha for a young tree (Kc 0.3) to 230 mm/yr/ha for a mature tree (Kc 0.9) and increased transpiration from 183 mm/yr for a young tree to 517 mm/yr for a mature tree (Table 6). The effect of tree age on drainage and runoff were minor, in which drainage and runoff decreased 41.5 mm and 3.3 mm between the young and mature trees. Tree age also influenced nitrogen fertilizer requirement from 5 kg/ha/yr in young trees to 75 kg/ha/yr in mature trees (Table 6).

Table 6: Selected long term (1980-2015) simulations of the effect of tree age (crop factor) on components of the water and nitrogen balance.

	Long term Simulation 1980-2015		
Canopy size / Tree age approximation	Young (Kc 0.3)	Intermediate (Kc 0.75)	Mature (Kc 0.9)
Rainfall (mm/yr)	726	726	726
N fertilizer input (kg-N/ha/yr)	15.01	60.01	75.01
Irrigation (mm/yr)	80	217.5	229.6
Transpiration (mm/yr)	183	434	517
Evaporation Soil (mm/yr)	426	342	283
Tree Nitrate Uptake (kg-N/ha)	46.2	94.4	117.2
Drainage (mm/yr)	166	136	124
Runoff (mm/yr)	12.4	9.9	9.1
Leached Nitrogen (kg-N/ha)/yr	35.8	12.5	13.6
Leached Nitrate (kg/ha/yr)	32.9	11.4	12.5

Note: SPASMO assumes Kc 0.75, PAWC of 184 mm, no net change in soil N. Results in Kg/ha/yr represent whole of orchard values not just the tree row, and therefore are not absolutely comparable to measured values.

Scenario analysis

The strongest influence on nitrate leaching was tree size (crop factor) in which predicted nitrate leaching decreased from 53 to 16 kg-N/ha/yr as the Kc value increased from 0.15 to 0.45, after which increase tree canopy (Kc value) had minimal influence on nitrogen leaching. Nitrogen leaching also increased with irrigation, rainfall and nitrogen fertilizer rate, and decreased with PAWC (Figure 9: a, b, c, d). Drainage below 1.0 meters depth decreased with tree size (Kc value) and PAWC, and increased with rainfall and irrigation. Likewise, the irrigation requirement increased as tree size increased, and decreased with increasing rainfall and PAWC. SPASMO indicated that nitrogen leaching was relatively insensitive to irrigation rate at the Lucaston site. Decreased irrigation from 217 mm to 96 mm (56% reduction) only decreased nitrogen leaching by 1.4 kg /ha (10% reduction) despite drainage having decreased by 51.6 mm (38 % decrease). The scenario analysis also demonstrated that nitrogen leaching was also relatively insensitive to nitrogen fertilizer application rate below 120 kg-N/ha/yr. Reducing the nitrogen fertilizer application from 60 to 30 kg/ha/yr reduced nitrogen leaching by 0.3 kg/ha/yr (2 % increase), whilst doubling nitrogen fertilizer to 120 kg/ha/yr increased yield by 9 t/ha (11 % increase) and increased nitrogen leaching from by 4.0 kg/ha (29 % increase). Interestingly a zero synthetic fertilizer regime was still predicted to result in 12.3 kg/ha nitrogen leaching, a 9.6 % reduction in nitrogen leaching compared to the current practice of applying 60 kg /ha.

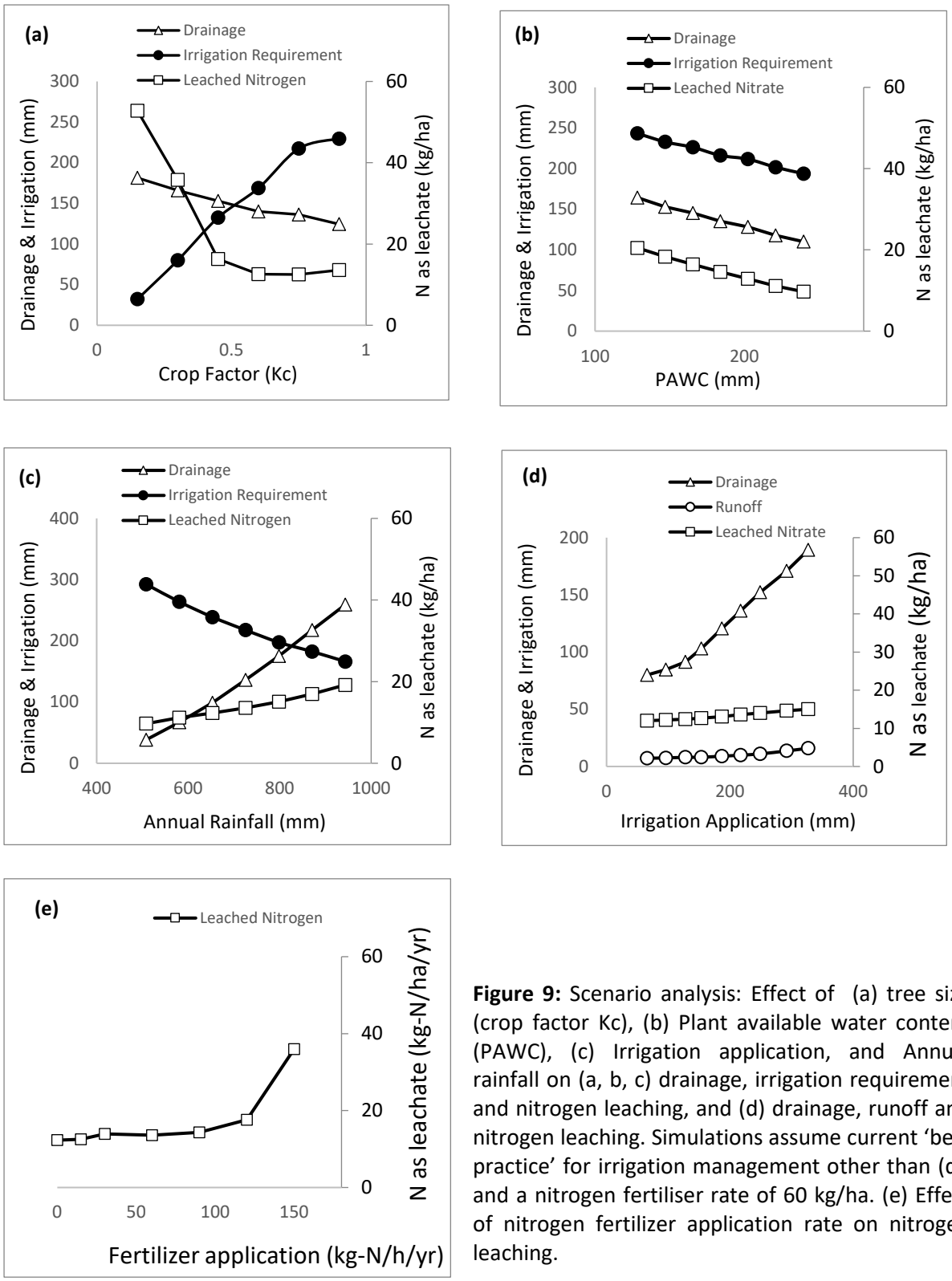

Figure 9: Scenario analysis: Effect of (a) tree size (crop factor Kc), (b) Plant available water content (PAWC), (c) Irrigation application, and Annual rainfall on (a, b, c) drainage, irrigation requirement and nitrogen leaching, and (d) drainage, runoff and nitrogen leaching. Simulations assume current 'best practice' for irrigation management other than (d), and a nitrogen fertiliser rate of 60 kg/ha. (e) Effect of nitrogen fertilizer application rate on nitrogen leaching.

Discussion

Error and uncertainty

Drainage flux and leached nitrate concentration were highly variable between fluxmeters, even within the same treatment. For example, within the medium irrigation treatment fluxmeter 7, & 8 recorded a total of 113 mm drainage over the 30 month monitoring period, whilst fluxmeter 8 located only 2 meters away only recorded 32 mm drainage. Likewise, nitrate concentration was also highly variable, for example adjacent fluxmeters 8 & 9 in August 2014 had nitrate concentrations of 0.5 mg/l and 45.2 mg/l. Variability was attributed to preferential flow, specifically a combination of finger flow in the A11 and A12 horizons, lateral flow along A12 / A2 horizon boundary and macropore flow within the BHs and B22 horizons, as described for the site in Hardie et al. (2018). Similar levels of variability between fluxmeters was also observed in a Bleached Mottled Grey Kurosol in the Huon Valley, Tasmania (Hardie et al., 2015).

The fluxmeters installed within the shoulder area (between the tree line and the inter-row) of the high treatment had substantially higher drainage flux, (average 534 mm) than the fluxmeters installed within the tree line (average 236), despite being in the same treatment. Nitrate concentration in the shoulder fluxmeters (average 7.1 mg/L), was also noted to be substantially lower than the adjacent tree line fluxmeters (average 21.9 mg/L). Notably 59 % of the drainage and 94 % of the leached nitrate in the shoulder region was collected over a 3 month period between June to August 2013. This suggests that drainage and nitrate leakage from the shoulder area resulted from the development of subsurface lateral flow between either in the A12 and A2 horizons or the A2 and Bhs horizons (Hardie et al., 2012) following saturation of the soil profile and development of a perched watertable over winter, rather than direct vertical leaching from the fertigation emitters.

Nitrate flux

The average volume of drainage collected at the Lucaston site at 7.8 mm/month (excluding shoulder area) was substantially lower than at the Mountain River site (Hardie et al., 2015), average 73.1 mm/month, located six km away on a similar soil type. Nitrate concentration in the leachate averaged 27.3 mg/L with individual flux meters recording nitrate concentrations as high as 235 mg/L. The nitrate-nitrogen concentration in the fertigation supply water varied between 800 and 1500 mg/L, such that the corresponding concentration in the drainage water, at a depth of 600 mm, was reduced by a factor of 20 or more, as a result of dilution with additional irrigation water and antecedent soil water, plus uptake by the tree's root system. Notably, monthly nitrate concentration exceeded the drinking water standard (DWS) of 50 mg $N\text{-}NO_3$/L of nitrate-nitrogen (NHMRC-ARMCANZ, 2011), 44 times (out of 279 samples) over the 30 month monitoring period. Average nitrate concentration at the Lucaston site at 27.3 mg/L was lower than that at Mountain River at 40.4 mg/L. Similar nitrate concentration in subsoil leachate in apple orchards has been reported by Atucha et al. (2011) who reported that monthly nitrate concentration in leachate from apple orchard under four different groundcover treatments ranged from 0.51 to 32.74 mg/L. Toselli et al. (2011) reported nitrate concentration in the water collected by lysimeters within an apple orchard ranged from less than 10 mg /L in late summer to more than 40 mg/L in winter. Stevenson and Neilsen (1990) reported annual average nitrate concentration in leachate from lysimeters installed in an apple orchard ranged from 211 to 439 mg/L.

Nitrate flux below the rootzone did not appear to be related to irrigation treatment as nitrate flux in the high irrigation treatment was 9.7 kg -N/ha/y, compared to 79.2 kg-N/ha/yr in the low treatment.

The average nitrate flux below 60 cm depth was 33.17 kg-N/ha/yr from below the tree row and 43.46 kg/Ha/yr from the shoulder area. Excluding nitrate additions from mineralisation and the shoulder area, this represents a loss of 55 % of the applied nitrogen fertilizer (60 kg-N/ha/yr) from the tree row. Average monthly nitrate flux following pre-harvest (October to February) Nitrogen application was 0.54 kg-N/ha/month, compared to 1.03 kg-N/ha/month post-harvest (March to May). Measured rates of nitrate flux were substantially higher than the SPASMO predicted average longterm nitrate leaching rate (Kc 0.75) at 12.5 kg/ha/yr.

Levels of nitrate leaching beneath the tree row at the Lucaston site at 30.25 kg -N/ha/yr (all treatment plus shoulder area) were substantially lower than those recorded at the Mountain River site at 220 kg -N/ha/yr. Given similarity of rainfall and irrigation strategy between the Lucaston and Mountain River sites (located approximately 6 km apart), the difference in drainage flux, nitrate concentration and thus nitrate leaching was attributed to the shallower installation of the fluxmeters at Mountain River at 30 cm at the base of the A1 horizon as opposed to 60 cm in the B21 horizon at Lucaston, and smaller tree size at Mountain River (LAI 0.34). The level of nitrate leaching at the Lucaston site appears to be at the lower end of nitrate leaching rates reported for apple orchards (Filipović et al., 2013; Stevenson and Neilsen, 1990; Toselli et al., 2011; Ventura et al., 2013). Stevenson and Neilsen (1990) reported nitrate leaching below 1.5 meters in a 'Macspur McIntosh' apple orchard averaged 42 - 271 kg ha^{-1} yr^{-1} nitrate. Atucha et al. (2011) reported nitrogen leaching from the subsoil of an apple orchard at 5.2 - 20.9 kg ha^{-1} yr^{-1}, whilst Filipović et al. (2013) reported seasonal nitrate leaching from an apple orchard was around 17 kg-N ha^{-1}.

Management

The modelling scenarios provide an insight to management at the site. They indicate that with an average rainfall of 726 mm the irrigation requirement at the current canopy size (Kc 0.71) is on average 217 mm/yr resulting in an average fruit yield of 85 t/ha, 136 mm drainage and 12.4 kg/ha yr nitrate leaching. A 30% reduction in rainfall to 508 mm/yr was predicted to resulted in an average fruit yield of 83.2 t/ha, an irrigation requirement of 293 mm, 38 mm drainage and 8.9 kg/ha yr nitrate leaching. This suggests that whilst nitrate leaching and drainage were reduced in the 30% lower rainfall year, the additional irrigation required to prevent crop moisture stress kept the soil profile sufficiently moist such that drainage and nitrogen leaching were not greatly affected. In a wet year with 30% above the average annual rainfall at 943 mm (similar to 2013-2014 909 mm), the irrigation requirement was 166 mm, drainage was 259 mm and nitrate leaching was 17.5 kg/ha/yr. This analysis indicates that even in a wet year, that supplementary irrigation is still required due to the mismatch in timing between rainfall events and crop moisture stress, however this results in greater storage of moisture within the soil profile, such that a greater proportion of rainfall results in drainage. Notably this increase in drainage results in only a modest increase in leached nitrate, of an additional 5.1 kg /ha.

The SPASMO modelling indicates that the current fertilizer practice of applying split pre and post-harvest 30 + 30 kg of nitrogen resulted in 12.4 kg/ha nitrate leaching per year and a yield of 85 t/ha. Zero application of nitrogen fertilizer still resulted in 11.2 kg/ha nitrate leaching and a 26.3 t/ha yield penalty. Consequently, efforts to eliminate nitrate leaching by shifting management to a zero inorganic nitrogen system is predicted to be ineffective at preventing nitrate leaching whilst having considerable impact on fruit production (31 % reduction). Doubling the current fertilizer application

to 120 kg /ha resulted in fruit yield from 85 t/ha to 94 t/ha, without a substantial increase in nitrate leaching from 12.4 kg/ha to 16.1 kg/ha, however fruit nitrogen content was estimated to increase from 0.56 (%) to 0.71 % which may lead to negative fruit quality outcomes.

The SPASMO modelling for the Lucaston site, indicates that nitrate leaching is somewhat insensitive to both irrigation and fertilizer application rates, and thus is largely beyond the control or influence of orchard management. SPASMO indicated that the amount of nitrate leaching at the site was most profoundly influenced by kc factor a surrogate for canopy size or tree age, in which nitrate leaching reduced up to a Kc factor 0.5 after which, nitrate leaching was largely unaffected by further increases in canopy size. HYDRUS-2D modelling at the nearby Mountain River site (Hardie, 2017) also reported that nitrate leaching was largely controlled by canopy size, in which nitrate leaching could be substantially reduced in mature but not young trees by conversion from spray to drip irrigation and ceasing manure application, neither of which are relevant to the Lucaston site.

Conclusion

Results demonstrated that over the 30 month monitoring period, leakage below 60 cm depth within the tree row of a commercial apple orchard at Lucaston, Tasmania, (excluding the shoulder area) averaged 93 mm/yr drainage, 33.2 kg/ha/yr nitrate at an average concentration of 30.5 mg/L. Irrigation treatment had no obvious effect on drainage volume or nitrate leaching, and only a small influence on apple yield. Differences between the measured and modelled drainage and nitrate flux were attributed to the extreme variability between fluxmeters, even within the same irrigation treatment. This variability resulted from preferential flow processes and occurrence of subsurface lateral flow in 2013. Options to reduce nitrate leaching are limited, as SPASMO modelling indicated that both the drainage flux and nitrate leaching were largely insensitive to irrigation and nitrogen fertilizer application rate, whilst having considerable impact on fruit yield.

Albornoz, F., 2016. Crop responses to nitrogen overfertilization: A review. Scientia Horticulturae 205, 79-83.

Allen, R.G., Pereira, L.S., Raes, D., Smith, M., 1998. Crop evapotranspiration: guidelines for computing crop water requirements. FAO Irrigation and Drainage Paper No. 56, FAO, Rome, Italy, 300 pp.

Atucha, A., Merwin, I.A., Purohit, C.K., Brown, M.G., 2011. Nitrogen dynamics and nutrient budgets in four orchard groundcover management systems. HortScience 46, 1184-1193.

BOM, 2015. Climate statistics for Australian locations: Grove, Tasmania. Bureau of Meterology.

Cichota, R., Snow, V.O., 2009. Estimating nutrient loss to waterways - An overview of models of relevance to New Zealand pastoral farms. New Zealand Journal of Agricultural Research 52, 239-260.

Close, M.E., Pang, L., Magesan, G.N., Lee, R., Green, S.R., 2003. Field study of pesticide leaching in an allophanic soil in New Zealand. 2: Comparison of simulations from four leaching models. Australian Journal of Soil Research 41, 825-846.

Crescimanno, G., Garofalo, P., 2005. Application and evaluation of the SWAP model for simulating water and solute transport in a cracking clay soil. Soil Science Society of America Journal 69, 1943-1954.
Di, H.J., Cameron, K.C., 2002. Nitrate leaching in temperate agroecosystems: Sources, factors and mitigating strategies. Nutrient Cycling in Agroecosystems 64, 237-256.
Dong, S., Cheng, L., Scagel, C.F., Fuchigami, L.H., 2004. N uptake, soil retention and loss of soil-applied 15NH 4 15NO3 in young Fuji/M.26 apple trees with different N status. Journal of Horticultural Science and Biotechnology 79, 395-399.
Fernández-Escobar, R., Benlloch, M., Herrera, E., García-Novelo, J.M., 2004. Effect of traditional and slow-release N fertilizers on growth of olive nursery plants and N losses by leaching. Scientia Horticulturae 101, 39-49.
Filipović, V., Kodešová, R., Petošić, D., 2013. Experimental and mathematical modeling of water regime and nitrate dynamics on zero tension plate lysimeters in soil influenced by high groundwater table. Nutrient Cycling in Agroecosystems 95, 23-42.
Gärdenäs, A.I., Hopmans, J.W., Hanson, B.R., Šimůnek, J., 2005. Two-dimensional modeling of nitrate leaching for various fertigation scenarios under micro-irrigation. Agricultural Water Management 74, 219-242.
Gee, G.W., Newman, B.D., Green, S.R., Meissner, R., Rupp, H., Zhang, Z.F., Keller, J.M., Waugh, W.J., van der Velde, M., Salazar, J., 2009. Passive wick fluxmeters: Design considerations and field applications. Water Resources Research 45, W04420.
Gee, G.W., Zhang, Z.F., Ward, A.L., Keller, J.M., 2004. Passive-wick water fluxmeters: theory and practice, Supersoil 2004: 3rd Australian New Zealand Soils Conference, University of Sydney, Australia.
Green, S., Clothier, B., Caspari, H., Neal, S., 2002. Rootzone processes, tree water-use, and the equitable allocation of irrigation water to olives, Geophysical Monograph Series, pp. 337-345.
Green, S., Clothier, B., Jardine, B., 2003a. Theory and Practical Application of Heat Pulse to Measure Sap Flow. Agronomy Journal 95, 1371-1379.
Green, S., Clothier, B.E., 2016a. SPASMO Modelling of Precision Fertigation: Appendix 3 Final Report, PIPS Precision Fertigation for Improved Apple Orchard Productivity: Milestone 8 Final Report. Tasmanian Institute of Agriculture, University of Tasmania, and Plant and Food Research, New Zealand.
Green, S., Clothier, B.E., 2016b. SPASMO Modelling of Precision Fertigation: Appendix Final Report, PIPS Precision Fertigation for Improved Apple Orchard Productivity: Milestone 8 Final Report. Tasmanian Institute of Agriculture, University of Tasmania, and Plant and Food Research, New Zealand.
Green, S., McNaughton, K., Wünsche, J.N., Clothier, B., 2003b. Modeling Light Interception and Transpiration of Apple Tree Canopies. Agronomy Journal 95, 1380-1387.
Green, S.R., Clothier, B.E., 1988. Water use of kiwifruit vines and apple trees by the heat-pulse technique. Journal of Experimental Botany 39, 115-123.
Green, S.R., Deurer, M., Clothier, B.E., 2012a. A Consumptive water footprint analysis for apple fruit production. Acta Horticulturae 951, 197-204.
Green, S.R., Deurer, M., Clothier, B.E., 2012b. A Consumptive water footprint analysis for apple fruit production, Acta Horticulturae, pp. 197-204.
Green, S.R., Sivakumaran, S., Van Den Dijssel, C., Mills, T.M., Blattmann, P., Snelgar, W.P., Clearwater, M.J., Judd, M., 2007. A water and nitrogen budget for 'Hort16A' kiwifruit vines. Acta Horticulturae, pp. 527-534.
Green, S.R., Snow, V., Clothier, B.E., 2003c. Modelling the nitrogen dynamics under pasture irrigated with dairy effluent. HortResearch Client Report No. 2003/6115.
Green, S.R., Vogeler, I., Clothier, B.E., Mills, T.M., Van Den Dijssel, C., 2003d. Modelling water uptake by a mature apple tree. Australian Journal of Soil Research 41, 365-380.

585 Greven, M., Green, S., Robinson, B., Clothier, B., Vogeler, I., Agnew, R., Neal, S., Sivakumaran, S.,
586 2007. The impact of CCA-treated posts in vineyards on soil and ground water, Water Science and
587 Technology, pp. 161-168.
588 Hardie, M., 2017. Two dimensional modelling of nitrate flux in a commercial apple orchard. Soil
589 Science Society of America Journal 81, 1235-1246.
590 Hardie, M., Doyle, R., Cotching, W.E., Lisson, S., 2012. Subsurface lateral flow in texture-contrast
591 (duplex) soils and catchments with shallow bedrock. Applied and Environmental Soil Science, Article
592 ID 861358, 861310 pages.
593 Hardie, M., Ridges, J., Swarts, N., Close, D., 2018. Drip irrigation wetting patterns and nitrate
594 distribution: comparison between electrical resistivity (ERI), dye tracer, and 2D soil–water modelling
595 approaches. Irrigation Science 36, 97-110.
596 Hardie, M.A., Oliver, G., Clothier, B.E., Bound, S.A., Green, S.A., Close, D.C., 2015. Effect of biochar on
597 nutrient leaching in a young apple orchard. Journal of Environmental Quality 44, 1273-1282.
598 Isbell, R.F., 2002. The Australian Soil Classification. CSIRO Publishing, Melbourne.
599 Jones, C.A., Kiniry, J.R., 1986. CERES-Maize: A simulation model of maize growth and development.
600 Texas A&M University Press, College Station, TX.
601 Keating, B.A., Carberry, P.S., Hammer, G.L., Probert, M.E., Robertson, M.J., Holzworth, D., Huth, N.I.,
602 Hargreaves, J.N.G., Meinke, H., Hochman, Z., McLean, G., Verburg, K., Snow, V., Dimes, J.P., Silburn,
603 M., Wang, E., Brown, S., Bristow, K.L., Asseng, S., Chapman, S., McCown, R.L., Freebairn, D.M., Smith,
604 C.J., 2003. An overview of APSIM, a model designed for farming systems simulation. European
605 Journal of Agronomy 18, 267-288.
606 Klein, I., Levin, I., Bar-Yosef, B., Assaf, R., Berkovitz, A., 1989. Drip nitrogen fertigation of 'Starking
607 Delicious' apple trees. Plant and Soil 119, 305-314.
608 Lehmann, J., Schroth, G., 2003. Nutrient leaching, in: Schroth, G., Sinclair, F.L. (Eds.), Trees, Crops
609 and Soil Fertility: Concepts and Research Methods, University of Wales, Bangor, UK pp. 151-166.
610 Loescher, W.H., Mccamant, T., Keller, J.D., 1990. Carbohydrate reserves, translocation, and storage
611 in woody plant-roots. HortScience 25, 274-281.
612 Ma, L., Scott, H.D., Shaffer, M.J., Ahuja, L.R., 1998. RZWQM simulations of water and nitrate
613 movement in a manured tall fescue field. Soil Science 163, 259-270.
614 McKenzie, N.J., Coughlan, K.L., Cresswell, H.P., 2002. Soil Physical Measurement and Interpretation
615 for Land Evaluation. CSIRO Publishing, Melbourne.
616 Mualem, Y., 1976. New model for predicting the hydraulic conductivity of unsaturated porous
617 media. Water Resources Research 12, 513-522.
618 Neilsen, D., Neilsen, G.H., 2002. Efficient use of nitrogen and water in high-density apple orchards.
619 HortTechnology 12, 19-25.
620 Neilsen, G.H., Neilsen, D., Hogue, E.J., Herbert, L.C., 2004. Zinc and boron nutrition management in
621 fertigated high density apple orchards. Can J Plant Sci 84, 823-828.
622 NHMRC-ARMCANZ, 2011. Australian Drinking Water Guidlines 6, National Water Quality
623 Management Strategy, national health and medical Research Council.
624 O'Dell, J., 1993. US EPA Method 353.2, Revision 2.0.
625 Oberly, G., Boynton, D., 1966. Nutrition of fruit crops, in: Childers, F. (Ed.), Apple nutrition.
626 Horticultural Publications, Rutgers, The State University. New Brunswick, pp. 22-26.
627 Ongley, E.D., 1996. Control of water pollution from agriculture. Food and Agriculture Organisation of
628 the United Nations, Rome.
629 Peters, A., Durner, W., 2008. Simplified evaporation method for determining soil hydraulic
630 properties. Journal of Hydrology 356, 147-162.
631 Phogat, V., Skewes, M.A., Cox, J.W., Alam, J., Grigson, G., Šimůnek, J., 2013. Evaluation of water
632 movement and nitrate dynamics in a lysimeter planted with an orange tree. Agricultural Water
633 Management 127, 74-84.
634 Rayment, G.E., Higginson, F.R., 1992. Australian Laboratory Handbook of Soil and Water Chemical
635 Methods. Inkata Press, Melbourne.

Reynolds, W.D., 2008. Chapter 77: Saturated hydraulic properties: Ring infiltrometer, in: Carter, M.R., Gregorich, E.G. (Eds.), Soil Sampling and Methods of Analysis, 2nd Edition ed. Canadian Society of Soil Science, CRC Press, Boca Raton, pp. 1043-1056.
Reynolds, W.D., Elrick, D.E., 1990. Ponded infiltration from a single ring: I. Analysis of steady flow. Soil Science Society of America Journal 54, 1233-1241.
Rosen, M.R., Reeves, R.R., Green, S., Clothier, B., Ironside, N., 2004. Prediction of groundwater nitrate contamination after closure of an unlined sheep feedlot. Vadose Zone Journal 3, 990-1006.
Sarmah, A.K., Close, M.E., Pang, L., Lee, R., Green, S.R., 2005. Field study of pesticide leaching in a Himatangi sand (Manawatu) and a Kiripaka bouldery clay loam (Northland). 2. Simulation using LEACHM, HYDRUS-1D, GLEAMS, and SPASMO models. Australian Journal of Soil Research 43, 471-489.
Saseendran, S.A., Nielsen, D.C., Ma, L., Ahuja, L.R., Halvorson, A.D., 2004. Modeling nitrogen management effects on winter wheat production using RZWQM and CERES-Wheat. Agronomy Journal 96, 615-630.
Šimůnek, J., van Genuchten, M.T., 2008. Modeling nonequilibrium flow and transport processes using HYDRUS. Vadose Zone Journal 7, 782-797.
Sokalska, D.I., Haman, D.Z., Szewczuk, A., Sobota, J., Dereń, D., 2009. Spatial root distribution of mature apple trees under drip irrigation system. Agricultural Water Management 96, 917-924.
Stefanelli, D., Goodwin, I., Jones, R., 2010. Minimal nitrogen and water use in horticulture: Effects on quality and content of selected nutrients. Food Res Int 43, 1833-1843.
Stevenson, D.S., Neilsen, G.H., 1990. Nitrogen additions and losses to drainage in orchard-type irrigated lysimeters. Canadian Journal of Soil Science 70, 11-19.
Stöckle, C.O., Donatelli, M., Nelson, R., 2003. CropSyst, a cropping systems simulation model. European Journal of Agronomy 18, 289-307.
Swarts, N., Montagu, K., Oliver, G., Southam-Rogers, L., Hardie, M., Corkrey, R., Rogers, G., Close, D., 2016a. Benchmarking nitrous oxide emissions in deciduous tree cropping systems. Soil Research 54, 500-511.
Swarts, N.D., Hardie, M., Close, D.C., 2016b. Precision nitrogen fertigation and irrigation management for improved apple quality, Acta Horticulturae, pp. 485-489.
Thorburn, P.J., Cook, F.J., Bristow, K.L., 2003. Soil-dependent wetting from trickle emitters: Implications for system design and management. Irrigation Science 22, 121-127.
Toselli, M., Perry, R.L., Flore, J.A., 2011. Evaluation of nitrate-nitrogen leaching from lysimeter-grown bearing apple trees. Soil Science 176, 280-287.
UMS, 2013. HYPROP User Manual. UMS GmbH München, Art. no. HYPROP.
van Dam, J.C., Huygen, J., Wesseling, J.G., Feddes, R.A., Kabat, P., van Walsum, P.E.V., Groenendijk, P., van Diepen, C.A., 1997. Theory of SWAP version 2.0; Simulation of water flow, solute transport and plant growth in the Soil-Water-Atmosphere-Plant environment. Wageningen Institute for Environment and Climate Research DLO Winand Staring Centre, Wageningen.
Van der Kooij, S., Zwarteveen, M., Boesveld, H., Kuper, M., 2013. The efficiency of drip irrigation unpacked. Agricultural Water Management 123, 103-110.
van Genuchten, M.T., 1980. Closed-form equation for predicting the hydraulic conductivity of unsaturated soils. Soil Science Society of America Journal 44, 892-898.
Ventura, M., Sorrenti, G., Panzacchi, P., George, E., Tonon, G., 2013. Biochar reduces short-term nitrate leaching from a horizon in an apple orchard. Journal of Environmental Quality 42, 76-82.
Wendroth, O., Ehlers, W., Hopmans, J.W., Kage, H., Halbertsma, J., Wosten, J.H.M., 1993. Reevaluation of the evaporation method for determining hydraulic functions in unsaturated soils. Soil Science Society of America Journal 57, 1436-1443.

Appendix 5: Draft manuscript on NPK trial

Interactions of nitrogen, phosphorus and potassium fertilization on 'Gala' apple tree nutrition

Bi Zheng Tan*, Nigel Swarts, Dugald Close

Tasmania Institute of Agriculture, College of Sciences and Engineering, Private Bag 98, University of Tasmania, Hobart TAS 7001, Australia.

*Email address: bi.tan@utas.edu.au

Highlights

They consist of a short collection of bullet points that capture the novel results of your research as well as new methods that were used during the study (if any). Please have a look at the examples here: example Highlights. Highlights should be submitted in a separate editable file in the online submission system. Please use 'Highlights' in the file name and include 3 to 5 bullet points (maximum 85 characters, including spaces, per bullet point).

Abstract

A concise and factual abstract is required. The abstract should briefly state the purpose of the research, the principal results, and major conclusions. No word limits.

Keywords

maximum of 6 keywords, using American spelling and avoiding general and plural terms and multiple concepts (avoid, for example, 'and', 'of'). Be sparing with abbreviations: only abbreviations firmly established in the field may be eligible. These keywords will be used for indexing purposes.

Introduction

Nutrient management via the application of fertilizer is a key factor determining the sustainable productivity of quality fruit. The challenges of negative environmental impacts from excessive fertilizer application (Neilsen and Neilsen, 2002, Swarts et al., 2016), depletion of natural resources and increasing demand for sustainable production from retailers and consumers requires precise management of mineral nutrition in fruit production. Precise management requires understanding of mineral nutrient uptake dynamics. The macronutrients N, P, and K particularly affect apple fruit quality (Neilsen et al., 2008) and yield (Nava and Dechen, 2009).. However, few studies have investigated interactions in

uptake between the key macronutrient minerals. and how/if these affect fruit quality and yield at harvest.

Uptake of macronutrient minerals from the soil is determined by both plant ion-transport mechanisms and the physicochemical properties of the ions (Mengel et al., 2001a). Each form of ions has various specific transport mechanisms to transport across the soil-root interface including both active and passive transport (Mengel et al., 2001a). The ions in the soil solution can also interact with other forms of ion, transport across root epidermis, and fixed onto soil surface to maintain electrochemical equilibrium (Mengel et al., 2001b). As a result, the interactions between mineral ions within the soil solution and the soil-root interface will be crucial to understand how apple tree take up nutrient and affect the fruit production and quality.

N, P and K fertilisers are precisely applied through fertigation in order to replace nutrients lost through harvest and pruning to ensure sustainable production. In a typical orchard soil, N is predominantly present for plant uptake in the form of nitrate ion, NO_3^-, rather than ammonium ion, NH_4^+ (Miller and Cramer, 2005). Nitrate ion has high mobility in the soil solution which renders it prone to leaching below the rootzone after an irrigation or rainfall event (Neilsen and Neilsen, 2002). However, a relatively high abundance of nitrate ensure it is more likely to flow to the root epidermis for uptake. In contrast, more than 90% of the P is fixed and not available for plant uptake, while the remaining P, in the inorganic form releases the plant available dihydrogenphosphate ion, $H_2PO_4^-$ extremely slowly into soil solution (Maathuis, 2009). As a result, plant roots mostly rely on active uptake to transport the $H_2PO_4^-$ ion across the root epidermis so there is not competition for uptake with N. On the other hand K, present as potassium ion K^+ in the soil solution, can be readily taken up through both active and passive uptake pathways. Although cations can be bound onto negatively charged clay particles and organic matter, the abundance and the monovalency of

K^+ results in exchang into the soil solution with other cations of more valence electrons, such as Ca^{2+} and Mg^{2+} (Dontsova et al., 2004). It is believed that constant cycling of K^+ in and out from vascular system can mediate the uptake and translocation of anions to the shoot (Maathuis, 2009) in order to maintain electrochemical neutrality within the plant system.

Due to the distinct uptake mechanisms and physicochemical characteristics of N, P and K, there is a need to understand antagonistic or synergistic uptake effects of macronutrients into apple tree and fruit. This study aimed to examine interactions of N, P, and K fertilization at various rates on the tree and fruit uptake dynamics .

Materials and Methods

Experiment site and plant materials

The experiment was conducted from April 2018 to June 2019 over a growing season in a commercial orchard located in the Derwent Valley, southern Tasmania (42°44'31"S 146°58'22"E), Australia. The area has a cool temperate climate with a cool and rainy winter, and mild summer. Mean maximum and minimum temperatures are 24 ˚C and 10 ˚C respectively in the summer months, and 11.5 ˚C and 1.5 ˚C respectively in the winter months. Mean annual rainfall is 572.2 mm, with summer being the driest of a fairly even seasonal distribution.

The apple trees were ‘Gala’ cultivar grown on M26 rootstock planted in 2005 at a density of 1667 tree ha^{-1}, trained to a central leader system supported by trellis. The trees were planted on a Dermosol with a sandy loam A horizon approximately 40 cm deep and subjected to commercial management practices prior to the experiment. Prior to the experiment, a total of 254 mm of water was irrigated over the winter dormancy period from 8^{th} to 12^{th} April 2018 attemping to deep drain the mobile mineral nutrients from the top soil. Following the deep drainage irrigation the soil N and P were below the suggested level and

soil K within the optimal range when measured at 3 WAFB (Table 1), before the application of treatments. A 1.0 m wide weed-free strip along the tree line was maintained with application of 'Basta' herbicide. During the growing season, trees were irrigated using microjet sprinklers (50 L hr^{-1}), for 2-3 hours when low soil moisture level was detected using soil moisture probes.

Table 1 Soil mineral nutrients concentration and chemical properties of soil at 0-10 cm depth measured at 3 WAFB, prior to application of experiment treatments and the recommended ranges for orchard.

	NH_4^+ (mg kg^{-1})	**NO_3^- (mg kg^{-1})**	**P (mg kg^{-1})**	**K (mg kg^{-1})**	**$C_{organic}$ (%)**	**EC (dS m^{-1})**	**pH ($CaCl_2$)**	**pH (H_2O)**	
3 WAFB	4.36	3.14	95.09	274.5	1.38	0.082	6.49	7.27	
Recommended range		10	100-300	195-390	1.0-3.0	< 0.2	5.5-6.0		FAO 6. Orchard management and plant husbandry

Experiment treatments and design

This experiment deployed a 2 × 2 × 2 factorial completely randomized design of N, P and K fertilizer rate, replicated five times to give a total of 40 tree plots. Each plot consisted of three sampling trees and one buffering tree on both sides. Nitrogen fertilizer was delivered in the form of calcium nitrate either at the rate of 10 (N1) or 50 (N2) kg N ha^{-1}; phosphorus fertilizer was delivered in the form of calcium phosphate monobasic either at the rate of 10 (P1) or 40 (P2) kg P ha^{-1}; potassium fertilizer was delivered in the form of potassium sulphate either at the rate of 50 (K1) or 150 (K2) kg K ha^{-1}. Fertilizer treatments were divided equally

over four successive weekly applications from 8th November 2018, 4 WAFB. During each application, calcium phosphate monobasic was broadcasted, and calcium nitrate and potassium sulphate were dissolved in 5 L of water separately and fertigated evenly within the herbicide strip of each tree plot.

Leaf petiole sampling and vascular sap analysis

The uptake and translocation of mineral nutrients to the tree canopy was assessed by monitoring the nutrient concentration of vascular sap of leaf petiole over the growing season. The leaf petiole samples were collected on: 1; 3rd December 2018 (8 WAFB), 2; 4th February 2019 (17 WAFB), and 3; 18 March 2019 (23 WAFB). The respective sampling times were selected as they represented: 1; the vascular sap status during active uptake of nutrients to the canopy, 2; ceased to translocate nutrient into fruit, and 3; the physiological change post-harvest. Samples were taken between 8–10 a.m. for consistency when the tissue has high turgor. Forty fully expanded leaves were randomly sampled from the middle section of each tree and separated into leaf petiole and lamina. Leaf petiole samples were packed in zip-lock bags and kept in an insulated cooler box between transportation. Leaf petiole samples were then analyzed by a commercial laboratory within 48 hours of sampling.

Vascular sap of leaf petiole was extracted using in-house designed and manufactured precision hydraulic presses (AgVita, Australia), filtered, and diluted for chemical analysis. Ammonium-N, nitrate-N, and chloride (Cl) were measured using QUIKCHEM® 8500 Series 2 flow injection analyzer (Lachat, USA). Other macro-nutrients including phosphorus (P), potassium (K), calcium (Ca), sulfur (S), magnesium (Mg), and micro-nutrients including boron (B), molybdenum (Mo), copper (Cu), iron (Fe), manganese (Mn), zinc (Zn), sodium (Na) were measured using 5110 inductively coupled plasma-optical emission spectrometer (Agilent Technologies, USA).

Plant tissue and soil sampling

Fruits were harvested on 28th February 2019 from the middle tree of each sampling plot, and yield was measured. Twenty fruits were subsampled for fruit quality analysis and another five fruits were cut for mineral nutrient analysis. Leaf laminae and cut fruit samples were dried at 60 ˚C until a constant weight was obtained.

Soil was sampled on 2nd November 2018 (3 WAFB) and 18th March 2019 (23 WAFB), which were prior to the application of fertilizer treatments and three weeks after harvest, respectively. At each sampling, a step probe was used to collect four 2.2 × 10.0 cm soil core samples. Two samples were taken from soil midway between two trees, another two were taken within 10 cm radius of two random tree trunks. All four samples were homogenously mixed into one, soil samples were air-dried until a constant weight and passed through 2 mm sieve.

Plant tissue and soil mineral nutrient analysis

Dried leaf and fruit samples, and sieved soil samples were sent to a commercial laboratory (CSBP Soil and Plant Analysis Laboratory, Western Australia) for chemical properties and mineral nutrient analysis. Leaf and fruit samples were measured for total N with Dumas method using a Truspec FP628 high temperature combustion analyser (LECO Corporation, USA), and nitrate-N and Cl were analyzed using a QUIKCHEM® 8500 Series 2 flow injection analyzer (LaChat, USA) (Rayment and Lyons, 2011). Phosphorus, K, Ca, S, Mg, B, Cu, Fe, Mn and Na were measured using an iCAP6500 Radial inductively coupled plasma spectrometer (Thermo Scientific, Germany) (McQuaker et al., 1979).

Soil ammonium-N and nitrate-N were measured as described above. Total organic carbon was measured colorimetrically using Ledetect 96 (Dynamica, USA). P and K was prepared using the Colwell method (Rayment and Lyons, 2011) and measured

colorimetrically using AquaKem 600 Series (Thermo Scientific, Finland) and SpectrAA 55 atomic absorption spectrometer (Varian, Australia), respectively. Electrical conductivity was measured using a 122216 EC Probe (TPS, Australia), while pH (water) and pH ($CaCl_2$) were measured using a LL Solitrode pH Electrode (Metrohm, Switzerland).

Fruit quality assessment

Fruit weight and size were measured using Vernier callipers. Peel red colour coverage was visually rated using a colour chart ranging from 1–5, where 1 represented 0-20% red coverage over the fruit and successive ranks increased in 20% steps. Red colour intensity was measured visually with a 'Royal Gala' colour chart (Enza, New Zealand) ranging from 1-11, where 1 represents light red and 11 represents a dark red colour. Background colour of peel where red pigmentation was not developed was visually assessed with a colour chart ranging from 1-10, where the colour shift from green (1) to light green (5) to yellow (10). A Delta absorbance meter was used to assess the maturity of the fruit by measuring the chlorophyll-a in the fruit mesocarp (Costa et al., 2009). Peel blush colour was also assessed by using a CR-400 chroma meter (Konica Minolta, USA) to take an average of three random measurements from the red blush area of each fruit. Peel blush colour was reported in L*a*b* colour space. A thin slice of peel was removed on the blush side of each apple to measure flesh firmness using a GUSS Fruit Texture Analyser (GUSS, South Africa). Juice was collected to measure total soluble solids (TSS) by using a digital refractometer (Atago, Japan). The fruit was then cut horizontally in half, the cut surface of the bottom half was sprayed with iodine solution and left to dry for five minutes before starch index was visually measured against the Cornell Starch-Iodine Index (1, full starch; 8, no starch)(Blanpied and Silsby, 1992).

Statistical analysis

Data were subjected to three-way ANOVA test assumption tests prior to analysis. Three-way ANOVA and Tukey's HSD test were used to compare treatment means at 95% confidence level using the R statistic package (Team, 2019).

Results

Result highlights

1) Interactions between N, P, and K fertilizer application at two different rates did not resulted in significant difference in fruit yield, size (weight), and quality attributes (Table S1) from a single season of fertilizer treatment.

2) Leaf petiole analyses over growing season (8, 17, 23 WAFB) showed that the uptake of macronutrients, including ammonium-N, nitrate-N, P, K, Ca, Mg (Table S2) were not affected by interactions between N, P, and K fertilizer application at two different rates.

3) Among the micronutrients (Zn, B, Mn, Mo), interaction between N:P significantly affect the petiole Zn content at 17 WAFB and petiole Mo content at 8 WAFB (Figure 1). At low N application rate (10 kg N ha^{-1}), a synergistic impact of increase in P application rate can significantly improve the petiole Zn content as measured at 17 WAFB. In contrast, when both N and P rates were increased to 50 and 40 kg ha^{-1} respectively, an antagonistic impact of excess N and P resulted to the petiole Mo content was significantly reduced at 8 WAFB. Both observations might be an indirect impact of the fertilizer application of N and P which present as anions in the soil and Zn and Mo present as cation in the soil.

   Petiole Mo content was also significantly affected interaction between N and K (Figure 2). low N application rate (10 kg K ha^{-1}), an increase of K rate from 50 to 150 kg K ha^{-1} significantly increase petiole Mo content at 8 wafb. In contrast, interaction between P and K (Figure 3) significantly reduced the petiole Mo content at 23 WAFB when K application rate increase from 50 to 150 kg K ha^{-1} and P application rate was low (10 kg P ha^{-1}). At earlier in the season, fertilizer K application can synergistically improve the uptake of Mo, however, the influence of K fertilization was the opposite at the later of the season.
4) Leaf lamina N content (Figure 4a) was significantly increased by increase in N application rate between 8 and 23 WAFB. An antagonistic impact was observed

between N application rate and leaf P content (Figure 4b), where an increase in N application rate significantly reduce the leaf P content from 17 WAFB to 23 WAFB. At low N application rate, a synergistic effect of increase in K fertilization rate from 50 to 150 kg K ha^{-1} significantly increase leaf lamina P content at 23 WAFB. A similar trend was also observed at 17 WAFB was also observed although the result was not significantly different, possibly due to large variation within sample population.

5) Fruit and leaf B content at 20 WAFB (fruit harvest) and 23 WAFB respectively (Figure 6) were significantly reduced by increasing P application rate. This indicate a possible antagonistic relationship between P fertilizer application and fruit and lead B content/uptake.

6) Soil N, P and K (Table S3) were significantly affected by the increase in N, P, and K fertilization rates, respectively. Interestingly, nitrate N was significantly lower in the soil that received high P fertilization rate (40 kg P ha^{-1}) than that received low P fertilization rate. Potassium application rate at 150 kg K ha^{-1} also significantly increased soil electric conductivity at 23 WAFB (after fruit harvest) than those received 50 kg K ha^{-1}.

Table S1 Fruit yield, weight, and quality attributes of 'Gala' apple on M26 rootstock under different N, P, and K fertilization rates at harvest of 2018-19 growing season.

Treatment	Fruit yield (kg tree^{-1})	Fruit weight (g)	Firmness (kg)	TSS (Brix°)	Starch index	Delta absorbance	Hue angle (h°)	Chroma	Blush coverage
N rate (N)									
N1	7.48	164.22	164.22	7.48	5.49	0.27	30.78	42.56	3.91
N2	6.87	164.11	164.11	6.87	5.98	0.33	32.00	42.19	3.84
Significance	ns.	ns.	ns.	ns.	ns.	ns.	ns.	ns.	ns.
P rate (P)									
P1	7.65	160.47	160.47	7.65	4.33	0.37	38.55	40.34	2.44
P2	6.70	167.68	167.68	6.70	5.63	0.30	30.06	41.93	4.08
Significance	ns.	ns.	ns.	ns.	ns.	ns.	ns.	ns.	ns.
K rate (K)									
K1	8.32	163.37	163.37	8.32	5.56	0.31	32.67	42.57	3.72
K2	6.03	165.01	165.01	6.03	5.89	0.30	30.07	42.16	4.04
Significance	ns.	ns.	ns.	ns.	ns.	ns.	ns.	ns.	ns.
Interaction									
N × P	ns.	ns.	ns.	ns.	ns.	ns.	ns.	ns.	ns.
N × K	ns.	ns.	ns.	ns.	ns.	ns.	ns.	ns.	ns.
P × K	ns.	ns.	ns.	ns.	ns.	ns.	ns.	ns.	ns.
N × P × K	ns.	ns.	ns.	ns.	ns.	ns.	ns.	ns.	ns.

Value represent the mean, n = 5. The effect of each factor and interactions between the factors are examined with three-way ANOVA at ($\alpha = 0.05$) and the respective significance level is indicated by the following symbols: "ns.", ($P > 0.05$); "*", ($P < 0.05$); "**", ($P < 0.01$); "***", ($P < 0.001$).

Table S2 Macronutrients (nitrate-N, ammonium-N, P, K, Ca, Mg) of 'Gala' apple leaf petiole at 8, 17, 23 WAFB under different N, P, and K fertilization rates at harvest of 2018-19 growing season.

	Ammonium-N (ppm)			**Nitrate-N (ppm)**			**P (ppm)**			**K (ppm)**			**Ca (ppm)**		
WAFB	**8**	**17**	**23**	**8**	**17**	**23**	**8**	**17**	**23**	**8**	**17**	**23**	**8**	**17**	**23**
Treatment															
N rate (N)															
N1	6.52	7.34	3.90	29.18	22.39	31.63	432.5	397.8	417.0	7864	12447	11968	1335	1881	2301
N2	7.34	7.66	3.76	32.74	24.25	37.23	423.1	393.6	395.2	7693	12136	11979	1256	1858	2231
Significance	ns.	ns.	ns.	ns.	ns.	ns.	ns.	ns.	ns.	ns.	ns.	ns.	ns.	ns.	ns.
P rate (P)															
P1	7.32	7.51	3.86	30.29	24.11	28.78	422.8	381.5	394.2	7886	12001	11842	1335	1853	2289
P2	6.54	7.49	3.81	31.63	22.54	37.46	432.8	409.9	418.0	7671	12583	12105	1256	1886	2243
Significance	ns.	ns.	ns.	ns.	ns.	ns.	ns.	ns.	ns.	ns.	ns.	ns.	ns.	ns.	ns.
K rate (K)															
K1	6.53	7.65	4.01	29.42	23.52	37.76	430.9	398.2	400.0	7965	12232	11707	1357	1935	2297
K2	7.33	7.35	3.66	32.50	23.12	31.22	424.7	393.2	411.8	7591	12351	12239	1234	1804	2235
Significance	ns.	ns.	ns.	ns.	ns.	ns.	ns.	ns.	ns.	ns.	ns.	ns.	ns.	ns.	ns.
Interaction															
N × P	ns.	ns.	ns.	ns.	ns.	ns.	ns.	ns.	ns.	ns.	ns.	ns.	ns.	ns.	ns.
N × K	ns.	ns.	**	*	ns.	ns.	ns.	*	ns.	ns.	ns.	ns.	ns.	ns.	ns.
P × K	ns.	ns.	ns.	ns.	ns.	ns.	ns.	ns.	ns.	ns.	ns.	ns.	ns.	ns.	ns.
N × P × K	ns.	ns.	ns.	ns.	ns.	ns.	ns.	ns.	ns.	ns.	ns.	ns.	ns.	ns.	ns.

Value represent the mean, n = 5. The effect of each factor and interactions between the factors are examined with three-way ANOVA at ($\alpha = 0.05$) and the respective significance level is indicated by the following symbols: "ns.", ($P > 0.05$); "*", ($P < 0.05$); "**", ($P < 0.01$); "***", ($P < 0.001$).

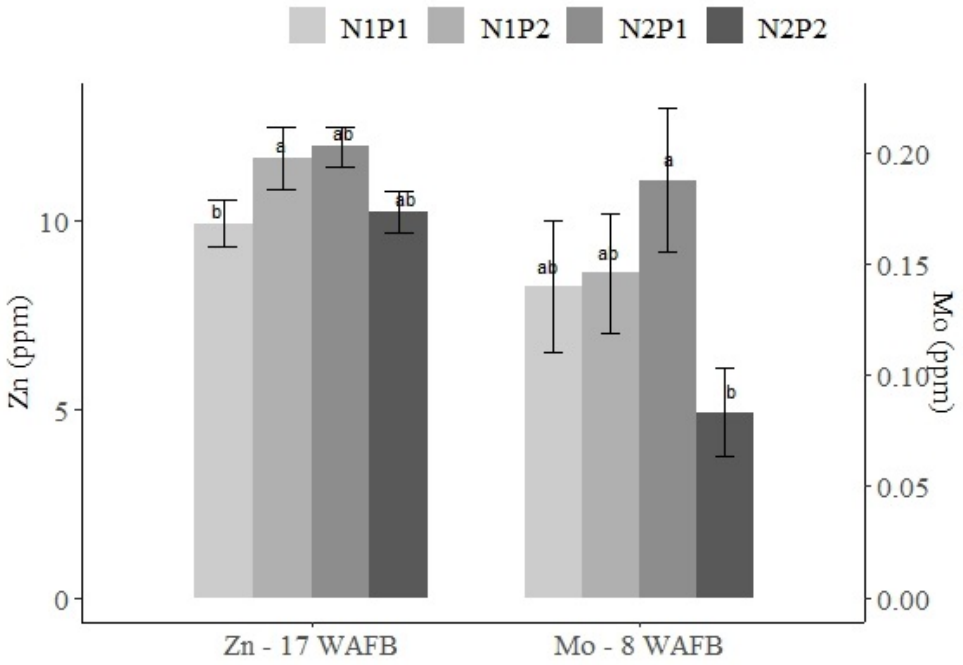

Figure 1 Zinc (ppm) and Molybdenum (ppm) content of leaf petiole at 17 and 8 WAFB respectively affected by the interactions between N and P fertilization rates at harvest of 2018-19 growing season.

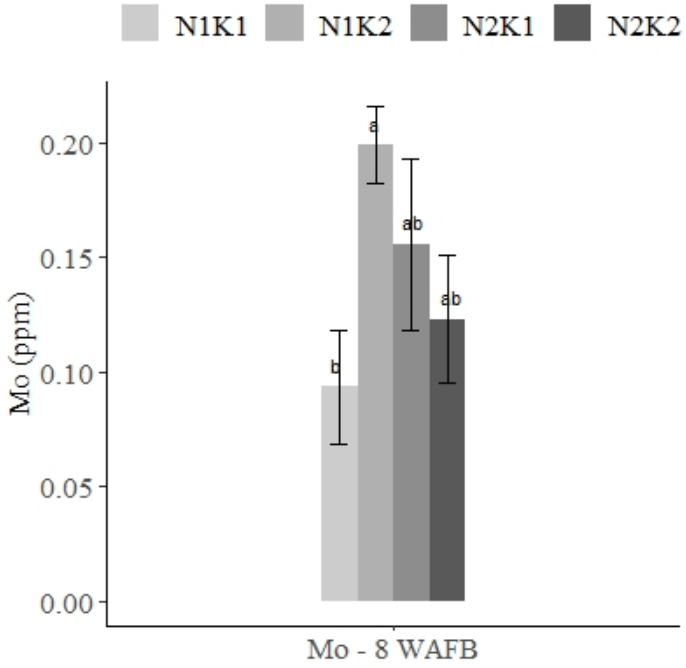

Figure 2 Molybdenum (ppm) content of leaf petiole at 8 WAFB affected by the interactions between N and K fertilization rates at harvest of 2018-19 growing season.

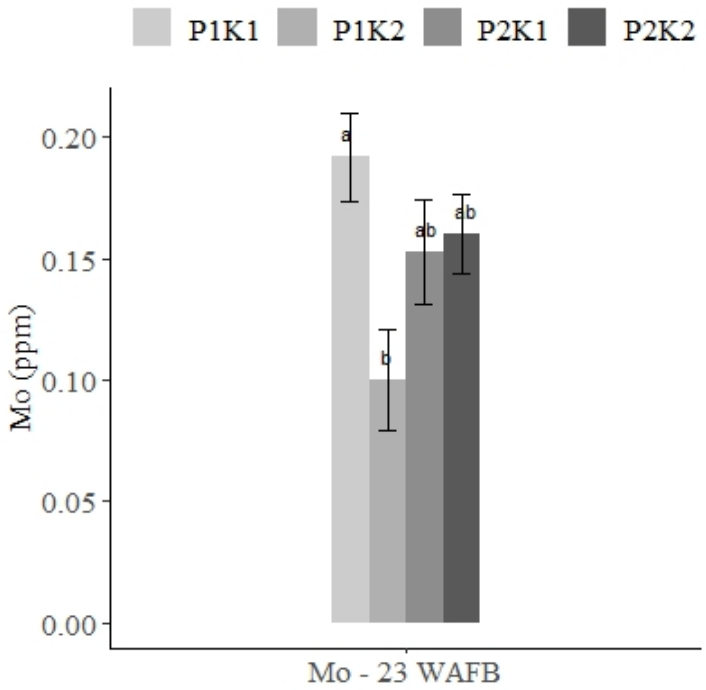

Figure 3 Molybdenum (ppm) content of leaf petiole at 8 WAFB affected by the interactions between P and K fertilization rates at harvest of 2018-19 growing season.

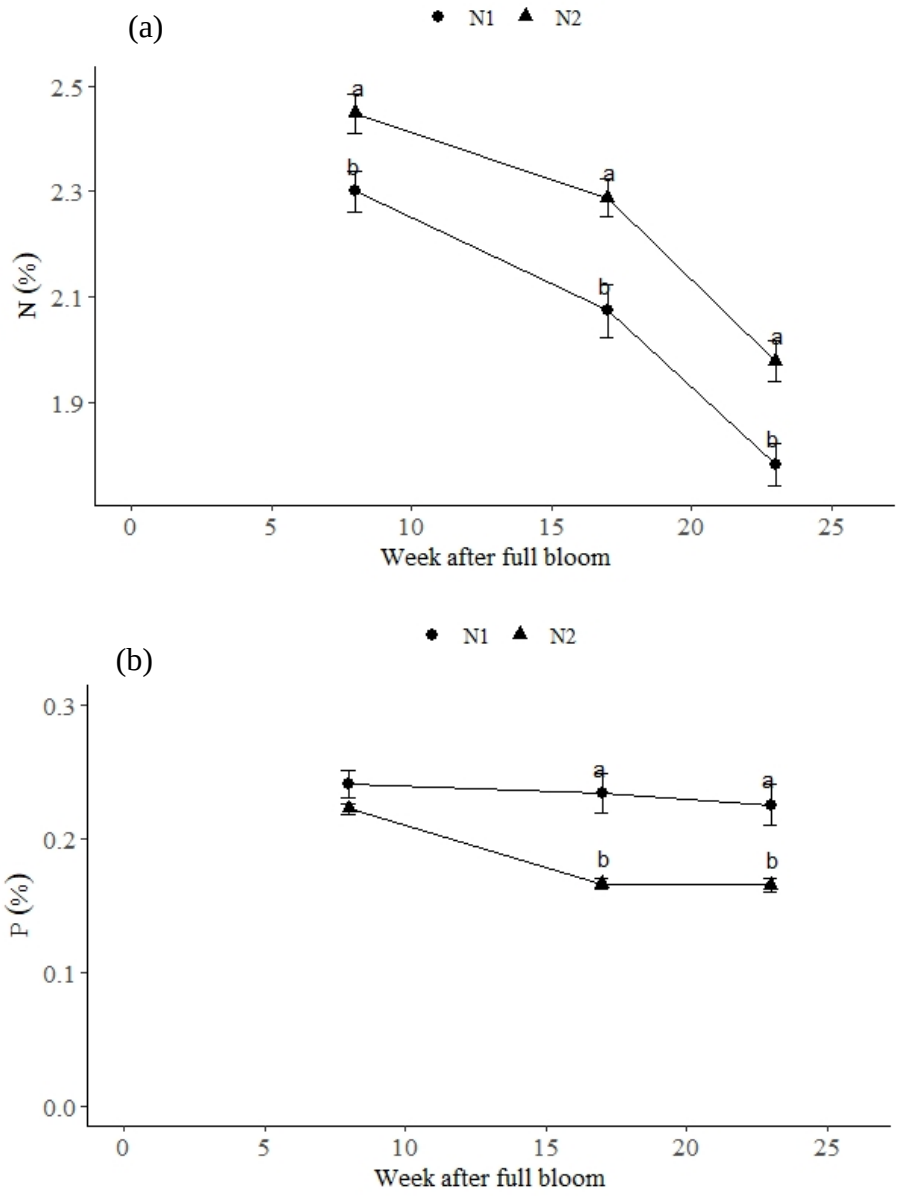

Figure 4 Nitrogen (a) and phosphorus (b) content (% dry weight) of 'Gala' apple leaf lamina at 8, 17, 23 WAFB under different N, P, and K fertilization rates at harvest of 2018-19 growing season.

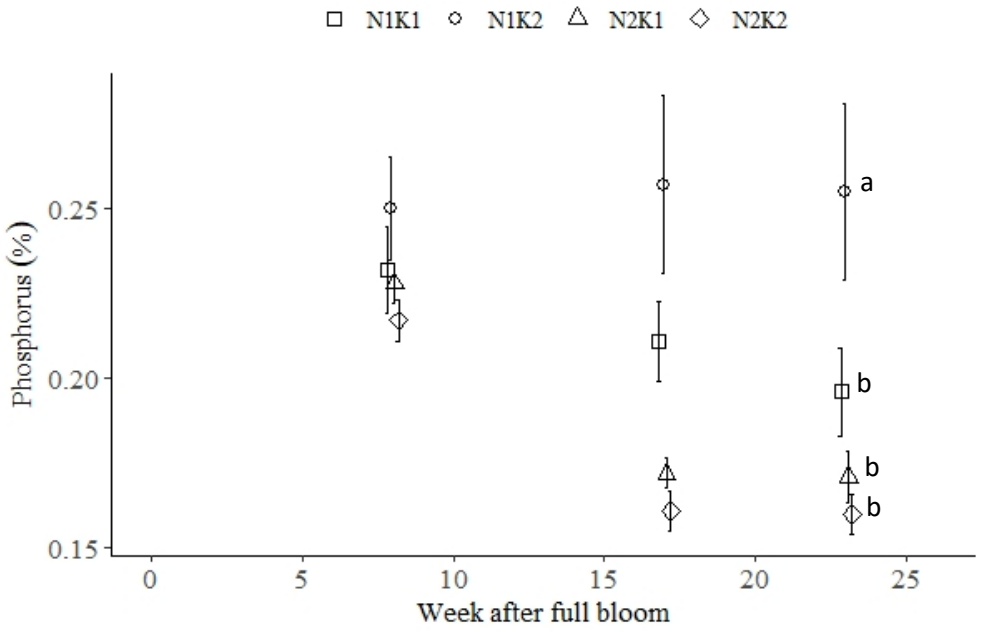

Figure 5 Phosphorus content (% dry weight) of 'Gala' apple leaf lamina at 8, 17, 23 WAFB affected by the interaction between N and K fertilization rates at 2018-19 growing season.

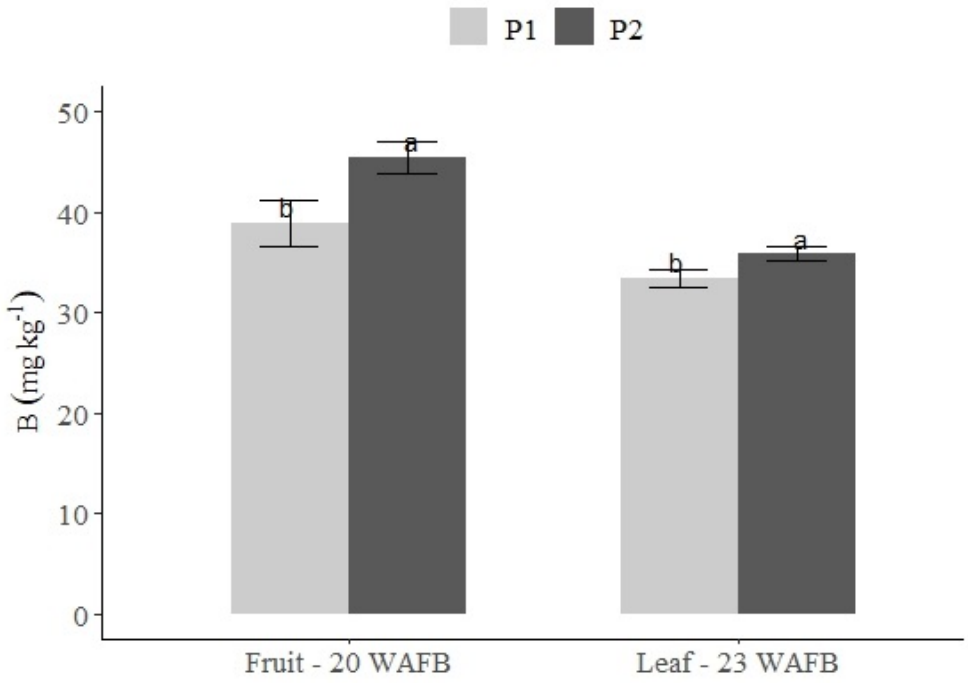

Figure 6 Fruit and leaf B content at 20 and 23 WAFB respectively influenced by P fertilization rates at 2018-19 growing season.

Table S3 Soil mineral content and physicochemical properties at 3 and 23 WAFB under different N, P, and K fertilization rates at harvest of 2018-19 growing season.

	Ammonium-N (mg kg^{-1})		Nitrate-N (mg kg^{-1})		P (mg kg^{-1})		K (mg kg^{-1})		EC (dS m^{-1})		pH ($CaCl_2$)		pH (H_2O)	
WAFB	**3**	**23**	**3**	**23**	**3**	**23**	**3**	**23**	**3**	**23**	**3**	**23**	**3**	**23**
Treatment														
N rate (N)														
N1	6.12	3.55	4.07	2.75 b	131.0	148.9	323.2	574.8	0.112	0.120	6.47	6.44	7.22	7.20
N2	6.67	3.40	4.57	12.37 a	147.7	155.2	365.5	511.2	0.112	0.127	6.48	6.42	7.25	7.16
Significance	ns.	ns.	ns.	**	ns.	ns.	ns.	ns.	ns.	ns.	ns.	ns.	ns.	ns.
P rate (P)														
P1	6.35	3.55	3.95	12.00 a	137.1	132.6 b	344.9	546.5	0.115	0.127	6.48	6.43	7.25	7.21
P2	6.45	3.40	4.70	3.12 b	141.5	171.5 a	343.8	539.5	0.108	0.120	6.46	6.43	7.21	7.15
Significance	ns.	ns.	ns.	**	ns.	**	ns.	ns.	ns.	ns.	ns.	ns.	ns.	ns.
K rate (K)														
K1	6.32	3.35	4.22	8.05	139.9	149.1	339.9	432.3 b	0.108	0.106 b	6.43 b	6.47	7.22	7.22
K2	6.47	3.60	4.42	7.07	138.8	155.0	348.8	653.7 a	0.115	0.141 a	6.52 a	6.39	7.25	7.15
Significance	ns.	ns.	ns.	ns.	ns.	ns.	ns.	***	ns.	*	*	ns.	ns.	ns.
Interaction														
N × P	ns.	ns.	ns.	**	ns.	ns.	ns.	ns.	ns.	ns.	ns.	ns.	ns.	ns.
N × K	ns.	ns.	ns.	ns.	ns.	ns.	ns.	ns.	ns.	ns.	ns.	*	ns.	*
P × K	ns.	ns.	ns.	ns.	ns.	ns.	ns.	ns.	ns.	ns.	ns.	ns.	ns.	*
N × P × K	ns.	ns.	ns.	ns.	ns.	ns.	ns.	ns.	ns.	ns.	ns.	**	ns.	***

Value represent the mean, n = 5. The effect of each factor and interactions between the factors are examined with three-way ANOVA at (α = 0.05) and the respective significance level is indicated by the following symbols: “ns.”, ($P > 0.05$); “*”, ($P < 0.05$); “**”, ($P < 0.01$); “***”, ($P < 0.001$).

The yield from each tree was generally low and uneven due to the heavy crop load from the previous season.

Conclusions

References

BLANPIED, G. & SILSBY, K. J. 1992. Predicting harvest date windows for apples. Cornell Cooperative Extension.

COSTA, G., NOFERINI, M., FIORI, G. & TORRIGIANI, P. 2009. Use of Vis/NIR spectroscopy to assess fruit ripening stage and improve management in post-harvest chain. *Fresh Prod,* 1**,** 35-41.

DONTSOVA, K. M., NORTON, L. D., JOHNSTON, C. T. & BIGHAM, J. M. 2004. Influence of exchangeable cations on water adsorption by soil clays. *Soil Science Society of America Journal,* 68**,** 1218-1227.

MAATHUIS, F. J. 2009. Physiological functions of mineral macronutrients. *Current opinion in plant biology,* 12**,** 250-258.

MCQUAKER, N., BROWN, D. & KLUCKNER, P. 1979. *AOAC Official Methods of Analysis*, Association of Pfficial Analytical Collaboration International.

MENGEL, K., KIRKBY, E. A., KOSEGARTEN, H. & APPEL, T. 2001a. Nutrient uptake and assimilation. *Principles of plant Nutrition.* Springer.

MENGEL, K., KIRKBY, E. A., KOSEGARTEN, H. & APPEL, T. 2001b. The soil as a plant nutrient medium. *Principles of plant nutrition.* Springer.

MILLER, A. & CRAMER, M. 2005. Root nitrogen acquisition and assimilation. *Root physiology: from gene to function.* Springer.

NAVA, G. & DECHEN, A. R. 2009. Long-term annual fertilization with nitrogen and potassium affect yield and mineral composition of'Fuji'apple. *Scientia Agrícola,* 66**,** 377-385.

NEILSEN, D. & NEILSEN, G. 2002. Efficient use of nitrogen and water in high-density apple orchards. *HortTechnology,* 12**,** 19-25.

NEILSEN, G., NEILSEN, D., PERYEA, F., FALLAHI, E. & FALLAHI, B. Effects of mineral nutrition on fruit quality and nutritional disorders in apples. VI International Symposium on Mineral Nutrition of Fruit Crops 868, 2008. 49-60.

RAYMENT, G. E. & LYONS, D. J. 2011. *Soil chemical methods: Australasia*, CSIRO publishing.

SWARTS, N., MONTAGU, K., OLIVER, G., SOUTHAM-ROGERS, L., HARDIE, M., CORKREY, R., ROGERS, G. & CLOSE, D. 2016. Benchmarking nitrous oxide emissions in deciduous tree cropping systems. *Soil Research,* 54**,** 500-511.

TEAM, R. C. 2019. R: A language and environment for statistical computing. Vienna, Austria: R Foundation for Statistical Computing.

Appendix 6: Draft 15N Manuscript

Nitrogen Use and Allocation in Apple Trees: pre-harvest N supply optimizes uptake efficiency

Bi Zheng Tan*, Dugald C. Close, Peter Quin, Nigel D. Swarts

Key-words: nitrogen uptake, NUE, ^{15}N, partitioning, storage, remobilization, application timing

Running head: Nitrogen Use and Allocation in Apple Trees

Tasmania Institute of Agriculture, College of Sciences and Engineering, University of Tasmania, Hobart TAS 7005, Australia

*Email: bi.tan@utas.edu.au

Abstract

Optimizing the utilization of applied nitrogen (N) in trees requires that tree N demand over time is matched by supply. We investigated how the timing of N application affected uptake, allocation, and remobilization within 14-year-old Gala/M26 apple trees (*Malus domestica Borkh*) over two seasons. In the 2017-18 season, 30 g N tree^{-1} of 5.5 atom % ^{15}N-calcium nitrate was fertigated weekly over four weeks commenced either at four weeks after full bloom (WAFB) (pre-harvest), one week after harvest (post-harvest), or equally divided to pre- and post-harvest (50:50 split). Uptake was monitored by leaf sampling before destructively harvested the whole trees at dormancy of the first season (to quantify N uptake and allocation), and at harvest of the second season (to quantify the remobilization of N derived from fertilizer [NDF]). The uptake efficiency of applied N fertilizer (NUpE) was significantly higher ($p < 0.05$) in the pre-harvest fertigation treatment (32.0%) than for the other treatments (~17%). Nitrogen fertigated in pre-harvest was rapidly translocated into leaves until nine WAFB, whilst N translocation into leaves when fertigated at post-harvest was negligible. Pre-harvest fertigated trees allocated 53.3 and 7.6% of the NDF taken up into fruit and leaves, respectively, and stored the same amount (approximately 4.1 g ^{15}N tree^{-1}) of NDF into perennial organs as the post-harvest treatment. However, the remobilization of NDF in the subsequent spring was not affected by the fertigation timing of current season. A seasonal effect of remobilization was observed with 4.6 g N tree^{-1} decreased in roots N status being reciprocated with 4.3 g N tree^{-1} increased in branches N status in season two, relative to season one. Fertigating N at pre-harvest optimized uptake efficiency with no detriment to fruit quality and provided adequate storage N to support early spring growth of the following season.

Introduction

Deciduous fruit trees internally cycle and reuse stored N from one growing season to the next. Nitrogen is withdrawn from leaves prior to leaf abscission and stored into roots, branches and the trunk for over-wintering (Millard and Thomson 1989). Stored N is remobilized for early spring growth and makes an important contribution to the seasonal N budget for tree fruit crops (Masclaux-Daubresse et al. 2010). Seasonal N requirements are thus comprised of internal stored N (Chapin III et al. 1990) and N uptake by the roots during the growing season (Millard and Grelet 2010). In a commercial orchard, root N uptake is predominantly from the application of N fertilizer which has been demonstrated to be vital to supply demand of vegetative and reproductive growth (Klein et al. 1989; Maathuis 2009). However, N fertilizer can be oversupplied in production systems, due to the perceived cost-effectiveness of achieving increased yield per unit area (Drake et al. 2002; Neilsen et al. 2009). This can cause reductions in fruit quality (Carew 2000) and the low use efficiency of N resources (Neilsen et al. 2001a) contributing to the pollution of underground water supplies (Neilsen and Neilsen 2002), and emissions of the potent greenhouse gas, nitrous oxide via denitrification (Freney 1997; Swarts et al. 2016). Conversely, matching N supply with tree uptake requirements optimizes marketable yield and minimizes environmental impact (Gebbers and Adamchuk 2010), is the primary objective of precision agriculture production.

Nitrogen uptake efficiency, defined here as 'the proportion of fertilizer N recovered in tree organs when applied in a growing season' (Neilsen et al. 2001b), has also been referred as apparent fertilizer N recovery by Benincasa et al. (2011) . Cassman et al. (2002) defined a similar term, fertilizer N recovery efficiency (NRec) for annual crops, which is modified for this study as the proportion of fertilizer N recovered in tree organs either in the year of application or any single subsequent year. Hill-Cottingham and Lloyd-Jones (1975) showed that NUpE for young apple trees was about 16 or 40% when N fertilizer was applied soon after fruit harvest or in early spring, respectively. The low NUpE in perennial tree crops, is

61 suspected to be caused by sparse distribution of root systems (Neilsen and Neilsen 2002)
62 and/or mismatched rate and timing of applied N to tree demand (Aguirre et al. 2001; Drake et
63 al. 2002; Hill-Cottingham and Lloyd-Jones 1975; Neilsen et al. 2001a).

64 The allocation of N throughout the tree is strongly influenced by the timing of
65 application. Toselli et al. (2000) showed that the majority of spring applied N in apple tree
66 was allocated into fruits and leaves and a relatively small amount was stored in root and
67 wood tissue, whilst most of the summer applied N was allocated into perennial structures.
68 Furthermore, an increase in stored N in the roots and wood of newly planted apple trees can
69 influence the manner of N remobilization in the subsequent season. Neilsen et al. (2001a)
70 showed that trees supplied with early N application at 2–8 weeks after planting remobilized
71 7% more N into fruitlets (18% of total remobilized N) and 6% less N (77% of total
72 remobilized N) into leaves from N storage than those with late summer N application at 8–14
73 weeks after planting. Whilst storage and uptake in young trees has been investigated (Dong et
74 al. 2001; Neilsen et al. 2001a), a key knowledge gap exists in the uptake, allocation and
75 internal cycling of N in commercially managed mature apple trees. This knowledge is key to
76 establishing an accurate N budget for precise nitrogen management in an orchard.

77 A comprehensive six-year study on the macronutrients budget in apple production
78 was conducted through destructive harvest of whole trees and mass balance between the
79 input, storage and output using conventional fertilizer (Scandellari et al. 2008). However, this
80 approach does not differentiate between NDF and pre-existing N in the soil, nor does it allow
81 for investigation of tree internal N remobilized from previous season/s. This can be achieved
82 by using an N source enriched with the stable isotope ^{15}N, to trace applied N throughout the
83 tree (Hauck and Bremner 1976; Masclaux-Daubresse et al. 2010), as has been used to
84 quantify fertilizer N uptake in both deciduous fruit tree crops including apples (Guak et al.
85 2003; Neilsen et al. 1997; Zhang et al. 2012), pears (Quartieri et al. 2002), cherries (Rivera et

al. 2016; San-Martino et al. 2010) and evergreen fruit trees such as citrus (Martínez-Alcántara et al. 2011). For instance, when 10-year-old field grown apple trees were supplied with ^{15}N-labelled fertilizer at bud burst and destructively sampled periodically over two seasons, the NUpE was quantified as low as 9.9 to 12.2% and that the majority of NDF was allocated into perennial organs (Zhang et al. 2012). A similar approach with the addition of successive xylem sap sampling was deployed on two-year-old apple trees (Guak et al. 2003); this demonstrated that leaf growth was mostly supported by remobilized N and root uptake did not commence until 14 days after remobilization had started.

The majority of studies using the ^{15}N isotope tracing method have been conducted in pot trials using young or newly planted trees, whereas the requirement for N varies with tree age and phenological stages (Schenk 1996) and more significantly, in commercial settings with higher crop loads. A challenge to the success of this technique *in situ* has been the recovery of ^{15}N in plant material from a large tree structure for complete mass-balancing. However, the utilization of dwarfing rootstocks in modern apple orchards and usage of netting to retain all shed materials has made recovery of the whole tree structure a more practical procedure.

This study aimed to address the knowledge gaps identified above in a high-density commercial orchard through the destructive sampling of whole trees at two different timings. Specifically we aimed to (1) quantify apple tree N uptake and NUpE under early (pre-harvest), late (post-harvest) and split (50:50 split) N fertigation application, (2) determine the impact of N application timing on N allocation and storage and; (3) quantify the remobilization of internal-tree stored N in the following season after fertigation treatments had been applied.

Materials and methods

Experiment site and trees

The experiment was conducted from August 2017 to June 2019 over two growing seasons in a commercial orchard located at Plenty in the Derwent Valley, southern Tasmania (42°44'31"S 146°58'22"E), Australia. The area has a cool temperate climate with a mild and rainy winter, and cool summer. Mean maximum and minimum temperatures are 24 ˚C and 10 ˚C respectively in the summer months, and 11.5 ˚C and 1.5 ˚C respectively in the winter months. Mean annual rainfall is 572.2 mm, with summer being the driest of a fairly even seasonal distribution. The orchard block was planted on a Dermosol with a sandy loam A horizon approximately 40 cm deep. The apple trees were 'Gala' cultivar grown on M26 rootstock planted in 2005 at a density of 1667 tree ha^{-1}, trained to a central leader system supported by trellis. A 1.0 m wide weed-free strip along the tree line was maintained with application of 'Basta' herbicide. The trees were subjected to commercial management practices prior to the experiment. Trees were irrigated using microjet sprinklers (50 L hr^{-1}) for 2-3 hours when low soil moisture level was detected using soil moisture probes throughout growing season.

Experiment treatments and design

The experiment treatments were the application of 5.5 atom % ^{15}N-labelled calcium nitrate (N_f) at the rate of 30 g N $tree^{-1}$ at different timings. The timings were either at pre-harvest (spring – commencing on 7th November 2017, four WAFB), post-harvest (autumn – commencing on 21st March 2018, one week post-harvest), 50:50 split (fertigation was equally divided to pre- and post-harvest), or control (N fertigation was excluded throughout the experiment duration). The pre- and post-harvest treatments were divided equally over four successive weekly applications. The 50:50 split treatment was divided equally over two pairs

of fortnightly applications, each commencing at the same time as the pre- and post-harvest treatments. All treatments were also applied to one buffer tree on either side of a sampling tree. Treatments were delivered via a fertigation system with electric pumps (SHURflo 4009-101-A87, Pentair, U.S.A.) at a flow rate of 11.3 L min^{-1}, and four pressure compensated drippers at 2 L hr^{-1} placed 20 cm away from the tree trunk of each tree in a square grid formation. During each fertigation event, water was pumped through the fertigation line for 10 min, followed by 30 min of N_f solution at 1.875 g N L^{-1}, and finished by 10 min of flushing with water. A total of 7.5 g N was delivered to each tree during each fertigation event. Nitrogen supply was excluded in the 2018-19 season to examine the fate of applied N_f from the 2017/18 season. All non-N nutrients, pest and weed control was carried out in line with standard orchard practice.

The experiment was established over three sampling rows with two buffering rows of trees in between, where the first, second and third sampling row had 11, 12, and five trees, respectively. A set of 16 trees from the first and third sampling row (hereinafter referred as 'first set') deployed a complete randomized design, received all four fertigation treatments and replicated four times. The remaining 12 trees from the second sampling row (hereinafter referred as 'second set') deployed a randomized complete block design, the 50:50 split treatment was excluded, and all other treatments were replicated four times. Different experimental designs were used for each set of tree plots due to the limitation of number of trees per row on the same soil type and profile.

Leaf, fruit, and soil sampling, and whole tree excavation

Ten randomly selected fully-grown bourse leaves were sampled from the middle section of each tree, on a weekly basis from three WAFB until leaf fall throughout the 2017-18 growing season. Orchard netting was installed below each tree early in the season and was lifted to

158 cover the whole tree canopy after fruit harvest to ensure the capture of all leaves during
159 autumn. All fruits were harvested at commercial maturity in both growing seasons, on 13th
160 March 2018 and 28th February 2019 respectively, to calculate the total biomass and N_f
161 recovery. Fifty fruits were sub-sampled for fruit quality assessment, 25 on harvest and the
162 remaining were assessed at eight weeks post-harvest.

163 Soil samples were taken at about the middle of dormancy on 11th July 2018, 14 weeks
164 before bud break of 2018-19 season, by taking 2.2 × 10.0 cm soil core samples of 0-10 cm
165 depth with a step probe. At each soil sampling, two samples were taken from soil within 10
166 cm radius of two fertigation drippers, another two were taken from soil midway between two
167 adjacent drippers these positions were repeated to sample each tree. All four samples were
168 homogenously mixed into one, soil samples were air-dried until a constant weight and passed
169 through 2 mm sieve.

170 The first set of trees were destructively harvested at dormancy of the 2017-18 season
171 (June 2018) to examine the uptake, allocation and storage of NDF (nitrogen derived from
172 fertilizer) in 2017-18 season. The second set of trees were destructively harvested at
173 commercial harvest of the 2018-19 season (March 2019), to measure the contribution of
174 stored and remobilized NDF to the subsequent season's tree growth. The above ground
175 portions of the trees were first removed to just above the graft union. The remaining tree
176 structure including roots were harvested by carefully digging the soil to 0.6 m depth and 1 m
177 radius around the tree trunk, the remaining soil being thoroughly examined for any broken
178 root material by two independent groups of people, to ensure recovery of as much of the root
179 systems as possible. Trees were separated into different organs, including: leaf, bud, spur,
180 first-year wood, branch (≥2 years), trunk, coarse root (>1 cm), medium root (<1 cm and >2
181 mm) and fine root (<2 mm), before fresh weight and a representative sub-sample were taken
182 for each organ. Sub-sampled organs and collected leaf samples were dried at 60 ˚C until a

183 constant weight was obtained. Plant material and seived-soil samples were then ground into a
184 fine powder using a ball mill (Retsch, Haan, Germany).

185 *Total N and ^{15}N analysis*

186 Powdered samples were analyzed for N percentage and ^{15}N atom percentage ($^{15}N_{apc}$) at the
187 Central Science Laboratory, University of Tasmania. Weight of the sample used for the
188 analysis varied with N percentage of the sample to achieve a 50 µg N target weight. Samples
189 were weighed in tin capsules and N stable isotopes were analysed using flash combustion
190 isotope ratio mass spectrometry (varioPYRO cube coupled to Isoprime100 mass
191 spectrometer). Stable isotope abundances were reported in delta (∂) values as the deviations
192 from conventional standards in parts per mil (‰) from the following equation:

193 $$\partial\ ^{15}N\ (‰) = [(^{15}N/^{14}N \text{ sample}) / (^{15}N/^{14}N \text{ standard}) - 1] \times 1000$$

194 $\delta^{15}N$ values were reported relative to atmospheric air. Certified Reference Materials
195 (USGS40, USGS41, IAEA-N1 and IAEA N2) were used to correct for instrumental drift and
196 quality assurance purposes. As recommended by IUPAC (Coplen et al. 1992), the value of
197 272 was employed for $^{14}N/^{15}N$ of N_2 in air for the calculation of atom fraction ^{15}N from
198 measured $\delta^{15}N$ values; the applied formula (Hauck 1982) is valid for low enrichments (<5%).
199 Enriched laboratory standards were prepared from mixtures of enriched and natural
200 abundance fertilizer and calibrated against international reference standard IAEA311. The
201 analytical performance of the instrumentation, drift correction and linearity performance were
202 calculated from the repetitive analysis of these standards. Precision of the elemental data was
203 0.2 %. For isotopic measurements precision was < 0.06 ‰ up to the highest enrichment level.
204 ^{15}N atom percentage was calculated from the measured $\delta^{15}N$ values and the calibration curve
205 produced from the enriched laboratory standards. Natural abundance (NA) of ^{15}N used in the
206 calculation was the $^{15}N_{apc}$ measured from the leaf sample prior to the application of enriched

calcium nitrate. The proportion of N within a plant organ that was derived from N_f was represented by NDF_{organ}, and:

NDF_{organ} (%) = ($^{15}N_{apc}$ of an organ - NA) / (N_f - NA);

N_f recovery represented the sum of NDF of all organs, and:

NDF recovery (g N tree^{-1}) = Sum of (NDF_{organ} × dry weight of organ) of all organs

NUpE represented the proportion of applied N_f taken up from soil and recovered in the 2017-18 season and NRec represented the proportion of stored NDF from the first season recovered in the second season. These were calculated with the following formulae:

NUpE (%) = (NDF recovery in 2017-18 season / N_f) x 100

NRec (%) = (NDF recovery in 2018-19 season / N_f) x 100

The N status of the tree represented the total N component of the whole tree structure at the time of measurement and comprised of native N (non-fertilizer derived N) and NDF. The native N and NDF of both leaf foliage and fruit organs for the first season, and of fruit organ at the fruit harvest for the second season were excluded from the calculation. These organs were excluded from the calculations such that the overall N remained within the tree system can be assessed and compared between the time of storage and after remobilization.

Fruit quality analysis

At harvest, 25 fruit per tree from each treatment and replicate were sub-sampled for the assessment of fruit quality. Fruit weight and size were measured using Vernier callipers. Peel red colour coverage was visually rated using a colour chart ranging from 1-5, where 1 represented 0-20% red coverage over the fruit and successive ranks increased in 20% steps. Red colour intensity was measured visually with a ‘Royal Gala’ colour chart (Enza, New Zealand) ranging from 1-11, where 1 represents light red and 11 represents a dark red colour.

Background colour of peel where red pigmentation was not developed was visually assessed with a colour chart ranging from 1-10, where the colour shift from green (1) to light green (5) to yellow (10). A Delta absorbance meter was used to assess the maturity of the fruit by measuring the chlorophyll-a in the fruit mesocarp (Costa et al. 2009). Peel blush colour was also assessed by using CR-400 chroma meter (Konica Minolta, USA) to take an average of three random measurements from the red blush area of each fruit. Peel blush colour was reported in L*a*b* colour space. A thin slice of peel was removed on the blush side of each apple to measure flesh firmness using a GUSS Fruit Texture Analyser (GUSS, South Africa). Juice was collected to measure total soluble solids (TSS) by using a digital refractometer (Atago, Tokyo, Japan). The fruit was then cut horizontally in half, the cut surface of the bottom half was sprayed with iodine solution and left to dry for five minutes before starch index was visually measured against the Cornell Starch-Iodine Index (1, full starch; 8, no starch)(Blanpied and Silsby 1992).

Statistical analysis

Data were subjected to one-way ANOVA test assumption tests prior to analysis. One-way ANOVA and Tukey's HSD test were used to compare treatment means at 95% confidence level using the R statistic package (Team 2019).

Results

N uptake efficiency and tree N status

At winter dormancy following the fertigation treatments in the first season, NUpE was significantly ($p < 0.05$) higher in the pre-harvest fertigated trees (32.0%) than for the post-harvest and 50:50 split fertigated trees, which had comparatively similar NUpE of approximately 17.2% (Figure 1). For the pre-harvest fertigated trees, NDF recovered (11.6%

NRec) in the second season was significantly ($p < 0.05$) less than the NDF recovered (32% NUpE) in the first season. The NRec of trees receiving post-harvest N fertigation was 15.1% and not significantly different to the NDF recovered in the previous season (NUpE 17.2%) and was not significantly different to the NRec of pre-harvest fertigated trees (Figure 1).

At the first winter dormancy (2017-18) following the treatment applications, the trees that received the pre-harvest and post-harvest treatments had a N status of just under 35 g tree^{-1} and were not significantly different to the 50:50 split treatment which was approximately 23.8 g tree^{-1} (Figure 2). In second season (2018-19), the N status of the whole tree for the pre-harvest treatment was not significantly different to the post-harvest treatment. The tree N status of all fertigation treatments in 2017-18 were also not significantly different to those of 2018-19. Post-harvest fertigated trees showed a non-significant trend towards higher NDF content at winter dormancy (5.17 g tree^{-1}) than in pre-harvest and 50:50 split fertigated trees (3.7 and 2.7 g tree^{-1}, respectively), yet the proportion of NDF to native N was not significantly different.

Leaf N dynamics

Leaf N concentration [N] (% of leaf dry weight) (Figure 3a) and concentration of NDF [NDF] (mg NDF (g dry leaf)$^{-1}$) (Figure 3b) of pre-harvest fertigated trees were generally higher than that of trees of other fertigation treatments over the season. Significant ($p < 0.05$) differences in leaf [N] between the pre-harvest and other treatments commenced one week after pre-harvest fertigation began (5 WAFB) and were less apparent after 20 WAFB (Figure 3a and Table S1). Leaf [N] significantly ($p < 0.05$) increased during the period of pre-harvest fertigation with the full rate application whereas leaf [N] of the other treatments remained static for two weeks after the pre-harvest fertigation commenced. Thereafter the dynamics of leaf [N] were similar across treatments with a gradual decrease over the season until a sharp

increase from 22 to 23 WAFB (when fruit harvest occurred) (Figure 3a). This was followed by a continued decrease to just under 1.6% dry weight of leaf [N] for all treatments at the last sampling date in April, approximately 26 WAFB.

The dynamics of leaf [NDF] for the pre-harvest and 50:50 split fertigated trees increased steadily from 4 WAFB, peaked at approximately 2.8 and 1.7 mg N (g leaf)$^{-1}$ at nine WAFB, respectively, before a gradual decrease to approximately 1.5 and 0.9 mg N (g leaf)$^{-1}$ at 26 WAFB, respectively (Figure 3b). For the post-harvest treatment leaf [NDF] was around 0.0 mg N (g leaf)$^{-1}$ for the duration of the experiment with a slight non-significant increase commencing at 23 WAFB, following post-harvest N application (Figure 3b; Table S1).

N allocation and remobilization

The NDF of pre-harvest fertigated trees was nearly double that of post-harvest fertigated trees, at 9.6 and 5.2 g N tree^{-1} respectively (Table S2). Pre-harvest fertigated trees allocated significantly ($p < 0.05$) higher percentage of NDF into fruit, leaves and other first year growth (bud, spur, and first year wood) organs (53, 7.6, 4.6% of total NDF taken up, respectively) than post-harvest fertigated trees (0, 0.14, 2.8% of total NDF taken up, respectively) (Figure 4a). The amounts of NDF allocated to fruit, leaf, and first year growth organs were also significantly ($p < 0.05$) higher for pre-harvest fertigated trees than those of post-harvest (Figure 4b). In contrast, post-harvest fertigated trees allocated significantly ($p < 0.05$) more NDF to perennial organs of branch, trunk and root (13.6, 36.1, 47.3% of total NDF taken up, respectively) than pre-harvest fertigated trees (5.4, 12.5, 26% of total NDF taken up, respectively) (Figure 4a). However, the amounts of NDF allocated to branches, trunk, or roots (Figure 4b) were not significantly different between treatments.

The N status of each tree organ when the trees were destructively harvested in March 2019 (aligned with commercial harvest) is shown in Figure 5; those sources include N

remobilized in spring (native N and NDF stored from the previous season) plus any native N taken up in the current season. No significant differences were found in the NDF and native N of various organs between pre- and post-harvest fertigation treatments at the destructive harvest in March 2019. Nonetheless, the mean values of native N and NDF status were slightly higher for post-harvest treatment than of pre-harvest treatment. A trend towards higher total N recovered in leaf (8.4-11.0 g tree^{-1}) than fruit (3.0-3.9 g tree^{-1}) was also observed for both fertigation treatments.

The fertigation timing did not result in significant differences in N status (native N or NDF), hence, the N composition of each organ was pooled between treatments and used for comparison of each season (Figure 6). The changes in N status of perennial organs from the dormancy of 2017-18 season to the fruit harvest of 2018-19 season represents the net N remobilization and translocation during that period (Figure 6). The total N status, comprised of both native and NDF, of root organs declined significantly ($p < 0.05$) from winter dormancy of 2017-18 season (15.2 g tree^{-1}) to destructive harvest in March 2019 (10.7 g tree^{-1}) (Table S3). Similarly, the NDF in the root was significantly ($p < 0.05$) declined at dormancy following 2017-18 season and was remobilized in the 2018-19 season, regardless of fertigation timings. In contrast, both the total N and NDF of the trunk organ remained not significantly different from the dormancy of 2017-18 season to after the harvest of 2018-19 season (Figure 6). The total N status of branch organs increased significantly ($p < 0.05$) from 2017-18 (3.5 g tree^{-1}) to 2018-19 (7.8 g tree^{-1}), while the NDF, at approximately 0.7 g N tree^{-1}, was not significantly different (Table S3).

Soil N status

The soil [N] and [^{15}N] at 0-10 cm depth were not significantly different between any treatments at the winter dormancy prioir to 2018-19 season (Table 1).

Fruit quality

Fruit yield and quality attributes (Table S4a and S4b) were not significantly different between all fertigation treatments over each season of assessment, with the exception of dry matter content and skin colour attributes. Post-harvest fertigated trees had fruit of significantly ($p < 0.05$) higher dry matter content than of 50:50 split fertigated trees in the first season. Fruits of the post-harvest treatment also had lower a^* index (duller), higher peel redness and red colour coverage than of 50:50 split fertigation treatments in the first season. A significantly yellower peel background colour was also observed in fruits of post-harvest than of 50:50 split fertigation treatments in the first season.

Discussion

From our application of ^{15}N-enriched fertiliser to commercial apple trees at different timings we have made important findings that could assist industry in better utilisation of N, to the benefit of growers and the environment. The uptake of N applied pre-harvest was significantly greater ($p < 0.05$) than that applied post-harvest, or split 50:50 between the two (Figure 1). It was also very clear that when applied post-harvest, the allocation of NDF to tree organs was demonstrably different to that of N applied pre-harvest, with little allocation to leaves (Figure 4) being one aspect of this. It was then unsurprising that leaf [NDF] was found to be a good indicator for the timing of uptake of any N applied pre-harvest (Figure 3b, pre-harvest and 50:50 split treatments), but a poor indicator for the uptake of any N applied post-harvest. In the discussion that follows the differences and their importance, in relation to timing of N application, of uptake of applied N, its allocation to tree organs and its remobilization for the following season were examined in detail.

N uptake and allocation

Pre-harvest fertigation had the highest NUpE of 32%, nearly double that of the other treatments (Figure 1; ~17.2%). Although the 50:50 split treatment received, to harvest, only half the rate of N of the pre-harvest treatment, its NUpE was not significantly different from that of the post-harvest treatment. This indicates that the NUpE was dependent on the availability of N in the soil at the time of highest demand and thus, a crucial factor in optimizing NUpE. The soil [^{15}N] of all applied-N treatments at 14 weeks before the bud burst of 2018-19 season (Table 1) was not significantly different from that of the controls (natural abundance) . Hence, any remaining fertilizer may have been lost to the immediate environment either via leaching (Hardie et al. 2018), nitrous oxide emission (Swarts et al. 2016), taken up by roots of neighbouring trees, or underwent dissimilatory nitrate reduction to ammonium (Giblin et al. 2013). Comparable NUpE was found for 3-year-old apple trees (22.3%, Neilsen et al. (2001b)) and apple trees in newly planted orchards (16-19%, Neilsen et al. (2001a)) with pre-harvest applied N via dripper fertigation. San-Martino et al. (2010) also found that NUpE was higher after spring N fertilizer application (65.7%) compared to summer application (37.4%) in 7-year-old sweet cherry trees. The much higher NUpE of that study relative to the current study might be due to a combination of: hand application of fertilizer below the soil surface; installation of plastic barriers 2 m from the trunk and 1 m deep around each tree, and the usage of ammonium nitrate, with ammonium being much less prone to leaching than nitrate – these factors all potentially reducing N loss (San-Martino et al. 2010). In addition, the extended post-harvest transpiration of cherry as a summer crop, relative to that of later apple harvest, could account for greater N uptake in the intervening period. The latter factor is also consistent with the much reduced NUpE of post-harvest fertilizer application observed in our study, where the amount of N taken up is likely to be limited by reduced transpiration pull associated with reduced sap flow activity (Fujii and Kennedy 1985). Quartieri et al. (2002) also demonstrated this, where only 3.1% of the late

summer applied N was found in the leaves of 2-year-old pear trees compared to the 23.1% for those of N applied in spring. This is further support for our finding of the low uptake of post-harvest applied N, being at least partly attributed to decreased canopy demand (Figure 4).

A significantly higher ($p < 0.05$) proportion of NDF was allocated to perennial organs from post-harvest applied N than from the pre-harvest or 50:50 split treatments (Table S2). However, given the reduced NUpE of post-harvest applied N, the absolute amount (as opposed to %) of NDF allocated into perennial organs was not significantly different between treatments (Figure 4b, Table S2). This indicates that the allocation of NDF was dependent on the timing of fertigation, as has been reported in sweet cherry (San-Martino et al. 2010) and nectarine (Tagliavini et al. 1999) trees. A large difference in the amount of NDF allocated to leaves, buds and spurs was observed between treatments. Post-harvest fertigated trees allocated 0.01 and 0.04 g NDF $tree^{-1}$ into buds and spurs respectively, 80 % less than the 0.04 and 0.21 g NDF $tree^{-1}$ for pre-harvest fertigated trees (Table S2). This suggests that the allocation of N into the buds and spurs occurred earlier in the season, rather than post-harvest, and is dependent on soil N availability. Furthermore, subsequent season buds develop in apples in early summer (Landsberg 1974) and is likely to be improved by non-limiting N supply. These results contradict general grower practice to apply N post-harvest to improve N nutrition in bud and spur with a goal to improve fruit quality of the following season.

Influence of N fertigation timing on leaf N dynamics

Uptake of N applied pre-harvest was reflected in significantly higher ($p < 0.05$) leaf [N] than for the post-harvest and control treatments following the commencement of pre-harvest fertigation and remained so until 20 WAFB (Figure 1a, 7-20WAFB). The leaf [N] for the 50:50 split treatment did not differ from any other treatment throughout the monitored period,

399 except at 20 WAFB when it was significantly ($p < 0.05$) lower than that of the pre-harvest
400 treatment but of seemingly little consequence. Leaf [N] of all treatments peaked at around
401 four to five WAFB (one week after pre-harvest fertigation), which coincided with the
402 commencement of fruit cell expansion. From that time leaf [N] decreased gradually over the
403 season in all treatments, as has been reported elsewhere (e.g. Aguirre et al. 2001; Grassi et al.
404 2002). Gradual seasonal decrease is likely due to the fruit becoming a stronger sink for both
405 carbohydrates and N than leaves as the season progresses (Neilsen et al. 2005), with the result
406 that as leaf bulk continues to increase and the ratio of N content to leaf biomass declines.

407 We observed that leaf [N] increased sharply a week after fruit harvest from 22 to 23
408 WAFB for all treatments (Figure 3a) – significantly ($p < 0.05$) for the pre- and post-harvest
409 treatments. This rapid increase into the leaves immediately after fruit removal strongly
410 supports that prior to harvest fruit was a stronger sink for N than leaves. The sharp increase in
411 leaf [N] at 23 WAFB indicates re-allocation of N uptake via the vascular system into the
412 leaves. From this point onward leaf [N] continued to drop, this being consistent with the
413 onset of leaf senescence accompanied by a reduction of chlorophyll level and related activity
414 (Fang et al. 1998), even when N availability was high as with the post-harvest application
415 (Figure 3b). In addition, the sink of N translocation changed from leaves to perennial storage
416 organs before dormancy (Munoz et al. 1993). Thus, the reduction in transpiration facilitated
417 N uptake induced by both reduced photosynthetic activity and shifted N translocation sink
418 explained the compromisation of post-harvest applied N uptake (from 23 WAFB).

419 The dynamics of leaf [NDF] clearly reflected the movement of all pre-harvest NDF
420 into or away from the leaf after fertigation (Figure 3b). After pre-harvest N fertigation
421 commenced at 4 WAFB, leaf [NDF] increased rapidly until nine WAFB (one week after
422 cessation of all pre-harvest N application), before decreasing slowly until dormancy. The rate
423 of N uptake was almost two-fold higher in the pre-harvest only treatment than for the 50:50

split treatment, indicative of the increased N supply. As expected, 0 mg NDF (g dry leaf)$^{-1}$ were recorded at nine WAFB for control and post-harvest treatments. At leaf fall (26 WAFB), leaf [NDF] decreased to 1.7 and 0.9 mg NDF (g leaf)$^{-1}$ for pre-harvest and 50:50 split fertigated trees, respectively. These values, having declined from their respective 9 WAFB maxima of 2.8 and 1.7 mg NDF (g leaf)$^{-1}$, indicated that a respective 39% and 47 % of NDF was either translocated to fruit or recycled into perennial organs before dormancy. The proportion of NDF from leaves translocated into the fruit or withdrawn into storage could not be distinguished, as the labelled N in both fruit and perennial organs could have originated from either root N uptake or translocation. Millard and Thomson (1989) reported that one-year-old apple trees that were fertigated with N withdrew approximately 69% (summer fertigation) or 41% (autumn fertigation) of N from the leaves into perennial storage organs prior to dormancy. Whilst the N withdrawal from summer fertigation (Millard and Thomson 1989) was 30% higher than of the pre-harvest treatment of our finding, these trees did not have fruit, thus the impact of crop load on N withdrawal to perennial organs cannot be determined. Importantly, leaf [NDF] of our post-harvest treatment was 0.0 mg NDF (g leaf)$^{-1}$ for the duration of the experiment, with only an insignificant increase from 24 to 26 WAFB (Figure 3b), indicating little relationship between N supplied and leaf [NDF] after fruit harvest. Both the poor relationship between N supply and leaf [NDF] post-harvest and the preferered allocation of post-harvest N towards perennial organs strongly suggests that the tree has greatly reduced N demand post-harvest, at a time when it has begun to shift physiologically from an active, growing phase toward a winter, dormant phase (Fadón et al. 2020).

N storage and remobilization

Tree N status at dormancy was comprised of the NDF and native N recovered from tree organs, including root, trunk, branch, and first year wood. Although the pre-harvest fertigated

449 trees took up 4.4 g tree^{-1} more NDF (equivalent to ~10% of tree N status at winter dormancy)
450 than the other treatments, at winter dormancy of the 2017/18 season the overall tree N status
451 did not differ between all treatments (Figure 2). This was because 60% and 47% of NDF
452 taken up by pre-harvest and 50:50 split fertigated trees was allocated to fruit and leaves and
453 lost from the system via harvest and leaf fall (Figure 4a & b). On the other hand, both overall
454 tree N and NDF status of pre- and post-harvest treated trees at the harvest of 2018-19 season
455 (Figure 2), were not significantly different to that of the previous season, when no additional
456 N had been provided to the trees. These findings suggest that when N supply is sufficient,
457 there could be a physiological mechanism to ensure a critical level of N is stored over winter
458 regardless of single season variation in fertilizer N supply, and availability of soil native N.
459 This could be influenced by stored N within the 14-year-old deciduous trees buffering the
460 single season variation in N availability. In contrast, demonstrated that the levels of
461 remobilized N in younger trees with less biomass of perennial organs (and possibly less N
462 storage capacity) were highly dependent on the rate of N supplied the previous season (Cheng
463 and Fuchigami 2002; Millard and Proe 1993). Hence, the tree age and N status at dormancy is
464 particularly important for deciduous fruit trees, as it determines the N available for the
465 remobilization in the following season and the trees ability to buffer the seasonal variation in
466 soil N availability caused by enrironmental condition or orchard practices.

467 Remobilization of N into fruit and new vegetative organs has found to be critical to
468 fruit development (Neilsen et al. 2001b) and shoot growth (Millard et al. 2006). Although the
469 amount of stored NDF in the buds and spurs at dormancy after the 2017-18 season (Table S2)
470 was significantly higher in the pre- than post-harvest treatment, the amounts of both native N
471 and NDF remobilized into fruit, leaf and first year growth organs in the 2018-19 season
472 (Figure 5) were not significantly different. This indicates that the amount of NDF remobilized
473 into new growth was not affected by the differences in NDF of bud and spur organs. This is

perhaps to be expected as the overall N in buds and spurs only contribute to ~3% of the total N for the whole tree, and of that 3%, ~87% of the total N was constituted by native N. A study of three-year-old apple trees found that the contribution of remobilized N in stems to leaf growth was 28 and 34% when N was supply in the autumn or autumn of the previous season, respectively (Millard and Thomson 1989). A similar study of four-year-old trees that compare low (30 mg dm^{-3}) and high N (150 mg dm^{-3}) supply in the summer of previous season showed respective values of 87 and 61% contribution to shoot tissues (spur, shoot, and reproductive tissues) (Guak et al. 2003). The contribution of remobilization of stored N to newly grown tissue are ~20% (three-year-old) and ~70% (four-year-old) higher than the our findings, ~9% for both pre- and post-harvest treatment in our study of 14 year-old trees. This indicates the likelihood that the contribution from previously stored N relative to NDF stored from last season uptake may generally increases with tree age (Millard and Grelet 2010).

Our finding that N remobilization was not affected by the timing of N fertigation, is not consistent with the report of preferential remobilization of N taken up in autumn than N taken up in spring and summer (Millard and Thomson 1989). A possible reason for the relatively small contribution of NDF to N remobilization and insignificant impact of fertigation timings on N remobilization observed in this study could again be due to differences in structure and function of our 14 year-old trees relative to young material studied by Guak et al. (2003) (4 years-old) and Millard and Thomson (1989) (2 years-old). In our study, a subtantial portion of remobilized N was comprised of unlabelled N absorbed prior to the experiment and was not able to be quantified, while NDF contributed to a minor fraction of the total remobilized N.

In this study, we found that the root was the main source of remobilized N and that the main sinks were branches, new vegetative organs, and fruits. This was evident by the significant reduction of native (unlabelled N) and NDF in root organs between dormancy of

2017-18 season and commercial harvest of 2018-19 season along with a concomitant increase of native N in branches and presence of both native and NDF in fruit and new vegetative organs (Figure 6). Although, it is important to acknowledge that increased portion of native N in branches, new vegetative organs and fruit could originate from root uptake as well as the remobilization of unlabelled N from roots. In contrast, the substantial amounts of native and NDF within the trunk did not vary between seasons. This suggests that the trunks were not a primary source of N for remobilization, and that most of the recently provided NDF was unavailable for remobilization in the following season. Again this contrasts with studies of young trees, where apple (Millard and Neilsen 1989) utilized the main trunk and sweet cherry (Grassi et al. 2002) utilized root as a primary source of N. As no additional N supply was provided in the 2018-19 season and the ^{15}N remaining in the soil was not significantly different to that of control treatment (Table 1), the NDF component in vegetative organs and fruit in 2018/19 originated only from the remobilized NDF and constituted less than 15% of the organ's total N. This has demonstrated the strong N buffering capacity of mature deciduous trees and could explain why the impact of many N fertilization studies require multiple seasons of repeated treatments to show a significant impact on fruit quality. Indeed, in this study there were limited differences in fruit quality outcomes associated with timing of fertigation. Importantly, this indicates that pre-harvest N taken up into fruit does not negatively impact colour development or firmness, as has been reported in some cases where excessive N was applied pre-harvest (Neilsen et al. 1999; Shear and Faust 1980).

Conclusion

The pre-harvest fertigation treatment had the highest NUpE of 32 % among the tested treatments likely due to a combination of higher transpiration rate and fruits that provided a strong sink for N. The NUpE was also dependent on the soil N availability at the time of high N demand, as the equal splitting of N rate into pre- and post-harvest reduced the uptake

524 unproportionally to the amount applied at pre- and post-harvest. The NDF from pre-harvest
525 application was mainly allocated into fruit (without any negative impact on fruit quality) and
526 new canopy growth, while post-harvest applied NDF was largely stored in perennial organs.
527 Leaf dynamics of N demonstrated a strong response to pre-harvest applied N whereas post-
528 harvest applied N was not recovered in the leaves in any substantial quantity; this largely
529 reflected the difference in NUpE between the pre- and post-harvest treatments. The total
530 amount of NDF stored in the tree framework was not significantly affected, regardless of the
531 difference in NUpE and allocation between different fertigation timings. Hence, supplying N
532 at four WAFB is recommended to optimize NUpE without compromising N allocation to
533 winter storage. The amount of remobilized N in the following season was similar between
534 treatments despite there being significantly higher NDF stored in the buds and spurs in the
535 pre-harvest fertigation treatment. Between seasons, NDF and native N was remobilized from
536 roots, and not the trunk, to shoots. Growers practice post-harvest fertigation to increase stored
537 N in bud, spur and roots to be remobilized in the following season for a better bloom and fruit
538 quality. Our results indicate that the practice of post-harvest fertigation of N for storage to
539 support next season growth is not recommended from a resource use efficiency perspective,
540 nor as a practice to improve fruit quality. This study represents a paradigm shift in the
541 understanding of mature deciduous tree nitrogen dynamics that indicates that fertilizer
542 strategies need to pivot from post-harvest to adequate pre-harvest N application.

Supplementary data

Table S1. The N concentration, and N derived from fertilizer of leaf samples collected over 2018-18 season after pre-harvest fertigation of 'Gala' apple trees on M26 rootstock in 2018-19 season under the impact of different N fertigation timings. Each tree received no N fertilizer (control) or a total of 30 g N of N_f in November 2017 (pre-harvest), March 2018 (post-harvest), or evenly split over pre- and post-harvest (50:50 split). Mean, n = 4. Different letters indicate significant differences ($p < 0.05$) between four treatments.

Week after full bloom	**3**	**4**	**5**	**6**	**7**	**9**	**12**	**14**	**16**	**18**	**20**	**22**	**23**	**24**	**25**	**26**
Treatment	**N concentration (% dry weight)**															
Control	1.9	2.04	2.04 b	2.01	1.81 b	1.81 b	1.77 b	1.66 b	1.63 b	1.66	1.52 b	1.40 b	1.68	1.47 b	1.46 b	1.44 b
Pre-harvest	2.1	2.34	2.44 a	2.23	2.24 a	2.13 a	2.01 a	1.92 a	1.88 a	1.78	1.74 a	1.60 a	1.85	1.67 a	1.60 a	1.62 a
Post-harvest	2.12	2.19	2.13 ab	1.92	1.85 b	1.84 b	1.82 ab	1.72 b	1.66 b	1.55	1.53 b	1.48 ab	1.82	1.57 ab	1.54 ab	1.47 b
50:50 split	2.04	2.02	2.09 ab	1.92	1.88 ab	1.94 ab	1.86 ab	1.83 ab	1.78 ab	1.94	1.56 b	1.48 ab	1.73	1.59 ab	1.50 ab	1.53 ab
	N derived from fertilizer (mg N (g leaf)$^{-1}$)															
Control	0	0.00 b	0.00 b	0.00	0.00 c	0.00 c	0.00 c	0.00 b	0.00 b	0.00 b	0.00 c	0.00 c	0.00 c	0.00 c	0.00 c	0.00 c
Pre-harvest	0	0.58 a	1.18 a	2.07 a	2.02 a	2.81 a	2.62 a	1.96 a	1.95 a	1.85 a	1.92 a	1.59 a	1.63 a	1.50 a	1.37 a	1.54 a
Post-harvest	0	0.00 b	0.00 b	0.00 b	0.00 c	0.00 c	0.00 c	0.00 b	0.00 b	0.00 b	0.00 c	0.00 c	0.00 c	0.04 c	0.07 c	0.06 c
50:50 split	0	0.44 a	0.50 ab	0.96 ab	0.99 b	1.70 b	1.54 b	1.51 a	1.58 a	1.58 a	1.00 b	1.21 b	1.13 b	1.03 b	0.83 b	0.90 b

549 **Table S2.** The N derived from fertilizer (NDF) percentage, total NDF and NDF allocation of various tree organs harvested at dormancy in June
550 2018 of 'Gala' apple trees on M26 rootstock under the impact of different N fertigation timings. Each tree received no N fertilizer (control), or a
551 total of 30 g N of N_f, in November 2017 (pre-harvest), March 2018 (post-harvest), or evenly split over pre- and post-harvest (50:50 split). Mean,
552 n = 4. Different letters indicate significant differences ($p < 0.05$) between the four treatments.

Organ type	Bud	Spur	Leaf foliage	First year wood	Branch	Trunk	Old root	Fine root	Fruit
Treatment	**N derived from fertilizer (%)**								
Control	0.00 d	0.00 c	0.00 c	0.00 c	0.00 b	0.00 b	0.00 b	0.00 c	0.00 b
Pre-harvest	22.70 a	18.87 a	12.69 a	25.48 a	14.09 a	11.39 a	26.61 a	6.17 b	26.31 a
Post-harvest	6.38 c	3.82 c	0.22 c	11.90 b	15.03 a	16.00 a	41.91 a	12.66 a	0.00 b
50:50 split	15.01 b	13.18 b	7.48 b	16.62 b	10.02 a	11.31 a	32.14 a	9.31 ab	19.27 a
	Total NDF (g tree^{-1})								
Control	0.00 c	0.00 c	0.00 b	0.00 b	0.00 b	0.00 b	0.00 b	0.00 b	0.00 c
Pre-harvest	0.04 a	0.21 a	0.73 a	0.20 a	0.52 a	1.20 ab	1.46 a	0.10 a	5.15 a
Post-harvest	0.01 bc	0.04 c	0.01 b	0.10 ab	0.76 a	1.98 a	2.10 a	0.19 a	0.00 c
50:50 split	0.02 ab	0.13 b	0.29 ab	0.06 b	0.28 ab	0.84 ab	1.30 ab	0.10 a	2.14 b
	NDF allocation (%)								
Control	0.00 c	0.00 c	0.00 b	0.00 b	0.00 b	0.00 c	0.00 c	0.00 b	0.00 b
Pre-harvest	0.38 ab	2.23 a	7.64 a	2.07 a	5.37 b	12.48 bc	15.43 b	1.05 ab	53.36 a
Post-harvest	0.21 b	0.64 b	0.14 b	1.94 a	13.64 a	36.11 a	42.53 a	4.78 a	0.00 b
50:50 split	0.48 a	2.41 a	5.97 ab	1.16 ab	5.06 b	14.24 b	24.18 b	1.85 ab	44.65 a

553

Table S3. The N derived from fertilizer (NDF) percentage, total NDF and NDF allocation of various tree organs harvested at harvest in March 2019 of 'Gala' apple trees on M26 rootstock under the impact of different N fertigation timings. Each tree received no N fertilizer (control) or a total of 30 g N enriched with 5.5% ^{15}N in November 2017 (pre-harvest) or March 2018 (post-harvest). Mean, n = 4. Different letters indicate the significant differences among four fertigation timing treatments.

Organ type	Bud	Spur	Leaf	First year wood	Branch	Trunk	Old root	Fine root	Fruit
Treatment	**N derived from fertilizer (%)**								
Control	0.00 b	0.00 b	0.00 b	0.00 b	0.00 b	0.00 b	0.00 b	0.00 b	0.00 b
Pre-harvest	10.63 a	11.73 a	12.11 a	11.94 a	9.47 a	18.06 a	16.92 a	3.92 a	12.75 a
Post-harvest	12.81 a	10.24 a	13.74 a	13.54 a	9.18 a	20.52 a	20.32 a	7.18 a	13.46 a
	Total NDF (g tree^{-1})								
Control	0.00 b	0.00 b	0.00 b	0.00 a	0.00 b	0.00 b	0.00 b	0.00 b	0.00 b
Pre-harvest	0.01 a	0.03 a	1.03 ab	0.13 a	0.72 a	0.60 a	0.57 a	0.04 ab	0.36 ab
Post-harvest	0.02 a	0.04 a	1.56 a	0.19 a	0.72 a	0.74 a	0.68 a	0.07 a	0.53 a
	NDF allocation (%)								
Control	0.00 b	0.00 b	0.00 b	0.00 b	0.00 b	0.00 b	0	0.00 b	0.00 b
Pre-harvest	0.38 a	1.05 a	29.20 a	3.52 a	20.50 a	17.56 a	15.97 a	1.22 ab	10.59 a
Post-harvest	0.41 a	0.91 a	33.01 a	3.70 a	16.79 a	16.55 a	15.62 a	1.51 a	11.50 a

Table S4a. The fruit yield, and quality parameters at harvest and post-harvest of 'Gala' apple trees on M26 rootstock in 2017-18 season under the impact of different N fertigation timings. Each tree received no N fertilizer (control) or a total of 30 g N enriched with 5.5% ^{15}N in November 2017 (pre-harvest) or March 2018 (post-harvest) or half rate of N in both pre- and post-harvest (50:50 split). Mean, n = 4. Different letters indicate the significant differences among four fertigation timing treatments.

Treatment	Yield (kg tree^{-1})	Weight (g)	Dry matter content (%)	L index	a index	Delta absorbance	Red intensity	Red coverage	Background colour
Control	16.98	166.22	13.45 ab	44.11 ab	32.07 a	0.33	5.50 ab	4.03 a	7.73 ab
Pre-harvest	18.42	155.95	13.31 ab	43.71 ab	31.91 ab	0.40	5.69 ab	3.99 ab	7.62 ab
Post-harvest	14.57	172.59	14.19 a	42.16 b	32.78 a	0.33	6.43 a	4.38 a	8.09 a
50:50 split	14.63	138.12	12.43 b	47.65 a	27.71 b	0.47	4.30 b	3.28 b	6.64 b

Treatment	Length (mm)	Diameter (mm)	Firmness (kg)	Starch index	TSS (Brix°)	Post-harvest firmness (kg)	Post-harvest TSS (Brix°)
Control	69.71	70.65	7.61	5.46	11.80	5.69	11.70
Pre-harvest	68.07	69.67	8.11	5.68	11.45	5.38	11.55
Post-harvest	70.64	71.68	7.56	5.15	12.21	5.81	12.16
50:50 split	64.99	66.52	7.89	5.52	10.78	5.59	11.02

Table S4b. The fruit yield, and quality parameters at harvest and post-harvest of 'Gala' apple trees on M26 rootstock in 2018-19 season under the impact of different N fertigation timings. Each tree received no N fertilizer (control) or a total of 30 g N enriched with 5.5% ^{15}N in November 2017 (pre-harvest) or March 2018 (post-harvest). Mean, n = 4. There was no significant difference in fruit yield and any quality attributes between the treatments.

Treatment	Yield (kg tree^{-1})	Weight (g)	Dry matter content (%)	L index	a index	Delta absorbance	Red intensity	Red coverage	Background colour
Control	6.84	156.71	15.18	45.74	33.06	0.45	5.50	3.83	6.67
Pre-harvest	8.1	176.48	14.64	43.32	35.89	0.45	5.96	4.31	6.74
Post-harvest	9.56	173.79	14.94	44.98	34.43	0.45	5.32	3.79	6.95

	Length (mm)	Diameter (mm)	Firmness (kg)	Starch index	TSS (Brix°)		Post-harvest firmness (kg)	Post-harvest TSS (Brix°)	
Control	71.69	66.55	9.14	4.87	14.17		6.45	14.05	
Pre-harvest	75.17	68.98	8.82	4.68	13.58		6.49	14.33	
Post-harvest	73.54	69.06	8.91	4.98	14.08		6.64	14.20	

568

569 **Table S5.** The total dry matter content, nitrogen concentration and total N content of various tree organs harvested at dormancy in June 2018 of
570 'Gala' apple trees on M26 rootstock under the impact of different N fertigation timings. Each tree received no N fertilizer (control) or a total of
571 30 g N enriched with 5.5% ^{15}N in November 2017 (pre-harvest) or March 2018 (post-harvest) or half rate of N in both pre- and post-harvest
572 (50:50 split). Mean, n = 4. Different letters indicate the significant differences among four fertigation timing treatments.

Organ type	Bud	Spur	Leaf foliage	First year wood	Branch	Trunk	Old root	Fine root	Fruit
Treatment	**Total dry matter (g tree^{-1})**								
Control	9.18	38.5	377.16	82.76	612.51	2095.22	1593.9	102.56	4005.8
Pre-harvest	8.92	50.23	434.78	75.5	720.53	2140.88	1599.97	144.18	5531.6
Post-harvest	10.11	49.65	347.08	74.49	728.91	1939.37	1567.48	114.7	3448.22
50:50 split	8.74	46.25	308.66	28.27	540.3	1341.16	1203.94	77.94	3486.04
	Nitrogen concentration (% dry weight)								
Control	1.74	2.06	0.9	1.04	0.48 b	0.42 b	0.83	1.03 c	0.31
Pre-harvest	1.79	2.25	1.2	1.07	0.54 ab	0.50 ab	0.97	1.11 bc	0.37
Post-harvest	1.83	2.12	0.9	1.21	0.67 a	0.60 a	0.95	1.31 ab	0.26
50:50 split	1.88	2.04	1.22	1.25	0.51 ab	0.49 b	0.99	1.34 a	0.33
	Total N content (g tree^{-1})								
Control	0.16	0.8	3.41	0.87	2.69 b	8.58	13.28	1.04	11.52 b
Pre-harvest	0.16	1.13	5.3	0.8	3.83 ab	10.63	15.69	1.59	20.31 a
Post-harvest	0.19	1.06	3.1	0.89	4.86 a	11.66	14.85	1.5	8.99 b
50:50 split	0.17	0.95	3.81	0.33	2.68 b	6.72	11.97	1.01	11.41 b

573

574 **Table S6.** The total dry matter content, nitrogen concentration and total N content of various tree organs harvested at harvest in March 2019 of
575 'Gala' apple trees on M26 rootstock under the impact of different N fertigation timings. Each tree received no N fertilizer (control) or a total of
576 30 g N enriched with 5.5% ^{15}N in November 2017 (pre-harvest) or March 2018 (post-harvest) or half rate of N in both pre- and post-harvest (50-
577 50 split). Mean, n = 4. Different letters indicate the significant differences among four fertigation timing treatments.

Organ type	Bud	Spur	Leaf	First year wood	Branch	Trunk	Old root	Fine root	Fruit
Treatment	**Total dry matter (g tree^{-1})**								
Control	9.73	16.89	601.84	89.6	1165.43	2455.02	1800.55	116.03	998.89
Pre-harvest	8.84	15.77	534.02	93.6	1099.48	2383.03	1325.57	110.43	1195.72
Post-harvest	10.39	21.39	663.87	126.84	1342.98	2623.16	1453.83	119.04	1415.29
	Nitrogen concentration (% dry weight)								
Control	1.38	1.92	1.53	1.14	0.65	0.41	0.59	0.76	0.24
Pre-harvest	1.38	1.88	1.59	1.13	0.69	0.42	0.69	0.85	0.25
Post-harvest	1.39	1.8	1.64	1.23	0.64	0.39	0.67	0.74	0.27
	Total N content (g tree^{-1})								
Control	0.13	0.32	9.16	1.01	7.63	10.1	10.59	0.86	2.51
Pre-harvest	0.12	0.29	8.41	1.05	7.49	9.85	9.08	0.95	2.98
Post-harvest	0.14	0.38	10.97	1.39	8.31	10.09	9.65	0.9	3.91

578

Conflict of interest

None declared.

Funding

This project was funded by Hort Innovation, using the apple and pear research and development levy and contributions from the Australian Government. Hort Innovation is the grower owned, not-for-profit research and development corporation for Australian horticulture.

Acknowledgements

We thank Reid Fruits for contributing the experimental orchard and tree material to be destructive harvested for this study. We acknowledge Mark Salter, Nick Owens, Brad Ashlin and Andrew Hall for the maintenance of the trial site and assisting in tree excavation for two seasons. We acknowledge Justin Direen and Garth Oliver for field and laboratorial assistance, Christian Dietz for providing advice and Christine Cook for guidance in sample collection and preparation for ^{15}N analysis.

Authors' Contributions

N.D.S. and D.C.C. conceptualized the study; B.T., N.D.S and D.C.C. designed the experiment; B.T. and N.D.S. and P.Q. implemented the methodology; B.T. and N.D.S executed the experiment and data collection; B.T. performed statistical analysis and summarized results with consultation with N.D.S. and D.C.C. All authors discussed to interpret the data and result. B.T. took the lead in writing the manuscript, and received critical feedbacks and edits from all co-authors.

References

601 Aguirre, P.B., Y.K. Al-Hinai, T.R. Roper and A.R. Krueger. 2001. Apple tree rootstock and fertilizer
602 application timing affect nitrogen uptake. HortScience. 36:1202-1205.
603 Benincasa, P., M. Guiducci and F. Tei. 2011. The nitrogen use efficiency: meaning and sources of
604 variation—case studies on three vegetable crops in central Italy. HortTechnology. 21:266-
605 273.
606 Blanpied, G. and K.J. Silsby. 1992. Predicting harvest date windows for apples. Cornell Cooperative
607 Extension.
608 Carew, R. 2000. A hedonic analysis of apple prices and product quality characteristics in British
609 Columbia. Canadian Journal of Agricultural Economics/Revue canadienne d'agroeconomie.
610 48:241-257.
611 Cassman, K.G., A. Dobermann and D.T. Walters. 2002. Agroecosystems, nitrogen-use efficiency, and
612 nitrogen management. AMBIO: A Journal of the Human Environment. 31:132-140.
613 Chapin III, F.S., E. Schulze and H.A. Mooney. 1990. The ecology and economics of storage in plants.
614 Annual Review of Ecology and Systematics. 21:423-447.
615 Cheng, L. and L.H. Fuchigami. 2002. Growth of young apple trees in relation to reserve nitrogen and
616 carbohydrates. Tree Physiology. 22:1297-1303.
617 Coplen, T.B., J.K. Krouse and J.K. Böhlke. 1992. Reporting of Nitrogen-Isotope Abundances. Pure
618 Appl. Chem. 64:907-908.
619 Costa, G., M. Noferini, G. Fiori and P. Torrigiani. 2009. Use of Vis/NIR spectroscopy to assess fruit
620 ripening stage and improve management in post-harvest chain. Fresh Prod. 1:35-41.
621 Dong, S., C.F. Scagel, L. Cheng, L.H. Fuchigami and P.T. Rygiewicz. 2001. Soil temperature and plant
622 growth stage influence nitrogen uptake and amino acid concentration of apple during early
623 spring growth. Tree Physiology. 21:541-547.
624 Drake, S., J. Raese and T. Smith. 2002. Time of nitrogen application and its influence on 'Golden
625 Delicious' apple yield and fruit quality. Journal of Plant Nutrition. 25:143-157.

626 Fadón, E., E. Fernandez, H. Behn and E. Luedeling. 2020. A conceptual framework for winter
627 dormancy in deciduous trees. Agronomy. 10:241.
628 Fang, Z., J.C. Bouwkamp and T. Solomos. 1998. Chlorophyllase activities and chlorophyll degradation
629 during leaf senescence in non-yellowing mutant and wild type of Phaseolus vulgaris L.
630 Journal of Experimental Botany. 49:503-510.
631 Freney, J. 1997. Emission of nitrous oxide from soils used for agriculture. Nutrient Cycling in
632 Agroecosystems. 49:1-6.
633 Fujii, J.A. and R.A. Kennedy. 1985. Seasonal changes in the photosynthetic rate in apple trees: A
634 comparison between fruiting and nonfruiting trees. Plant Physiology. 78:519-524.
635 Gebbers, R. and V.I. Adamchuk. 2010. Precision agriculture and food security. Science. 327:828-831.
636 Giblin, A.E., C.R. Tobias, B. Song, N. Weston, G.T. Banta and V. H. RIVERA-MONROY. 2013. The
637 importance of dissimilatory nitrate reduction to ammonium (DNRA) in the nitrogen cycle of
638 coastal ecosystems. Oceanography. 26:124-131.
639 Grassi, G., P. Millard, R. Wendler, G. Minotta and M. Tagliavini. 2002. Measurement of xylem sap
640 amino acid concentrations in conjunction with whole tree transpiration estimates spring N
641 remobilization by cherry (Prunus avium L.) trees. Plant, Cell & Environment. 25:1689-1699.
642 Guak, S., D. Neilsen, P. Millard, R. Wendler and G.H. Neilsen. 2003. Determining the role of N
643 remobilization for growth of apple (Malus domestica Borkh.) trees by measuring xylem‐sap
644 N flux. Journal of Experimental Botany. 54:2121-2131.
645 Hardie, M., J. Ridges, N. Swarts and D. Close. 2018. Drip irrigation wetting patterns and nitrate
646 distribution: comparison between electrical resistivity (ERI), dye tracer, and 2D soil–water
647 modelling approaches. Irrigation science. 36:97-110.
648 Hauck, R.D. 1982. Nitrogen—isotope-ratio analysis. Methods of soil analysis. Part 2. Chemical and
649 microbiological properties:735-779.
650 Hauck, R.D. and J.M. Bremner. 1976. Use of tracers for soil and fertilizer nitrogen research. Advances
651 in Agronomy. 219-266 p.

652 Hill-Cottingham, D.G. and C.P. Lloyd-Jones. 1975. Nitrogen-15 in apple nutrition investigations.
653 Journal of the Science of Food and Agriculture. 26:165-173.
654 Klein, I., I. Levin, B. Bar-Yosef, R. Assaf and A. Berkovitz. 1989. Drip nitrogen fertigation of 'Starking
655 Delicious' apple trees. Plant and Soil. 119:305-314.
656 Landsberg, J. 1974. Apple fruit bud development and growth; analysis and an empirical model.
657 Annals of Botany. 38:1013-1023.
658 Maathuis, F.J. 2009. Physiological functions of mineral macronutrients. Current Opinion in Plant
659 Biology. 12:250-258.
660 Martínez-Alcántara, B., A. Quiñones, E. Primo-Millo and F. Legaz. 2011. Nitrogen remobilization
661 response to current supply in young citrus trees. Plant and Soil. 342:433-443.
662 Masclaux-Daubresse, C., F. Daniel-Vedele, J. Dechorgnat, F. Chardon, L. Gaufichon and A. Suzuki.
663 2010. Nitrogen uptake, assimilation and remobilization in plants: challenges for sustainable
664 and productive agriculture. Annals of Botany. 105:1141-1157.
665 Millard, P. and G.-a. Grelet. 2010. Nitrogen storage and remobilization by trees: ecophysiological
666 relevance in a changing world. Tree Physiology. 30:1083-1095.
667 Millard, P. and G. Neilsen. 1989. The influence of nitrogen supply on the uptake and remobilization
668 of stored N for the seasonal growth of apple trees. Annals of Botany. 63:301-309.
669 Millard, P. and M. Proe. 1993. Nitrogen uptake, partitioning and internal cycling in Picea sitchensis
670 (Bong.) Carr. as influenced by nitrogen supply. New Phytologist. 125:113-119.
671 Millard, P. and C. Thomson. 1989. The effect of the autumn senescence of leaves on the internal
672 cycling of nitrogen for the spring growth of apple trees. Journal of Experimental Botany.
673 40:1285-1289.
674 Millard, P., R. Wendler, G. Grassi, G.-A. Grelet and M. Tagliavini. 2006. Translocation of nitrogen in
675 the xylem of field-grown cherry and poplar trees during remobilization. Tree Physiology.
676 26:527-536.

677 Munoz, N., J. Guerri, F. Legaz and E. Primo-Millo. 1993. Seasonal uptake of 15 N-nitrate and
678 distribution of absorbed nitrogen in peach trees. Plant and Soil. 150:263-269.
679 Neilsen, D., P. Millard, L. Herbert, G. Neilsen, E. Hogue, P. Parchomchuk and B. Zebarth. 2001a.
680 Remobilization and uptake of N by newly planted apple (Malus domestica) trees in response
681 to irrigation method and timing of N application. Tree Physiology. 21:513-521.
682 Neilsen, D., P. Millard, G. Neilsen and E. Hogue. 1997. Sources of N for leaf growth in a high-density
683 apple (Malus domestica) orchard irrigated with ammonium nitrate solution. Tree Physiology.
684 17:733-739.
685 Neilsen, D., P. Millard, G.H. Neilsen and E.J. Hogue. 2001b. Nitrogen uptake, efficiency of use, and
686 partitioning for growth in young apple trees. Journal of the American Society for
687 Horticultural Science. 126:144-150.
688 Neilsen, D. and G. Neilsen. 2002. Efficient use of nitrogen and water in high-density apple orchards.
689 HortTechnology. 12:19-25.
690 Neilsen, D., G. Neilsen, L. Herbert, P. Millard and S. Guak. 2005. Allocation of dry matter and N to
691 fruit and shoots in dwarf apple in response to sink size and N availability. *In* V International
692 Symposium on Mineral Nutrition of Fruit Plants 721, pp 33-40.
693 Neilsen, G., E. Hogue and M. Meheriuk. 1999. Nitrogen fertilization and orchard-floor vegetation
694 management affect growth, nutrition and fruit quality of 'Gala' apple. Canadian Journal of
695 Plant Science. 79:379-385.
696 Neilsen, G.H., D. Neilsen and L. Herbert. 2009. Nitrogen fertigation concentration and timing of
697 application affect nitrogen nutrition, yield, firmness, and color of apples grown at high
698 density. HortScience. 44:1425-1431.
699 Quartieri, M., P. Millard and M. Tagliavini. 2002. Storage and remobilisation of nitrogen by pear
700 (Pyrus communis L.) trees as affected by timing of N supply. European Journal of Agronomy.
701 17:105-110.

Rivera, R., P. Bañados and M. Ayala. 2016. Distribution of 15N applied to the soil in the 'Bing'/'Gisela® 6'sweet cherry (Prunus avium L.) combination. Scientia Horticulturae. 210:242-249.

San-Martino, L., G.O. Sozzi, S. San-Martino and R.S. Lavado. 2010. Isotopically-labelled nitrogen uptake and partitioning in sweet cherry as influenced by timing of fertilizer application. Scientia Horticulturae. 126:42-49.

Scandellari, F., M. Ventura, D. Malaguti, C. Ceccon, G. Menarbin and M. Tagliavini. 2008. Net primary productivity and partitioning of absorbed nutrients in field-grown apple trees. *In* VI International Symposium on Mineral Nutrition of Fruit Crops 868, pp 115-122.

Schenk, M. 1996. Regulation of nitrogen uptake on the whole plant level. *In* Progress in Nitrogen Cycling Studies. Springer, pp 277-283.

Shear, C. and M. Faust. 1980. Nutritional ranges in deciduous tree fruits and nuts. Horticultural Reviews, Volume 2:142-163.

Swarts, N., K. Montagu, G. Oliver, L. Southam-Rogers, M. Hardie, R. Corkrey, G. Rogers and D. Close. 2016. Benchmarking nitrous oxide emissions in deciduous tree cropping systems. Soil Research. 54:500-511.

Tagliavini, M., P. Millard, M. Quartieri and B. Marangoni. 1999. Timing of nitrogen uptake affects winter storage and spring remobilisation of nitrogen in nectarine (Prunus persica var. nectarina) trees. Plant and Soil. 211:149-153.

Team, R.C. 2019. R: A language and environment for statistical computing. R Foundation for Statistical Computing, Vienna, Austria.

Toselli, M., C. Zavalloni, B. Marangoni and J.A. Flore. 2000. Nitrogen partitioning in apple trees as affected by application time. HortTechnology. 10:136-141.

Zhang, L., M. Han, C. Zhao, C. Liu, F. Zhang, L. Zhang and B. Li. 2012. 15 Nitrogen study on absorption, distribution and utilization of nitrogen applied in early summer in red fuji apple. Journal of plant nutrition. 35:1557-1571.

728 **List of Figures**

729 **Table 1** The [N] and [^{15}N] of soil samples of 0-10cm depth collected from each 'Gala' apple
730 tree on M26 rootstock on 11th July 2018, 14 weeks before bud break of 2018-19 season under
731 different N fertigation treatments. Value represent ± 1 standard error of the mean, n = 4.

732

733 **Table S1.** The N concentration, and N derived from fertilizer of leaf samples collected over
734 2018-18 season after pre-harvest fertigation of 'Gala' apple trees on M26 rootstock in 2018-
735 19 season under the impact of different N fertigation timings. Each tree received no N
736 fertilizer (control) or a total of 30 g N of N_f in November 2017 (pre-harvest), March 2018
737 (post-harvest), or evenly split over pre- and post-harvest (50:50 split). Mean, n = 4. Different
738 letters indicate significant differences ($p < 0.05$) between four treatments.

739 **Table S2.** The N derived from fertilizer (NDF) percentage, total NDF and NDF allocation of
740 various tree organs harvested at dormancy in June 2018 of 'Gala' apple trees on M26
741 rootstock under the impact of different N fertigation timings. Each tree received no N
742 fertilizer (control), or a total of 30 g N of N_f, in November 2017 (pre-harvest), March 2018
743 (post-harvest), or evenly split over pre- and post-harvest (50:50 split). Mean, n = 4. Different
744 letters indicate significant differences ($p < 0.05$) between the four treatments.

745 **Table S3.** The N derived from fertilizer (NDF) percentage, total NDF and NDF allocation of
746 various tree organs harvested at harvest in March 2019 of 'Gala' apple trees on M26
747 rootstock under the impact of different N fertigation timings. Each tree received no N
748 fertilizer (control) or a total of 30 g N enriched with 5.5% ^{15}N in November 2017 (pre-
749 harvest) or March 2018 (post-harvest). Mean, n = 4. Different letters indicate the significant
750 differences among four fertigation timing treatments.

Table S4a. The fruit yield, and quality parameters at harvest and post-harvest of 'Gala' apple trees on M26 rootstock in 2017-18 season under the impact of different N fertigation timings. Each tree received no N fertilizer (control) or a total of 30 g N enriched with 5.5% ^{15}N in November 2017 (pre-harvest) or March 2018 (post-harvest) or half rate of N in both pre- and post-harvest (50:50 split). Mean, n = 4. Different letters indicate the significant differences among four fertigation timing treatments.

Table S4b. The fruit yield, and quality parameters at harvest and post-harvest of 'Gala' apple trees on M26 rootstock in 2018-19 season under the impact of different N fertigation timings. Each tree received no N fertilizer (control) or a total of 30 g N enriched with 5.5% ^{15}N in November 2017 (pre-harvest) or March 2018 (post-harvest). Mean, n = 4. There was no significant difference in fruit yield and any quality attributes between the treatments.

Table S5. The total dry matter content, nitrogen concentration and total N content of various tree organs harvested at dormancy in June 2018 of 'Gala' apple trees on M26 rootstock under the impact of different N fertigation timings. Each tree received no N fertilizer (control) or a total of 30 g N enriched with 5.5% ^{15}N in November 2017 (pre-harvest) or March 2018 (post-harvest) or half rate of N in both pre- and post-harvest (50:50 split). Mean, n = 4. Different letters indicate the significant differences among four fertigation timing treatments.

Table S6. The total dry matter content, nitrogen concentration and total N content of various tree organs harvested at harvest in March 2019 of 'Gala' apple trees on M26 rootstock under the impact of different N fertigation timings. Each tree received no N fertilizer (control) or a total of 30 g N enriched with 5.5% ^{15}N in November 2017 (pre-harvest) or March 2018 (post-harvest) or half rate of N in both pre- and post-harvest (50-50 split). Mean, n = 4. Different letters indicate the significant differences among four fertigation timing treatments.

Figure 1 Fertigation NUpE and NRec of ‘Gala’ apple trees on M26 rootstock in the 2017-18 and 2018-19 seasons following different N fertigation treatments. Error bars represent ± 1 standard error of the mean, n = 4. Different uppercase letters denote significant interaction ($P < 0.05$) between fertigation treatments and seasons, and different lowercase letters indicate significant differences ($P < 0.05$) between fertigation treatments within a season.

Figure 2 The amount of NDF and unlabelled N (Native N) in each ‘Gala’ apple tree on M26 rootstock at dormancy of the 2017-18 and harvest of the 2018-19 seasons under different N fertigation treatments. Error bars represent ± 1 standard error of the mean, n = 4.

Figure 3 Dynamics of leaf N concentration [N] (a) and concentration of NDF [NDF] (b) of ‘Gala’ apple trees on M26 rootstock during the 2017-18 season following different N fertigation timings. Error bars represent ± 1 standard error of the mean, n = 4. Fruit was harvested at 22 WAFB.

Figure 4 The proportion (a) and total amount (b) of NDF allocated into different organs of ‘Gala’ apple tree on M26 rootstock at winter dormancy of the 2017-18 season under different N fertigation treatments. Error bars represent ± 1 standard error of the mean, n = 4. Different letters indicate significant differences ($p < 0.05$) between treatments for the same organ.

Figure 5 The total N in each organ showing composition of native N and NDF at one week after harvest of the 2018-19 season under different N fertigation treatments. Error bars represent ± 1 standard error of the mean, n = 4.

Figure 6 The total N contained in the roots, trunk, branches and seasonal canopy showing composition of N derived from native N and NDF at winter dormancy of 2017-18 season and at one week after harvest timing of the 2018-19 season (March 2019). Error bars represent ± 1 standard error of the mean, n = 12. Different letters indicate significant differences related to the time of sampling.

Tables

Table 1 The [N] and [^{15}N] of soil samples of 0-10cm depth collected from each 'Gala' apple tree on M26 rootstock on 11th July 2018, 14 weeks before bud break of 2018-19 season under different N fertigation treatments. Value represent ± 1 standard error of the mean, n = 4.

Treatment	[N] (% dry weight)	[^{15}N] (atom %)
Control	0.143 ± 0.013	$0.3696 \pm 8.8 \times 10^{-5}$
Pre-harvest	0.146 ± 0.008	$0.3802 \pm 2.6 \times 10^{-3}$
Post-harvest	0.139 ± 0.005	$0.3839 \pm 8.6 \times 10^{-3}$
50:50 split	0.152 ± 0.005	$0.3821 \pm 2.4 \times 10^{-3}$

OR

807

808

Treatment	23-Oct-17	11-Jul-18	2-Nov-18	21-Feb-19	12-Mar-19
			[N] (% dry weight)		
Control	0.178 ± 0.004	0.143 ± 0.013	0.185 ± 0.008	0.188 ± 0.007	0.149 ± 0.009
Pre-harvest	0.193 ± 0.016	0.146 ± 0.008	0.175 ± 0.006	0.172 ± 0.006	0.139 ± 0.023
Post-harvest	0.196 ± 0.020	0.139 ± 0.005	0.175 ± 0.009	0.178 ± 0.002	0.137 ± 0.018
50:50 split	0.192 ± 0.015	0.152 ± 0.005			
			[15N] (atom %)		
Control	$0.3690 \pm 5.3\times10^{-5}$	$0.3696 \pm 8.8\times10^{-5}$	$0.3701 \pm 2.0\times10^{-4}$	$0.3746 \pm 4.8\times10^{-3}$	$0.3740 \pm 4.3\times10^{-3}$
Pre-harvest	$0.3692 \pm 1.1\times10^{-4}$	$0.3802 \pm 2.6\times10^{-3}$	$0.3887 \pm 2.5\times10^{-3}$	$0.3851 \pm 5.4\times10^{-3}$	$0.3837 \pm 7.0\times10^{-4}$
Post-harvest	$0.3691 \pm 1.9\times10^{-4}$	$0.3839 \pm 8.6\times10^{-3}$	$0.3949 \pm 7.5\times10^{-3}$	$0.4005 \pm 8.9\times10^{-3}$	$0.3877 \pm 1.6\times10^{-3}$
50:50 split	$0.3688 \pm 2.0\times10^{-4}$	$0.3821 \pm 2.4\times10^{-3}$			

Figures

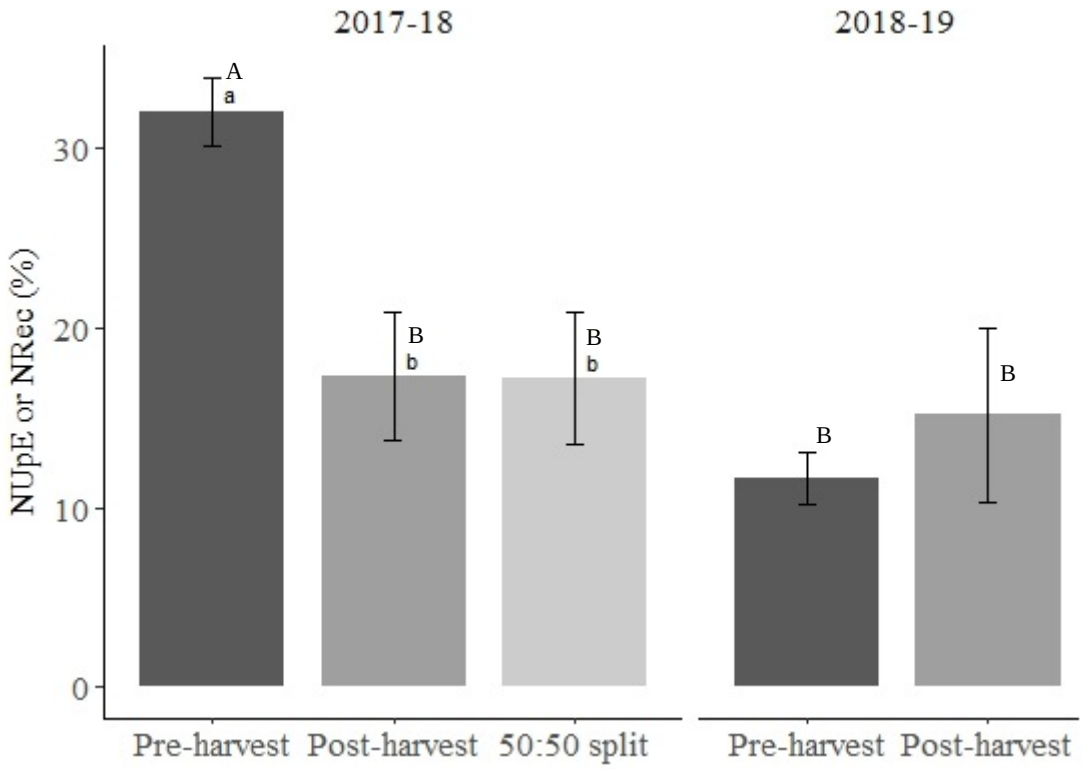

Figure 1 Fertigation NUpE and NRec of 'Gala' apple trees on M26 rootstock in the 2017-18 and 2018-19 seasons following different N fertigation treatments. Error bars represent ± 1 standard error of the mean, n = 4. Different uppercase letters denote significant interaction ($P < 0.05$) between fertigation treatments and seasons, and different lowercase letters indicate significant differences ($P < 0.05$) between fertigation treatments within a season.

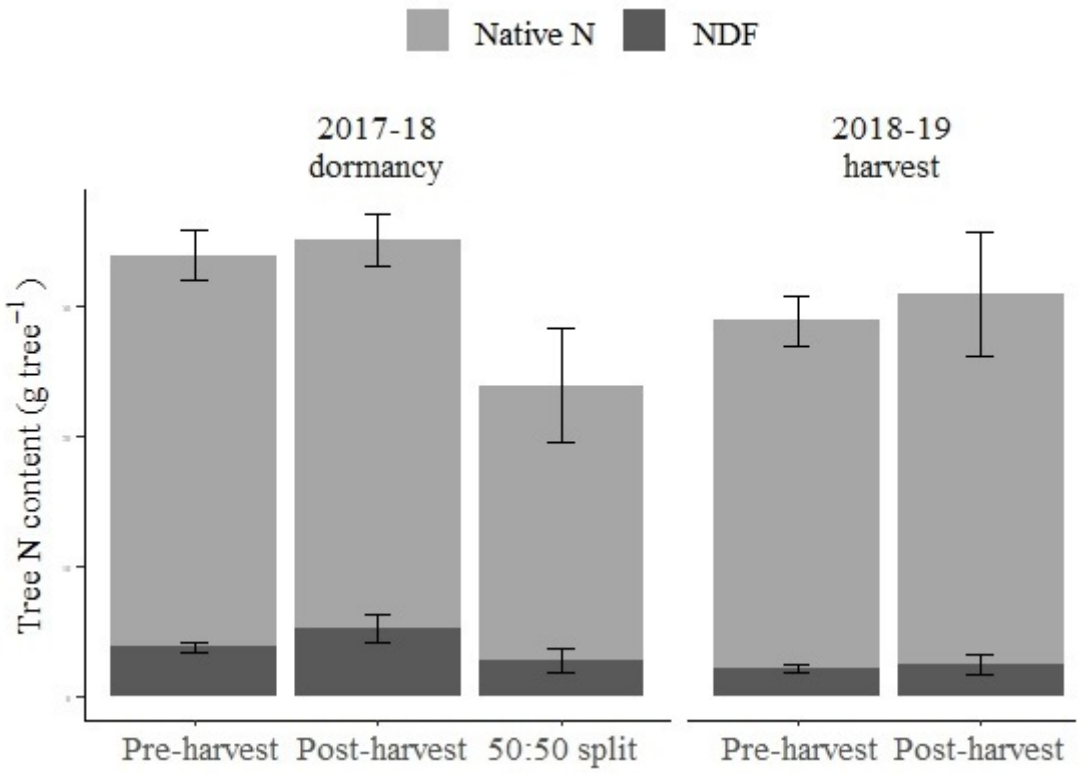

Figure 2 The amount of NDF and unlabelled N (Native N) in each 'Gala' apple tree on M26 rootstock at dormancy of the 2017-18 and harvest of the 2018-19 seasons under different N fertigation treatments. Error bars represent ± 1 standard error of the mean, n = 4.

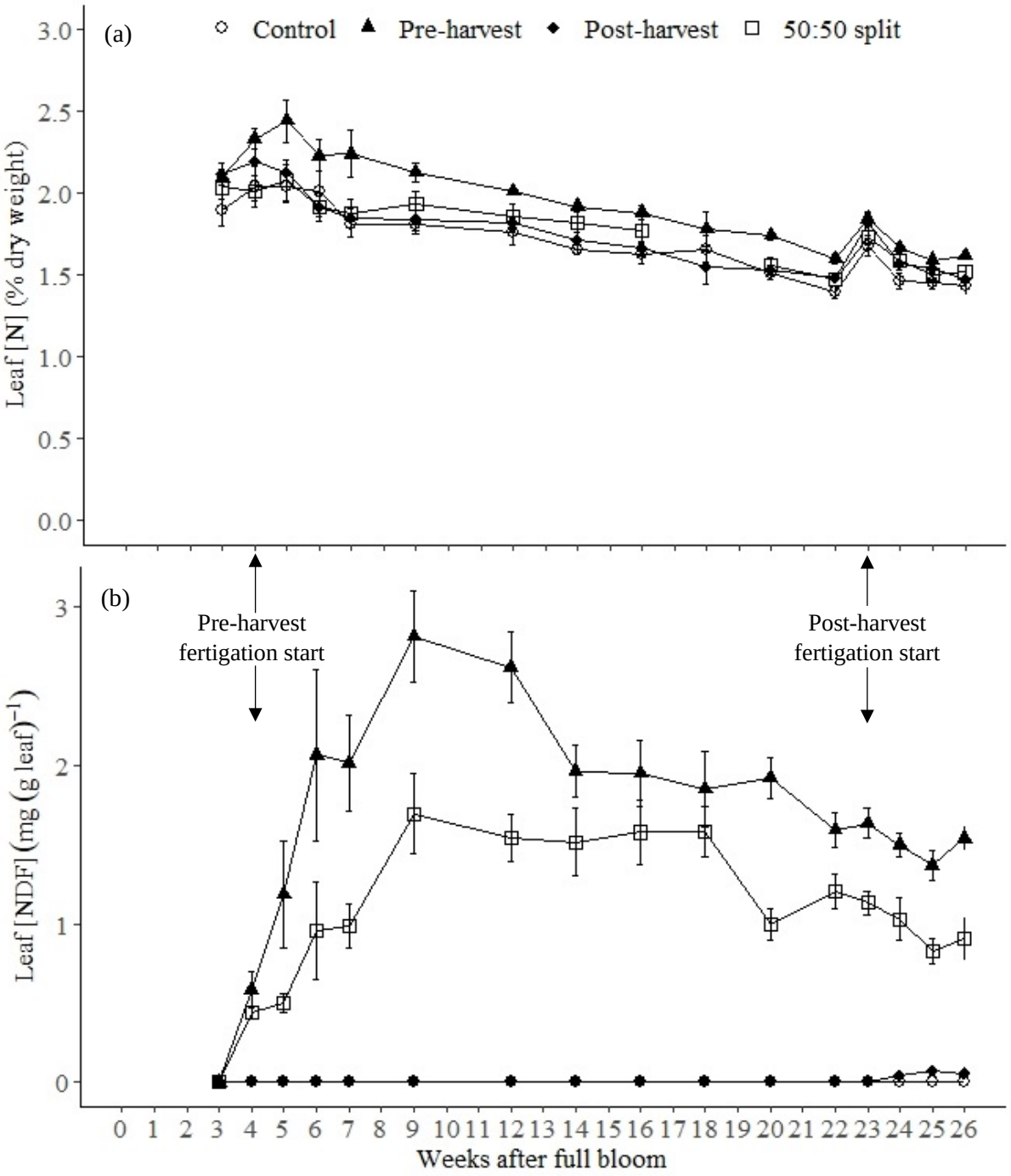

Figure 3 Dynamics of leaf N concentration [N] (a) and concentration of NDF [NDF] (b) of 'Gala' apple trees on M26 rootstock during the 2017-18 season following different N fertigation timings. Error bars represent ± 1 standard error of the mean, n = 4. Fruit was harvested at 22 WAFB.

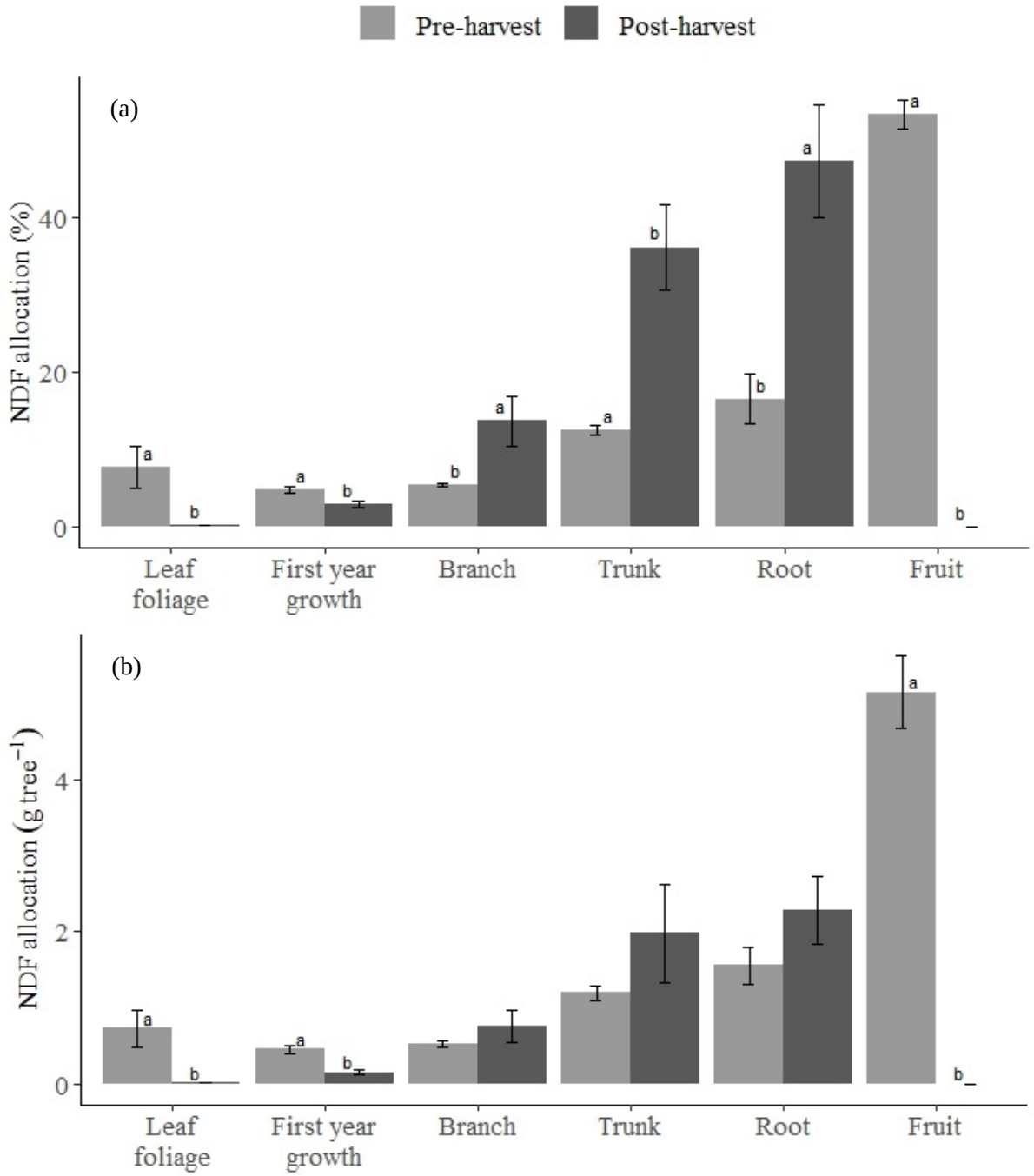

Figure 4 The proportion (a) and total amount (b) of NDF allocated into different organs of 'Gala' apple tree on M26 rootstock at winter dormancy of the 2017-18 season under different N fertigation treatments. Error bars represent ± 1 standard error of the mean, n = 4. Different letters indicate significant differences ($p < 0.05$) between treatments for the same organ.

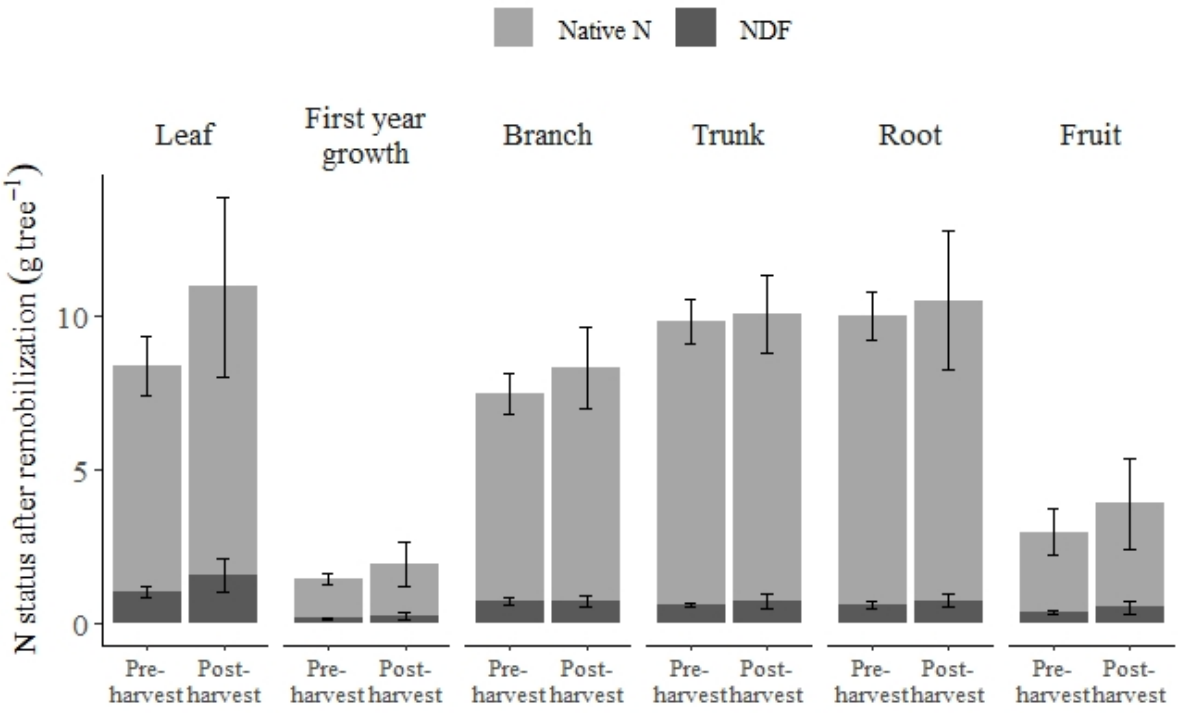

828 **Figure 5** The total N in each organ showing composition of native N and NDF at one week
829 after harvest of the 2018-19 season under different N fertigation treatments. Error bars
830 represent ± 1 standard error of the mean, n = 4.

831

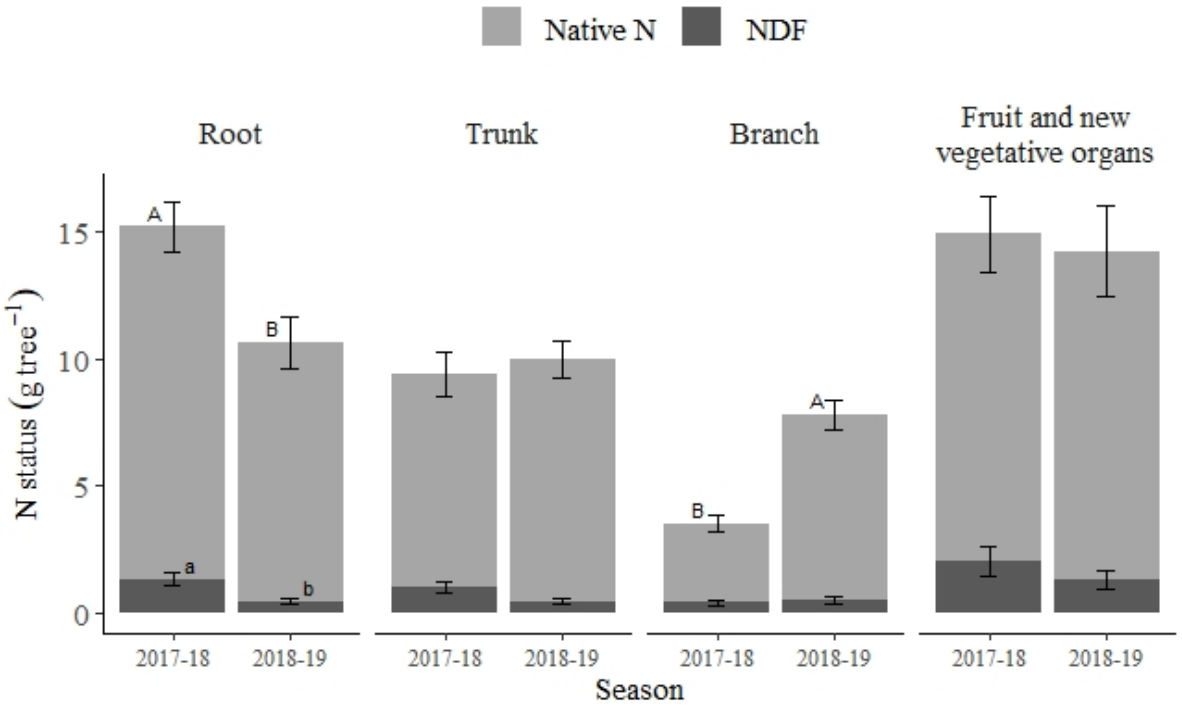

832 **Figure 6** The total N contained in the roots, trunk, branches and seasonal canopy showing
833 composition of N derived from native N and NDF at winter dormancy of 2017-18 season and
834 at one week after harvest timing of the 2018-19 season (March 2019). Error bars represent ±
835 1 standard error of the mean, n = 12. Different letters indicate significant differences related
836 to the time of sampling.

Appendix 7: Soil Mineralisation

Roberta Gentile, Plant and Food Research, New Zealand

Soil Nitrogen Mineralisation

Nitrogen (N) is generally the most common growth-limiting nutrient in agricultural production systems. In a perennial orchard system, external N uptake may occur through the roots via soil nutrient uptake or leaves from foliar nutrient applications. Soil available N is derived from a number of sources including fertiliser application, organic amendments, mineralisation of soil organic matter, and decomposition of orchard leaf litter, prunings and groundcover. The contribution of mineralisation to crop N supply may range from <20 to >200 kg N ha^{-1} (Cabrera et al. 1994) depending on the quantity of mineralisable organic N in the soil and environmental conditions (soil temperature and moisture) that control the rate of mineralisation and can have a significant contribution to plant N uptake.

Predicting the ability of the soil to supply N has economic and environmental importance as growers can tailor nutrient applications to crop requirements accounting for the N that mineralised from soil organic matter. Soil temperature and moisture control soil microbial activity and hence the rate of soil N mineralisation in the field. Refining our ability to accurately estimate mineralisable N based on soil indicators and modelled predictions is essential to improve fertiliser management.

Orchard soil mineralisable nitrogen

Soil collection

Soil was collected from two apple fertigation experiments at Lucaston and Plenty to determine the potentially mineralisable N. Soil was collected from the Lucaston experiment in December 2015 from the 50% pre- and post-harvest N medium irrigation treatment and from the Plenty experiment in September 2018 from the unfertilised treatment. In each of the four field replicates of both experiments, three soil samples were collected comprising the tree row topsoil (0-10 cm), alley topsoil (0-10 cm), and alley subsoil (20-30 cm). Soil samples were 5-mm sieved and air-dried in the laboratory. Soils were analysed for total carbon (C) and nitrogen, and labile C (hot-water extractable C), (Table 1).

Table 1. Mean values of organic carbon and total nitrogen content for soils sampled from the apple fertigation experiments in Tasmania.

Site	Soil	Total Carbon (g/kg)	Nitrogen (g/kg)	Labile Carbon (g/kg)	C:N ratio	Fraction labile carbon (% of total)
Lucaston	Tree row (0-10 cm)	36.0	2.13	1.04	16.6	2.88
	Alley (0-10 cm)	31.3	2.19	1.16	14.3	3.69
	Subsoil (20-30 cm)	11.6	0.54	0.35	21.5	3.04
Plenty	Tree row (0-10 cm)	21.0	1.87	0.69	11.2	3.29
	Alley (0-10 cm)	18.1	1.70	0.68	10.6	3.74
	Subsoil (20-30 cm)	5.4	0.58	0.14	9.3	2.64

Laboratory Incubation

Nitrogen mineralisation was measured during an 84-day aerobic incubation at 21 °C and -20 kPa moisture content to represent optimum conditions observed in the field. The equivalent of 25 g of oven-dry soil was weighed into 60 ml plastic containers. The soil samples were slowly wet to the target water potentials, and covered with a parafilm layer that had four pin-prick holes. Soils were pre-incubated for 14 days to allow for the flush of mineralisation upon re-wetting and then incubated for a further 84 days to measure nitrogen mineralisation rate. Soil moisture was monitored weekly by weighing the samples and adding back the same amount of water that was lost as evaporation during the incubation period.

Replicate soil samples were destructively sampled after pre-incubation and again at 14, 35, 56 and 84 days during the incubation. Soil samples were analysed for gravimetric water contents by oven-drying a subsample at 105 °C. Inorganic nitrogen concentrations in the soil samples were measured by extracting 5 g of soil with 25 ml 2M KCl solution and analysing the extract for NH4-N and NO3-N on a Lachat QuikChem 8500 Series 2 Flow Injection Analysis System (Lachat Instruments, Loveland, Colorado, USA).

Modelling the nitrogen mineralisation

We have previously reported on modelling the C and N dynamics of the soil organic matter in SINATA. In brief, mineralization is modelled by dividing the soil organic matter into two pools – a fast cycling litter pool (labile C and N) and an almost stable humus pool following Johnsson et al. (1987). This two-pool model then considers the total soil C and N that cycle within soil organic material. The relative amounts of these two components change daily to reflect inputs of new biomass and losses of older biomass as it decomposes. The nitrogen demand for the internal cycling of soil-C and soil-N is regulated by the C/N ratio of the soil biomass which is one of the important model inputs, and the other important factor is the fraction of labile C and N.

During all simulations reported here we chose typical values for equation parameters, and we used the fraction of labile C measured in the soils (Table 1) to estimate a parameter value for the fraction of stabilised organic matter. The comparison between measured mineralization rate and modelled outputs is shown in Figure 1. Simple modelling seems to works, at least for optimum environment conditions.

It is interesting to note that the while the topsoil samples from the tree row and alley have similar concentrations of total C and N (Table 1) the alley soil samples show larger amounts of N mineralised. This appears to be due to their lower C:N ratios and higher proportion of labile C than the tree row soils. This agrees with the findings of Swarts et al. (2016) who measured higher N2O emissions from the alley than tree row, which may have been due to greater microbial activity in this zone due to carbon input from the alley groundcover.

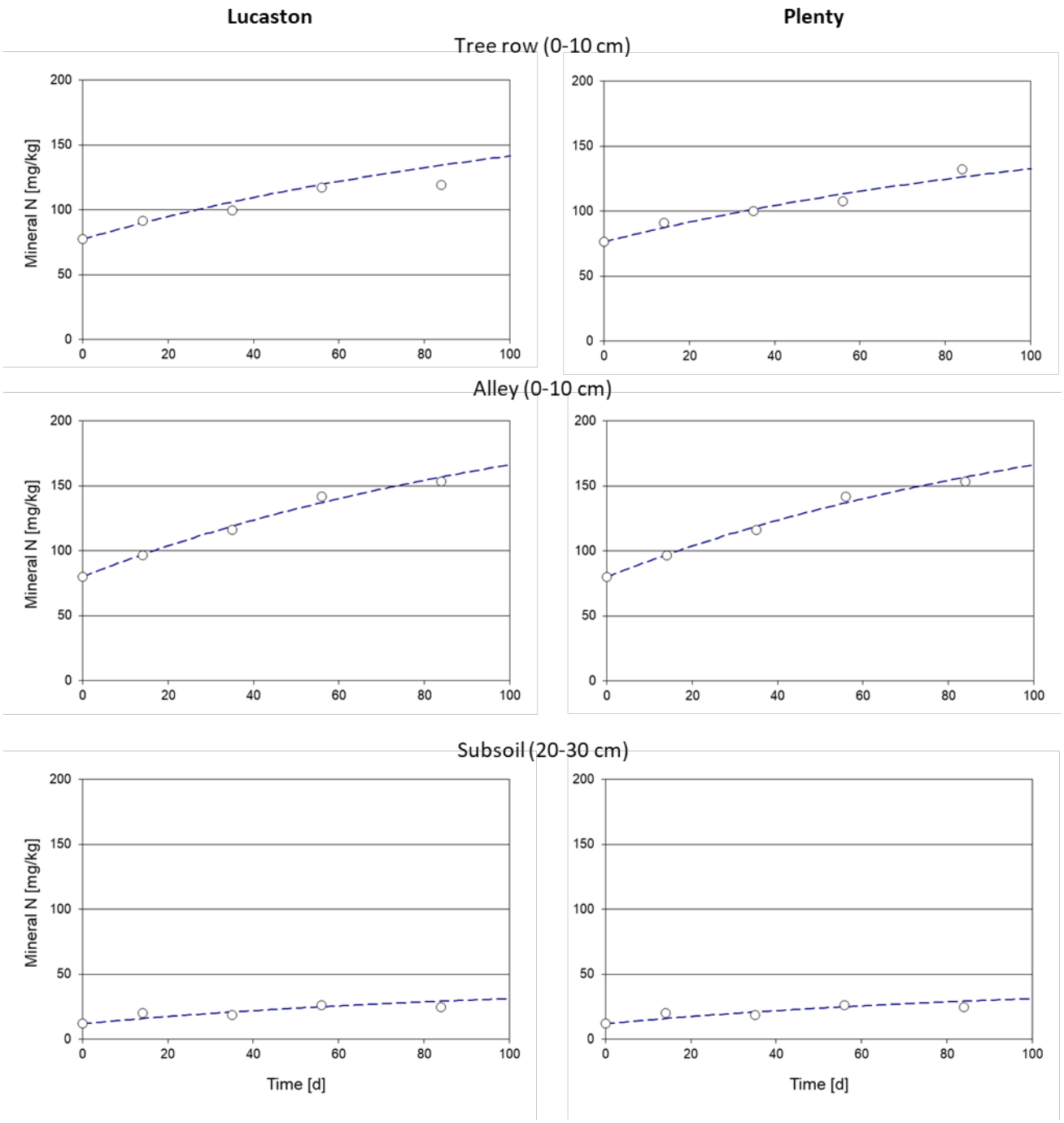

Figure 1. The change in soil mineral nitrogen (round marker) observed during laboratory incubations of soils sampled from the Lucaston (left-side) and Plenty (right-side) fertigation experiments, Tasmania. The broken line is model outputs from the mineralization sub-model of SINATA.

References

Cabrera ML, Kissel DE, Vigil MF 1994. Potential nitrogen mineralization: laboratory and field evaluation. In Havlin JL, Jacobsen JS, eds. Soil Testing: Prospects for Improving Nutrient Recommendations. Soil Science Society of America Special Publication No. 40. SSSA and ASA, Madison, WI, pp. 15–30.

Johnsson H, Bergstrom L, Jannson PE, Paustian K 1987. Simulated nitrogen dynamics and losses in a layered agricultural soil. Agriculture Ecosystems and Environment 18: 333–356.

Swarts N, Montagu K, Oliver G, Southam-Rogers L, Hardie M, Corkrey R, Rogers G, Close D 2016. Benchmarking nitrous oxide emissions in deciduous tree cropping systems. Soil Research 54: 500–511.

Appendix 8: Summary of the SINATA Tool
Steve Green, Plant and Food Research, New Zealand

The SINATA model

The purpose of this report is to provide a summary of how the SINATA (**S**trategic **I**rrigation and **N**itrogen **A**ssessment **T**ool for **A**pples) model comes together.

What is SINATA?

SINATA is a decision support tool, formulated in Excel™, to provide a guide for advisors and growers on optimization of irrigation and nitrogen application for the major apple-growing growing regions of Australia. The tool works at the block scale to determine water and nitrogen fertilizer needs based on local soil and climate conditions, tree age and anticipated crop yields. Being in Excel allows the model to be made more widely accessible, with the added potential to serve as a repository of knowledge that is already captured or may be advanced in the future.

The SINATA model in EXCEL™ comprises a number of worksheets that enable the USER to set inputs e.g. to describe details of the orchard block with appropriate soil and climate attributes (Fig. 1), and to view outputs and outcomes of management decisions e.g. annual and monthly water and nutrient balances (Fig. XX) in response to irrigation and N-fertilizer use.

What is the main purpose of SINATA?

The primary goal of SINATA is to understand how water and fertilizer application (rates, timings) can be managed to satisfy the tree's requirements, mitigating leaching and optimising productivity without cost to fruit quality.

What goes into the model?

The model includes local climate and soil data, and includes functional relations for different apple varieties (phenology and yield) to assess irrigation and N-fertilizer needs. The following list outlines what goes into the model.

- Inputs – soil (hydraulic and physio-chemial properties), plant (crop factors and productivity), atmosphere (long term climate including ETo and rainfall) data
- Processes – water (uptake, runoff, drainage, storage) and nitrogen (uptake, soil transformation, leaching, runoff) balances
- Functional descriptions of tree productivity (variety and age relationships including phenology and yield)
- Outputs – monthly and annual water and nitrogen balances

A number of factors e.g. associated with location, variety, irrigation and fertigation, are selected using pull-down menus from the tools 'Input page' worksheet (Fig. 2). The remaining factors are set internally, by default, and are from within a set of linked worksheets ('Parameters', 'soil', 'crop' and 'climate' data) that are normally hidden from the User's view.

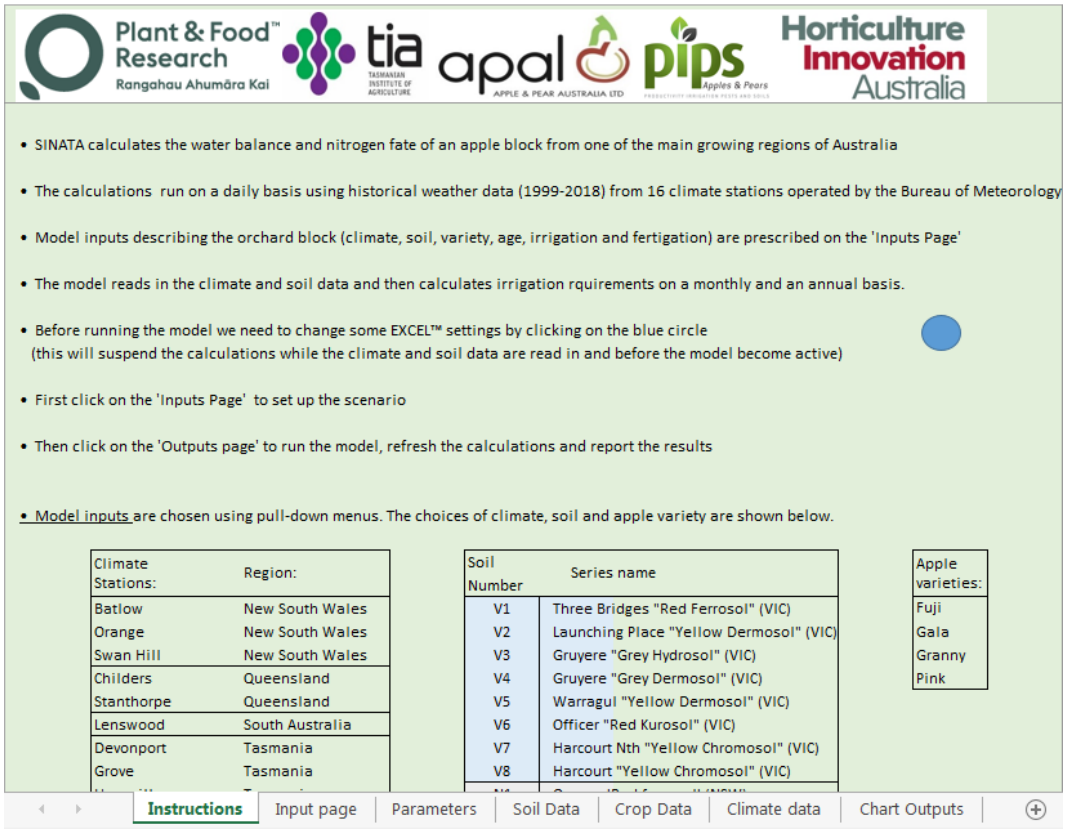

Figure 1. Instructions worksheet from the SINATA (**S**trategic **I**rrigation and **N**itrogen **A**ssessment **T**ool for **A**pples) model. The tool includes local climate and soils data. Functional relations are used to calculate dry-matter production and nitrogen demands for four of the commercial apple varieties. Several worksheets that are normally hidden ('Parameters', 'soil data', 'crop data' and 'climate data") contain default parameter values derived from the experimental findings of the PIPS (Production Irrigation pests and Soils) project.

What can the SINATA tool do?

The following list outlines what SINATA can do.

- Calculate a soil water balance – to provide advice on crop water use and irrigation
- Simulate crop growth, dry matter allocation, nitrogen distribution – to advise on tree nitrogen demands and returns of organic matters (leaves and prunings)
- Simulates N turnover in the soil – to advise how much nitrogen is mineralization fom soil organic matter
- Calculates a soil nitrogen balance – to provide advice on fate of surface applied fertilizer

- Estimate the environmental impact in terms of nitrogen losses

What can't the SINATA tool do?

The following list outlines some, but not all, of the things that SINATA can't do.

- simulate future scenarios (i.e. climate change, warmer, drier, etc)
- simulate fruit quality (size, colour etc)
- accommodate unknown soils or climates or apple varieties, without additional data
- make management decisions for the current year (uses historical rather than real-time climate data
- handle the 2- or 3-dimensional nature of an orchard such as mounding and contouring

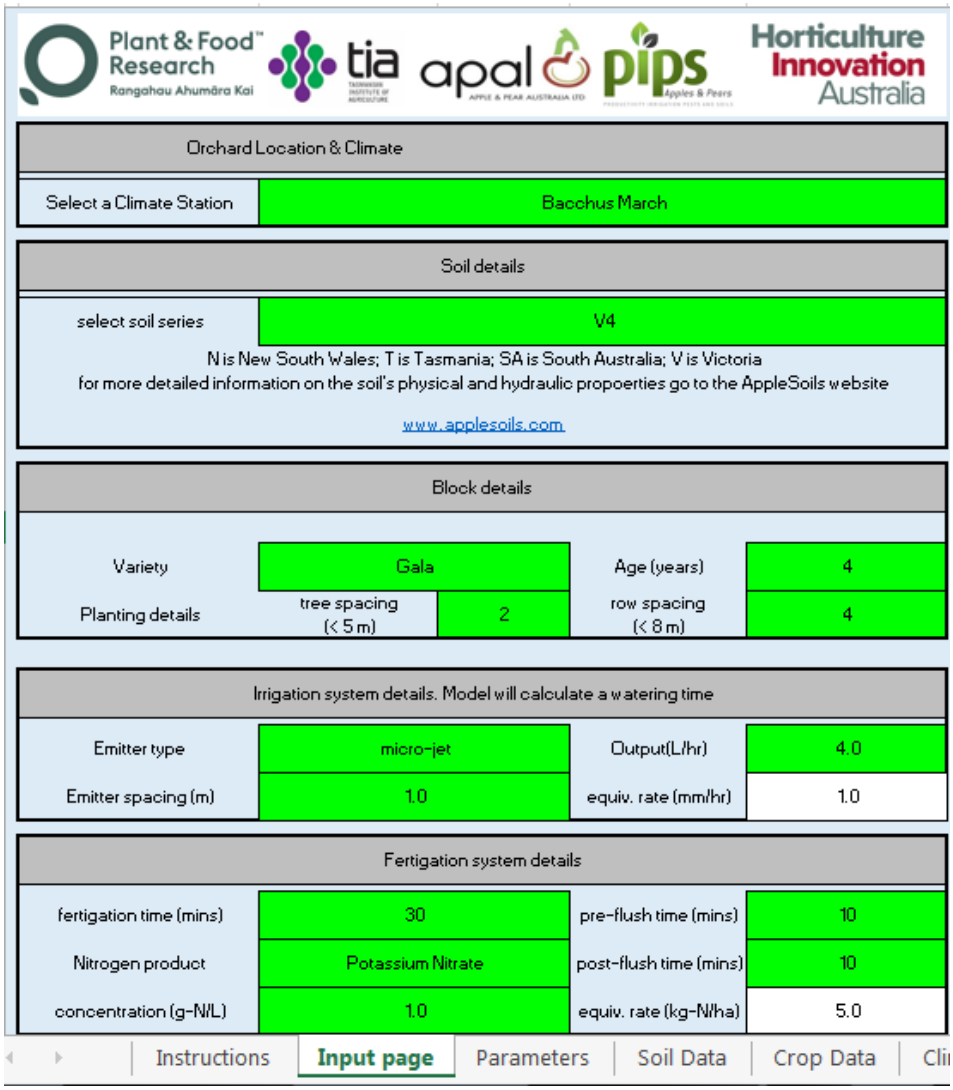

Figure 2. A screen image of the "Input page" worksheet from the SINATA (**S**trategic **I**rrigation and **N**itrogen **A**ssessment **T**ool for **A**pples) model. The tool includes local climate and soils data. Functional relations are used to calculate the dry-matter production and nitrogen demands for four of the

commercial apple varieties. Values in the green boxes are selected using a pull-down menu. All other cells are locked from entry.

What are the assumptions behind the calculations?

Tree water use

The daily climate variables from BOM include a value for the reference evaporation rate, ET_0 [mm/d], which defines the potential rate of evaporation from an extensive surface of green grass cover, of a short, uniform height, that is actively growing, completely shading the ground, and is not short of water or nutrients. On the other hand, the potential water use of the apple trees, ET_C, is calculated using a crop factor, K_C, as:

$$ET_C = K_C\, ET_O \qquad \text{[Eq. 1]}$$

For this calculation, the daily value of ET_C is represented by the tree water use (T, L/d), which we have measured with sap flow sensors for a ranges of tree ages and canopy sizes, divided by the ground area per tree (e.g. A_G = 3.85m^2 at a spacing of 1.1 m by 3.5 m (Fig. 3). A functional relationship has been derived for Kc in order to calculate the seasonal transpiration rate of apple trees, including adjustments for tree ages and different varieties.

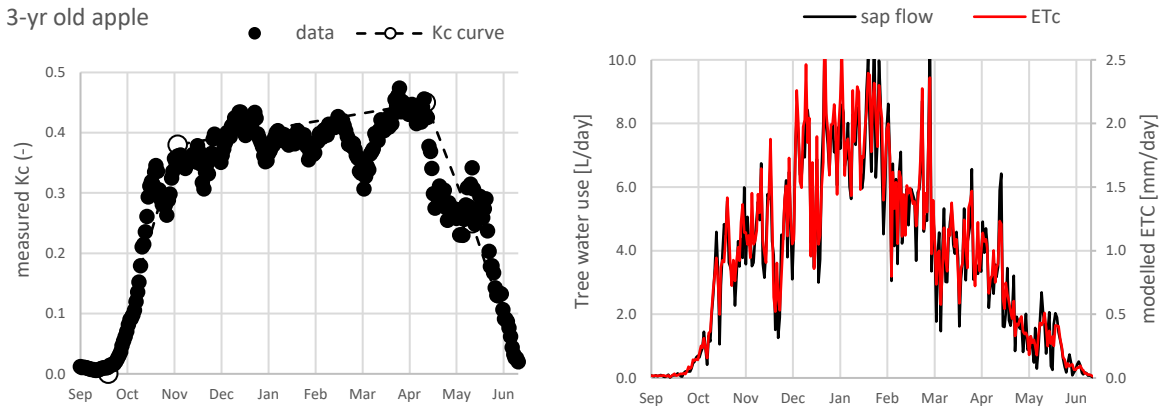

Figure 3. The top panel shows the seasonal pattern of the crop factor, *Kc*, used to calculate the water use of Envy™ apple trees (*Malus* x *domestica* var. 'Scilate'), as derived from measured sap flow and the local ETo value from climate data. The broken line represents a stylised envelope curve used by SINATA to represent the influence of leaf development on transpiration losses from these young apple trees. The bottom panel shows the seasonal pattern of daily transpiration (n=6) of 3-year-old Envy™ apple trees (*Malus* x *domestica* var. 'Scilate') at Lucaston Park Orchards, Tasmania, as measured using the compensation heat-pulse method. The red line shows the tree water use as calculated from the FAO-56 model using the seasonal crop factor from the top panel.

The ‘Parameter’ worksheet in SINATA holds a number of functional relationships used by the tool. For example, the left panel of Fig. 4 shows the mid-season crop factor as a function of time since planting, or tree age. Older trees tend to transpire more water than younger trees due to the increased size of the leaf canopy, if all other factors are equal. However, as the trees develop towards full canopy the leaf area stabilizes and the crop factor reaches a plateau with a maximum close to 1.0. The crop factor – tree age relationship in Fig. 4 comes from an extensive series of trunk sap-flow measurements on different-ages apple trees, carried out under the PIPS-I & PIPS-II research programmes in Victoria and Tasmania.

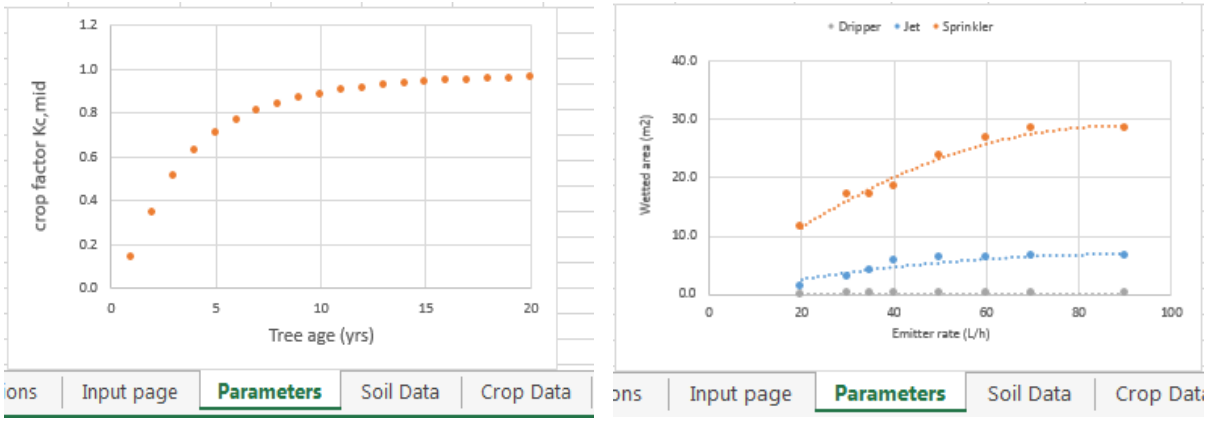

Figure 4. The left panel shows the assumed relationship between the mid-season crop factor and the tree age, as determined from the ratio of measured tree water use (L/day) per unit ground area (m2/tree) divided by potential evapotranspiration (ETo, mm/day). The right panel shows the assumed relationship between the size of the wetted area (m^2) and the emitter output (L/hr) for drippers (grey line), jets (blue line) and sprinklers (orange line) (Source: Netafim product guide downloaded from www.netafirm.com).

Irrigation

The fractional wetted area of the orchard block is important for determining how much of the recently-applied irrigation is lost to the atmosphere as surface evaporation. The right panel of Fig. 4 shows the relationship employed by SINATA to determine the area wetted by an emitter as a function of output rate. This relationship comes directly from manufacturer’s specification sheets and it is ‘hard-coded’ into SINATA.

Daily irrigation volumes are determined on the basis of need, by adding sufficient irrigation to maintain soil water contents above a strategic set-point curve which is illustrated by the grey line of Fig. 5. The default strategy is to raise soil moisture levels between budburst and flowering, then reduce soil moisture levels (with minimum water stress) between flowering through to harvest, then to allow for a gradual decline in soil moisture until leaf fall, and finally to halt irrigation until the next budburst occurs. Three other lines are shown in Fig.5. These are the field capacity (or the upper drained limit of the soil profile), the refill point and wilting point (FC = soil water content at a matric

potential of 0.1 kPa) which are integrated soil properties (see next section) summed from the soil surface to the bottom of the root-zone.

By default, SINATA employs the irrigation strategy of Fig. 5 to determine the irrigation demands. However, the USER can also change the set points for irrigation, to simulate a revised irrigation strategy and then assess the outcome in terms of changed water demands.

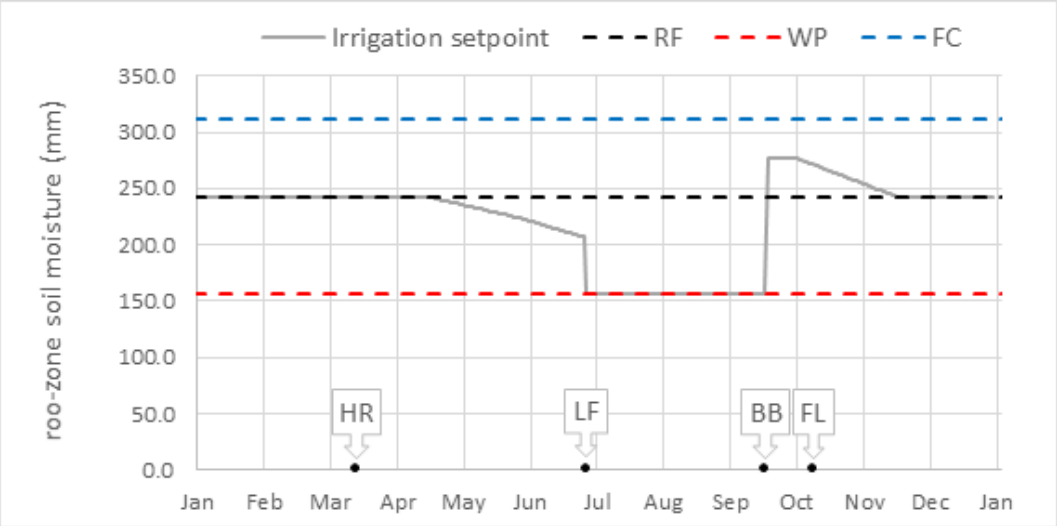

Figure 5. SINATA defines the irrigation strategy using a number of 'set-points' to maintain the root-zone water at critical times. These set points are defined by the soils water holding capacity at field capacity (FC) and wilting point (WP). The refill point (FP) represents the soil water content where trees begin to show signs of water stress. Boxes on the lower axis represent key phenological times of Budburst (BB), flowering (FL), harvest (HR) and leaf fall (LF).

Soil properties

A total of 57 soils are incorporated into SINATA. The soil's hydraulic properties are characterized by the water retention curve (WRC) and the hydraulic conductivity (HC) function. The WRC describes the relationship between the soil's water content, Θ [L/L] and matric potential, h [cm]. This curve is modelled using the van Genuchten (1980) equation:

$$\Theta = \frac{\theta - \theta_R}{\theta_S - \theta_R} = \left[\frac{1}{1+(\alpha h)^N}\right]^M \qquad \text{Eq. [1]}$$

Here S and R indicate saturated and residual values of the soil water content (θ) and the parameters α, N and M (=1-1/N) are fitting parameters that determine the 'shape' of the curve. The non-linear routine SOLVER in Microsoft® Excel® was used to determine each of the fitting parameters (Fig. 6).

Soil processes

The decomposition of soil organic matter (biomass) adds to the amount of mineral nitrogen in the soil. This process is known as mineralization. Mineralization is modelled by dividing the soil organic matter into two pools – a fast cycling litter pool (labile C and N) and an almost stable humus pool following Johnsson et al. (1987). This two-pool model then considers the total soil carbon and nitrogen that cycle within soil organic material. The relative amounts of these two components change daily to reflect inputs of new biomass (e.g. from leaf fall and root-turnover) and losses of older biomass as it decomposes. The nitrogen demand for the internal cycling of soil-C and soil-N is regulated by the C/N ratio of the soil biomass, r_O, which is one of the important model inputs, and the other important factor is the fraction of labile C & N. Figure 7 shows modelled mineralization rates compare favourably against laboratories studies from top-soil at Lucaston, Tasmania.

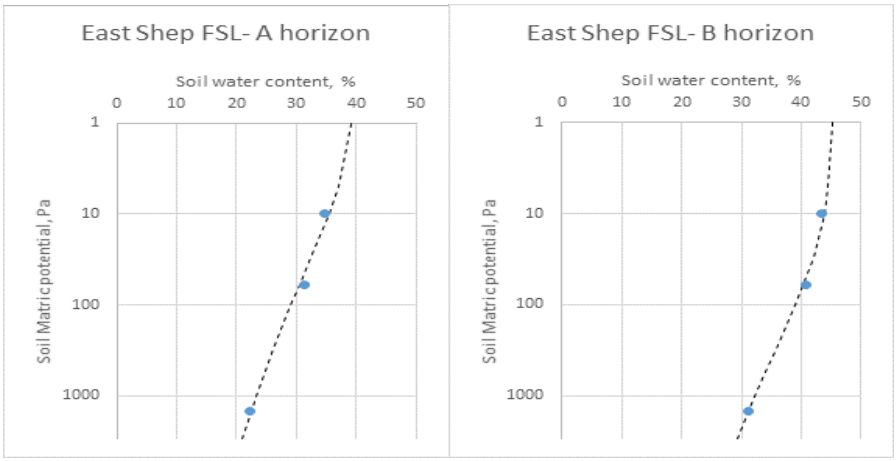

Figure 6. The soil's water retention curve (WRC) for a Lemnos Loam (top panels) and a Shepparton fine sandy loam (bottom panels) from near Shepparton, Victoria. Data (blue markers) were sourced from (Mehta and Wang, 2005). The broken lines are curves fitted for the van Genuchten model (1980) as described by Eq 1. The soil's field capacity (FC) is given by the water content at a potential of -10 kPa. The soil's wilting point (WP) is defined by the water content at a potential of -1500 kPa. The refill point for irrigation (RP) is typically at a potential of about -100 kPa.

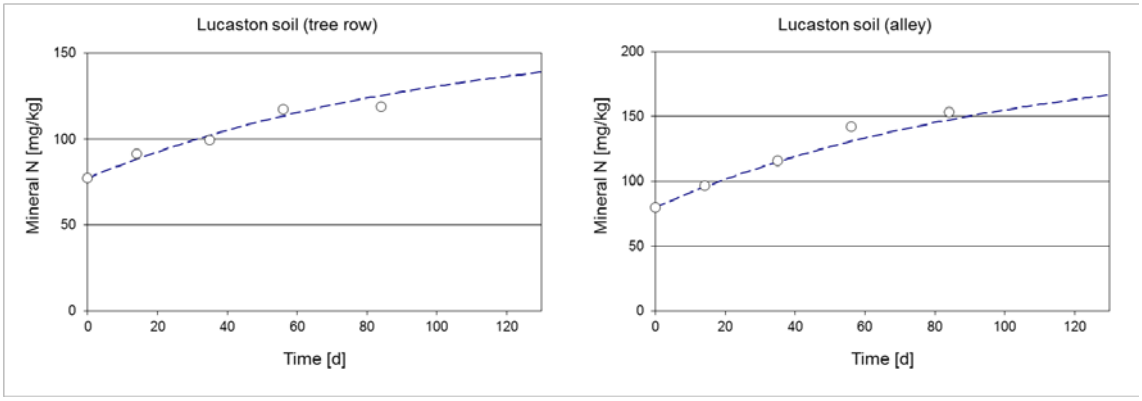

Figure 7. The change in soil mineral nitrogen (marker) observed during laboratory incubations of soils sampled from the Lucastion N-trial site, Tasmania. The broken line is model outputs from the mineralization sub-model of SINATA.

How the soil data is incorporated into SINATA

The soil properties for SINATA are compiled into a 'hidden' database that resides inside the tool. Data for a given soil type are selected using the pull-down menu of Fig. 2. An example of a subset of the soil property data is shown Fig. 8. The hydraulic conductivity and the water holding capacity of the top soil (10 cm) are used to classify the hydrologic status of the soil (e.g. well drained, poorly drained etc). This property modifies the surface runoff component of SINATA which is based on a daily rainfall totals with an adjustment to express the effect of slope and soil water content (Williams 1991).

Soil Number	Series name
1	Huon Loam (TAS)
2	Lucaston silty clay loam (TAS)
3	Congupna clay (VIC)
4	Congupna clay loam (VIC)
5	East Shepparton fine Sa Lo (VIC)
6	Goulburn clay loam (VIC)
7	Goulburn loam (VIC)
8	Katamatite loam (VIC)
9	Lemnos loam (VIC)
10	Shepparton fine Sa Lo (VIC)
11	Boosey Loam (VIC)
12	Cobram Loam (VIC)
13	Moira Loam (VIC)
14	Muckatah clay loam (VIC)
21	Koyuga clay loam (VIC)
22	Nanneella fine Sa Lo (VIC)
23	Rochester clay (VIC)
24	Timmering loam (VIC)
25	Wallenjoe clay (VIC)
26	Wanalta loam (VIC)

Choose a Soil Series 25 Wallenjoe clay (VIC)

phi values (kPa): 0, 10, 100, 1500

depth	_Rhob	% stones	K_sat	VF_sand	VF_clay	Org_C	Org_N	SAT	FC	SP	WP
0	1.42	0.00	643	8.9	65.0	1.25	0.08	62.40	47.9	42.7	39.1
20	1.49	0.00	74	7.4	61.0	0.84	0.06	62.50	51.5	45.7	40.7
40	1.49	0.00	74	7.4	61.0	0.56	0.04	62.50	51.5	45.7	40.7
60	1.49	0.00	74	7.4	61.0	0.38	0.03	62.50	51.5	45.7	40.7
80	1.49	0.00	74	7.4	61.0	0.25	0.02	62.50	51.5	45.7	40.7
100	1.49	0.00	74	7.4	61.0	0.17	0.01	62.50	51.5	45.7	40.7
120	1.49	0.00	74	7.4	61.0	0.13	0.01	62.50	51.5	45.7	40.7
140	1.49	0.00	74	7.4	61.0	0.13	0.01	62.50	51.5	45.7	40.7
160	1.49	0.00	74	7.4	61.0	0.13	0.01	62.50	51.5	45.7	40.7
180	1.49	0.00	74	7.4	61.0	0.13	0.01	62.50	51.5	45.7	40.7

Figure 8. A screenshot from the SINATA model (Version 2.0) showing the list of available soil series and a subset of parameter values for the hydraulic and physical properties. Data for each soil series can be selected using the filter tab on the "Input Page" worksheet. SINATA has compiled property data for 57 soil profiles from the main apple growing regions of Australia. Values for Western Australia will be added to SINATA once they have been determined.

Plant growth and nutrient uptake

Core components of SINATA's calculations of plant growth and nutrient uptake are derived from a series of model outputs generated by Plant and Food Research's SPASMO model (Soil Plant Atmosphere System Model). SPASMO has previously been parameterized for Australian apple orchards, and verified against field data on tree water use and tree nutrient uptake under the PIPS-1 project (Figs. 9 & 10). Functional relationships in SINATA for plant growth and nitrogen uptake are expressed in a simplified form (Figs 11 & 12). This empirical approach maintains the functionality and integrity of the model outputs.

The empirical curves for crop development are representative of mature trees (i.e. 10 years). The model computes the seasonal development of dry-matter in the various plant components (Fig. 11) and includes temporal adjustments related to key phenological events such as the timing of budburst and harvest (Table 1). This approach accommodates differences in early (e.g. gala) and late (e.g. Pink) apple varieties.

SINATA offers two options to establish nutrient demands of the trees. The first option is a statistical approach, based on yield data provided the by apple-industry, to estimate and expected yield for the four main apple varieties (Gala, Fuji, Pink Lady and Granny Smith). Two yields are suggested: an average orchard with an average yield, or a more productive orchard a higher yield (the upper quartile) as shown in Fig. 13. Some rescaling is applied to the crop-development curves, to account for tree age, and this is done in a non-linear way that mimics the age-related changes in the mid-season crop factor (Fig. 4). The second option to establish the nutrient demands is for tool users to input their anticipated crop yields at harvest time. In this case the crop developmental curves are also re-scaled to match the expected yields.

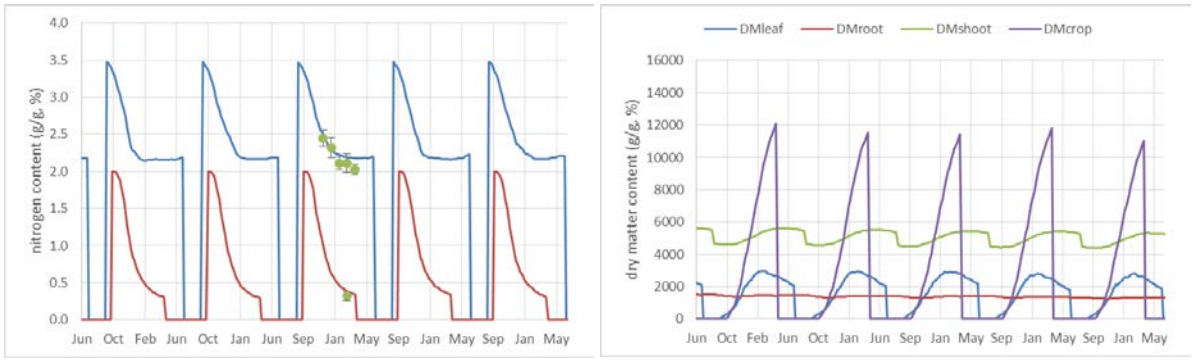

Figure 9. The left panel shows the nitrogen content of leaf (blue lines) and fruit (red lines) material as simulated using Plant and Food Research's SPASMO (**S**oil **P**lant **A**tmosphere **S**ystem **M**odel) model and as measured on Gala trees at Lucaston, Tasmania (green markers). The right panel shows the corresponding dry-matter content of the leaf (blue line), root (red line), shoot (green line) and crop (purple line) material from an orchard of mature (10 years) Gala trees, as simulated using SPASMO.

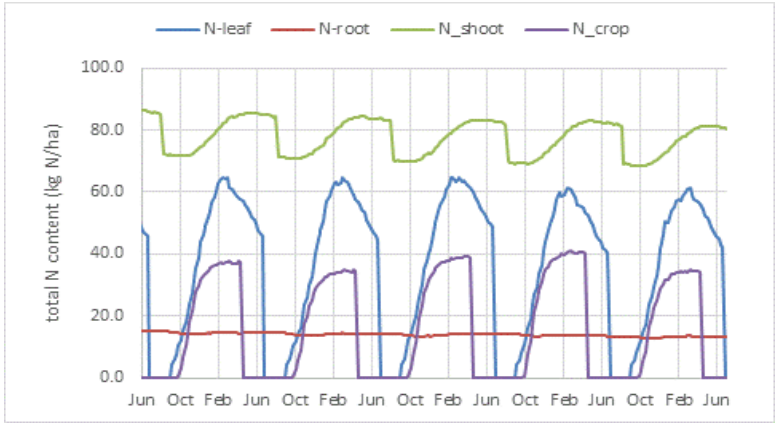

Figure 10. The mass distribution of nitrogen to various components of a model apple orchard, as simulated using Plant and Food Research's SPASMO (**S**oil **P**lant **A**tmosphere **S**ystem **M**odel) model. Trees on the model orchard comprise of leaves (blue line), fine roots (red line), shoots (green line), fruit (purple line) and the woody trunks and structural roots (> 125 kg-N/ha; data not shown).

Fruit are harvested on a set day of year, with all of that nitrogen being removed from the orchard system. Meanwhile a fraction (50%) of the nitrogen in the leaves (at leaf fall) and all of the nitrogen in the pruned shoots (during winter pruning) is returned to the soil surface, as a littler layer, that slowly decomposes releasing organic carbon and nitrogen back to the top soil. The remaining fraction (50%) leaf nitrogen at leaf fall is transferred back to the main structural (woody) components of the tree, to maintain the nitrogen balance. Figure 11 shows functional relationships in SINATA to simulate the temporal development of leaf and fruit dry matter. Figure 12 shows similar functional relationships for the corresponding nitrogen contents. Table 1 lists average dates for key phenological events. The seasonal development of the fruit-N content is adjusted to the length of the fruit-growing season.

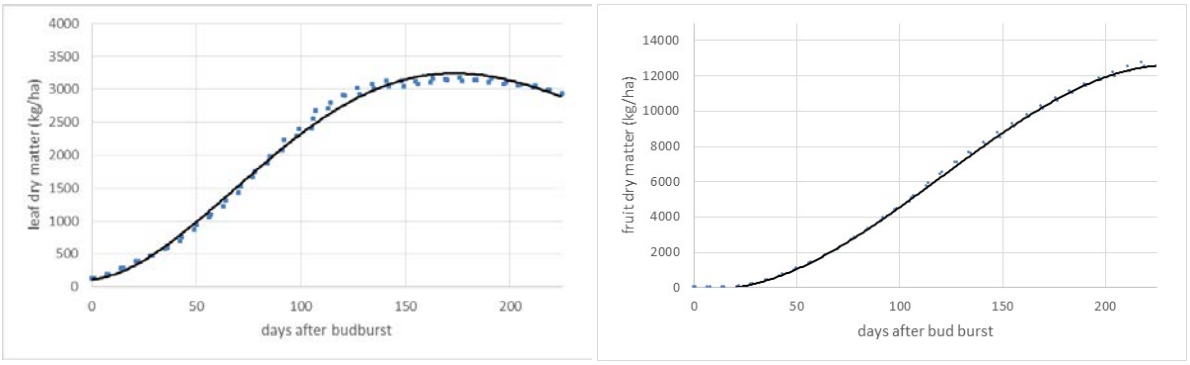

Figure 11. Functional relationships used to describe the temporal development of leaf dry matter (left panel) and fruit dry matter (right panel) of a model orchard of mature Gala apple. The blue markers are average weekly values generated using a range of soils and years. The black lines represent a 4th order polynomial fitted to the model outputs using least-square regression. These functional relations are used in SINATA to calculate dry-matter development and potential nutrient uptake demands. Different developmental curves have been developed the each apple variety, namely (Fuji, Gala, Granny and Pink).

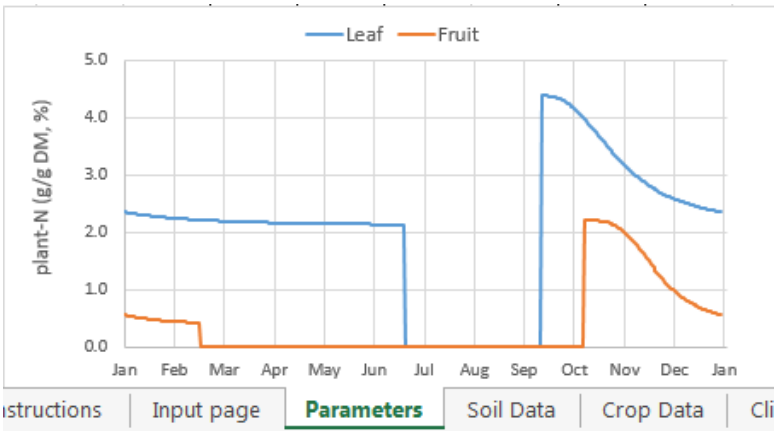

Figure 12. Functional relationships used to describe the temporal development of the nitrogen content of leaf (blue line) and fruit (orange line) material from a model Gala apple tree. SINATA assumes the same N-content range for all apple varieties, and rescales the developmental curves to match the phenology (e.g. Table 1).

Table 1. The average dates for key phenological events occurring on four commercial apple varieties from Australia (Source: adapted from data compiled from the OrchardNet focus orchards (source: HIA database assembled by AgFirst NZ Ltd)

Variety	Budburst	Flowering	Harvest	season (d)
Fuji	18Sep	10Oct	15Mar	178
Gala	13Sep	09Oct	18Feb	157
Granny	10Sep	07Oct	06Apr	208
Pink	09Sep	05Oct	24Apr	227

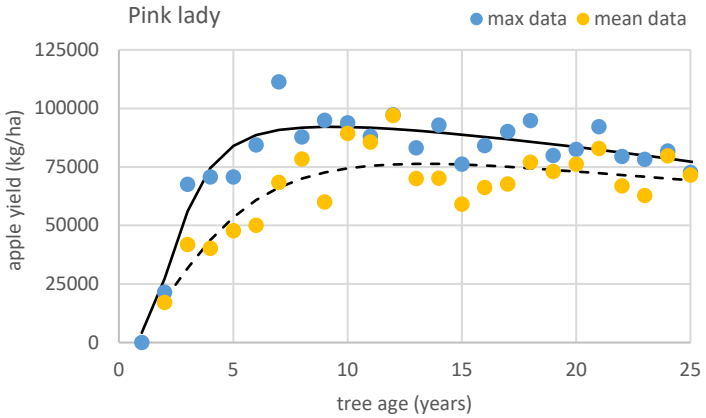

Fig 13. The relationship between harvested fruit yield and tree age for Pink Lady apples grown in Australia (source: HIA database assembled by AgFirst NZ Ltd). Data are regional averages.

Model Outputs

The soil water balance component of the model includes a calculation of the irrigation requirements (Figs 14 & 15). The results are presented on a monthly and an annual basis, using a mean and a standard deviation along with a value for any level of probability e.g. the one in 10 year high.

- Climate data is selected from a pull-down menu on the 'Inputs page' worksheet.
- Users can select one of twenty two climate stations and the press the 'recalculate' button (Fig. 14) to update the model outputs
- All results are summarized on the 'Chart outputs' worksheet
- The tool provides an estimates of the daily tree water use in L per tree. It also shows the water content of the root-zone soil compared against the irrigation strategy. Irrigation volumes are expressed as a depth equivalent (mm) or as a volume ML/ha)
- The tool also displays a monthly summary of the local climate and water balance, reporting values for the long term average (LTA) and the standard deviation of each f the water baace terms (evapotranspiration (ETo), crop water use (ETc), rainfall, irrigation, drainage and runoff components (Fig. 15)

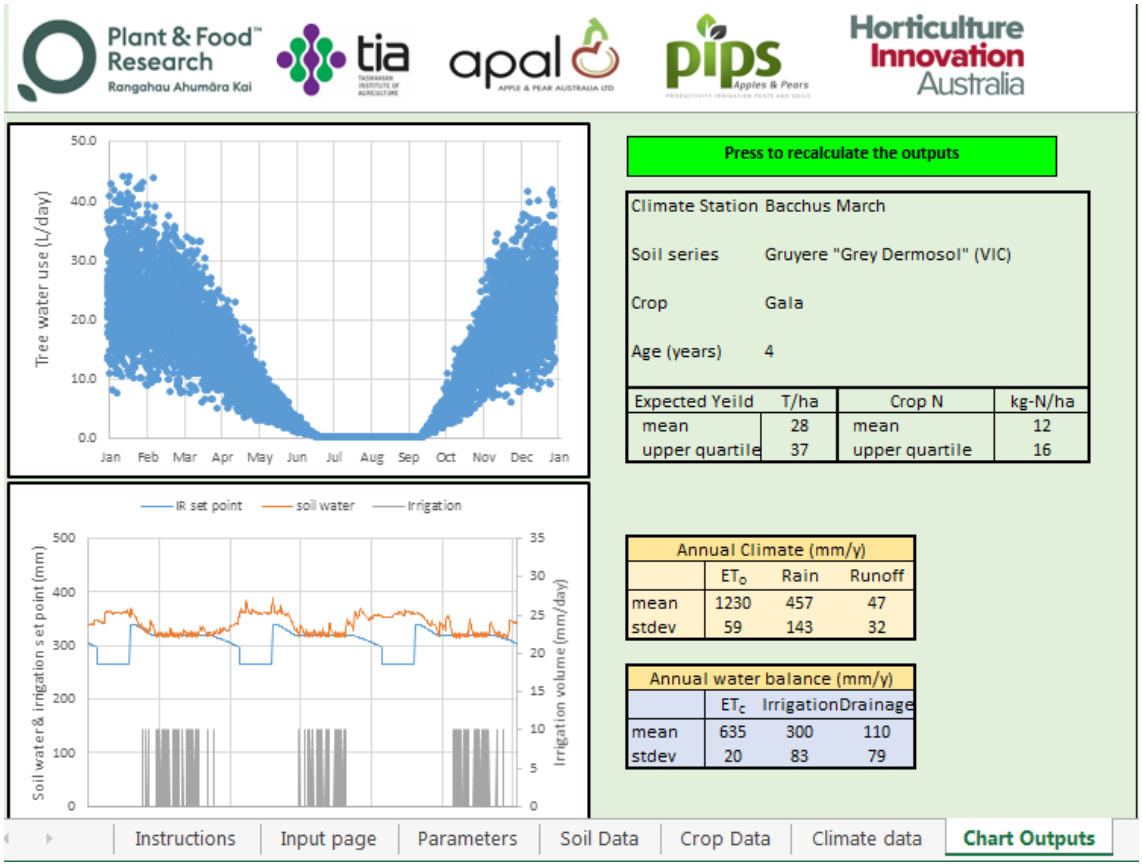

Figure 14. A screen image of the 'Chart Outputs' worksheet from the SINATA (**S**trategic **I**rrigation and **N**itrogen **A**ssessment **T**ool for **A**pples) model. The upper right panel records the selected inputs of climate and soil, along with the apple variety (Gala) and the tree age (4 years). Expected values of crop yield and crop nitrogen are derived from the national harvest database (Source: OcrhardNet, AgFirst). The upper left panel shows the daily tree water use computed using 25 years of climate data. The lower left panel shows the water content of the root-zone soil (orange line) compared with irrigation volumes (grey line) required to maintain the set-points for the irrigation strategy (blue line). The lower right panel shows the annual means and standard deviations of the water balance components.

What work remains to be completed?

At the time of writing this report, Plant and Food Research are still finalizing the remaining component of SINATA that deals with nitrogen fate in the soil domain including the potential for N leaching. In most of the apple growing regions of Australia, rainfall is much less that ET_O and so irrigation is essential to maintain production of high quality fruit. SINATA proves guideline values to help with planning for monthly and annual water takes.

Many of the orchard soils in Australia have very poor drainage characteristics, especially in the subsoils. For example, on some of the duplex soils the saturated hydraulic conductivity is reported to be less than 1 mm/day. Drainage is shown to be a relatively small component of the overall water balance. There is a knowledge gap about rooting depth and the impact of soil restrictions such as hard-pan layers or heavy clay subsoils with poor drainage.

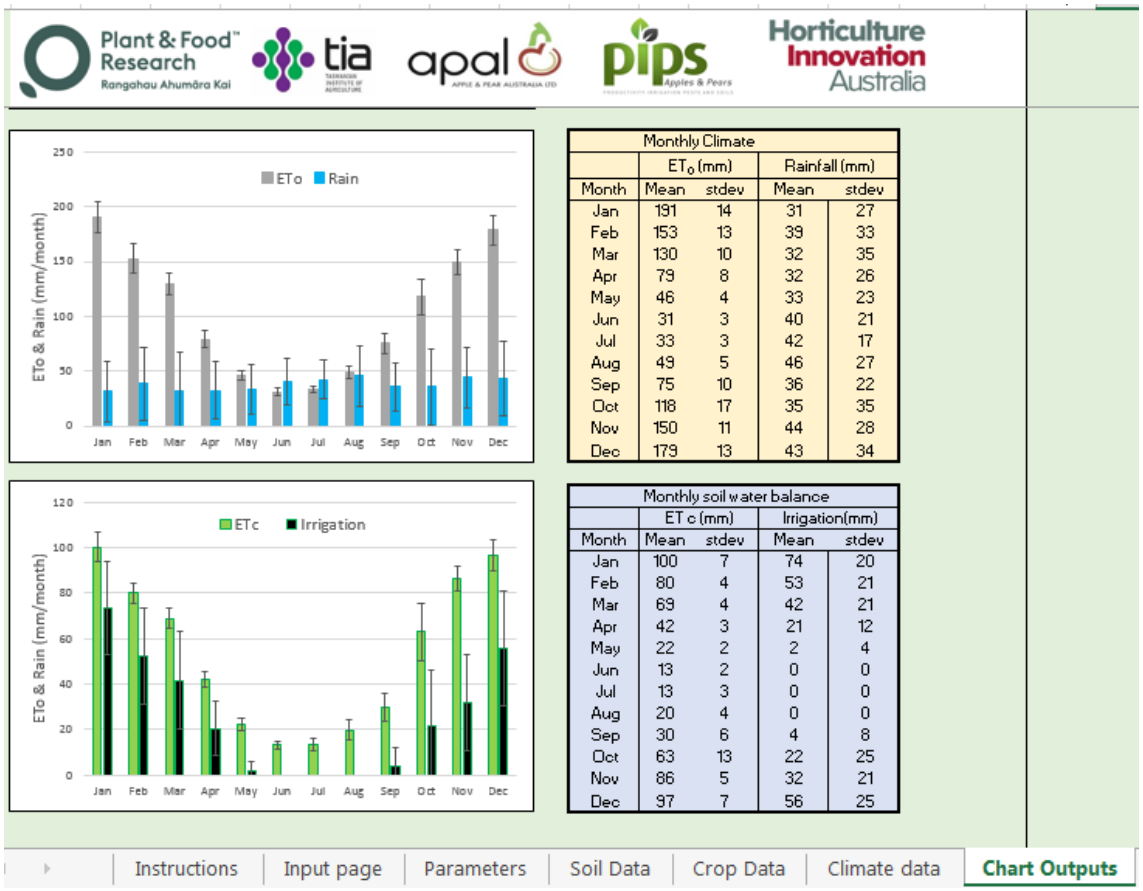

Monthly Climate

	ET_o (mm)		Rainfall (mm)	
Month	Mean	stdev	Mean	stdev
Jan	191	14	31	27
Feb	153	13	39	33
Mar	130	10	32	35
Apr	79	8	32	26
May	46	4	33	23
Jun	31	3	40	21
Jul	33	3	42	17
Aug	49	5	46	27
Sep	75	10	36	22
Oct	118	17	35	35
Nov	150	11	44	28
Dec	179	13	43	34

Monthly soil water balance

	ETc (mm)		Irrigation(mm)	
Month	Mean	stdev	Mean	stdev
Jan	100	7	74	20
Feb	80	4	53	21
Mar	69	4	42	21
Apr	42	3	21	12
May	22	2	2	4
Jun	13	2	0	0
Jul	13	3	0	0
Aug	20	4	0	0
Sep	30	6	4	8
Oct	63	13	22	25
Nov	86	5	32	21
Dec	97	7	56	25

Figure 15. A screen image of the 'Chart Outputs' worksheet from the SINATA (**S**trategic **I**rrigation and **N**itrogen **A**ssessment **T**ool for **A**pples) model showing monthly values of the climate, as represented by evapotranspiration (ETo, mm/day) and rainfall (mm/day), the crop water use (ETc, mm/day), and the irrigation demands.

Do these soils factors limit root depth and should such behaviours be included in the SINATA tool? One way to simulate the behaviour of a root restriction would be to 'set' the root depth on the 'Inputs' worksheet. If the User prescribed root depth then they could do a 'what-if' simulation to gauge the outcome e.g how much impact does a restricted rooting depth have on irrigation demand?

It must be remembered that SINATA is primarily a strategic planning tool to enable advisors and growers to estimate the seasonal pattern of irrigation demand for orchards of different ages, climates and soils. A lot of the data needed to populate the model inputs is not yet available so, in some instances, we are still using literature values to fill in some of the knowledge gaps.

In particular there is some uncertainty around the set points for irrigation, and whether they should be derived from a soil matric-potential or from a relative soil water content and where that irrigation trigger-point should be observed (i.e. at what depth in the root zone?)

SINATA will provide outputs for the water and nitrogen balance of an apple orchard. We are yet to gauge the interest in modifying outputs and providing different metrics of production that might

include water use efficiency or a cost-benefit analysis of irrigation and fertilizer use. At this stage, SINATA serves as a framework onto which additional features can be added if requested.